

Topics in Current Chemistry 372

Takeo Kawabata *Editor*

# Site-Selective Catalysis

 Springer

**Editorial Board**

H. Bayley, Oxford, UK  
K.N. Houk, Los Angeles, CA, USA  
G. Hughes, CA, USA  
C.A. Hunter, Sheffield, UK  
K. Ishihara, Chikusa, Japan  
M.J. Krische, Austin, TX, USA  
J.-M. Lehn, Strasbourg Cedex, France  
R. Luque, Córdoba, Spain  
M. Olivucci, Siena, Italy  
J.S. Siegel, Tianjin, China  
J. Thiem, Hamburg, Germany  
M. Venturi, Bologna, Italy  
C.-H. Wong, Taipei, Taiwan  
H.N.C. Wong, Shatin, Hong Kong  
V.W.-W. Yam, Hong Kong, China  
C. Yan, Beijing, China  
S.-L. You, Shanghai, China

## **Aims and Scope**

The series Topics in Current Chemistry presents critical reviews of the present and future trends in modern chemical research. The scope of coverage includes all areas of chemical science including the interfaces with related disciplines such as biology, medicine and materials science.

The goal of each thematic volume is to give the non-specialist reader, whether at the university or in industry, a comprehensive overview of an area where new insights are emerging that are of interest to larger scientific audience.

Thus each review within the volume critically surveys one aspect of that topic and places it within the context of the volume as a whole. The most significant developments of the last 5 to 10 years should be presented. A description of the laboratory procedures involved is often useful to the reader. The coverage should not be exhaustive in data, but should rather be conceptual, concentrating on the methodological thinking that will allow the non-specialist reader to understand the information presented.

Discussion of possible future research directions in the area is welcome.

Review articles for the individual volumes are invited by the volume editors.

**Readership: research chemists at universities or in industry, graduate students.**

More information about this series at <http://www.springer.com/series/128>

Takeo Kawabata

Editor

# Site-Selective Catalysis

With contributions by

M. Canta · M. Costas · M.W. Giuliano · M. Kanai ·  
T. Kawabata · M.J. Krische · K. Manabe · S.J. Miller · J. Ni ·  
T. Ooi · M. Rodríguez · I. Shin · M.S. Taylor · Y. Ueda ·  
D. Uraguchi · M. Yamaguchi

 Springer

*Editor*  
Takeo Kawabata  
Institute for Chemical Research  
Kyoto University  
Kyoto  
Japan

ISSN 0340-1022  
Topics in Current Chemistry  
ISBN 978-3-319-26331-1  
DOI 10.1007/978-3-319-26333-5

ISSN 1436-5049 (electronic)  
ISBN 978-3-319-26333-5 (eBook)

Library of Congress Control Number: 2016933316

Springer Cham Heidelberg New York Dordrecht London  
© Springer International Publishing Switzerland 2016

This work is subject to copyright. All rights are reserved by the Publisher, whether the whole or part of the material is concerned, specifically the rights of translation, reprinting, reuse of illustrations, recitation, broadcasting, reproduction on microfilms or in any other physical way, and transmission or information storage and retrieval, electronic adaptation, computer software, or by similar or dissimilar methodology now known or hereafter developed.

The use of general descriptive names, registered names, trademarks, service marks, etc. in this publication does not imply, even in the absence of a specific statement, that such names are exempt from the relevant protective laws and regulations and therefore free for general use.

The publisher, the authors and the editors are safe to assume that the advice and information in this book are believed to be true and accurate at the date of publication. Neither the publisher nor the authors or the editors give a warranty, express or implied, with respect to the material contained herein or for any errors or omissions that may have been made.

Printed on acid-free paper

Springer International Publishing AG Switzerland is part of Springer Science+Business Media (www.springer.com)

# Preface

Chemoselectivity and stereoselectivity have been key factors in the development of fine organic synthesis. In addition to these selectivities, site-selectivity has recently been receiving much attention, because site-selective catalysis enables conventionally difficult molecular transformations such as late-stage functionalization of biologically active complex molecules, which provides straightforward access to structurally diverse compounds with related biological activity. However, methods for site-selective molecular transformation of complex molecules have not been well explored. This may be because of the lack of reliable strategy for site-selective catalysis. Recently, site-selective catalysis has been expanding its scope and significance as a new challenge in organic synthesis to realize conventionally difficult, yet valuable molecular transformations.

During the last few decades, asymmetric synthesis has been extensively developed. “Steric approach control” is the key principle for the extensive development of asymmetric synthesis. For example, if one of the two potentially reactive enantiofaces is effectively shielded by steric interaction, a highly enantioselective reaction would be expected. On the other hand, this principle seems not to be effective for achieving site-selective molecular transformation of complex molecules because, to functionalize a desirable reactive site, the remaining many undesirable potentially reactive sites have to be sterically shielded by the catalyst or the reagent. One of the promising approaches to achieve site-selective functionalization may be taking advantage of the acceleration of the reaction at the desirable site based on precise molecular recognition with the properly designed catalyst, rather than the deceleration of the reactions at many undesirable sites by steric shielding. Under such catalyst-controlled conditions, selective molecular transformation is expected to take place at the desirable site independently from the intrinsic reactivity of the substrate.

From these scientific backgrounds, this book focuses on (1) ligand-controlled site-selective cross-coupling, (2) iron-catalyzed site-selective oxidation of alkyl C–H bonds, (3) catalytic site-selective conjugate addition of conjugated dienones and trienones, (4) site-selective redox-triggered C–C coupling of diols, (5) site-selective

cleavage of peptides and proteins, (6) catalyst-controlled site-selective molecular transformations of carbohydrates, (7) site-selective functionalization of complex natural products by peptide-based catalysts, and (8) site-selective acylation of carbohydrates and its application to unconventional retrosynthesis of natural glycosides.

Site-selective molecular transformations can be performed in either a substrate-controlled or a catalyst-controlled manner, at least in principle. More arbitrary and diverse molecular transformation is expected, especially by such catalyst-controlled transformations. The molecular recognition process with its dynamic nature seems to be responsible for the performance of catalyst-controlled site-selective molecular transformation. Various examples of catalyst-controlled site-selective functionalization and its application to biological active natural products with complex structures are described. We know, however, that we are still at the preliminary stage in this emerging scientific field of site-selective catalysis. I believe that publication of this book can stimulate extensive development of methods for these future-oriented molecular transformations.

Uji, Kyoto, Japan  
2015

Takeo Kawabata

# Contents

<b>Ligand-Controlled Site-Selective Cross-Coupling . . . . .</b>	<b>1</b>
Miyuki Yamaguchi and Kei Manabe	
<b>Recent Advances in the Selective Oxidation of Alkyl C–H Bonds Catalyzed by Iron Coordination Complexes . . . . .</b>	<b>27</b>
Mercè Canta, Mònica Rodríguez, and Miquel Costas	
<b>Site-Selective Conjugate Addition Through Catalytic Generation of Ion-Pairing Intermediates . . . . .</b>	<b>55</b>
Daisuke Uraguchi and Takashi Ooi	
<b>Asymmetric Iridium-Catalyzed C–C Coupling of Chiral Diols via Site-Selective Redox-Triggered Carbonyl Addition . . . . .</b>	<b>85</b>
Inji Shin and Michael J. Krische	
<b>Site-Selective Peptide/Protein Cleavage . . . . .</b>	<b>103</b>
Jizhi Ni and Motomu Kanai	
<b>Catalyst-Controlled, Regioselective Reactions of Carbohydrate Derivatives . . . . .</b>	<b>125</b>
Mark S. Taylor	
<b>Site-Selective Reactions with Peptide-Based Catalysts . . . . .</b>	<b>157</b>
Michael W. Giuliano and Scott J. Miller	
<b>Organocatalytic Site-Selective Acylation of Carbohydrates and Polyol Compounds . . . . .</b>	<b>203</b>
Yoshihiro Ueda and Takeo Kawabata	
<b>Index . . . . .</b>	<b>233</b>

# Ligand-Controlled Site-Selective Cross-Coupling

Miyuki Yamaguchi and Kei Manabe

**Abstract** Site-selective mono-cross-coupling reactions involving dichloro- or dibromo(hetero)aryl substrates are utilized to prepare substituted monochloro- or monobromo(hetero)arenes, which are used as drug components and synthetic precursors. In these reactions, selectivity toward the preferred reaction site of a dihalo (hetero)arene can vary depending on the ancillary ligand of the transition metal catalyst. This review summarizes the examples of ligand-controlled site-selective cross-coupling reactions, specifically those mediated by Pd complexes.

**Keywords** Kumada–Tamao–Corriu coupling • Palladium • Sonogashira coupling • Suzuki–Miyaura coupling • Transition metal catalyst

## Contents

1	Introduction .....	2
2	Suzuki–Miyaura Coupling .....	4
3	Kumada–Tamao–Corriu Coupling .....	12
4	Sonogashira Coupling .....	17
5	Conclusion .....	23
	References .....	23

## Abbreviations

Ar            Aryl  
Cy            Cyclohexyl

---

M. Yamaguchi and K. Manabe (✉)  
School of Pharmaceutical Sciences, University of Shizuoka, 52-1 Yada, Suruga-ku,  
Shizuoka 422-8526, Japan  
e-mail: [manabe@u-shizuoka-ken.ac.jp](mailto:manabe@u-shizuoka-ken.ac.jp)

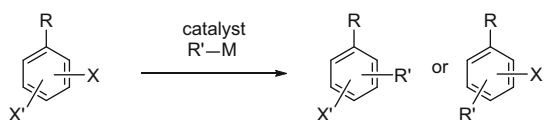
dba	Dibenzylideneacetone
DHTP	Dihydroxyterphenylphosphine
DPEPhos	Bis[2-(diphenylphosphino)phenyl] ether
DPPF	1,1'-Bis(diphenylphosphino)ferrocene
HTP	Hydroxyterphenylphosphine
LUMO	Lowest unoccupied molecular orbital
NMP	<i>N</i> -Methylpyrrolidone
PMP	4-Methoxyphenyl
PXPd2	Dichloro(chlorodi- <i>tert</i> -butylphosphine)palladium(II) dimer
Q-Phos	1,2,3,4,5-Pentaphenyl-1'-(di- <i>tert</i> -butylphosphino)ferrocene
TBAC	Tetrabutylammonium chloride
Th	Thienyl
Tol	4-Methylphenyl
Ts	Tosyl, <i>p</i> -toluenesulfonyl
Xantphos	4,5-Bis(diphenylphosphino)-9,9-dimethylxanthene
XPhos	2-Dicyclohexylphosphino-2',4',6'-triisopropylbiphenyl

## 1 Introduction

Cross-coupling reactions between organic halides (or pseudohalides such as triflates) with organometallic reagents are among the most important transition metal-catalyzed transformations and have various synthetic applications in academia and industry [1–3]. Recently, organic dihalides, which are molecules containing two halo substituents, have attracted considerable interest as cross-coupling substrates. For example, double-cross-coupling of organic dihalides affords disubstituted compounds, whereas mono-cross-coupling of dihalides affords monohalogenated compounds. The latter are versatile synthetic intermediates exhibiting interesting structural motifs and have therefore inspired efforts to develop efficient methods for mono-cross-coupling reactions.

Selectivity between the two halo groups in organic dihalide substrates is an important topic which needs to be considered in the chemistry of mono-cross-coupling reactions. For instance, *chemoselective* cross-coupling between two different halo groups is easily achieved through the intrinsic reactivity order of halo groups (i.e.,  $I > Br > Cl > F$ ) [4–7], but *site-selective* cross-coupling between two identical halo groups is more challenging (Scheme 1,  $X = X'$ ). The latter

**Scheme 1** Chemoselective and site-selective cross-coupling of organic dihalides



$X, X' = \text{halogen}$

$X \neq X'$  : **chemoselective cross-coupling**

$X = X'$  : **site-selective cross-coupling**

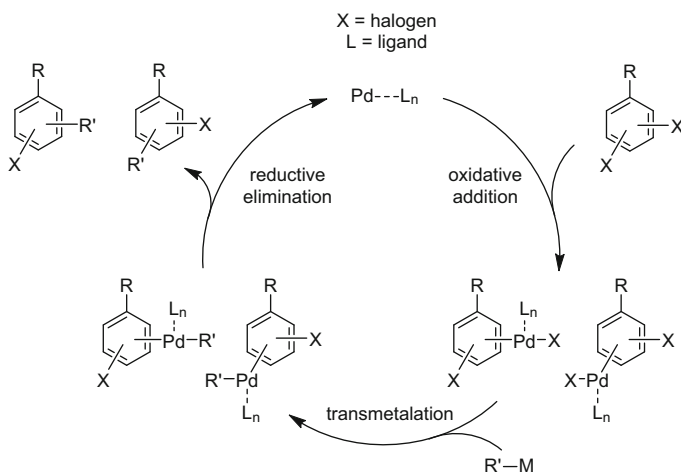
transformation is highly desired because dihalide substrates with two identical halo groups can generally be prepared more easily than their counterparts with two different halo groups [8–11].

Traditionally, the site-selective cross-coupling of organic dihalides has been based on the “substrate-controlled” strategy, in which the selectivity between the two halo groups is controlled by the structures of the substrates. Two general rules exist: the reaction preferentially occurs (1) at the less sterically hindered position, and (2) at the carbon–halogen bond bearing the less electron-rich carbon [12]. Detailed studies on the factors influencing site-selectivity in heteroaromatic dihalides have been reported [13–16]. These factors include the strength of the carbon–halogen bonds and  $\pi^*$  LUMO coefficients.

Recently, another strategy for site-selective cross-coupling has emerged in which the selectivity can be controlled by the catalyst. This “catalyst-controlled” strategy has several advantages over the substrate-controlled strategy. For example, the major product can, in principle, be obtained regardless of the steric and electronic nature of the substrates. Furthermore, the site-selectivity can be tuned merely by changing the catalyst; different products can be obtained selectively from the same dihalide substrate [17].

Most catalyst-controlled site-selective cross-coupling reactions have employed palladium complexes as catalysts. The key to attaining the desired site-selectivity lies in the use of the appropriate ancillary ligand in the Pd catalyst. Accordingly, designing and developing new ligand platforms for “ligand-controlled” site-selective cross-coupling reactions can make unprecedented site-selectivity accessible.

Scheme 2 depicts a general cross-coupling catalytic cycle involving organic dihalides. Although the oxidative addition step is proposed to be reversible in some cross-coupling reactions [18], it is generally considered to be irreversible in many



**Scheme 2** General catalytic cycle of Pd-catalyzed cross-coupling involving organic dihalides

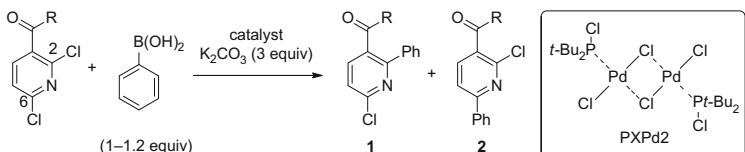
cases. Thus, selectivity in the oxidative addition of one of the two carbon–halogen bonds is essential in ligand-controlled site-selective cross-coupling, and is influenced by the nature of the supporting ligand in the Pd catalyst.

In this review, examples of the ligand-controlled site-selective cross-coupling reactions are summarized. This review is not intended to be an exhaustive summary of the topic, but rather to showcase the concepts of the strategies for selective reactions. The examples are categorized by the type of cross-coupling reaction: Suzuki–Miyaura coupling, Kumada–Tamao–Corriu coupling, and Sonogashira coupling. Examples of enantioselective cross-coupling, in which one of the two enantiotopic halo groups is selected [19], as well as examples of catalyst-controlled chemoselectivity between two different (pseudo)halo groups [20–22], are omitted.

## 2 Suzuki–Miyaura Coupling

In 2003, Yang and coworkers reported the site-selective Suzuki–Miyaura coupling [23] of 2,6-dichloronicotinic acid derivatives with phenylboronic acid (Table 1) [24]. When the methyl ester derivative of 2,6-dichloronicotinic acid ( $R = \text{OMe}$ ) was employed as the substrate and  $\text{Pd}(\text{PPh}_3)_4$  as the catalyst, C6-arylated **2** was obtained as the major product (entry 1, Table 1). This selectivity presumably resulted from a less sterically hindered environment, thereby promoting oxidative addition of the catalytically active Pd(0) complex to the C6 carbon–chloride bond. Pd catalysts supported by bidentate ligands also promoted similar C6-selectivity. On the other hand, a 1:1 ratio of Pd/ $\text{P}(t\text{-Bu})_3$  resulted in C2-arylated **1** as the major product (entry 2, Table 1). Among the catalysts tested, PXPd2 [25], a 1:1 Pd/chlorophosphine complex by formulation, gave the highest regioselectivity (entry 3,

**Table 1** Site-selective Suzuki–Miyaura coupling of 2,6-dichloronicotinic acid derivatives



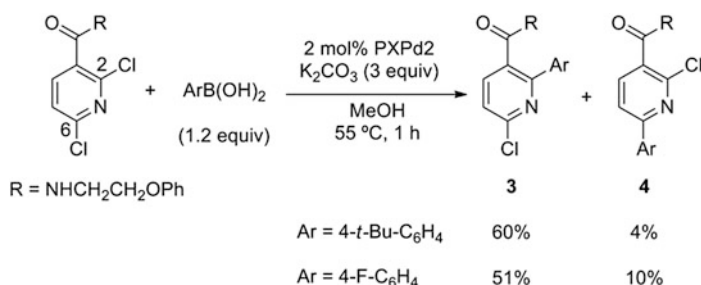
Entry	R	Catalyst (mol%)	Conditions	<b>1</b> : <b>2</b>
1	OMe	$\text{Pd}(\text{PPh}_3)_4$ (5)	THF, reflux, 16 h	1:5 <sup>a</sup>
2	OMe	$\text{Pd}_2(\text{dba})_3$ (1.5)/[HP( <i>t</i> -Bu) <sub>3</sub> ]BF <sub>4</sub> (3)	THF, reflux, 16 h	1.7:1 <sup>a</sup>
3	OMe	PXPd2 (1)	MeOH, reflux, 30 min	2.5:1 <sup>a</sup>
4	NHCH <sub>2</sub> CH <sub>2</sub> OPh	PXPd2 (2)	MeOH, 55°C, 1 h	9:1 <sup>b</sup>

<sup>a</sup>Yields are not indicated

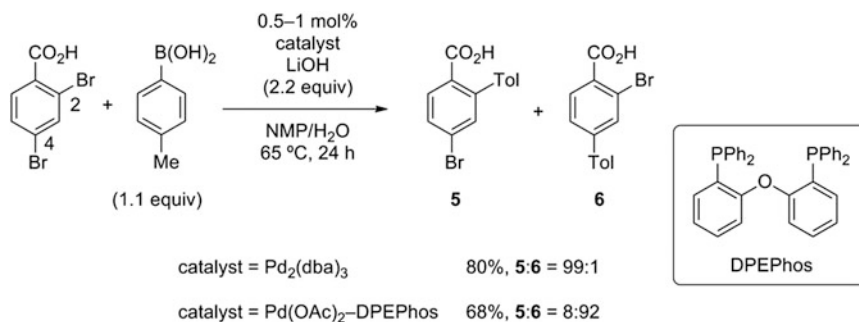
<sup>b</sup>Yield of **1** is 61%

Table 1). The observed preference toward the C2 position can be explained by coordination of the carbonyl oxygen to the catalytically active Pd(0) species. This coordination is promoted by increase of the Pd/ligand ratio, which makes the Pd more coordinatively unsaturated. Use of reagent-grade methanol as the solvent helped achieve a higher yield; in contrast, the reaction became sluggish when anhydrous methanol was used. From these results, it is reasoned that a trace amount of water in reagent-grade methanol accelerates the reaction either by solvolysis of the catalyst to form more active species, or by increasing the solubility of the inorganic salt. Use of 2,6-dichloronicotinamide, which has enhanced coordinating ability, largely improved site-selectivity (entry 4, Table 1). This catalyst system was employed for both electron-rich and electron-deficient boronic acids to afford C2-arylated product **3** with moderate to good selectivity (Scheme 3). Although the selectivity could be significantly improved upon and greatly depends on the neighboring group, this early example introduced the possibility of site-selective cross-coupling of nitrogen-containing heterocycles.

In a more recent example, Houpis and coworkers demonstrated the site-selective Suzuki–Miyaura coupling of 2,4-dibromobenzoic acid with arylboronic acids (Scheme 4) [26]. In reactions with Pd<sub>2</sub>(dba)<sub>3</sub> as the catalyst in the absence of phosphine ligands, cross-coupling occurred with excellent *ortho*-selectivity to



**Scheme 3** Scope of site-selective Suzuki–Miyaura coupling of 2,6-dichloronicotinamide derivative



**Scheme 4** Site-selective Suzuki–Miyaura coupling of 2,4-dibromobenzoic acid

afford C2-arylated product **5**. This selectivity was attributed to the coordination of the carboxylate anion to Pd, which places the *ortho* bromo group close to Pd, and therefore promotes oxidative addition at this position. The choice of the base (LiOH), solvent system (NMP/H<sub>2</sub>O), and base equivalents (2.2 equiv.) was essential to achieve such a high yield and selectivity. In contrast, reactions with a Pd catalyst supported by bulky bidentate phosphines such as DPEPhos preferentially produced C4-arylated isomer **6**. This result is attributed to both the strong chelating effect of the phosphine, which inhibits coordination of the carboxylate anion to Pd, and the bulkiness of the catalyst species, which promotes oxidative addition at the less sterically hindered *para*-position. In both catalyst systems, less than 3% of di-coupled product was observed.

Subsequent work by Houpis and coworkers further applied the directing effect of the carboxylate anion to the site-selective Suzuki–Miyaura coupling of 2,6-dichloronicotinic acid (Table 2) [27]. Reactions that employed Pd<sub>2</sub>(dba)<sub>3</sub> as the catalyst, K<sub>2</sub>CO<sub>3</sub> as the base, and ethanol as the solvent produced C2-arylated compound **7** with high selectivity (entry 1, Table 2). The carboxylate moiety presumably serves as a directing group, which is likewise proposed above in the reaction involving 2,4-dibromobenzoic acid [26]. Similar to the report by Yang et al. [24], trace amounts (1–5%) of water in ethanol was crucial for the reaction to succeed. The particle size of the carbonate base also affected the efficiency of the reaction; that is, milled K<sub>2</sub>CO<sub>3</sub> resulted in higher yields. On the other hand, the opposite site-selectivity was observed in the presence of phosphine ligands: a PPh<sub>3</sub>-based catalyst exclusively afforded C6-arylated isomer **8** (entry 2, Table 2). It is noteworthy that a less sterically bulky monodentate phosphine as a supporting ligand was ineffective in the case of 2,4-dibromobenzoic acid [26], yet exhibited excellent selectivity in this case. The catalyst systems described here could also be used to couple successfully a variety of electron-rich and electron-deficient boronic acids with the same site-selectivities (Scheme 5).

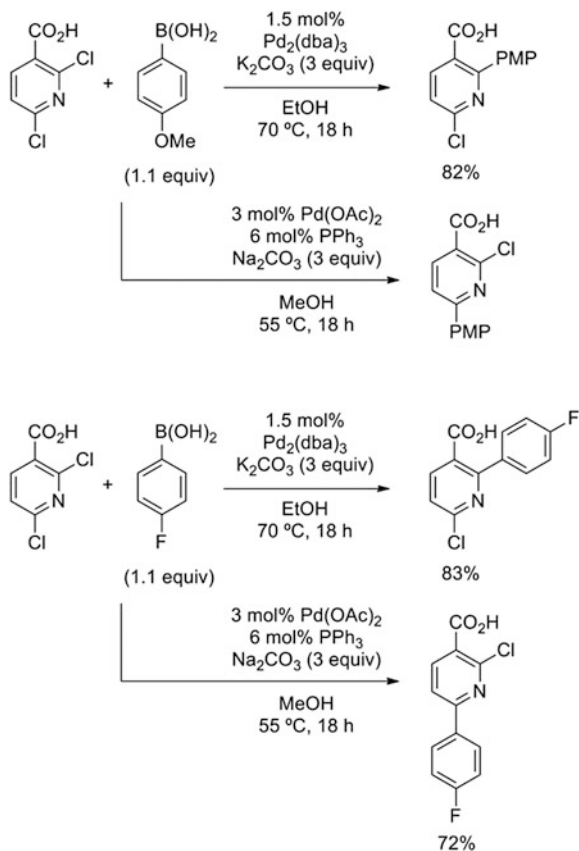
Dai, Chen, and coworkers reported another example of ligand-dependent site-selectivity switching in the Suzuki–Miyaura coupling of 3,5-dichloropyridazines [28]. Calculations of bond dissociation energies [15] predicted preferential reaction

**Table 2** Site-selective Suzuki–Miyaura coupling of 2,6-dichloronicotinic acid

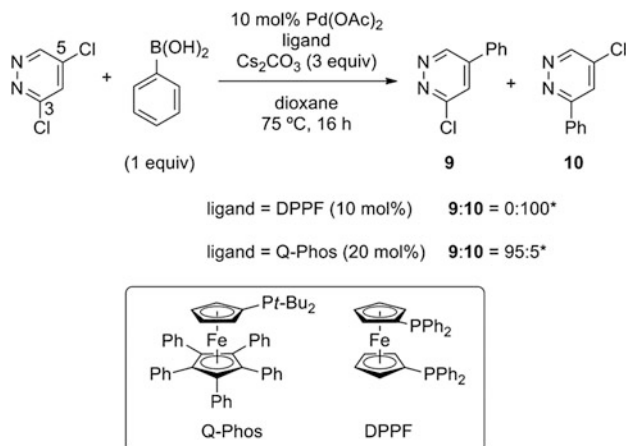
Entry	Catalyst (mol%)	Base	Solvent	Temp (°C)	Yield (%)	
					<b>7</b>	<b>8</b>
1	Pd <sub>2</sub> (dba) <sub>3</sub> (1.5)	K <sub>2</sub> CO <sub>3</sub>	EtOH	70	86	2
2	Pd(OAc) <sub>2</sub> –PPh <sub>3</sub> (3) <sup>a</sup>	Na <sub>2</sub> CO <sub>3</sub>	MeOH	55	0	86

<sup>a</sup>Pd/PPh<sub>3</sub> ratio was 1:2

**Scheme 5** Scope of site-selective Suzuki–Miyaura coupling of 2,6-dichloronicotinic acid



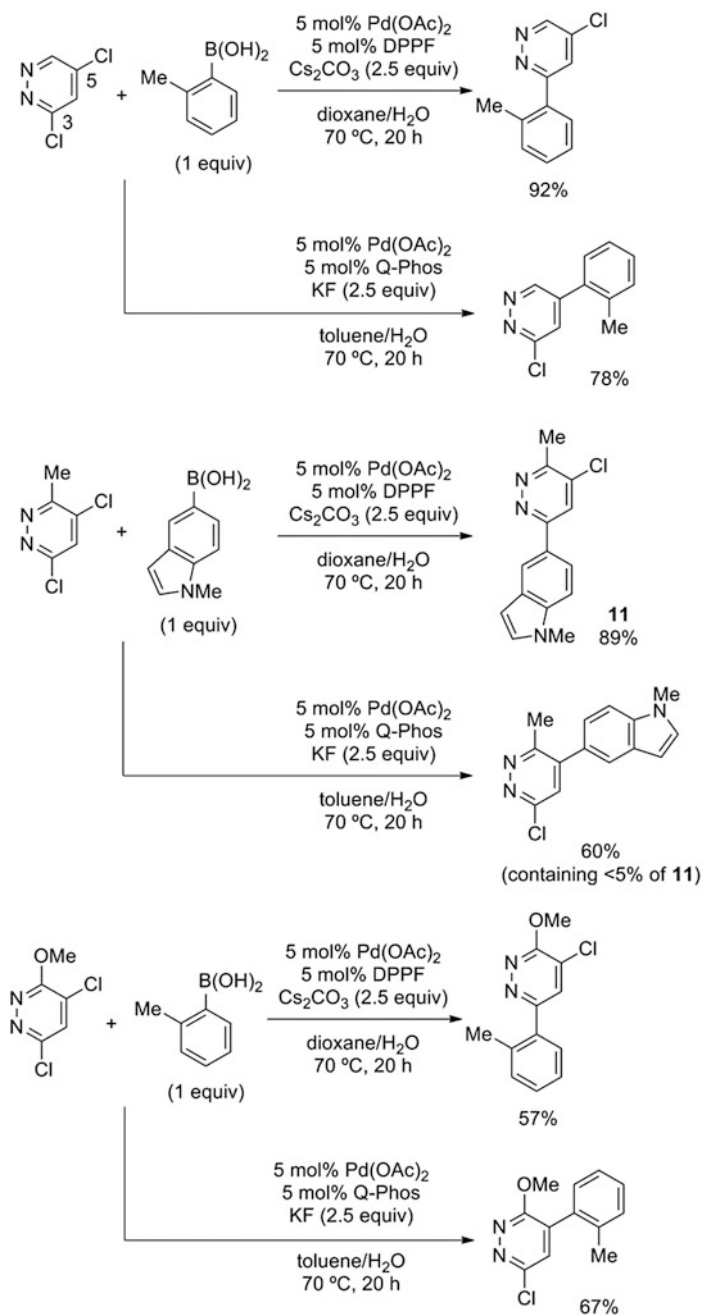
at the C3 position. The effect of the ancillary ligands was examined using a model reaction under the following conditions: 3,5-dichloropyridazine and phenylboronic acid as substrates, dioxane as the solvent, Pd(OAc)<sub>2</sub> as the catalyst, ligand, and Cs<sub>2</sub>CO<sub>3</sub> as the base. In accord with theoretical predictions, electron-deficient bidentate ligands facilitated the predominant formation of C3-coupled product **10**. In particular, DPPF served as the best ligand for C3-selective coupling and demonstrated complete selectivity (Scheme 6). Additional investigation demonstrated that reducing the amount of the base and employing dioxane/H<sub>2</sub>O as the solvent improved the yields (Scheme 7). Meanwhile, electron-rich monodentate ligands promoted the formation of C5-coupled product **9**, and the use of Q-Phos [29] resulted in the highest observed site-selectivity (Scheme 6). Further optimization of reaction conditions revealed that a 1:1 ratio of Pd/Q-Phos with KF as the base and toluene/H<sub>2</sub>O as the solvent provided the best results (Scheme 7). Under these optimized reactions conditions, various boronic acids were successfully coupled (Scheme 7), and both C3- and C5-coupled products could be synthesized in good yields.

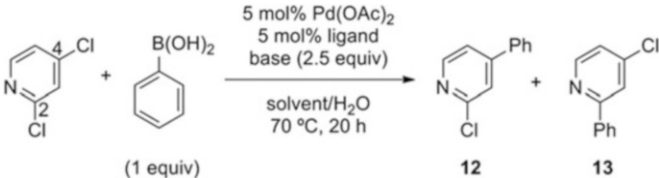


**Scheme 6** Site-selective Suzuki–Miyaura coupling of 3,5-dichloropyridazine. \*Yields are not indicated

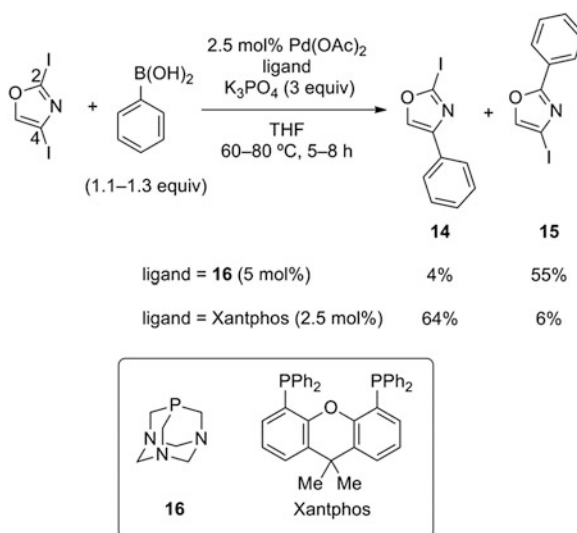
The catalyst systems described above were also employed in the site-selective Suzuki–Miyaura coupling of 2,4-dichloropyridine with phenylboronic acid (Table 3) [28]. Reactivity at the C2 position was predicted to be greater than at the C4 position according to the calculations of bond dissociation energies [15]. In accord with this theoretical prediction, the use of DPPF as an ancillary ligand exclusively gave 2-phenylated product **13** (entry 1, Table 3). On the other hand, a Q-Phos-based catalyst promoted the opposite site-selectivity to give 4-phenylated product **12** (entry 2, Table 3) with a 2.4:1 ratio of **12:13**. It should be noted that the site-selectivity could be switched in reactions employing a substrate without a directing substituent.

In another example, Strotman, Chobanian, and coworkers screened a series of phosphine ligands for the ligand-controlled, site-selective Suzuki–Miyaura coupling of 2,4-diiodooxazole with phenylboronic acid (Scheme 8) [30]. Their results revealed that the use of highly electron-rich phosphines was selective toward C2-phenylated product **15**, although some exceptions to this electronic trend exist. Among the electron-rich phosphines examined, 1,3,5-triaza-7-phosphaadamantane (**16**) afforded the highest C2-selectivity to yield product **15**. In the presence of electron-deficient ligands, however, coupling occurred predominantly at the C4-position. In particular, the use of Xantphos provided the highest selectivity toward C4-phenylated product **14** in 64% yield. Although the underlying mechanism is still unclear, the observed site-selectivities are presumably affected by steric and electronic factors. Other examples that showcase the aforementioned site-selectivities based on the phosphine ligand employed are shown in Scheme 9, featuring a variety of electron-deficient and electron-rich arylboronic acids.

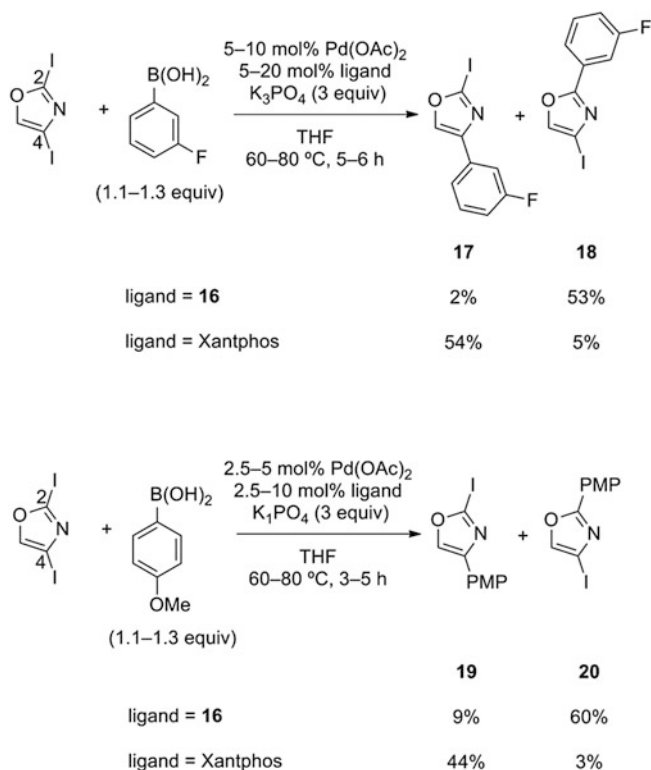
**Scheme 7** Examples of site-selective Suzuki–Miyaura coupling of 3,5-dichloropyridazines

**Table 3** Site-selective Suzuki–Miyaura coupling of 2,4-dichloropyridine


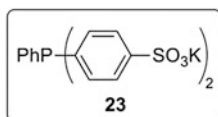
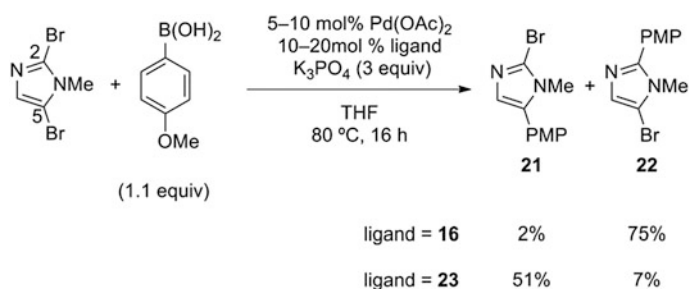
Entry	Ligand	Base	Solvent	Yield (%)	
				12	13
1	DPPF	Cs <sub>2</sub> CO <sub>3</sub>	Dioxane	0	90
2	Q-Phos	KF	Toluene	36	15

**Scheme 8** Site-selective Suzuki–Miyaura coupling of 2,4-diiodooxazole

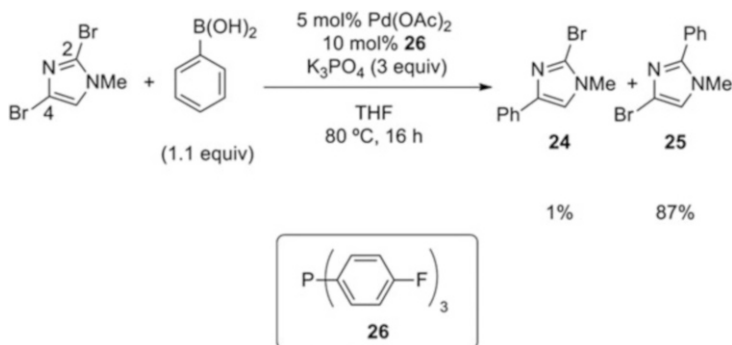
The same report also featured phosphine ligand effects on the site-selectivity in Suzuki–Miyaura coupling reactions of 2,5-dihalo-1-methylimidazoles [30]. For example, when 2,5-dibromo-1-methylimidazole was the substrate, the use of phosphine **16** promoted cross-coupling at the C2 position to give product **22**, whereas phosphine **23** promoted cross-coupling at the C5 position to give product **21** (Scheme 10). In the case of 2,5-diiodo-1-methylimidazole, phosphine **16** was also found to be effective in C2-selective cross-coupling. On the other hand, use of Xantphos afforded the C5-coupled product with high selectivity. C2-selectivity was also observed when electron-deficient phosphine **26** was employed in the reaction featuring 2,4-dibromo-1-methylimidazole as the substrate (Scheme 11), as well as when the Xantphos-based catalyst system was applied in the arylation of 2,4- and 2,5-dibromothiazoles (Scheme 12).



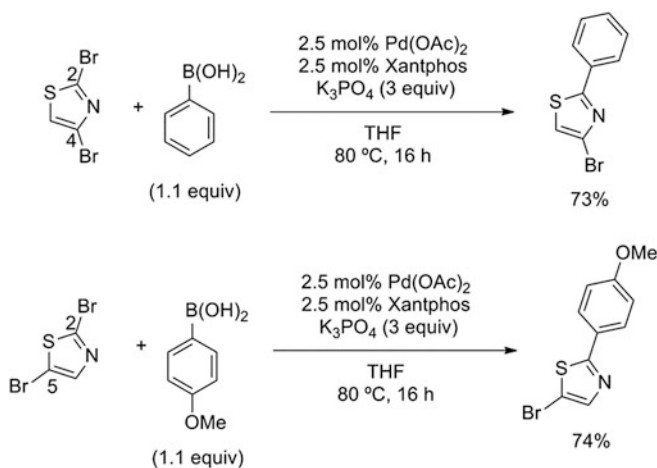
**Scheme 9** Examples of site-selective Suzuki–Miyaura coupling of 2,4-diiodooxazole



**Scheme 10** Site-selective Suzuki–Miyaura coupling of 2,5-dibromo-1-methylimidazole



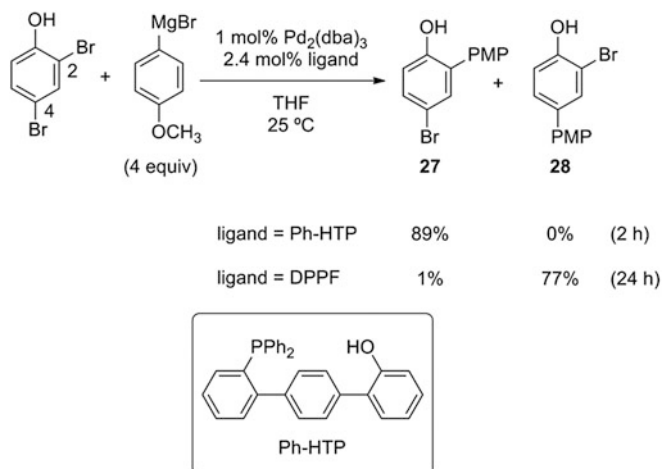
**Scheme 11** Site-selective Suzuki–Miyaura coupling of 2,4-dibromo-1-methylimidazole



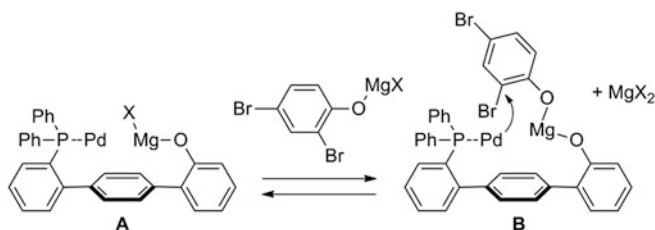
**Scheme 12** Site-selective Suzuki–Miyaura coupling of 2,4- and 2,5-dibromothiazoles

### 3 Kumada–Tamao–Corriu Coupling

The first example of ligand-controlled site-selective Kumada–Tamao–Corriu coupling was reported by Manabe and Ishikawa [31, 32] and employed dihaloarene substrates with Grignard reagents [33]. Treatment of 2,4-dibromophenol with excess Grignard reagent in the presence of  $\text{Pd}_2(\text{dba})_3$  and hydroxy-substituted terphenylphosphine (Ph-HTP) [34, 35] promoted coupling *ortho* to the hydroxy group to produce **27** with excellent selectivity (Scheme 13). Because electron-donating hydroxy groups, which are converted to more electron-donating oxido groups in the presence of a strong base, generally retard oxidative addition of *ortho* C–X bonds, it is remarkable that Ph-HTP accelerated this transformation to reach completion in 2 h. Replacing the Ph-HTP ligand with DPPF reversed the site-selectivity toward the *para* C–X bond to generate isomer **28**. It should be noted that



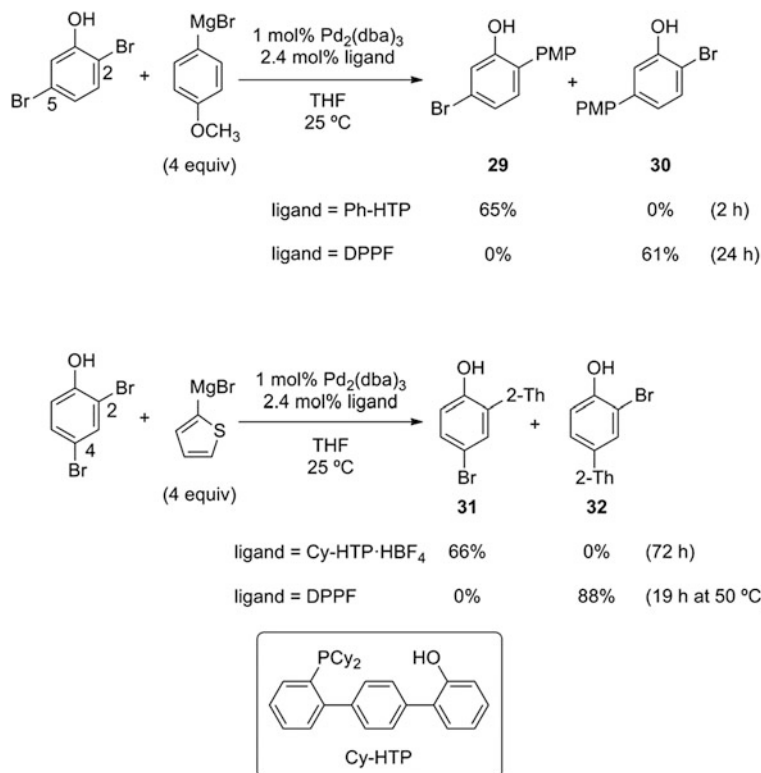
**Scheme 13** Site-selective Kumada–Tamao–Corriu coupling of 2,4-dibromophenol with a Grignard reagent



**Scheme 14** Mechanism to explain the *ortho*-selectivity in the site-selective cross-coupling using Ph-HTP

the di-cross-coupled product, in which both bromo groups were substituted with 4-methoxyphenyl groups, was obtained in just less than 5% yield despite the presence of excess Grignard reagent.

The *para*-selectivity exhibited in the DPPF-based catalytic system can be attributed to steric effects; that is, oxidative addition occurs preferentially at the less sterically hindered position *para* to the hydroxy group. On the other hand, this reasoning does not explain the high reactivity and exclusive *ortho*-selectivity of the Ph-HTP-based catalytic system. Rather, the key lies in the formation of an intermediate in which the hydroxy groups of the Ph-HTP ligand and the substrate are bridged, as shown in Scheme 14. A mechanism is proposed in which the Grignard reagent deprotonates the hydroxy group of palladium-bound Ph-HTP to form palladium/magnesium bimetallic species **A**. The magnesium oxido moiety of **A** subsequently binds the hydroxy group of the substrate, which also exists as a magnesium salt, to form magnesium bisphenoxide complex **B**. Consequently, the *ortho* bromo group of the substrate is brought closer to the palladium center, and,

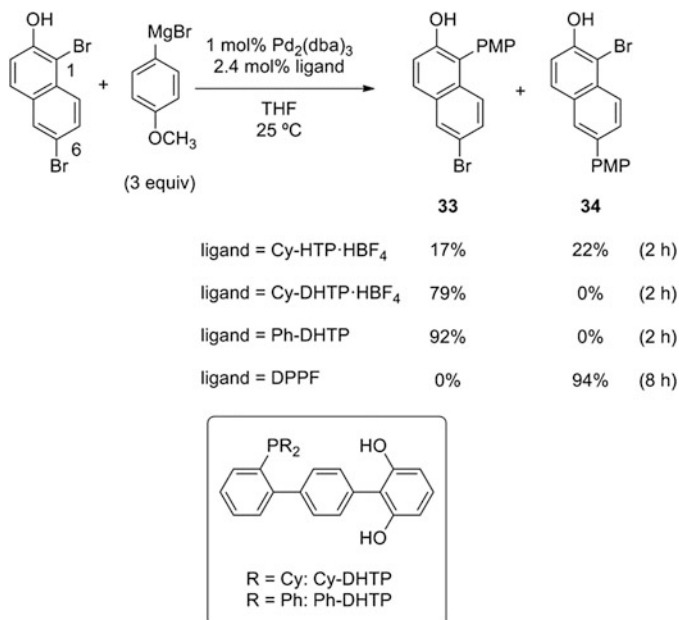


**Scheme 15** Examples of site-selective cross-coupling of dibromophenols with Grignard reagents

therefore, it is more prone to oxidative addition, which is the turnover-limiting and selectivity-determining step. It is worth mentioning that replacement of these hydroxy groups with methoxy groups resulted in reactions exhibiting poor yields and selectivity.

These catalyst systems were successfully applied to site-selective cross-coupling reactions of other substrates and Grignard reagents (Scheme 15). In the case of substrate 2,5-dibromophenol, Ph-HTP similarly promoted *ortho* coupling to give product **29** in good yields, whereas DPPF promoted *meta* coupling to give product **30**. It should be mentioned that the Ph-HTP-based catalyst enabled the reaction at the more sterically hindered and less electronically reactive (i.e., more electron-rich) position. Interestingly, the coupling reaction between 2,4-dibromophenol and 2-thienylmagnesium bromide afforded *ortho*-coupled product **31** in a very low yield for unknown reasons in the presence of the Ph-HTP-based catalyst. However, it was found that the use of the HBF<sub>4</sub> salt of Cy-HTP, which is the cyclohexyl analogue of Ph-HTP, dramatically improved the yield.

As demonstrated thus far, the use of hydroxyterphenylphosphines, Cy-HTP and Ph-HTP, promoted *ortho*-coupling of dibromophenols. However, catalytic systems

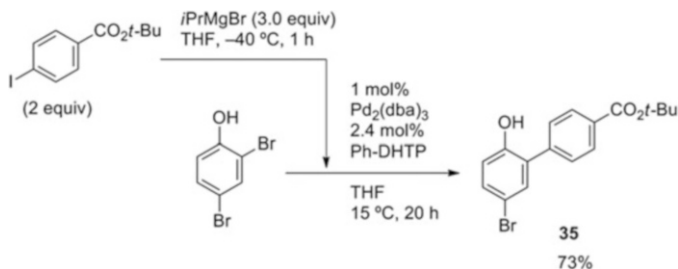


**Scheme 16** Site-selective cross-coupling of 1,6-dibromo-2-naphthol

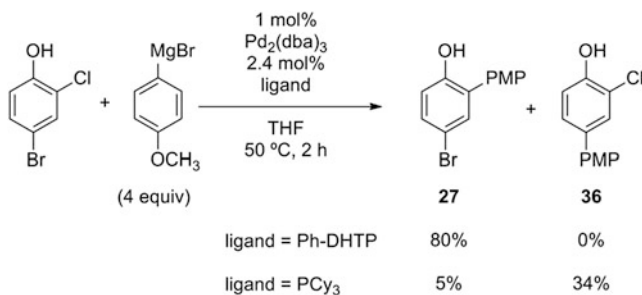
employing these ligands were only effective on a limited substrate scope. In subsequent reports by Manabe and Ishikawa, it was found that dihydroxyterphenylphosphines, Cy-DHTP and Ph-DHTP, greatly broadened the substrate scope and increased the *ortho*-selectivity of reactions [36, 37]. Representative examples are shown in Scheme 16. For instance, Cy-HTP hardly promoted any selectivity in the reaction of 1,6-dibromo-2-naphthol, whereas the use of Cy-DHTP resulted in exclusive *ortho*-selectivity to afford product **33** in good yields. Furthermore, Ph-DHTP effected complete selectivity to afford **33** in high yields. The effectiveness of DHTP over HTP is attributed to the increased chance for the magnesium phenoxide moiety to be situated close to the palladium because of the presence of two hydroxy groups in DHTP vs only one in HTP. Additionally, site-selectivity switching was observed with the use of DPPF to generate **34** in 94% yield.

Because the DHTP ligands remarkably accelerate the reaction rate at the position *ortho* to the hydroxy group, cross-coupling can be conducted at lower temperatures to increase the tolerance of additional functional groups such as esters. In the presence of Ph-DHTP, the reaction of 2,4-dibromophenol with a *tert*-butoxycarbonyl-substituted Grignard reagent, which was prepared from *tert*-butyl 4-iodobenzoate at  $-40\text{ }^{\circ}\text{C}$  according to a literature procedure [38], could be conducted at  $15\text{ }^{\circ}\text{C}$  to afford *ortho*-coupled product **35** in good yields (Scheme 17).

The high *ortho*-selectivity induced by Ph-DHTP was also demonstrated in the reaction featuring 4-bromo-2-chlorophenol as the substrate (Scheme 18). Interestingly, the *ortho*-selectivity of Ph-DHTP predominated over the intrinsic reactivity



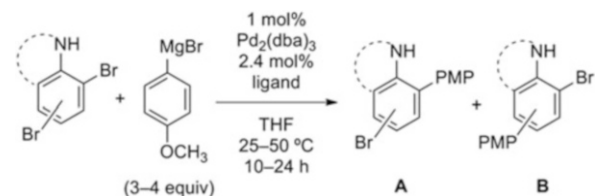
**Scheme 17** Site-selective cross-coupling of 2,4-dibromophenol with a *tert*-butoxycarbonyl-substituted Grignard reagent

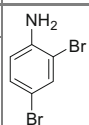
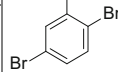
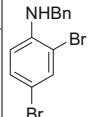
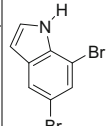
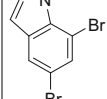


**Scheme 18** Site-selective cross-coupling of 4-bromo-2-chlorophenol

order of the halo groups (Br > Cl) to generate product **27** in good yields. In the presence of a simple phosphine, such as PCy<sub>3</sub>, the reaction occurred selectively at the *para*-bromo group instead.

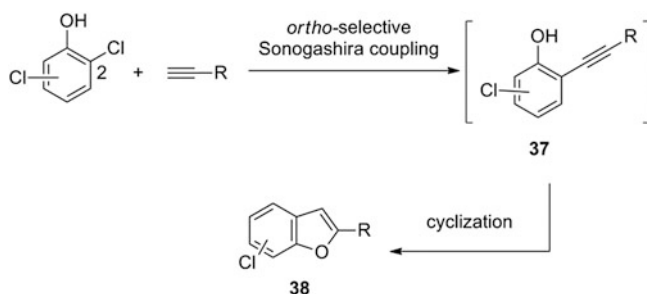
The *ortho*-selectivities of the catalytic systems described above for the reactions of dihalophenols were also observed in the reactions of the dibromoaniline analogues (Table 4) [36, 37]. That is, Ph-DHTP promoted cross-coupling at the position *ortho* to the NH functionality in dibromoaniline derivatives (entries 1, 3, and 5, Table 4) and in dibromoindole (entry 7, Table 4). These reactions are likely to occur by a mechanism similar to the one proposed for dibromophenol shown in Scheme 14. On the other hand, the use of DPPF resulted in poor yields and limited *para*-selectivity (entries 2, 4, 6, and 8, Table 4), for which the reasons are unclear.

**Table 4** Site-selective cross-coupling of dibromoaniline analogues


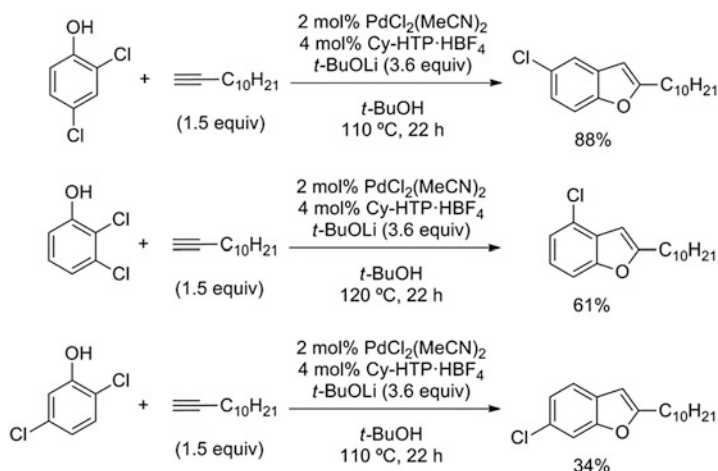
Entry	Substrate	Ligand	Yield (%)	
			A	B
1		Ph-DHTP	90	0
2		DPPF	9	15
3		Ph-HTP	63	0
4		DPPF	15	32
5		Ph-DHTP	70	0
6		DPPF	29	21
7		Ph-DHTP	81	0
8		DPPF	0	37

## 4 Sonogashira Coupling

Manabe and Wang reported one-pot syntheses of substituted chlorobenzo[*b*]furan derivatives via the *ortho*-selective Sonogashira coupling–cyclization sequence (Scheme 19) [39, 40] using dichlorophenols and terminal alkynes [41]. In this sequence, the first step is the *ortho*-selective Sonogashira coupling of dichlorophenol and terminal alkynes in the presence of a Pd-bound Cy-HTP catalyst and *t*-BuOLi as base to afford 2-alkynylchlorophenol **37**, followed by subsequent cyclization to afford chlorobenzo[*b*]furans **38** (Scheme 19). Various dichlorophenols could be successfully employed as substrates in this sequence (Scheme 20), and only small amounts (<10%) of di-coupled alkynylbenzo[*b*]furan were observed in these reactions. It should be noted that the Sonogashira coupling proceeded preferentially at the sterically hindered 2-position. In addition, the reaction was possible at a chloro group, which is less reactive than bromo or iodo groups. The high reactivity and *ortho*-selectivity are attributed to the formation of a heteroaggregate similar to the one shown in Scheme 14: the hydroxy groups of both the 2-dichlorophenol substrate and the Pd-bound Cy-HTP catalyst



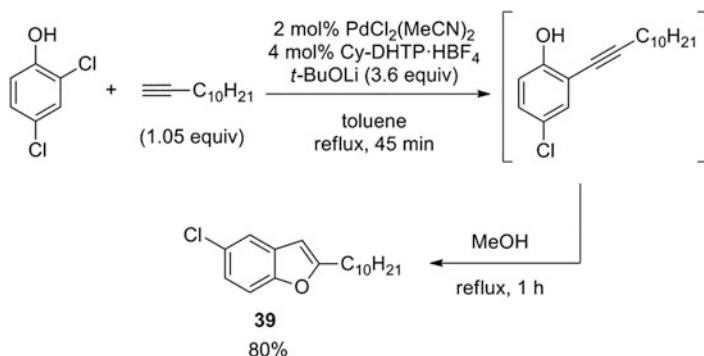
**Scheme 19** One-pot syntheses of substituted chlorobenzo[*b*]furan derivatives via the *ortho*-selective Sonogashira coupling–cyclization sequence



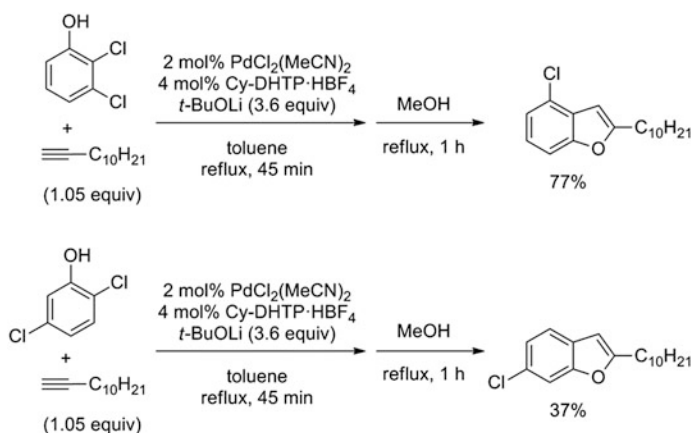
**Scheme 20** One-pot syntheses of substituted chlorobenzo[*b*]furan derivatives using Cy-HTP

are deprotonated by *t*-BuOLi and the resulting lithium-bridged phenoxides are arranged such that Pd is within the proximity of the *ortho* chloro group. Other phosphine ligands such as  $P(t\text{-Bu})_3$  and XPhos, which have often been used for cross-coupling of chloroarenes, gave poor results.

Manabe and coworkers further improved this protocol by changing the ligand from Cy-HTP to Cy-DHTP, which has also shown to be more effective in Kumada–Tamao–Corriu coupling [36]. For example, the Sonogashira coupling reaction between 2,4-dichlorophenol and 1-dodecyne in toluene was greatly accelerated in the presence of Cy-DHTP and reached completion in 45 min. Addition of MeOH as the cosolvent facilitated the subsequent cyclization step to afford the desired 5-chlorobenzo[*b*]furan **39** in good yields within 1 h (Scheme 21) [42]. Moreover, neither C4-alkynylated phenol nor the di-coupled product was observed. Because the use of *t*-BuOLi as a base was also crucial to achieve high reactivity and *ortho*-selectivity, the authors propose a mechanism similar to that proposed for Kumada–



**Scheme 21** One-pot syntheses of substituted chlorobenzo[*b*]furan using Cy-DHTP

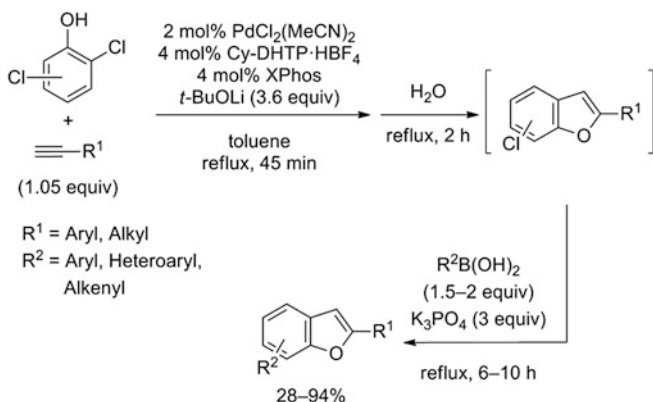


**Scheme 22** Examples of substituted chlorobenzo[*b*]furan synthesis from 2,3- and 2,5-dichlorophenols

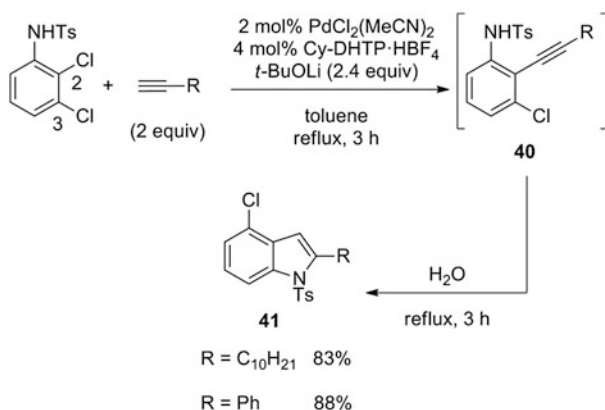
Tamao–Corriu coupling; the effectiveness of DHTP over HTP can also be attributed to the increased probability for the lithium phenoxide moiety to be situated close to the palladium.

Chlorobenzo[*b*]furan isomers with chloro groups at different positions were also synthesized using this protocol (Scheme 22). The reaction employing 2,3-dichlorophenol as the substrate afforded the corresponding 4-chlorobenzo[*b*]furan in good yields. However, the reaction employing 2,5-dichlorophenol exhibited poor reactivity, affording 6-chlorobenzo[*b*]furan in 37% yield along with by-products such as di-coupled 6-(1-dodecynyl)-2-decylbenzo[*b*]furan.

This transformation was applied in the sequential one-pot synthesis of disubstituted benzo[*b*]furan from dichlorophenol, terminal alkyne, and boronic acid [42]. In this case, water was used as the cosolvent to conduct successfully the Suzuki–Miyaura coupling reaction after chlorobenzo[*b*]furan formation (Scheme 23). The use of two ligands, Cy-DHTP and XPhos, was necessary to promote the formation



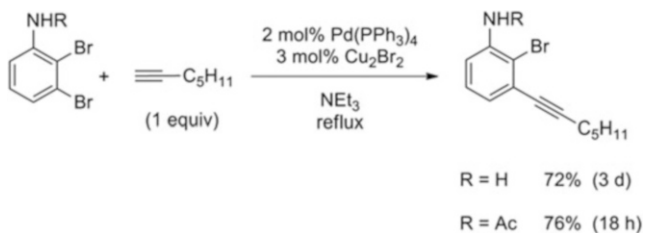
**Scheme 23** One-pot syntheses of disubstituted benzo[*b*]furans



**Scheme 24** One-pot syntheses of 4-chloroindole derivatives using Cy-DHTP

of the desired disubstituted product in good yields. The results of the mechanistic study suggest that the Pd–Cy-DHTP catalyst promotes the *ortho*-selective Sonogashira coupling step, whereas the Pd–XPhos catalyst accelerates the Suzuki–Miyaura coupling step.

According to a report by Manabe and Yamaguchi, the Pd–Cy-DHTP system also facilitates the one-pot synthesis of chloro-substituted indoles from dichloroaniline derivatives and terminal alkynes [43]. Under conditions similar to those employed for benzo[*b*]furan synthesis, Sonogashira coupling reactions between *N*-tosylated 2,3-dichloroaniline with terminal alkynes occurred selectively at the 2-chloro position, which is electronically deactivated and more sterically hindered. The resulting 2-alkynylaniline derivatives **40** underwent cyclization to afford the desired 4-chloroindoles **41** in high yields (Scheme 24). Neither 3-alkynylated isomers nor dialkynylated products were observed. The choice of the appropriate nitrogen-protecting group was also key to the success of the reaction, and the



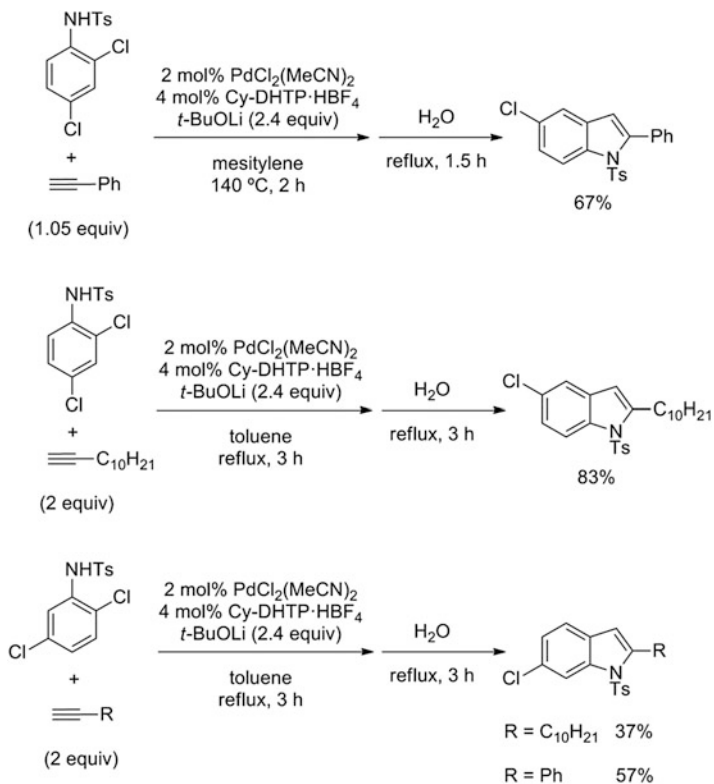
**Scheme 25** Examples of *meta*-selective Sonogashira coupling of 2,3-dibromoanilines

tosyl group was found to give the best result. In the case of *N*-acetylated substrates, Sonogashira coupling reactions also proceeded selectively at the *ortho*-position, yet the subsequent cyclization reaction did not complete.

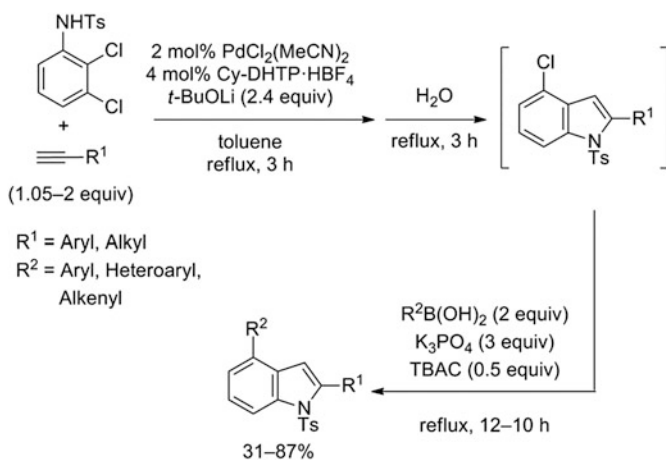
The *ortho*-selectivity promoted by Cy-DHTP is the opposite of that promoted by simple phosphines; Singh and Just previously reported that, in the presence of the latter, the use of Pd(PPh<sub>3</sub>)<sub>4</sub> as the catalyst promoted coupling exclusively at the less electron-rich *meta*-position in reactions between 2,3-dibromoaniline derivatives with 1-heptyne (Scheme 25) [12]. It is speculated that the high *ortho*-selectivity of Cy-DHTP can also be attributed to heteroaggregate formation between Cy-DHTP and the substrate, as similarly proposed for chlorobenzo[*b*]furan synthesis.

Indoles bearing chloro groups at different positions could also be synthesized by this method. *N*-Tosylated 2,4-dichloroaniline and 2,5-dichloroaniline were successfully converted into the corresponding 5-chloroindoles and 6-chloroindoles, respectively, in moderate to high yields (Scheme 26).

This protocol was also successfully applied to the one-pot synthesis of 4-substituted indoles, which are known to be challenging synthetic targets [43]. These reactions first produced 4-chloroindoles via a Sonogashira coupling–cyclization step, followed by a Suzuki–Miyaura coupling step with boronic acids to give the desired 4-substituted indoles in moderate to good yields (Scheme 27). In the Suzuki–Miyaura coupling, the use of a quaternary ammonium salt was crucial to promote the reaction. Among the quaternary ammonium salts screened, TBAC was found to be the most effective. The authors speculate that TBAC serves as a phase-transfer agent that transports boronic acids to the organic phase. It should be noted that the Pd–Cy-DHTP system catalyzed both the Sonogashira and Suzuki–Miyaura coupling reactions, whereas a two-ligand system consisting of both Cy-DHTP and XPhos, which was effective in benzo[*b*]furan synthesis [42], gave poor results.



**Scheme 26** One-pot syntheses of 5- and 6-chloroindole derivatives



**Scheme 27** One-pot syntheses of 2,4-disubstituted indole derivatives

## 5 Conclusion

Pd-catalyzed site-selective cross-coupling reactions demonstrate the influential role of ligands in transition metal catalysis. The reactions described in this review discuss efficient approaches to introduce various substituents at specific halo-substituted positions on (hetero)aromatic compounds. The commercial availability of a variety of dihalo-substituted starting materials makes site-selective cross-coupling reactions practical for the rapid production of diverse (hetero)arenes with multiple substituents. In all examples described here, the reactions proceeded successfully only on substrates containing hetero atoms, and this field of chemistry aims to include substrates without hetero atoms in the substrate scope.

At present, examples of ligand-controlled site-selective cross-coupling reactions are rather limited, and the origin of the site-selectivity is still unclear in many cases. However, the high *ortho*-selectivity of HTP and DHTP ligands, for example, is encouraging the design of new ligands that can promote different site-selectivities. Additional progress in the future of this exciting field is highly anticipated.

## References

1. Negishi E (2002) Handbook of organopalladium chemistry for organic synthesis. Wiley, New York
2. Tsuji J (2004) Palladium reagents and catalysts. Wiley, West Sussex
3. de Meijere A, Bräse S, Oestreich M (2014) Metal-catalyzed cross-coupling reactions and more. Wiley-VCH, Weinheim
4. Unrau CM, Campbell MG, Snieckus V (1992) Directed ortho metalation – Suzuki cross coupling connections. Convenient regiospecific routes to functionalized *m*- and *p*-teraryls and *m*-quinquearyls. *Tetrahedron Lett* 33:2773–2776
5. Goodby JW, Hird M, Lewis RA, Toyne KJ (1996) 5-Bromo-2-iodopyrimidine: a novel, useful intermediate in selective palladium-catalysed cross-coupling reactions for efficient convergent syntheses. *Chem Commun* 2719–2720
6. Heinrich ACJ, Thiedemann B, Gates PJ, Staubitz A (2013) Dual selectivity: electrophile and nucleophile selective cross-coupling reactions on a single aromatic substrate. *Org Lett* 15:4666–4669
7. Montoir D, Tonnerre A, Duflos M, Bazin MA (2014) Differential functionalization of 1,6-naphthyridin-2(1*H*)-ones through sequential one-pot Suzuki–Miyaura cross-couplings. *Eur J Org Chem* 1487–1495
8. Wang JR, Manabe K (2009) Transition-metal-catalyzed site-selective cross-coupling of di- and polyhalogenated compounds. *Synthesis* 1405–1427
9. Schröter S, Stock C, Bach T (2005) Regioselective cross-coupling reactions of multiple halogenated nitrogen-, oxygen-, and sulfur-containing heterocycles. *Tetrahedron* 61:2245–2267
10. Fairlamb IJS (2007) Regioselective (site-selective) functionalization of unsaturated halogenated nitrogen, oxygen and sulfur heterocycles by Pd-catalysed cross-couplings and direct arylation processes. *Chem Soc Rev* 36:1036–1045
11. Hassan Z, Patonay T, Langer P (2013) Regioselective Suzuki–Miyaura reactions of aromatic bis-triflates: electronic versus steric effects. *Synlett* 24:412–423

12. Singh R, Just G (1989) Rates and regioselectivities of the palladium-catalyzed ethynylation of substituted bromo- and dibromobenzenes. *J Org Chem* 54:4453–4457
13. Handy ST, Zhang Y (2006) A simple guide for predicting regioselectivity in the coupling of polyhaloheteroaromatics. *Chem Commun* 299–301
14. Legault CY, Garcia Y, Merlic CA, Houk KN (2007) Origin of regioselectivity in palladium-catalyzed cross-coupling reactions of polyhalogenated heterocycles. *J Am Chem Soc* 129:12664–12665
15. Garcia Y, Schoenebeck F, Legault CY, Merlic CA, Houk KN (2009) Theoretical bond dissociation energies of halo-heterocycles: trends and relationships to regioselectivity in palladium-catalyzed cross-coupling reactions. *J Am Chem Soc* 131:6632–6639
16. Herrebout WA, Nagels N, Verbeek S, van der Veken BJ, Maes BUW (2010) A DFT study of site-selectivity in oxidative addition reactions with Pd<sup>0</sup> complexes: the effect of an azine nitrogen and the use of different types of halogen atoms in the substrate. *Eur J Org Chem* 3152–3158
17. Manabe K, Yamaguchi M (2014) Catalyst-controlled site-selectivity switching in Pd-catalyzed cross-coupling of dihaloarenes. *Catalysts* 4:307–320
18. Newman SG, Lautens M (2010) The role of reversible oxidative addition in selective palladium(0)-catalyzed intramolecular cross-couplings of polyhalogenated substrates: synthesis of brominated indoles. *J Am Chem Soc* 132:11416–11417
19. Hayashi T (2002) Palladium-catalyzed asymmetric cross-coupling. In: Negishi E, de Meijere A (eds) *Handbook of organopalladium chemistry for organic synthesis*, vol 1. Wiley, New York, pp p791–806, Chapter III.2.16
20. Kamikawa T, Hayashi T (1997) Control of reactive site in palladium-catalyzed Grignard cross-coupling of arenes containing both bromide and triflate. *Tetrahedron Lett* 38:7087–7090
21. Littke AF, Dai C, Fu GC (2000) Versatile catalysts for the Suzuki cross-coupling of arylboronic acids with aryl and vinyl halides and triflates under mild conditions. *J Am Chem Soc* 122:4020–4028
22. Ashcroft CP, Fussell SJ, Wilford K (2013) Catalyst controlled regioselective Suzuki cross-coupling of 2-(4-bromophenyl)-5-chloropyrazine. *Tetrahedron Lett* 54:4529–4532
23. Suzuki A (2011) Cross-coupling reactions of organoboranes: an easy way to construct C–C bonds (Nobel lecture). *Angew Chem Int Ed* 50:6722–6737
24. Yang W, Wang Y, Corte JR (2003) Efficient synthesis of 2-aryl-6-chloronicotinamides via XPd<sub>2</sub>-catalyzed regioselective Suzuki coupling. *Org Lett* 5:3131–3134
25. Li GY (2002) Catalysis using phosphine oxide and phosphine sulfide complexes with Pd and Ni for the synthesis of biaryls and arylamines. *Int Patent WO2002000574A2*, 3 Jan 2002
26. Houpis IN, Huang C, Nettekoven U, Chen JG, Liu R, Canters M (2008) Carboxylate directed cross-coupling reactions in the synthesis of trisubstituted benzoic acids. *Org Lett* 10:5601–5604
27. Houpis IN, Liu R, Wu Y, Yuan Y, Wang Y, Nettekoven U (2010) Regioselective cross-coupling reactions of boronic acids with dihalo heterocycles. *J Org Chem* 75:6965–6968
28. Dai X, Chen Y, Garrell S, Liu H, Zhang LK, Palani A, Hughes G, Nargun R (2013) Ligand-dependent site-selective Suzuki cross-coupling of 3,5-dichloropyridazines. *J Org Chem* 78:758–7763
29. Shelby Q, Kataoka N, Mann G, Hartwig J (2000) Unusual in situ ligand modification to generate a catalyst for room temperature aromatic C–O bond formation. *J Am Chem Soc* 122:10718–10719
30. Strotman NA, Chobanian HR, He J, Guo Y, Dormer PG, Jones CM, Steves JE (2010) Catalyst-controlled regioselective Suzuki couplings at both positions of dihaloimidazoles, dihalooxazoles, and dihalothiazoles. *J Org Chem* 75:1733–1739
31. Tamao K, Sumitani K, Kumada M (1972) Selective carbon–carbon bond formation by cross-coupling of Grignard reagents with organic halides. Catalysis by nickel–phosphine complexes. *J Am Chem Soc* 94:4374–4376

32. Corriu RJP, Masse JP (1972) Activation of Grignard reagents by transition-metal complexes. A new and simple synthesis of *trans*-stilbenes and polyphenyls. *J Chem Soc Chem Commun* 144a
33. Ishikawa S, Manabe K (2007) *Ortho*-selective cross coupling of dibromophenols and dibromoanilines with Grignard reagents in the presence of palladium catalysts bearing hydroxylated oligoarene-type phosphine. *Chem Lett* 36:1304–1305
34. Ishikawa S, Manabe K (2007) Oligoarene strategy for catalyst development hydroxylated oligoarene-type phosphines for palladium-catalyzed cross coupling. *Chem Lett* 36:1302–1303
35. Ishikawa S, Manabe K (2010) Synthesis of hydroxylated oligoarene-type phosphines by a repetitive two-step method. *Tetrahedron* 66:297–303
36. Ishikawa S, Manabe K (2010) DHTP ligands for the highly *ortho*-selective, palladium-catalyzed cross-coupling of dihaloarenes with Grignard reagents: a conformational approach for catalyst improvement. *Angew Chem Int Ed* 49:772–775
37. Ishikawa S, Manabe K (2011) Hydroxylated terphenylphosphine ligands for palladium-catalyzed *ortho*-selective cross-coupling of dibromophenols, dibromoanilines, and their congeners with Grignard reagents. *Tetrahedron* 67:10156–10163
38. Boymond L, Rottländer M, Cahiez G, Knochel P (1998) Preparation of highly functionalized Grignard reagents by an iodine–magnesium exchange reaction and its application in solid-phase synthesis. *Angew Chem Int Ed* 37:1701–1703
39. Heravi MM, Sadjadi S (2009) Recent advances in the application of the Sonogashira method in the synthesis of heterocyclic compounds. *Tetrahedron* 65:7761–7775
40. Najera C, Chinchilla R (2007) The Sonogashira reaction: a booming methodology in synthetic organic chemistry. *Chem Rev* 107:874–922
41. Wang JR, Manabe K (2010) Hydroxyterphenylphosphine–palladium catalyst for benzo[*b*]furan synthesis from 2-chlorophenols bifunctional ligand strategy for cross-coupling of chloroarenes. *J Org Chem* 75:5340–5342
42. Yamaguchi M, Katsumata H, Manabe K (2013) One-pot synthesis of substituted benzo[*b*]furans from mono- and dichlorophenols using palladium catalysts bearing dihydroxyterphenylphosphine. *J Org Chem* 78:9270–9281
43. Yamaguchi M, Manabe K (2014) One-pot synthesis of 2,4-disubstituted indoles from *N*-tosyl-2,3-dichloroaniline using palladium–dihydroxyterphenylphosphine catalyst. *Org Lett* 16:2386–2389

# Recent Advances in the Selective Oxidation of Alkyl C–H Bonds Catalyzed by Iron Coordination Complexes

Mercè Canta, Mònica Rodríguez, and Miquel Costas

**Abstract** Selective and stereoretentive oxidation of alkyl C–H bonds has been described over the last decade by employing biologically inspired iron coordination complexes as catalysts and hydrogen peroxide as oxidant. Examples of catalyst dependent C–H site selectivity have started to appear. The current paper describes an account of these findings.

**Keywords** Alkyl C–H oxidation · Aminopyridine ligands · Bioinspired catalysis · Hydrogen peroxide · Iron coordination complexes · Nonheme oxygenases · Selectivity

## Contents

1	Importance and Scope of Alkyl C–H Oxidation Reactions .....	28
2	Precedents for Selective C–H Hydroxylations at Non-Heme Iron-Dependent Enzymes .....	29
2.1	Biological Precedents .....	29
3	Iron Coordination Complexes as Catalysts for Selective C–H Bond Oxidation .....	31
4	Tuning the Selectivity in Alkane Oxidation Reactions .....	35
4.1	Predictably Selective Oxidations and Selectivity Patterns .....	35
4.2	Novel Selectivity for Alkane Oxidation Reactions .....	40
5	Novel Reactivity on C–H Oxidation .....	51
5.1	$\alpha$ -Oxygenation .....	51
5.2	Desaturation .....	51
	References .....	53

---

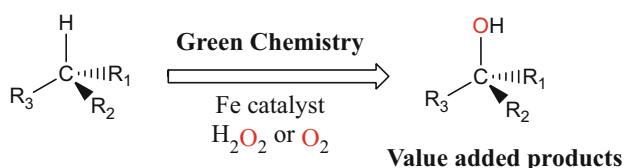
M. Canta, M. Rodríguez, and M. Costas (✉)

Departament de Química i Institut de Química Computacional i Catàlisi, Universitat de Girona, Facultat de Ciències, Campus de Montilivi, 17071 Girona, Catalonia, Spain  
e-mail: [Miquel.costas@udg.edu](mailto:Miquel.costas@udg.edu)

# 1 Importance and Scope of Alkyl C–H Oxidation Reactions

The functionalization of nonactivated alkyl C–H groups is a reaction of general interest and significance which remains as a challenge for modern chemistry [1–5]. Alkanes are convenient feedstocks because they are abundant and can be extracted from crude oil and natural gas. The catalytic oxidation of alkyl C–H groups is also highly important in organic synthesis because oxidized alkane frameworks are ubiquitous in organic molecules of industrial and biological relevance. Therefore the construction of such structures is of fundamental interest in modern organic synthesis. However, selective oxidation of alkyl C–H bonds in an environmentally sustainable manner remains as one of the main current challenges in organic synthetic chemistry (Scheme 1).

Although the oxidation of C–H groups is thermodynamically favorable, it also has large activation barriers that translate into their characteristic inert nature against most reagents. This lack of reactivity is because C–H bonds are strong, non-polarized, and localized, with a highly stabilized HOMO and a high lying LUMO. Therefore highly reactive oxidizing reagents are required to overcome these barriers, and this most commonly compromises selectivity [6, 7]. The main difficulties are (1) to control chemoselectivity, i.e., to direct the oxidation toward C–H groups in the presence of other functionalities in the molecule, usually more reactive, (2) to stop the functionalization at the desired oxidation state, thus avoiding undesired over-oxidized products, and (3) to discriminate among the various C–H groups present in a substrate, because most organic molecules contain multiple C–H sites with only slight electronic and structural differences. Given these difficulties, even though oxygenated alkyl frameworks are basic constituents of the majority of organic molecules, selective C–H oxidation is very rarely considered in synthetic planning. Instead, already oxygenated small molecules are employed in the building up of more complex structures, relying on protecting and deprotecting sequences [6–9]. On top of that, it is becoming increasingly necessary for chemical transformations to be carried out in a sustainable manner, using non-toxic and available reagents that could generate minimum waste (Scheme 1). In this regard, selective C–H oxidation is envisioned as a very powerful tool in organic synthesis because it converts ubiquitous alkyl moieties into functional groups. This translates into the rapid built-up of molecular complexity from



**Scheme 1** Selective Oxidation of alkane hydrocarbons into value added product through Fe-catalyzed reactions as example of a challenging and environmentally sustainable transformation

inert functionalities, limiting the use of protecting groups, and enabling new and shorter synthetic strategies [10–13].

The development of catalysts for C–H oxidation is regarded as a highly appealing approach. These catalysts are expected to enable mild reaction conditions and introduce distinct chemo- and regioselectivities based on their electronic and steric properties, as well as their ability to engage in weak and reversible noncovalent interactions with the substrate [14]. Toward this endeavor, nature constitutes an excellent inspirational source. A number of metalloenzymes exist that perform selective C–H oxidation with high levels of chemo-, regio-, and stereoselectivity, and iron constitutes the most common metal source found in these metalloenzymes. This prominent role of iron in biological C–H oxidative transformations in combination with the availability and lack of toxicity of this element, has made this metal very attractive in synthetic catalyst development [15, 16]. Iron porphyrins have been traditionally regarded as powerful oxidation catalysts but most recently iron coordination complexes have emerged as promising and convenient alternatives with improved catalytic performance in terms of product yields and selectivities [14]. Major findings and challenges of the topic are discussed below.

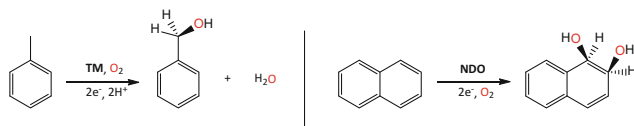
## 2 Precedents for Selective C–H Hydroxylations at Non-Heme Iron-Dependent Enzymes

### 2.1 *Biological Precedents*

Iron is the metal ion of choice for many biological oxidations because of its natural abundance in the geosphere, its inherent electronic properties, and its accessible redox potentials [17]. It is a ubiquitous element in living systems and its versatility is unique. The high availability of this metal and its various attainable oxidation states has led to the evolutionary selection of iron in many life processes. Iron-containing biological molecules play important roles in biologically essential transformations, such as biological oxidations and oxygen transport [18]. There is a myriad of remarkable transition-metal-dependent oxidative enzymes capable of activating dioxygen and catalyzing the selective oxidation of C–H bonds (alkane hydroxylation) or C=C groups (olefin epoxidation or *cis*-dihydroxylation) [19–24].

#### 2.1.1 Rieske Oxygenases

In the past 15–20 years, several studies have been performed on mononuclear non-heme iron(II) enzymes. Among them, Rieske oxygenases constitute a relevant and paradigmatic example of mononuclear non-heme iron(II) proteins involved in O<sub>2</sub> activation reactions. Their efficiency and versatility are even greater than those of the related heme-containing Cyt P450, being able to catalyze stereoselective



**Scheme 2** Benzylic hydroxylation and aromatic *cis*-dihydroxylation reactions catalyzed by Rieske oxygenases (toluene monooxygenase and naphthalene-1,2-dioxygenase, respectively)

benzylic hydroxylation and *cis*-dihydroxylation reactions (Scheme 2), among other reactions. They are also the only enzymes among both heme and non-heme iron enzymes capable of stereospecific and enantioselective *cis*-dihydroxylation of arene and olefin double bonds, which are reactions of high biotechnological interest as they initiate the biodegradation of aromatics in the soil [24–31].

Rieske oxygenases are part of a superfamily of enzymes that share a characteristic structure consisting of an oxygenase component (a mononuclear non-heme iron(II) high spin center containing a 2-His-1-carboxylate facial triad motif in the active site) [31–33]. Besides, the active site contains a reductase component (an Fe<sub>2</sub>-S<sub>2</sub> Rieske center) that delivers electrons from NAD(P)H to the oxygenase center [34].

Naphthalene-1,2-dioxygenase (NDO) is one of the best studied examples of the Rieske dioxygenases family, and a catalytic cycle has been proposed [26, 34]. Studies on crystals of NDO exposed to O<sub>2</sub> indicate that a side-on-bound peroxy (or -hydroperoxy)-iron(III) species is the last detectable intermediate before substrate oxidation occurs [35]. In this reaction, both O<sub>2</sub> atoms are incorporated in the *syn*-diol product. Interestingly, labeling studies also show H<sub>2</sub><sup>18</sup>O incorporation into the *syn*-diol product, suggesting that the O–O bond heterolytic cleavage can generate a putative Fe<sup>V</sup>=O species before substrate attack, although direct evidence for this high-valent oxo species has yet to be obtained [26, 34, 36]. Moreover, phthalate dioxygenase, an enzyme of the Rieske oxygenase family, can elicit catalytic chemistry when H<sub>2</sub>O<sub>2</sub> is used as oxidant thus resembling the peroxide shunt of Cyt P450 [37].

Rieske oxygenases can be naïvely taken as a precedent that simple non-heme iron sites, bound to nitrogen and oxygen based ligands, can form oxidizing species that attack oxidatively robust functionalities via mechanisms that depart from Fenton transformations, and, because of that, this family of enzymes serves to inspire development of oxidation catalysts based on simple iron coordination complexes associated with nitrogen and oxygen ligands.

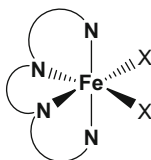
Convincing evidence for a metal-based mechanism in non-heme catalyzed C–H oxidation reactions with a synthetic catalyst appeared in 1997 in work by Que and co-workers [38] where a family of tpa-based (tpa = tris-(2-pyridylmethyl)amine) iron(II) complexes were investigated as stereospecific C–H oxidation catalysts using H<sub>2</sub>O<sub>2</sub> as oxidant. Beyond their mechanistic significance, these findings were key for the future development of this chemistry with a synthetic aim, because a metal-based mechanism bears implicitly the possibility of modulating the

reactivity and thus the selectivity of the iron-based species that attack the C–H bond by means of ligand design. Instead, C–H breaking reactions initiated by hydroxyl or alkoxy radicals are devoid of this control. Therefore, the bona fide settling on an iron-based C–H functionalization mechanism is the basis of the following past and present efforts to develop non-heme iron complexes as selective C–H oxidation catalysts [14, 17, 39].

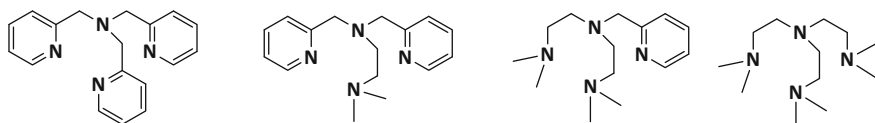
### 3 Iron Coordination Complexes as Catalysts for Selective C–H Bond Oxidation

Mononuclear non-heme iron(II) complexes containing *N*-based ligands, especially those containing pyridine heterocycles, have been extensively explored in metal-catalyzed transformations over the last decade [14, 17, 39, 40]. A particularly relevant aspect of the use of *N*-based ligands is that they led to the discovery of very selective C–H and C=C oxidation iron catalysts, and synthetically useful methodologies have also emerged from the use of these complexes. A very challenging aspect of this chemistry is that the catalytic activity of a complex is dramatically dependent on its ligand structure; therefore accurate design of the ligand is necessary yet not obvious [41]. The vast majority of iron complexes that can mediate stereospecific hydroxylation of alkanes contain an Fe<sup>II</sup> center and tetradentate *N*-based ligands that leave two coordination positions vacant in a *cis* relative position that are occupied by weakly bound ligands (Scheme 3). The lability of these positions is a key aspect to ensure a fast reaction with the oxidant. Tripodal and linear families of complexes bearing tetradentate ligands have mostly been studied in the oxidation of alkanes employing H<sub>2</sub>O<sub>2</sub> as oxidant.

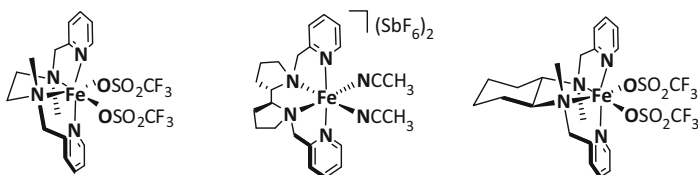
An illustrative example of tripodal ligand is tpa. As mentioned above, the combination of [Fe(tpa)(CH<sub>3</sub>CN)<sub>2</sub>](ClO<sub>4</sub>)<sub>2</sub> with H<sub>2</sub>O<sub>2</sub> proved to oxidize alkanes effectively. The oxidation is highly stereospecific (>99% retention of configuration for the oxidation of *cis*- and *trans*-1,2-dimethylcyclohexane (DMCH)), this being the first example of non-heme iron catalysts capable of stereospecific alkane oxidation [42, 43]. Studies with [Fe(OTf)<sub>2</sub>(tpa)] (OTf = trifluoromethylsulfonate anion) and derivatives where pyridine heterocycles were later systematically replaced by aliphatic amines (Scheme 4) were performed by Britovsek and coworkers [44]. These studies showed that at least two pyridine donors were needed



**Scheme 3** Representation of N<sub>4</sub>-tetradentate iron complexes with two *cis* coordination positions occupied by labile ligands (X)



**Scheme 4** Tpa-based ligands introducing aliphatic amines used for the preparation of Fe<sup>II</sup> complexes



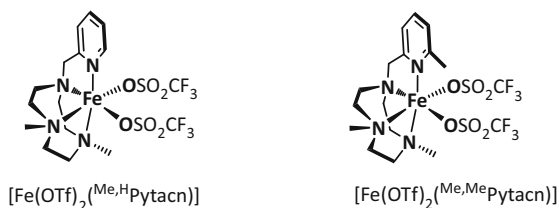
**Scheme 5** Structure of [Fe(OTf)<sub>2</sub>(mep)], [Fe(pdp)(CH<sub>3</sub>CN)<sub>2</sub>](SbF<sub>6</sub>)<sub>2</sub>, and [Fe(OTf)<sub>2</sub>(mcp)] catalysts

in the ligand to show reactivity distinct from Fenton-type chemistry, and are essential for high catalytic activity and selectivity in these systems.

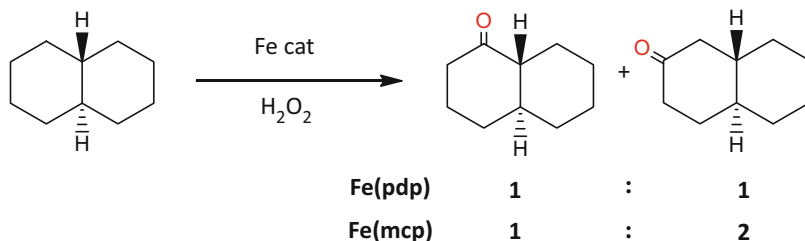
An arguably more interesting catalyst is [Fe(OTf)<sub>2</sub>(mep)] (mep = *N,N'*-dimethyl-*N,N'*-bis(2-pyridylmethyl)-ethane-1,2-diamine, Scheme 5) [43, 45, 46], which proved to be more efficient in stereospecific alkane hydroxylation than its tpa analogue but still worked under conditions of large excess of substrate [42–44, 47, 48]. Interestingly, Bermejo and coworkers recently reported the selective oxidation of steroids and terpenoids using [Fe(OTf)<sub>2</sub>(mep)] [49, 50]. In this case, substrate limiting conditions were employed, and synthetically useful yields (up to 70%) were achieved.

Another interesting ligand platform which has been extensively studied is the Pytacn (Pytacn = *N*-methyl-2-pyridyl *N,N''*-dialkylsubstituted triazacyclononane) family (Scheme 6) [51]. [Fe(OTf)<sub>2</sub>(<sup>Me,H</sup>Pytacn)] proved to be capable of mediating the hydroxylation of alkanes with retention of configuration [51–53]. Substitution on the N atoms of the triazamacrocycle and on the pyridine 6th position were studied in order to explore steric effects in catalytic oxidations. The 6-methyl pyridine substituted [Fe(OTf)<sub>2</sub>(<sup>Me,Me</sup>Pytacn)] showed unusually high efficiency in the stereospecific oxidation of alkanes and alkenes with H<sub>2</sub>O<sub>2</sub>. This catalyst was also described to mediate the oxidation of alkyl C–H bonds with product yields that may be amenable for synthetic purposes [54]. Besides its high activity, this catalyst also exhibits enhanced selectivity toward methylene sites.

A major breakthrough in the field was introduced by White and Chen [55] in 2007, reporting the predictably selective oxidation of C–H bonds for the synthesis of complex molecules employing H<sub>2</sub>O<sub>2</sub> as oxidant and a non-heme iron catalyst. In this case the catalyst employed was [Fe(pdp)(CH<sub>3</sub>CN)<sub>2</sub>](SbF<sub>6</sub>)<sub>2</sub> (pdp = *N,N'*-bis(2-pyridylmethyl)-2,2'-bipyrrrolidine), a coordination complex that bears a relatively bulky tetradentate ligand framework (Scheme 5). The C–H site of oxidation with this system could be predicted in complex organic molecules on the basis of



**Scheme 6** Structure of relevant Pytaccin-based complexes for C–H oxidation reactions

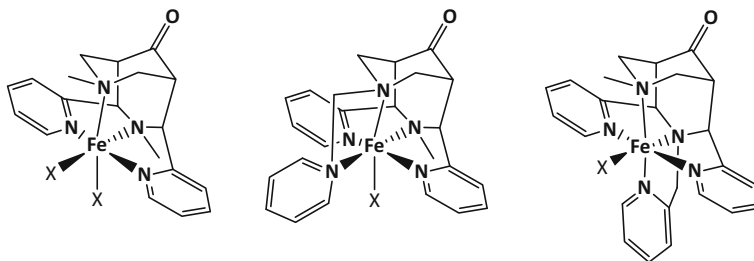


**Scheme 7** Selectivity for methylenic sites of  $[\text{Fe}(\text{OTf})_2(\text{pdp})]$  and  $[\text{Fe}(\text{OTf})_2(\text{mcp})]$  in the oxidation of *trans*-decaline

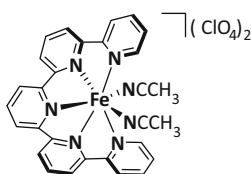
the electronic and steric environment of the C–H bonds. Additionally, when a carboxylic acid functionality was present, this group could direct oxidations toward five-membered ring lactone formation. Three years later, these authors used the same catalyst to study the effect of the combination of different effects on dictating selectivity in methylene oxidations [56]. The authors reported the site-selective oxidation of nonactivated secondary C–H bonds to afford monooxygenated products in preparative useful yields without the use of directing or activating groups. For natural products, useful levels of chemo-, site-, and diastereoselective methylene oxidations were obtained.

More recent work showed that  $[\text{Fe}(\text{OTf})_2(\text{mcp})]$  (Scheme 5), based on the cyclohexyldiamine backbone is a convenient catalyst for preparative C–H oxidation reactions [57]. Use of the cyclohexyldiamine instead of the bipyrrrolidine makes the iron catalyst more easily obtained in large amounts. C–H site selectivity with this catalyst responds to electronic and stereoelectronic effects as  $[\text{Fe}(\text{pdp})(\text{CH}_3\text{CN})_2](\text{SbF}_6)_2$ , but the former appears to be more selective for discriminating among multiple methylenic sites. For example,  $[\text{Fe}(\text{OTf})_2(\text{mep})]$  and  $[\text{Fe}(\text{pdp})(\text{CH}_3\text{CN})_2](\text{SbF}_6)_2$  oxidize the two distinct methylenic sites of *trans*-decaline, the second complex yields a roughly 1:1 ratio, whereas  $[\text{Fe}(\text{OTf})_2(\text{mcp})]$  yields a 2:1 ratio in favor of the sterically less demanding methylene site (Scheme 7).

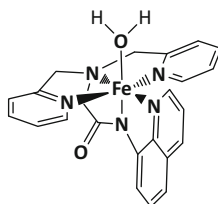
Comba and coworkers [58] described a set of rigid pentadentate iron complexes based on bispidine derivatives (Scheme 8) for the catalytic oxidation of cyclohexane, obtaining reasonably good turnover numbers (TON) (up to 34 TON).



**Scheme 8** Bispidine-based catalysts, where X is solvent molecule or oxo group



**Scheme 9** Structure of  $[\text{Fe}(\text{qpy})](\text{ClO}_4)_2$  catalyst reported for the oxidation of cyclohexane



**Scheme 10** Structure of  $[\text{Fe}^{\text{III}}(\text{dpaq})(\text{H}_2\text{O})]^{2+}$  catalyst

A different approach was proposed by Che and coworkers [59], who used  $[\text{Fe}(\text{qpy})](\text{ClO}_4)_2$  ( $\text{qpy} = 2, 2' : 6', 2'' : 6'', 2''' : 6''', 2''''$ -quinquepyridine, Scheme 9) in combination with Oxone for the oxidation of cyclohexane, obtaining modest TON of products. Activated substrates were tested affording up to 85% yield for the oxidation of xanthene.

Finally, Hitomi et al. recently presented a catalytic system based on the pentadentate H-dpaq ligand ( $\text{dpaq} = 2$ -[bis-(pyridine)-2-ylmethyl]amino-*N*-quinolin-8-yl-acetamidate, Scheme 10) [60]. The complex  $[\text{Fe}^{\text{III}}(\text{dpaq})(\text{H}_2\text{O})]^{2+}$  was used in combination with various oxidants to show a metal-based oxidation mechanism suggested by the high alcohol/ketone (A/K) ratios obtained in the oxidation of cyclohexane, regardless of the oxidant employed. This catalyst presented a performance virtually identical to that of  $[\text{Fe}(\text{pdp})(\text{CH}_3\text{CN})_2](\text{SbF}_6)_2$  in the oxidation of *cis*-4-methylcyclohexyl-1-pivalate and 1-substituted 3,7-dimethyl-octane without the addition of acetic acid.

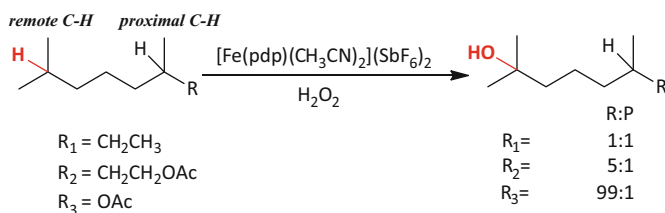
## 4 Tuning the Selectivity in Alkane Oxidation Reactions

One of the major subjects of interest over the last decade in metal-catalyzed alkane oxidation reactions has been the understanding of the factors determining the C–H site selectivity of such processes [61]. This knowledge is necessary to face the challenge of devising chemical tools for overcoming the innate reactivity of C–H bonds, introducing novel selectivities in these reactions.

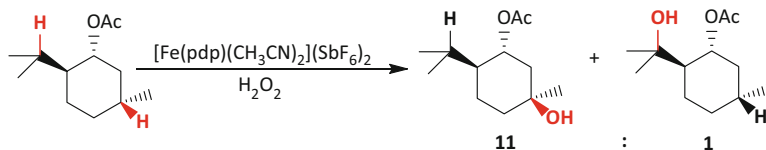
### 4.1 Predictably Selective Oxidations and Selectivity Patterns

A major breakthrough in predictable selectivity on aliphatic C–H oxidation reactions was introduced by White and Chen in 2007 [55]. In this landmark work, predictable selectivity when using the  $[\text{Fe}(\text{pdp})(\text{CH}_3\text{CN})_2](\text{SbF}_6)_2$  catalyst was achieved on the basis of the electronic and steric properties of the C–H bonds, without the need for directing groups. The iron catalyst  $[\text{Fe}(\text{pdp})(\text{CH}_3\text{CN})_2](\text{SbF}_6)_2$  (15 mol%), together with  $\text{H}_2\text{O}_2$  as oxidant and acetic acid as additive, was capable of performing selective oxidations of nonactivated C–H bonds for a broad range of substrates. Very interestingly, this predictability could also be used to oxidize selectively complex natural products at specific C–H bonds in preparative useful yields. Selectivity can be achieved by introducing directing groups (see below), or can be predicted by considering the steric and electronic properties of the different C–H bonds of the substrate. Hydroxylation occurred preferentially at the most electron-rich tertiary C–H bond, with complete retention of stereochemistry (provided that the tertiary site was part of a stereogenic center). To test the site selectivity among different tertiary C–H bonds, small molecules with two tertiary sites were oxidized, always obtaining preferential oxidation at the tertiary C–H bond more remote from electron-withdrawing groups (EWGs). The selectivity between the two tertiary sites ranges from 5:1 (remote:proximal, R:P) to 99:1 (R:P), depending on the substrate. However, when no EWGs were present in the molecule, no selectivity was obtained, affording ratios of 1:1 (R:P) (Scheme 11).

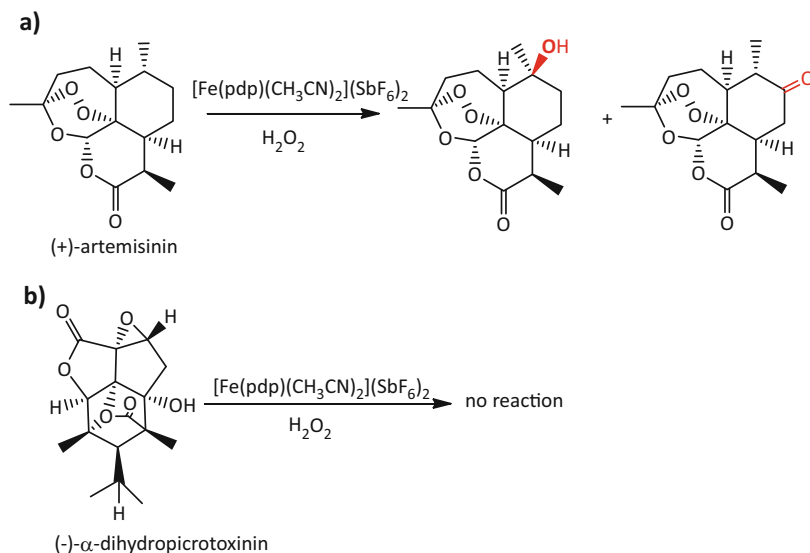
Regarding the steric effects, (–)-menthyl acetate was chosen as substrate, in which two of the three tertiary sites are virtually equivalent in terms of electronics.



**Scheme 11** Oxidation of substrates with electronically different groups by  $[\text{Fe}(\text{pdp})(\text{CH}_3\text{CN})_2](\text{SbF}_6)_2$



**Scheme 12** Selective oxidation of (-)-menthyl acetate with  $[\text{Fe}(\text{pdp})(\text{CH}_3\text{CN})_2](\text{SbF}_6)_2$  as catalyst



**Scheme 13** Oxidation of complex molecules by  $[\text{Fe}(\text{pdp})(\text{CH}_3\text{CN})_2](\text{SbF}_6)_2$

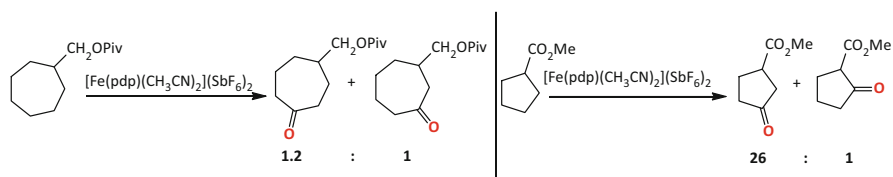
Oxidation occurred preferentially at the less hindered tertiary C–H bond, with 11:1 (accessible:hindered) selectivity and 55% combined yield (Scheme 12).

When steric and electronic effects were interplaying in a single substrate, experiments showed that the steric effects could override the electronic ones in site selectivities. The oxidation of the complex molecule (+)-artemisinin took place preferentially at the more electron-rich and less encumbered tertiary site with moderate yield (34%) which could be increased to 54% by recycling the starting material twice (Scheme 13a). More recent work showed that this oxidation also produced 22% of product arising from oxidation at a methylenic site [62]. On the other hand, in the highly hindered environment of (-)- $\alpha$ -dihydropicrotoxinin, no oxidation was attained, and 92% of the starting material was recovered after the oxidation process (Scheme 13b).

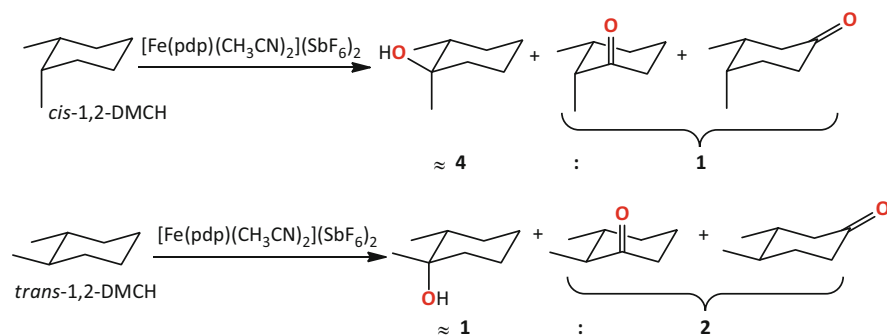
A study on methylene oxidation was presented by the same authors in 2010, using the  $[\text{Fe}(\text{pdp})(\text{CH}_3\text{CN})_2](\text{SbF}_6)_2$  catalyst again [56]. Secondary C–H bonds have intermediate electronic and steric properties between tertiary and primary sites. Primary C–H bonds are stronger but sterically more accessible. On the other

hand, tertiary C–H bonds are weaker but sterically more encumbered. Nonactivated secondary C–H bonds could be site-selectively oxidized to afford mono-oxygenated products in preparative useful yields. In substrates with no electronic biasing elements, such as *n*-hexane, no site selectivity was attained. However, when EWGs were present in the substrate (inductive effects), the oxidation is biased towards the more remote site of the EWG, with selectivities ranging from 1.2:1 (R:P) to 26:1 (R:P), depending on the substrate (Scheme 14). Substrates where all protons are close to the EWG, such as cyclopentanone, showed almost no conversion.

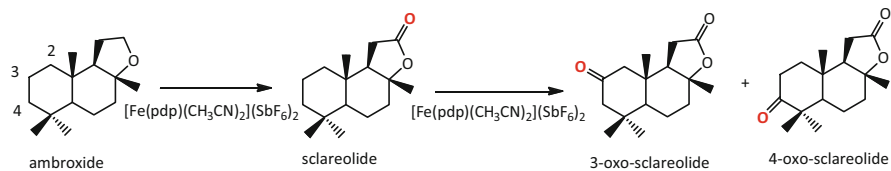
Interestingly, it was pointed out that stereoelectronic parameters based on conformational effects are also strong contributing factors to the product distribution in six-membered ring oxidations. Methylene sites adjacent to bulky groups were disfavored. However, the catalyst allows for subtle steric influence to have significant effects on the chemoselectivity of secondary vs tertiary C–H bonds. In the oxidation of *cis*-1,2-DMCH, the tertiary:secondary (3 ary:2 ary) ratio of products is 4:1, although for *trans*-1,2-DMCH the 3 ary:2 ary ratio is reversed to 1:2, favoring the oxidation at secondary sites (Scheme 15). The latter case might be explained because of the axial disposition of the tertiary C–H bonds, which are sterically more encumbered, and stronger than equatorial C–H sites. The reason is that breakage of the latter liberates strain and minimize 1,3-diaxial interactions of the methyl groups. As a result, predominantly secondary site oxidation was attained in the oxidation of *trans*-1,2-DMCH.



**Scheme 14** Electronic effects on secondary C–H group oxidation by  $[\text{Fe}(\text{pdpp})(\text{CH}_3\text{CN})_2](\text{SbF}_6)_2$



**Scheme 15** Chemoselectivity of secondary vs tertiary C–H bonds in *cis*- and *trans*-1,2-DMCH oxidation by  $[\text{Fe}(\text{pdpp})(\text{CH}_3\text{CN})_2](\text{SbF}_6)_2$



**Scheme 16** Combination of stereoelectronic factors in the oxidation of terpenes by  $[\text{Fe}(\text{pdp})(\text{CH}_3\text{CN})_2](\text{SbF}_6)_2$  [56]

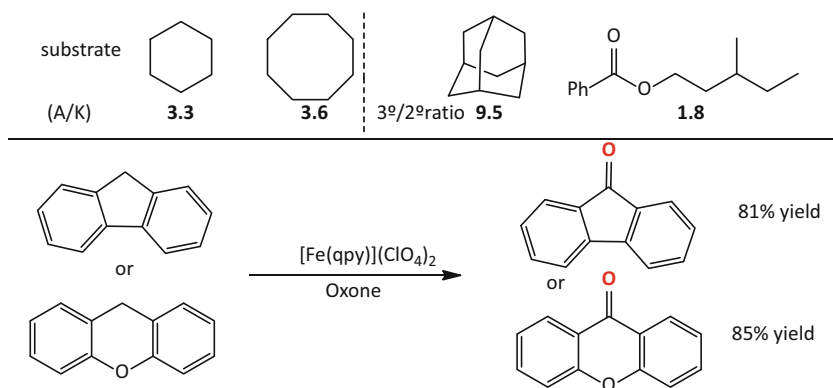
On the other hand, electronic activating groups (EAGs) were used to achieve orthogonal site selectivity to inductive or steric effects by means of hyperconjugation. For example, when a cyclopropane ring was fused to a cyclohexane ring, oxidation occurred preferentially at the position more proximal to the cyclopropane ring (1:5.2 R:P). Moreover, steric, electronic, and stereoelectronic factors can be synergistically combined in the oxidation of complex natural products, resulting in useful levels of chemo-, site-, and even diastereoselective methylene oxidations. For the oxidation of complex natural products, terpenoids were chosen as appropriate substrate platforms to study the predictability of the oxidations. An interesting example of hyperconjugative effects was the oxidation of (–)-ambroxide, which selectively afforded (+)-sclareolide in high yield (80%). (+)-Sclareolide contains a lactone deactivating group, and further oxidation of this molecule yielded a mixture of (+)-3-oxo-sclareolide and (+)-4-oxo-sclareolide (1.4:1), thus oxidizing the more distal secondary sites from the EWG (Scheme 16). More recent work questions this selectivity, showing that oxidation of this substrate with  $[\text{Fe}(\text{OTf})_2(\text{pdp})]$  also produces (+)-4-oxo-sclareolide in amounts comparable to the (+)-2-oxo and (+)-3-oxo-sclareolide isomers [63].

Inspired by the well-established principles in oxidation catalysis with heme complexes, Gómez et al. designed a new catalyst platform based on modifications at the well-known mep and mcp ligands (mcp = *N,N'*-dimethyl-*N,N'*-bis(2-pyridylmethyl)-cyclohexane-1,2-diamine) by introducing bulky pinene groups at positions 4 and 5 of the pyridine rings [64]. By doing so,  $[\text{Fe}(\text{OTf})_2((S,S,R)\text{-mcpp})]$ ,  $[\text{Fe}(\text{OTf})_2((R,R,R)\text{-mcpp})]$ , and  $[\text{Fe}(\text{OTf})_2((R)\text{-mcpp})]$  complexes were synthesized (Scheme 17).

The catalyst  $[\text{Fe}(\text{OTf})_2((S,S,R)\text{-mcpp})]$  stood as the most efficient of the series using very low catalyst loadings (1 mol%), even more efficient than  $[\text{Fe}(\text{pdp})(\text{CH}_3\text{CN})_2](\text{SbF}_6)_2$  under these catalytic conditions, for the oxidation of *cis*-1,2-DMCH. Using a low loading of this catalyst (2 mol%), cyclohexane oxidation yields the corresponding ketone in 70% yield. Under these conditions, electronic effects were studied with 2,7-dimethyl-octane derivatives (Scheme 18), affording yields and selectivities very similar to those previously reported by White and coworkers (compare with Scheme 11) [55].

Furthermore, (–)-menthyl acetate was also tested using 3 mol% catalyst, obtaining 62% combined yield of oxidation at the tertiary sites with 17:1 selectivity (accessible:hindered) (Scheme 19). This efficiency selectivity was even more remarkable than that obtained with 15 mol%  $[\text{Fe}(\text{pdp})(\text{CH}_3\text{CN})_2](\text{SbF}_6)_2$  [55] (compare with Scheme 12), most likely because of the well-defined chiral cavity





**Scheme 20** Chemoselectivity of secondary vs tertiary C–H bond oxidation by [Fe(qpy)](ClO<sub>4</sub>)<sub>2</sub>

interplaying were tested. Oxidation of cyclohexane yielded 15.6 TON and 3.3 A/K ratio ( $A/K = [\text{alcohol}]/[\text{ketone}]$ ,  $[\text{cyclohexanol}]/[\text{cyclohexanone}]$ ), whereas cyclooctane afforded 50% combined yield and 3.6 A/K ratio (Scheme 20). On the other hand, in the oxidation of adamantane, 42% yield was obtained with a 3°/2° ratio of 9.5. Hyperconjugation effects were used to direct the oxidation to the most proximal position to the EAGs. Interestingly, this catalyst supports aromatic groups on the substrate, and fluorene and xanthene were the most effectively and selectively oxidized, obtaining up to 85% yield of the ketone product (the sole product observed for these two substrates). Ester moieties were also employed as EAGs, as in the case of 3-methylpentyl benzoate, where the tertiary alcohol was obtained in 33% yield, and 18% of oxidation at the secondary most remote site (3°/2° = 1.8).

Oxidations proved to be stereospecific, as shown in the oxidation of *cis*- and *trans*-4-methylcyclohexyl benzoate, which occurred with retention of the configuration. In terms of yields, the former was more efficiently oxidized to the corresponding tertiary alcohol (45% yield) than the latter (19% yield). Finally, millimole scale oxidations of xanthene and tetrahydronaphthalene were performed, showing the practicability of this methodology. Xanthone was obtained as sole product in 83% yield in the oxidation of xanthene, whereas the products of tetrahydronaphthalene oxidation were a mixture of ketone (49%), secondary alcohol (12%), and overoxidized product (26%).

## 4.2 Novel Selectivity for Alkane Oxidation Reactions

It is now currently accepted that the factors governing selectivity in C–H oxidation reactions by traditional organic reagents are determined by the innate nature of the C–H bonds of the substrates [61]. Oxidations with iron catalysts such as [Fe(OTf)<sub>2</sub>(mep)] or [Fe(pdp)(CH<sub>3</sub>CN)<sub>2</sub>](SbF<sub>6</sub>)<sub>2</sub> mainly appear to obey the same

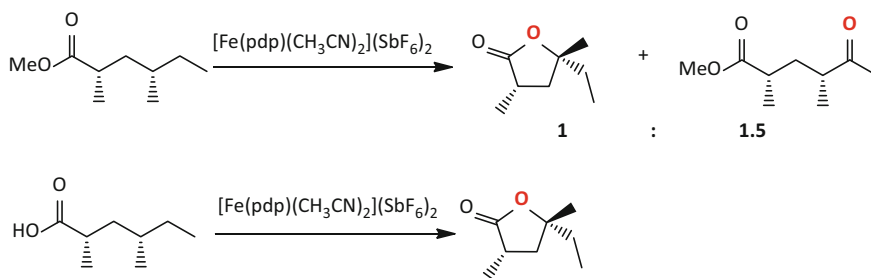
rules. Reagents that could override the intrinsic bias imposed by the general reactivity of the substrate are particularly valuable because they complement current methodologies and open novel synthetic pathways. To this end, two different approaches can be taken: the introduction of directing groups on the substrate and modifications on the catalyst architecture introducing structural aspects that condition substrate access to the catalyst active site, achieving novel selectivities differing from those dictated by the innate properties of the C–H bonds in the substrate. Both strategies are described in the following.

#### 4.2.1 Novel Selectivity Induced by Directing Groups on the Substrate

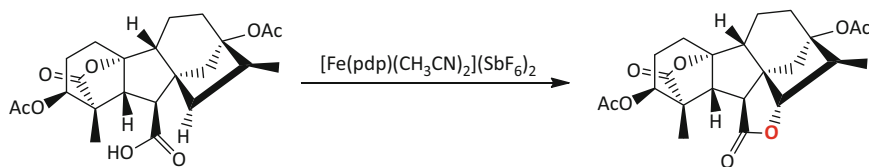
The use of directing groups on the substrate has been the most successful strategy to divert C–H regioselectivity in alkane oxidations [65–69]. In the particular case of non-heme iron-catalyzed oxidations, White and Chen presented the directed oxidation of carboxylic acid-containing substrates [55]. The authors postulated that a carboxylate group on the substrate could be used to direct the site of C–H oxidation, based on the role of carboxylates as ligands for non-heme iron complexes and the beneficial role of acetic acid on the catalytic activity of  $[\text{Fe}(\text{pdp})(\text{CH}_3\text{CN})_2](\text{SbF}_6)_2$ . Diastereoselective lactonizations at secondary C–H sites were achieved with this methodology. For example, (+)-2,4-dimethyl-hexanoic acid was oxidized using  $[\text{Fe}(\text{pdp})(\text{CH}_3\text{CN})_2](\text{SbF}_6)_2$  (15 mol%) and  $\text{H}_2\text{O}_2$ , furnishing a five-membered ring lactone in 70% yield, whereas the oxidation of the analogous methyl ester gave a methyl ketone as the major product (Scheme 21).

On the other hand, this methodology was evaluated with a tetrahydrogibberellic acid analog, which yielded the corresponding five-membered ring lactone as a single diastereoisomer in 52% yield (recycling the substrate once) (Scheme 22). In contrast, oxidation of the corresponding methyl ester resulted in mostly recovered starting material and mixtures of undefined oxidation products.

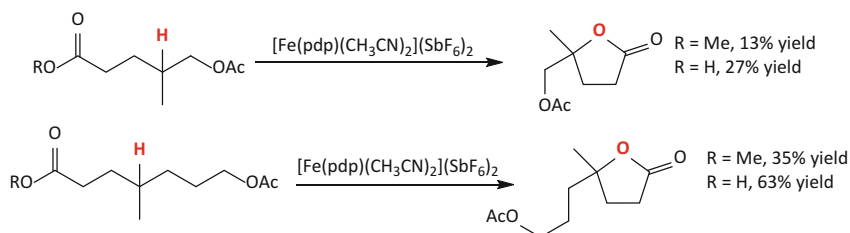
The same authors presented a more thorough study on the evaluation of the selectivity rules governing C–H oxidation of carboxylic acid-containing substrates in 2012 [70]. In this work it was shown that carboxylic acids not only controlled the



**Scheme 21** Directed oxidation of a carboxylic acid-containing substrate with  $[\text{Fe}(\text{pdp})(\text{CH}_3\text{CN})_2](\text{SbF}_6)_2$



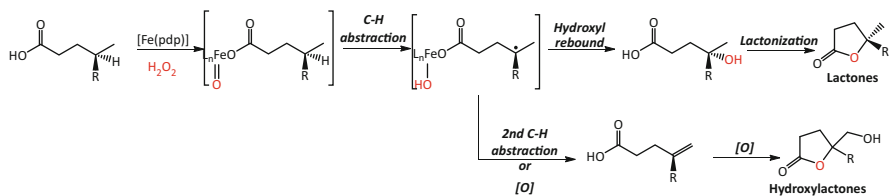
**Scheme 22** Oxidation of a tetrahydrogibberellic acid analog with  $[\text{Fe}(\text{pdp})(\text{CH}_3\text{CN})_2](\text{SbF}_6)_2$



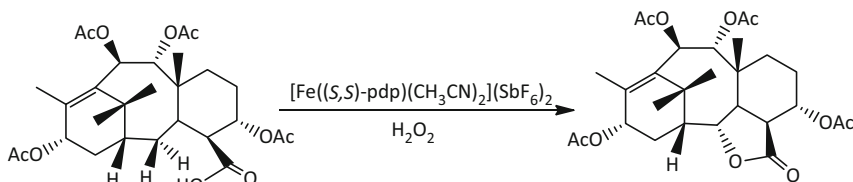
**Scheme 23** Lactonization reactions of ester- and carboxylic acid-based substrates with  $[\text{Fe}(\text{pdp})(\text{CH}_3\text{CN})_2](\text{SbF}_6)_2$

site selectivity but they were also capable of overcoming unfavorable electronic, steric, and stereoelectronic effects within the substrate by rendering the oxidation reaction intramolecular. Linear methyl esters with EWGs were tested, showing that the substrate became more reactive as the EWGs were shifted away from the tertiary center, but poor yields were obtained. However, analogous carboxylic acid substrates were significantly more reactive, affording moderate yields of the corresponding lactones (Scheme 23).

Moreover, matched/mismatched behavior with the chiral  $[\text{Fe}(\text{pdp})(\text{CH}_3\text{CN})_2](\text{SbF}_6)_2$  catalyst was detected when a chiral carboxylic acid was employed, although this behavior was not detected with analogous chiral methyl esters. This observation supported the proposal of carboxylic acid acting as ligand for the metal center. Enantiomeric enrichment of racemic carboxylic acid and lactone product was possible upon reaction with the chiral catalyst. In terms of steric effects, it was shown that yields of lactone products arising from oxidation of cyclohexane-derivatized carboxylic acids were virtually unaffected by the axial or equatorial disposition of the C–H bond to be oxidized, but instead methyl ester substrates were sensitive. From a mechanistic point of view, it is proposed that, analogous to C–H hydroxylation, the iron catalyst reacts with  $\text{H}_2\text{O}_2$  and carboxylic acid substrate to generate an iron-oxo carboxylate as the active oxidant species, capable of intramolecular hydrogen atom abstraction to afford a short-lived carbon-centered substrate radical. This radical can proceed via two different rebound pathways to furnish the lactone product: (1) carboxylate rebound to form lactone directly or (2) hydroxyl rebound followed by lactonization (Scheme 24). The latter pathway is favored according to labeling studies, which showed that doubly  $^{18}\text{O}$ -labeled carboxylic acid led to predominantly singly labeled lactone. Alternatively, the carbon-centered



**Scheme 24** Proposed mechanism for  $[\text{Fe}(\text{pdp})(\text{CH}_3\text{CN})_2](\text{SbF}_6)_2$ -catalyzed C–H lactonization reactions



**Scheme 25** Directed oxidation of a taxane-based substrate to its lactone product with  $[\text{Fe}(\text{pdp})(\text{CH}_3\text{CN})_2](\text{SbF}_6)_2$

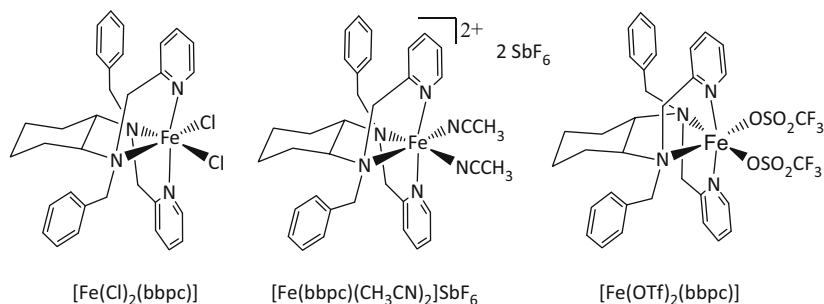
radical can undergo a second hydrogen abstraction to furnish an olefin intermediate, and further oxidation to yield hydroxylactones. Very interestingly, this strategy was employed in the site-directed oxidation of a taxane, obtaining moderate yield (49%) of the desired lactone (Scheme 25).

#### 4.2.2 Novel Selectivity Induced by Steric Modifications on the Catalyst Architecture

A more subtle and elaborated approach exploited by enzymes relies on employing highly spatially structured oxidizing sites that could regulate selectivity by controlling access and orientation of the substrate in its approach toward the oxidizing unit. Pursuing this strategy, new bioinspired iron catalysts have been designed introducing steric modifications on the catalyst architecture to overcome the innate reactivity of C–H bonds and achieve novel selectivities in C–H bond oxidations.

In an attempt to alter the regioselectivity of non-heme iron catalysis, Goldsmith and coworkers [71] described a new mcp-modified ligand framework, where they replaced the methyl groups on the amine nitrogens with benzyl groups. Three iron complexes were synthesized –  $[\text{FeCl}_2(\text{bbpc})]$ ,  $[\text{Fe}(\text{OTf})_2(\text{bbpc})_2]$ , and  $[\text{Fe}(\text{bbpc})(\text{CH}_3\text{CN})_2](\text{SbF}_6)_2$  (bbpc = *N,N'*-di(phenylmethyl)-*N,N'*-bis(2-pyridinylmethyl)-1,2-cyclohexanediamine) (Scheme 26) – and appeared to catalyze the oxidation of alkanes by  $\text{H}_2\text{O}_2$ , being the hexafluoroantimonate complex the most active and selective for alkane hydroxylation.

Interestingly, the bulk installed on the ligand architecture directs the oxidation toward the less sterically hindered positions of substrates. Reaction of  $[\text{Fe}(\text{bbpc})$



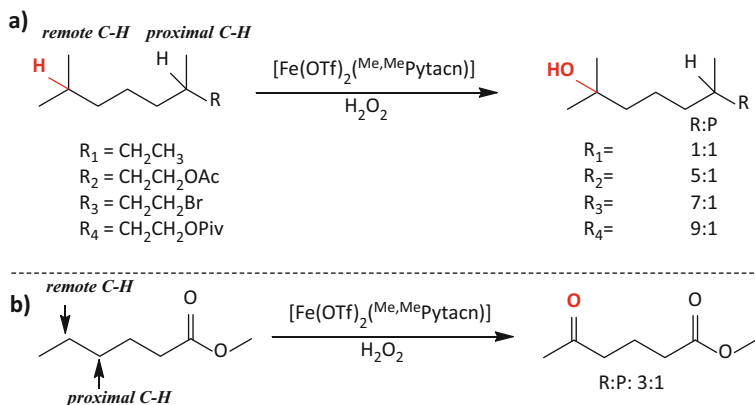
**Scheme 26** Benzyl-modified mcp iron catalysts for efficient alkane oxidation reactions

$(\text{CH}_3\text{CN})_2(\text{SbF}_6)_2$  (15 mol%) with *cis*- and *trans*-1,2-DMCH showed preferential oxidation for tertiary and secondary sites, respectively. As previously mentioned, this can be explained in terms of strain release of 1,3-diaxial interactions. Interestingly, when comparing these results with previously described catalysts under the same catalytic conditions, a clear preference for oxidation at the secondary position was observed for both substrates when the  $[\text{Fe}(\text{bbpc})]$  catalysts were employed. Despite the high catalyst loading employed, yields obtained are modest (~30%). This effect might be attributed to the steric hindrance offered by the *N*-benzyl group.

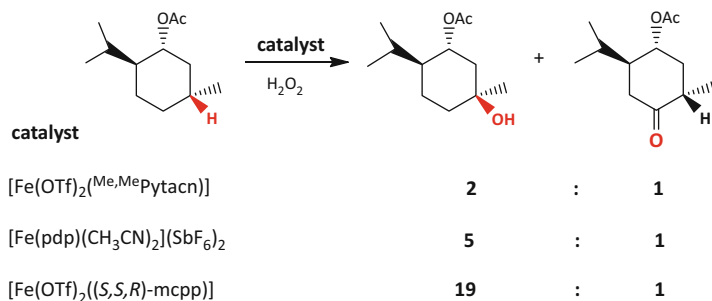
In recent work by Prat et al. [54],  $[\text{Fe}(\text{OTf})_2(\text{Me},\text{MePytacn})]$  ( $\text{Me},\text{MePytacn}$  = 1-(6-methyl-2-pyridylmethyl)-4,7-dimethyl-1,4,7-triazacyclononane) was described as an efficient catalyst with enhanced preference for oxidizing methylenic sites. Interestingly, low catalyst loadings (3 mol%) were used in this protocol, and the addition of acetic acid appeared not to be strictly required for efficient catalysis, indicating the remarkably facile O–O lysis for this catalyst.

Following the same trend as the previously mentioned catalysts, oxidation with  $[\text{Fe}(\text{OTf})_2(\text{Me},\text{MePytacn})]$  occurred preferentially at the tertiary position more remote from EWGs, indicating its electrophilic nature (Scheme 27a). The remote/proximal ratios obtained were virtually the same as those attained with catalysts  $[\text{Fe}(\text{pdp})(\text{CH}_3\text{CN})_2](\text{SbF}_6)_2$  and  $[\text{Fe}(\text{OTf})_2(\text{S},\text{S},\text{R}-\text{mcpp})]$  (for comparison see Schemes 11 and 18, respectively). However, using  $[\text{Fe}(\text{OTf})_2(\text{Me},\text{MePytacn})]$ , a significant amount of secondary site oxidation (ketone formation) was observed. Moreover, methylene oxidation was also sensitive to the electronic properties of the C–H bonds, as shown in the oxidation of methyl hexanoate (Scheme 27b).

Steric effects on the substrate also appeared to play a role in the oxidation reactions. An interesting example is 1,1-DMCH, where oxidation at adjacent position to the methyl groups was disfavored because of steric encumbrance, and the other two methylenic sites were thus favored. The enhanced selectivity for secondary sites was best illustrated in the oxidation of (–)-menthyl acetate, which furnished a ~2:1 mixture of tertiary alcohol:ketone after selective oxidation at the methylenic site. This behavior was in stark contrast with that offered by  $[\text{Fe}(\text{pdp})]$



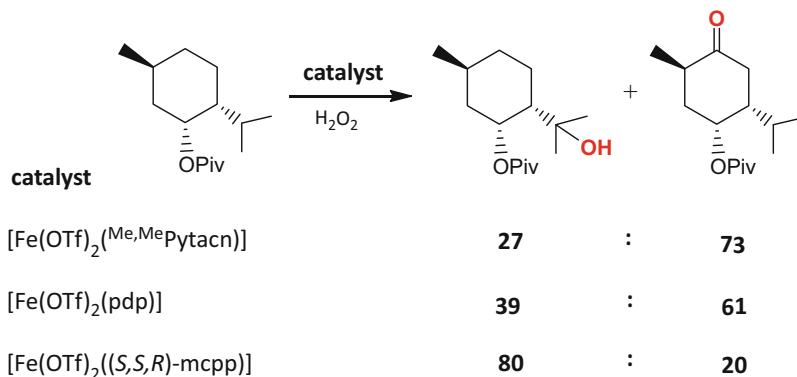
**Scheme 27** Oxidation of substrates with electronically different groups by  $[\text{Fe}(\text{OTf})_2]^{(\text{Me,MePytacn})}$ . a) Hydroxylation of tertiary C–H bonds, b) oxidation of methylenic sites.



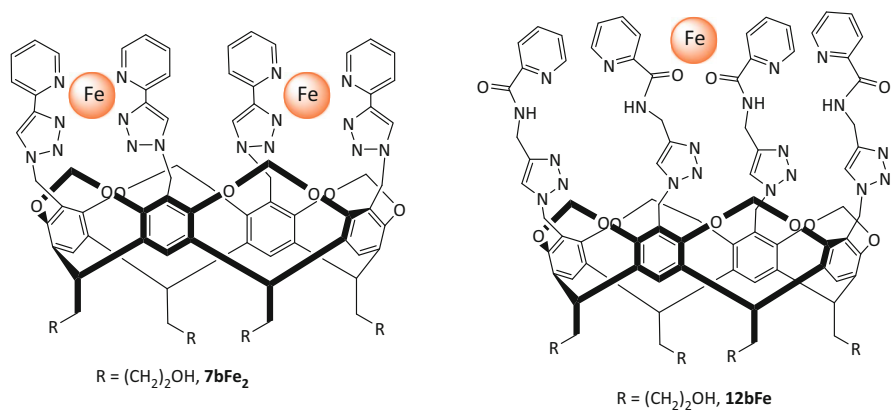
**Scheme 28** Oxidation of (–)-menthyl acetate with various catalysts described in the literature

$(\text{CH}_3\text{CN})_2](\text{SbF}_6)_2$  [55, 56] and  $[\text{Fe}(S,S,R)\text{-mcpp}](\text{OTf})_2$  [64] under analogous conditions, which fairly selectively hydroxylate the most sterically exposed tertiary C–H bond (5:1 A/K and 19:1 A/K, respectively, Scheme 28).

On the other hand, in the oxidation of *trans*-cyclohexane-based substrates, oxidation at methylenic positions was found to be in competition with that of tertiary C–H bonds. *trans*-1,2-DMCH yielded a normalized 24:76  $3^\circ/2^\circ$  ratio, and this trend was even more significant in the oxidation of *trans*-decaline (4:96), indicating that products arising from methylene oxidation are largely dominant. The rationale for this behavior lies on the steric demand exerted by the methyl group in the  $\alpha$ -position of the pyridine, which remains in close proximity to the iron site. This fact favors preferential oxidation at the spatially more accessible methylenic sites in contrast to the more embedded tertiary C–H bonds. More importantly, this could be applied to divert regioselectivity in the C–H oxidation of (+)-neomenthyl esters (Scheme 29). Whereas  $[\text{Fe}(\text{OTf})_2(\text{pdp})]$  offered poor discrimination between secondary and tertiary C–H bonds,  $[\text{Fe}(\text{OTf})_2]^{((S,S,R)\text{-mcpp})}$  and  $[\text{Fe}(\text{OTf})_2]^{(\text{Me,MePytacn})}$  were found to be complementary, the former



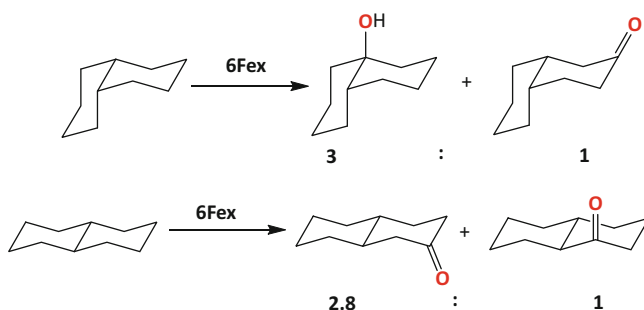
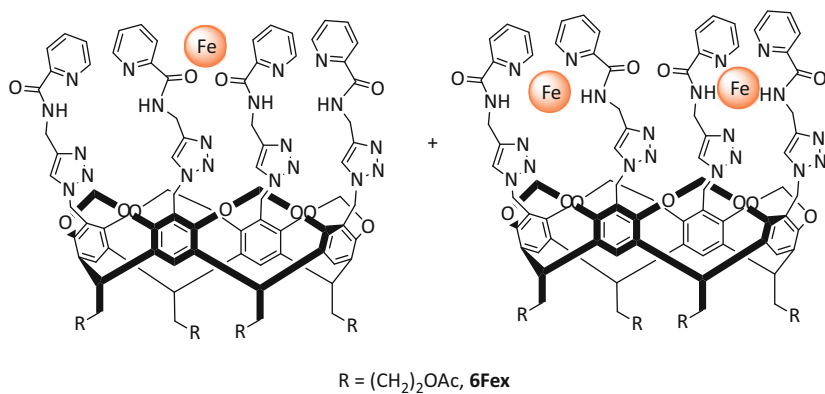
**Scheme 29** Oxidation of (+)-neomenthyl pivalate with various catalysts described in the literature



**Scheme 30** Resorcinarene-based cavitands used as catalysts for fluorene oxidation

yielding the tertiary alcohol as the major product (up to 80:20 normalized 3°/2° ratio) and the latter affording preferential oxidation at the methylenic site (up to 27:73 normalized 3°/2° ratio).

A different approach was proposed by Hooley and coworkers [72]. In this study resorcinarene-based cavitands were used as catalysts, which allow for binding of iron(II) by bidentate ligands, leaving empty sites for further reactivity at the metal sites. The iron-coordinated cavitands **7bFe<sub>2</sub>** and **12bFe** (Scheme 30) bore free coordination sites, and thus they were envisioned to perform C–H oxidation reactions under mild conditions, inspired by the mode of action of the Rieske oxygenases. However, these catalysts proved inactive towards cyclohexane and methylcyclohexane oxidations. In contrast, they were able to convert fluorene smoothly to fluorenone using TBHP as oxidant.

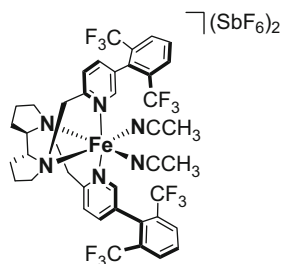


**Scheme 31** Regioselectivity in the oxidation of *cis*- and *trans*-decaline by 6Fex and structure of the catalyst

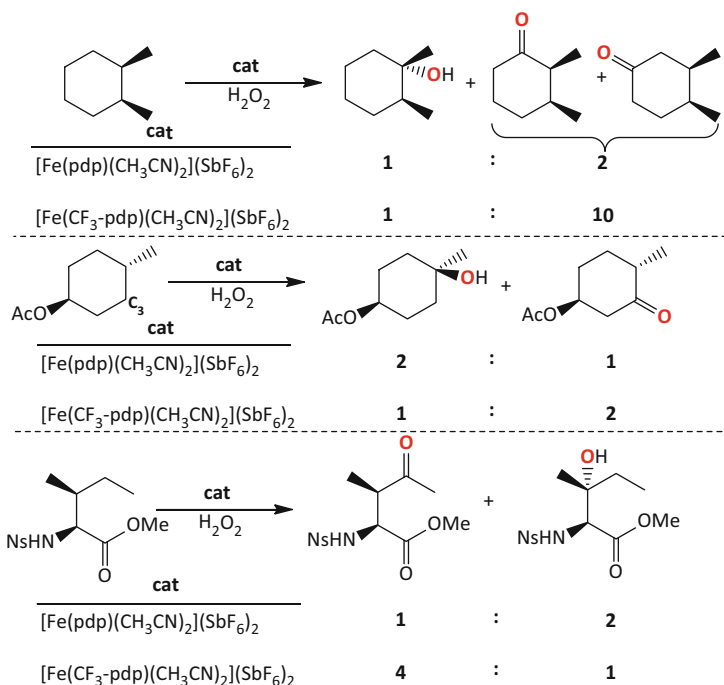
In a later study [73], the authors showed that 6Fex (Scheme 31) was capable of efficiently oxidizing *cis*-decaline to the tertiary alcohol (*cis*-2-decalol) and the ketone product (*cis*-2-decalone) (up to 69% yield) using TBHP. Interestingly, the addition of acetic acid was not strictly required for the outcome of the reaction, although long reaction times (24 h) and high temperatures (60 °C) were needed. Good selectivity for the tertiary alcohol was obtained (up to 75% normalized regioselectivity). On the other hand, *trans*-decaline afforded *trans*-2-decalone and *trans*-3-decalone as oxidized products in a 2.8:1 ratio with an overall yield of 46%. Interestingly, these catalysts were also able to oxidize benzylic methylenic sites very efficiently (up to 88% yield for the oxidation of 1-ethyl-4-methyl benzene).

Very recently White and coworkers [62] designed a new catalyst [Fe(CF<sub>3</sub>-pdp)(CH<sub>3</sub>CN)<sub>2</sub>](SbF<sub>6</sub>)<sub>2</sub> (CF<sub>3</sub>-pdp = *N,N'*-bis(5-(2,6-di-(trifluoro)-methyl-phenyl)-2-pyridylmethyl)-2,2'-bipyrrrolidine) that used a trajectory restriction strategy to achieve predictable, catalyst-controlled site-selectivity (Scheme 32).

In the oxidation of *trans*-1,2-DMCH, this catalyst exhibited enhanced selectivity towards secondary sites (10:1 2°/3° ratio), whereas the structurally related [Fe(pdp)(CH<sub>3</sub>CN)<sub>2</sub>](SbF<sub>6</sub>)<sub>2</sub> catalyst provided a 2:1 2°/3° ratio (Scheme 33). On the other

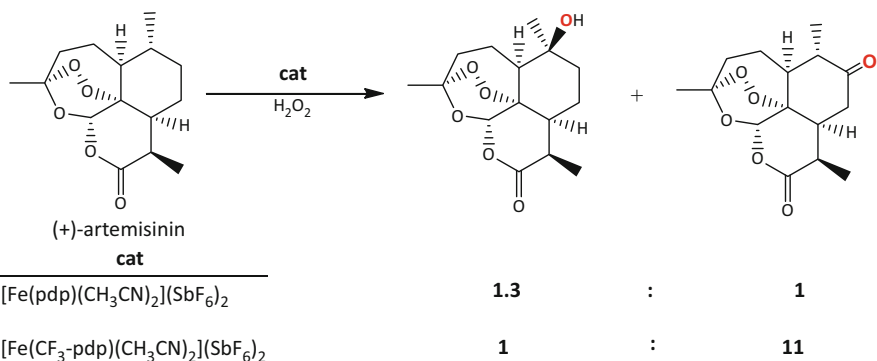


**Scheme 32** Structure of trajectory restrictive catalyst  $[\text{Fe}(\text{CF}_3\text{-pdp})(\text{CH}_3\text{CN})_2](\text{SbF}_6)_2$  for catalyst-controlled site-selectivity



**Scheme 33** Difference in regioselectivity attained with catalysts  $[\text{Fe}(\text{pdp})(\text{CH}_3\text{CN})_2](\text{SbF}_6)_2$  and  $[\text{Fe}(\text{CF}_3\text{-pdp})(\text{CH}_3\text{CN})_2](\text{SbF}_6)_2$

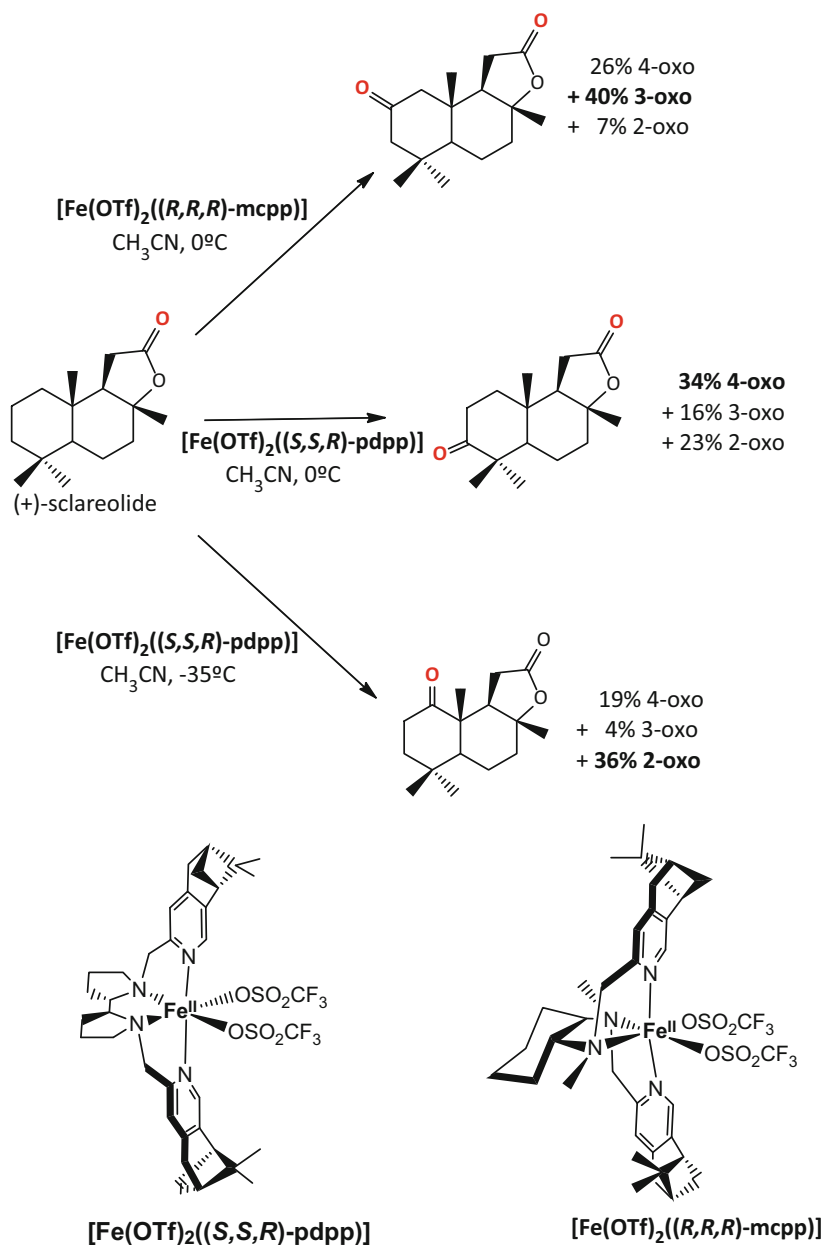
hand, this catalyst was able to overturn the inherent reactivity of the substrates. This was the case of *trans*-4-methylcyclohexyl acetate, which gave the tertiary alcohol as major product when  $[\text{Fe}(\text{pdp})(\text{CH}_3\text{CN})_2](\text{SbF}_6)_2$  was used (1:2 2°/3° ratio) but the C<sub>3</sub>-ketone was the major product when  $[\text{Fe}(\text{CF}_3\text{-pdp})(\text{CH}_3\text{CN})_2](\text{SbF}_6)_2$  was employed (2:1 2°/3° ratio). The protected (+)-isoleucine changed from 1:2 to 4:1 2°/3° ratio when the sterically encumbered catalyst was used to oxidize this substrate.



**Scheme 34** Oxidation of artemisinin with  $[\text{Fe}(\text{pdp})(\text{CH}_3\text{CN})_2](\text{SbF}_6)_2$  and  $[\text{Fe}(\text{CF}_3\text{-pdp})(\text{CH}_3\text{CN})_2](\text{SbF}_6)_2$

This strategy was further investigated in the oxidation of complex molecules such as (+)-artemisinin, where two products result: (+)-10 $\beta$ -hydroxy-artemisinin (3 $^\circ$  site) and (+)-9-oxo-artemisinin (2 $^\circ$  site). Whereas  $[\text{Fe}(\text{pdp})(\text{CH}_3\text{CN})_2](\text{SbF}_6)_2$  catalyst afforded 2:1 2 $^\circ$ /3 $^\circ$  ratio,  $[\text{Fe}(\text{CF}_3\text{-pdp})(\text{CH}_3\text{CN})_2](\text{SbF}_6)_2$  yielded 10:1 2 $^\circ$ /3 $^\circ$  ratio, the latter able to override strong electronic substrate bias (Scheme 34).

Modulation of selectivity among multiple methylene sites has been rarely observed and constitutes a major challenge. Nevertheless, changes in site selectivity in the functionalization of structurally rich natural product substrates using iron catalysts have been documented. For example, site selectivity in the oxidation of (+)-sclareolide was achieved by using highly structured non-heme iron catalysts containing pinene rings attached to pyridine moieties (Scheme 35). Hence, (+)-1-oxo-sclareolide, (+)-2-oxo-sclareolide, and (+)-3-oxo-sclareolide can be obtained as the main product in 36% (61% selectivity), 40% (55% selectivity), and 34% (47% selectivity) yield, respectively, by choosing the appropriate experimental conditions and catalyst. Although those yields may seem modest, they are competitive with enzymatic oxidations. For example, (+)-2-oxo-sclareolide is obtained enzymatically with reduced yields and longer reaction times.



**Scheme 35** Regioselective oxidation among multiple methylene sites with  $[\text{Fe}(\text{OTf})_2]((R,R,R)\text{-mcpp})$ ,  $[\text{Fe}(\text{OTf})_2]((S,S,R)\text{-pdpp})$ , and  $[\text{Fe}(\text{OTf})_2]((S,S,R)\text{-pdpp})$

## 5 Novel Reactivity on C–H Oxidation

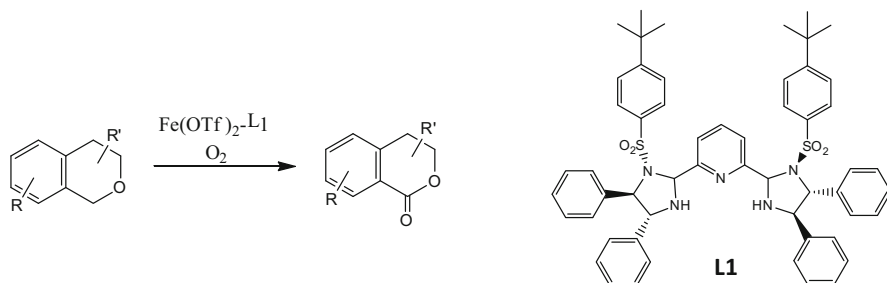
In addition to the most common C–H oxygenation reactions of alkanes employing peroxides as oxidants, novel reactivity for these substrates has emerged in the past few years. Remarkable examples of this emerging reactivity involves the  $\alpha$ -oxygenation of electron-rich substrates employing  $O_2$  as terminal oxidant, and desaturation of alkane C–H bonds.

### 5.1 $\alpha$ -Oxygenation

An original work in the field of C–H oxidation was reported by Xiao and coworkers [74] in 2014, when they developed novel iron catalysts with tridentate pyridine bisulfonylimidazolidine ligands for the  $\alpha$ -oxidation of ethers under 1 atm of  $O_2$  and additive-free conditions. This system relies on environmentally friendly conditions to oxidize electron-rich substrates selectively using  $O_2$  as oxidant, with excellent mass balance and high turnover numbers. Most remarkably,  $H_2$  is formed as the only side-product. The conditions mentioned provide the oxidation of important motifs for natural products as isochromans and phthalans. In case of isochromans (Scheme 36), the reaction proceeds with high chemoselectivity, with no alcohol byproduct formation and with good mass balance, with no degradation of the substrate. The presence of substituents in the alkyl ring does not affect the reaction yield. However, substituents in the aromatic ring show electronic effects because the electron-withdrawing groups induce higher TONs, whereas electron-donating substituents give the opposite effect. Moreover, very electron-rich isochromans can also be oxidized, but with lower TONs. This is the first reported iron system able to oxidize such electron-rich substrates.

### 5.2 Desaturation

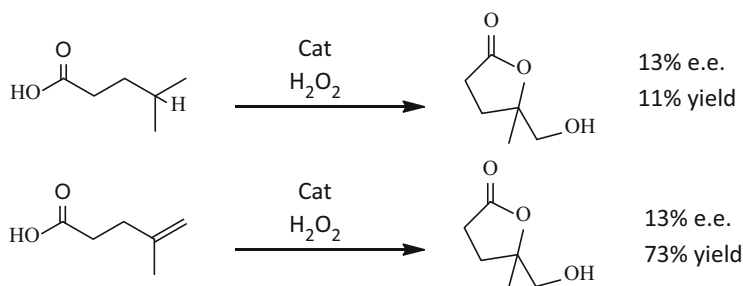
Nature has developed enzymes that have the ability to catalyze different type of reactions. An example is those enzymes that can perform hydroxylation or



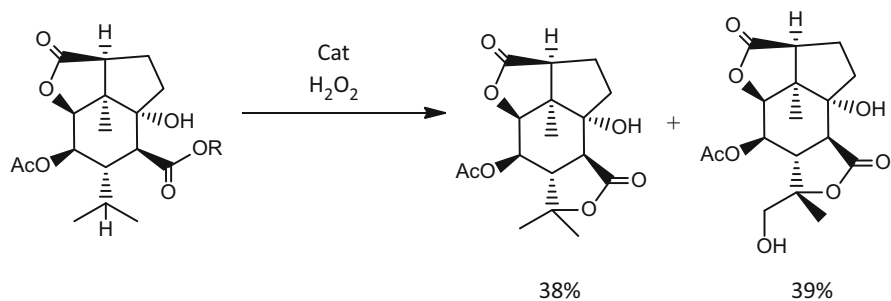
**Scheme 36** Oxidation of electron-rich isochromans using iron catalyst

desaturation activity depending on the substrate. Hydroxylation reactions have been described for a good number of iron oxidation catalysts, but it was in 2011 when White and coworkers [75] described that  $[\text{Fe}(\text{pdp})(\text{CH}_3\text{CN})_2](\text{SbF}_6)_2$  is able to disclose substrate-dependent hydroxylase/desaturase activity in aliphatic C–H bonds in substrates containing carboxylic acids. This ability was demonstrated when the 4-methylpentanoic acid was exposed to oxidizing conditions in the presence of  $[\text{Fe}(\text{pdp})(\text{CH}_3\text{CN})_2](\text{SbF}_6)_2$  catalyst (Scheme 37). The product is proposed to result from a desaturation reaction that rapidly oxidizes to an epoxide and finally an intramolecular lactonization takes place to give the final product. This proposal was demonstrated by exposing the supposed alkene product from the desaturation reaction to the same reaction conditions that finally give the same product. Moreover, with the use of the chiral  $[\text{Fe}(\text{pdp})(\text{CH}_3\text{CN})_2](\text{SbF}_6)_2$  catalyst, both reactions gave the same enantioenriched hydroxylactone product and also favored the same enantiomer.

This enzyme-like reactivity enables the synthesis of highly complex molecules from substrates containing carboxylic acids, such as picrotoxinin derivatives which, when exposed to the same oxidizing conditions, yield lactone and hydroxylactone products (Scheme 38).



**Scheme 37** Desaturation/hydroxylation reaction of 4-methylpentanoic acid using  $[\text{Fe}((R,R)\text{-pdp})(\text{CH}_3\text{CN})_2](\text{SbF}_6)_2$  as catalyst



**Scheme 38** Synthesis of highly complex lactone molecules using  $[\text{Fe}((S,S)\text{-pdp})(\text{CH}_3\text{CN})_2](\text{SbF}_6)_2$

## References

1. Sheldon RA, Kochi JA (1981) Metal-catalyzed oxidation of organic compounds. Academic, New York
2. Shilov AE, Shul'pin GB (2000) Activation and catalytic reaction of saturated hydrocarbons in the presence of metal complexes. Kluwer Academic, Boston
3. Dyker G (2005) Handbook of C–H transformation, vol 1–2. Wiley-VCH, Weinheim
4. Pérez PJ (2013) Alkane C–H activation by single-site metal catalysis, vol 38. Springer, The Netherlands
5. Bordeaux M, Galarneau A, Drone J (2012) *Angew Chem Int Ed* 51:10712
6. Gutekunst WR, Baran PS (2011) *Chem Soc Rev* 40:1976
7. McMurray L, O'Hara F, Gaunt M (2011) *Chem Soc Rev* 40:1885
8. Che C-M, Lo VK-Y, Zhou C-Y, Huang J-S (2011) *Chem Soc Rev* 40:1950
9. Yamaguchi J, Yamaguchi AD, Itami K (2012) *Angew Chemie Int Ed* 51:8960
10. Labinger JA, Bercaw JE (2002) *Nature* 417:507
11. Godula K, Sames D (2006) *Science* 312:67
12. Chen K, Baran PS (2009) *Nature* 459:824
13. White MC (2012) *Science* 335:807
14. Lloret J, Company A, Gómez L, Costas M (2013) Alkane C–H activation by single-site metal catalysis, vol 38. Springer, The Netherlands
15. Enthaler S, Junge K, Beller M (2008) *Angew Chemie Int Ed* 47:3317
16. Schröder K, Junge K, Bitterlich B, Beller M (2010) *Top Organomet Chem* 33:83
17. Que L Jr, Tolman WB (2008) *Nature* 455:333
18. Cotton FA, Wilkinson G, Murillo CA, Bochmann M (1999) *Advanced inorganic chemistry*. Wiley, New York
19. Meunier B, Bernadou J (2000) *Struct Bond* 97:1
20. Schlichting I, Berendzen J, Chu K, Stock AM, Maves SA, Benson DE, Sweet RM, Ringe D, Petsko GA, Sligar SG (2000) *Science* 287:1615
21. Meunier B, de Visser SP, Shaik S (2004) *Chem Rev* 104:3947
22. Montellano POD (2004) *Cytochrome P450: structure, mechanism and biochemistry*, 3rd edn. Springer, New York
23. Kovaleva EG, Lipscomb JD (2008) *Nat Chem Biol* 4:186
24. Barry SM, Challis GL (2013) *ACS Catal* 3:2362
25. Gibson DT, Subramanian V (1984) *Microbial degradation of aromatic hydrocarbons*. Marcel Dekker, New York
26. Gibson DT, Resnick SM, Lee K, Brand JM, Torok DS, Wackett LP, Schocken MJ, Haigler BE (1995) *J Bacteriol* 177:2615
27. Hudlicky T, Gonzalez D, Gibson DT (1999) *Aldrichimica Acta* 32:35
28. Gibson DT, Parales RE (2000) *Curr Opin Biotechnol* 11:236
29. Wolfe MD, Parales JV, Gibson DT, Lipscomb JD (2001) *J Biol Chem* 276:1945
30. Costas M, Mehn MP, Jensen MP, Que L Jr (2004) *Chem Rev* 104:939
31. Bruijninx PCA, van Koten G, Klein Gebbink RJM (2008) *Chem Soc Rev* 37:2581
32. Hegg EL, Que L Jr (1997) *Eur J Biochem* 250:625
33. Koehntop KD, Emerson JP, Que LJ (2005) *J Biol Inorg Chem* 10:87
34. Kauppi B, Lee K, Carredano E, Parales RE, Gibson DT, Eklund H, Ramaswamy S (1998) *Structure* 6:571
35. Karlsson A, Parales JV, Parales RE, Gibson DT, Eklund H, Ramaswamy S (2003) *Science* 299:1039
36. Wolfe MD, Altier DJ, Stubna A, Popescu CV, Münck E, Lipscomb JD (2002) *Biochemistry* 41:9611
37. Wolfe MD, Lipscomb JD (2003) *J Biol Chem* 278:829
38. Chen K, Que L (2001) *J Am Chem Soc* 123:6327
39. Costas M, Chen K, Que L Jr (2000) *Coord Chem Rev* 200–202:517

40. Talsi EP, Bryliakov KP (2012) *Coord Chem Rev* 256:1418
41. Codola Z, Lloret J, Costas M (2014) *Progress in Inorganic Chemistry*: Vol. 59. Wiley, p 447
42. Kim C, Chen K, Kim J, Que L Jr (1997) *J Am Chem Soc* 119:5964
43. Chen K, Que L Jr (1999) *Chem Commun* 1375
44. Britovsek GJP, England J, White AJP (2005) *Inorg Chem* 44:8125
45. Toftlund H, Pedersen E, Yde-Adersen S (1984) *Acta Chem Scand Ser A* 38:693
46. Okuno T, Ito S, Ohba S, Nishida Y (1997) *J Chem Soc Dalton Trans* 3547
47. England J, Davies CR, Banaru M, White AJP, Britovsek GJP (2008) *Adv Synth Catal* 350:883
48. England J, Gondhia R, Bigorra-Lopez L, Petersen AR, White AJP, Britovsek GJP (2009) *Dalton Trans* 27:5319
49. Clemente-Tejada D, López-Moreno A, Bermejo FA (2012) *Tetrahedron* 68:9249
50. Clemente-Tejada D, López-Moreno A, Bermejo FA (2013) *Tetrahedron* 69:2977
51. Company A, Gómez L, Güell M, Ribas X, Luis JM, Que L Jr, Costas M (2007) *J Am Chem Soc* 129:15766
52. Company A, Gómez L, Fontrodona X, Ribas X, Costas M (2008) *Chem Eur J* 14:5727
53. Prat I, Company A, Postils V, Ribas X, Que L Jr, Luis JM, Costas M (2013) *Chem Eur J* 19:6724
54. Prat I, Gómez L, Canta M, Ribas X, Costas M (2013) *Chem Eur J* 19:1908
55. Chen MS, White MC (2007) *Science* 318:783
56. Chen MS, White MC (2010) *Science* 327:566
57. Canta M, Font D, Gómez L, Ribas X, Costas M (2014) *Adv Synth Catal* 356:818
58. Comba P, Maurer M, Vadivelu P (2009) *Inorg Chem* 48:10389
59. Liu P, Liu Y, Wong E, Xiang S, Che C-M (2011) *Chem Sci* 2:2187
60. Hitomi Y, Arakawa K, Funabiki T, Kodera M (2012) *Angew Chemie Int Ed* 51:3448
61. Newhouse T, Baran PS (2011) *Angew Chemie Int Ed* 50:3362
62. Gormisky PE, White MC (2013) *J Am Chem Soc* 135:14052
63. Gómez L, Canta M, Font D, Prat I, Ribas X, Costas M (2013) *J Org Chem* 78:1421
64. Gómez L, Garcia-Bosch I, Company A, Benet-Buchholz J, Polo A, Sala X, Ribas X, Costas M (2009) *Angew Chemie Int Ed* 48:5720
65. Chen K, Richter JM, Baran PS (2008) *J Am Chem Soc* 130:7247
66. Kasuya S, Kamijo S, Inoue M (2009) *Org Lett* 11:3630
67. Simmons EM, Hartwig JF (2012) *Nature* 483:70
68. Wang Y-F, Chen H, Zhu X, Chiba S (2012) *J Am Chem Soc* 2012:11980
69. Zhang S-Y, He G, Zhao Y, Wright K, Nack WA, Chen G (2012) *J Am Chem Soc* 134:7313
70. Bigi MA, Reed SA, White MC (2012) *J Am Chem Soc* 134:9721
71. He Y, Gorden JD, Goldsmith CR (2011) *Inorg Chem* 50:12651
72. Djernes KE, Moshe O, Mettry M, Richards DD, Hooley RJ (2012) *Org Lett* 14:788
73. Djernes KE, Padilla M, Mettry M, Young MC, Hooley RJ (2012) *Chem Commun* 48:11576
74. Gonzalez-de-Castro A, Robertson CM, Xiao J (2014) *J Am Chem Soc* 136:8350
75. Bigi MA, Reed SA, White MC (2011) *Nat Chem* 3:216

# Site-Selective Conjugate Addition Through Catalytic Generation of Ion-Pairing Intermediates

Daisuke Uraguchi and Takashi Ooi

**Abstract** Site-selectivity in conjugate addition reactions is tightly associated with the principle of vinylogy. Various vinylogous nucleophiles and electrophiles have been applied to stereoselective conjugate additions directed by chiral small-molecule catalysts. This chapter focuses on the systems that control site- and stereoselectivity via chiral ion-pairing intermediates under organocatalytic conditions and describes individual vinylogous substrates in a separate section. Although site-selectivity originates largely from the intrinsic stereoelectronic nature of individual substrates, catalyst-controlled site-selectivity can be attained in certain cases.

**Keywords** Asymmetric catalysis • Ion-pairing • Organocatalysis • Vinylogy

## Contents

1	Introduction .....	56
2	Vinylogous Electrophiles .....	56
2.1	$\alpha,\beta,\gamma,\delta$ -Unsaturated Carbonyl Compounds .....	56
2.2	$\alpha,\beta,\gamma,\delta$ -Unsaturated Nitro Compounds .....	59
2.3	Iminium Activation of $\alpha,\beta$ -Unsaturated Ketones and Aldehydes .....	61
3	Vinylogous Nucleophiles .....	65
3.1	Azlactones .....	65
3.2	$\gamma$ -Butenolides .....	70

---

D. Uraguchi  
Department of Applied Chemistry, Graduate School of Engineering, Nagoya University,  
Furo cho, Chikusa ku, Nagoya, Aichi 464-8602, JAPAN

T. Ooi (✉)  
Institute of Transformative Bio-Molecules (WPI-ITbM) and Department of Applied  
Chemistry, Graduate School of Engineering, Nagoya University, and CREST, Japan Science  
and Technology Agency (JST), Furo cho, Chikusa ku, Nagoya, Aichi 464-8602, JAPAN  
e-mail: [tooi@apchem.nagoya-u.ac.jp](mailto:tooi@apchem.nagoya-u.ac.jp)

3.3	$\gamma$ -Butyrolactam .....	73
3.4	Alkylidene Malononitriles .....	76
3.5	$\alpha$ -Alkylidene Oxindoles and Lactones .....	79
3.6	Miscellaneous .....	81
4	Outlook .....	81
	References .....	81

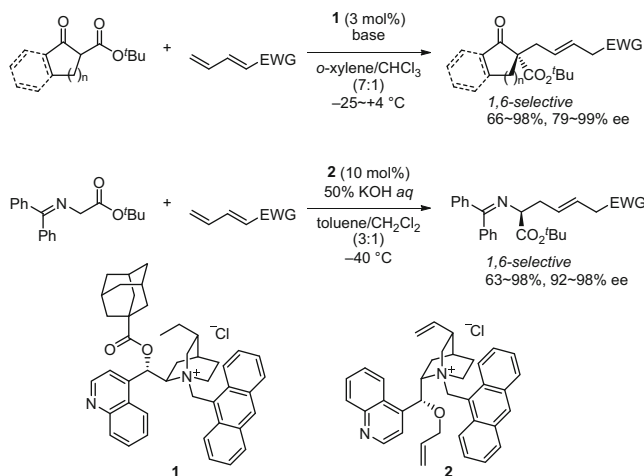
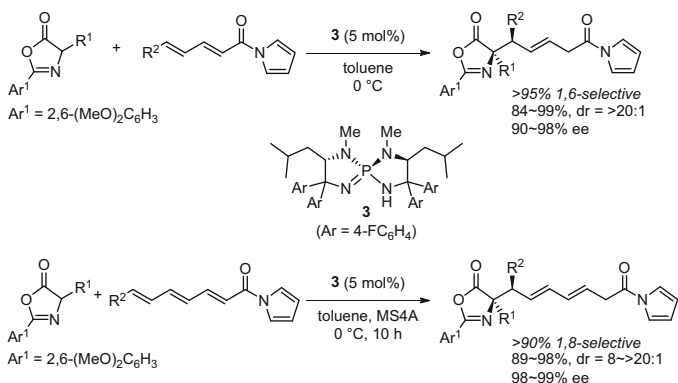
## 1 Introduction

The development of chemical transformations with the desired chemo-, site-, and/or stereoselectivity by exploiting reaction partners that embody several reactive and pro-stereogenic functionalities represents one of the main challenges at the forefront of organic synthesis. Among the requisite selectivity issues that should be addressed in the pursuit of this goal, control of the site-selectivity (regioselectivity) in conjugate addition poses a unique challenge which is tightly associated with the principle of vinylogy formulated by Reynold C. Fuson in 1935 for both electrophiles and nucleophiles [1]. According to this principle, when a double bond (s) is/are interposed between a functional group and the parent reactive site of a substrate, the influence of (that) functional group might sometimes be propagated along the chain and make itself apparent at some remote point in the molecule. Therefore, in addition reactions to the extended electron-deficient conjugate  $\pi$ -systems, discrimination of reaction sites is often required to afford defined, non-randomized products. Various useful protocols have been reported for vinylogous conjugate additions, such as copper-catalyzed asymmetric reactions of alkylmetals, and remarkable progress has been made in the field of enantioselective organocatalysis during the last 10 years [2–4]. Considering the critical importance of non-bonding interactions for achieving selectivity control by chiral organic molecules, this chapter focuses on a series of site-selective conjugate additions with vinylogous electrophiles/nucleophiles, which feature the involvement of ionic intermediates.

## 2 Vinylogous Electrophiles

### 2.1 $\alpha,\beta,\gamma,\delta$ -Unsaturated Carbonyl Compounds

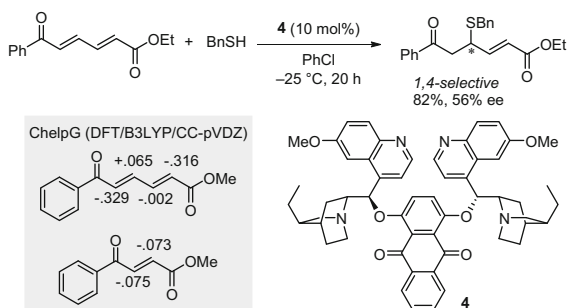
Conjugate addition to  $\alpha,\beta,\gamma,\delta$ -unsaturated carbonyl compounds is one of the simplest reactions involving site-selectivity. Because two reactive sites, the  $\beta$ - and  $\delta$ -positions relative to the carbonyl group, often have similar reactivity, nucleophiles can frequently attack both sites. Several catalysts effectively discriminate between two such sites, although it is generally difficult to understand the origin of the observed selectivity.

**Scheme 1** 1,6-Selective conjugate addition to  $\delta$ -unsaturated dienyl carbonyl compounds**Scheme 2** 1,6- and 1,8-Selective conjugate addition to polyenyl *N*-acyl pyrroles

The first highly site- and enantioselective conjugate addition of carbanionic nucleophiles to  $\alpha,\beta,\gamma,\delta$ -unsaturated carbonyl compounds was reported in 2007. The dihydrocinchoninium salt **1** was used as a phase-transfer catalyst in this reaction (Scheme 1) [5]. Under mild liquid–liquid biphasic conditions, various cyclic 1,3-dicarbonyl compounds were introduced into the  $\delta$ -position of electron-poor  $\delta$ -unsaturated  $\alpha,\beta,\gamma,\delta$ -unsaturated ketones, esters, and sulfones with excellent site- and enantioselectivities. In addition, cinchonidinium salt **2** appeared to be an effective catalyst for the 1,6-selective conjugate addition of a *tert*-butyl glycinate-derived Schiff base, allowing the synthesis of a series of highly enantioenriched,  $\alpha$ -tertiary chiral  $\alpha$ -amino acid derivatives possessing the  $\beta,\gamma$ -unsaturated carbonyl moiety as a side chain in good yield with high enantioselectivity.

In 2012, the site-, diastereo-, and enantioselective 1,6-conjugate addition to  $\delta$ -substituted dienyl *N*-acyl pyrroles was reported for the first time (Scheme 2)

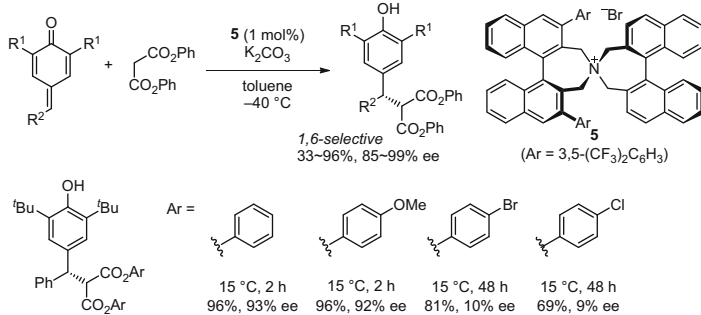
**Scheme 3** 1,4-Selective sulfa-Michael addition to 1,6-keto ester



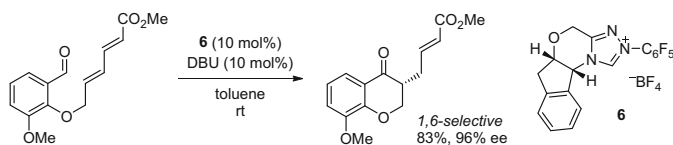
[6]. Natural L-leucine-derived *P*-spiro chiral triaminoiminophosphorane **3** deprotonated the acidic  $\alpha$ -proton of oxazol-5(*4H*)-one (azlactone) to form the chiral phosphonium enolate, which underwent selective carbon–carbon bond formation at the  $\delta$ -position of the vinylogous acceptor. Despite the similar steric nature of the  $\delta$ -carbon to that of the  $\beta$ -carbon, virtually complete site-selectivity was attained concurrently with rigorous diastereo- and enantiocontrol. Considering the known ambident character of azlactones (see Sect. 3.1), it was also remarkable that bond formation took place exclusively at the  $\alpha$ -carbon of the enolate, illustrating perfect site-selectivity with respect to the nucleophile. This catalytic system was successfully extended to the more challenging 1,8-selective conjugate addition to  $\zeta$ -substituted electron-deficient trienes. Use of 4-Å molecular sieves (MS4A) was crucial for achieving high site- and stereoselectivity in a firmly reproducible manner under the catalysis of iminophosphorane **3**.

Site-selectivity in the sulfa-Michael reaction of aliphatic thiols to divergently activated electron-deficient dienes has been studied (Scheme 3) [7]. Although (*2E,4E*)-6-oxo-2,4-dienoates possess four potentially reactive and electrophilic  $sp^2$ -carbons, benzylthiol predominantly attacked the  $\beta$ -position to the ketone carbonyl, affording the corresponding 1,4-addition product with moderate enantioselectivity with the aid of the cinchona alkaloid-derived dimeric catalyst **4**. To elucidate the origin of this selectivity profile, calculation of the electronic parameters, such as the ChelpG (i.e., Charges from Electrostatic Potentials using a Grid-based method), was attempted, revealing that the observed addition site was indeed the most electrophilic carbon having a positive ChelpG charge. However, this information relies only on the structure of the acceptor and thus provides no insight into the possible reaction mechanism.

Formal  $\alpha$ -diarylmethylation of malonates was achieved through the development of a 1,6-selective conjugate addition–aromatization sequence with *para*-quinone methides as vinylogous electrophiles (Scheme 4) [8]. The driving force toward aromatization would make nucleophilic addition to the  $\delta$ -position more thermodynamically favorable than addition to the  $\beta$ -position. Under solid–liquid biphasic conditions, the *N*-spiro chiral ammonium salt **5** appeared to be the most active and selective promoter. The electronic character of the aryl ester substituents on the malonate was linked to the stereochemical outcome, and introduction of a *para*-halophenyl group led to a significant decrease in the enantioselectivity. Based



**Scheme 4** 1,6-Selective conjugate addition/aromatization of *para*-quinone methides



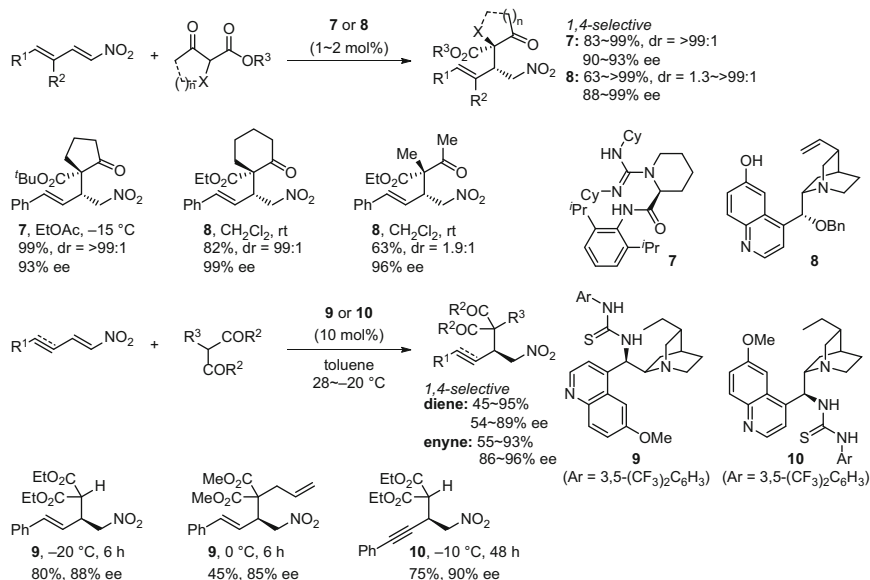
**Scheme 5** Intramolecular Stetter reaction with a 1,6-acceptor

on this finding, cooperative action of the ionic bonding and  $\pi$ - $\pi$  interaction between the 3,5-bis(trifluoromethyl)phenyl group [3,5-(CF<sub>3</sub>)<sub>2</sub>C<sub>6</sub>H<sub>3</sub>] of catalyst **5** and the aryloxy group of the nucleophile was proposed to be important in a plausible transition-state model.

Intramolecular reactions represent an attractive platform for achieving complete site-selectivity, as demonstrated in the Stetter reaction catalyzed by chiral tetracyclic carbene generated in situ from 1,2,4-triazolium salt **6** (Scheme 5) [9]. Subsequent to addition of the carbene to a formyl group of the substrate, the resulting Breslow intermediate smoothly reacted with the dienoate component in a 1,6-selective manner to form a six-membered ring. Because formation of an eight-membered ring incorporating a *trans*-alkene moiety through 1,4-addition is unfavorable, substrate-controlled complete site-selectivity was readily established.

## 2.2 $\alpha,\beta,\gamma,\delta$ -Unsaturated Nitro Compounds

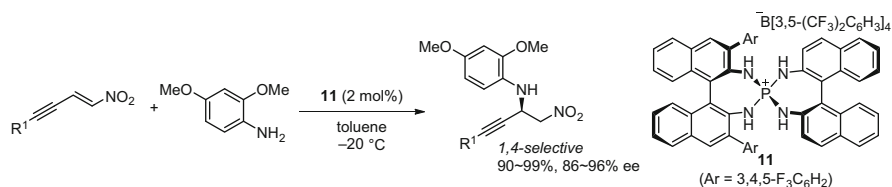
In contrast to the extensive use of nitroolefins in asymmetric Michael additions [10], the vinylogous analogues, nitrodienes and nitroenynes, are less frequently utilized in the conjugate addition of enolate equivalents, despite the significant synthetic utility of the resulting products which possess carbonyl, nitro, and olefin functionalities. Likewise, studies on the hetero-Michael reaction with these acceptors have been very limited, possibly because of apprehension of the site-selectivity issue [11].



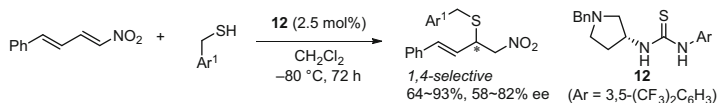
**Scheme 6** Conjugate addition of 1,3-dicarbonyl compounds to nitrodienes and nitroynes

In 2009, bifunctional guanidine **7** was found to be an effective catalyst for the 1,4-selective conjugate addition of cyclic  $\beta$ -ketoesters to nitrodienes to furnish unsaturated nitrocarbonyl compounds with vicinal quaternary-tertiary stereogenic carbon centers (Scheme 6) [12]. The products were subsequently derivatized into  $\beta$ -ramipril-type amino acid esters, which clearly demonstrated the synthetic utility of the site-selective adducts with the remaining olefinic moiety. This disclosure stimulated further research on this topic, and cinchona alkaloid-derived bifunctional amines such as **8** and **9** were discovered to be highly efficient catalysts for 1,4-selective conjugate addition of various 1,3-dicarbonyl compounds to nitrodienes [13, 14]. A proposed key element for achieving high selectivities is the simultaneous recognition of the electrophile and the nucleophile by the acidic group, arylhydroxide or thiourea, and a protonated bridgehead amino group of these catalysts through hydrogen-bonding interactions, although detailed experimental and theoretical mechanistic evaluation remain to be performed. These results suggest the intrinsic preference of nitrodiene to accept a nucleophile at the  $\beta$ -position. Moreover, the catalytic performance of amino-thiourea **10** was demonstrated in a similar conjugate addition to nitroynes, giving rise to non-conjugated nitroalkynes with moderate to high enantioselectivity [15]. The observed complete site-selectivity is partially derived from the general preference of nitroynes toward attack at the  $\beta$ -position.

When heteronucleophiles react with nitroolefins possessing extended conjugation at the  $\beta$ -position, the heteroatoms are appended to a stereogenic allylic or propargylic carbon, providing synthetically valuable nitro compounds. For example, aza-Michael addition to nitroynes under catalysis of the ionic Brønsted acid, chiral tetraarylammonium phosphonium barfate **11**, produced the propargylic amine



**Scheme 7** 1,4-Selective aza-Michael addition to nitroynes



**Scheme 8** 1,4-Selective sulfa-Michael addition to nitrodienes

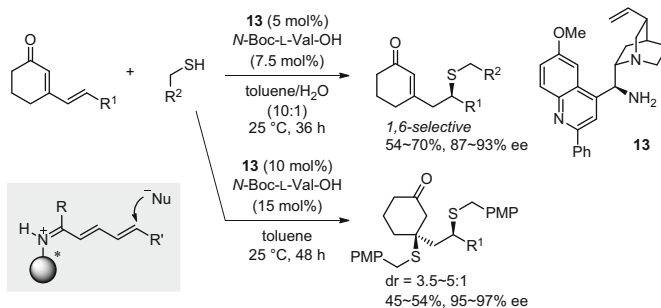
possessing a nitro group with high enantioselectivity (Scheme 7) [16]. Considering the rich chemistry associated with the transformation of the triple bond and the nitro group, this protocol could serve as a useful tool for accessing chiral amines, which was in fact demonstrated by derivatization of the product to chiral 1,2-diamine in three steps.

During study of the chiral thiourea **12**-catalyzed sulfa-Michael addition of aliphatic thiols to nitroolefins, benzylic mercaptans were subjected to the reaction with nitrodienes (Scheme 8) [17]. Exclusive formation of 1,4-adducts was observed in moderate to good chemical yield with moderate to fair enantioselectivity.

### 2.3 Iminium Activation of $\alpha,\beta$ -Unsaturated Ketones and Aldehydes

Since the seminal report by MacMillan in 2000 [18], LUMO-lowering activation via reversible formation of an iminium with chiral amines has been recognized as one of the most reliable and powerful strategies for catalyzing asymmetric conjugate addition to  $\alpha,\beta$ -unsaturated aldehydes and ketones with rigorous stereocontrol [19]. However, the marriage of this activation mode with the concept of vinylogy remained uninvestigated for over 10 years. Recently, the iminium activation has been extended to vinylogous acceptors and the effectiveness of this strategy has been demonstrated using various nucleophiles [20].

By exploiting the experiential development of vinylogous enamine catalysis, the first systematic study of iminium activation in conjunction with vinylogous acceptors was reported in 2012, which focused on sulfa-Michael addition to  $\beta$ -vinylic cyclohexenones as a model reaction (Scheme 9) [21]. The vinylogous iminium intermediate generated from the dienone and primary amine catalyst **13** having a tertiary amino group reacted with thiols at the  $\delta$ -position selectively and the corresponding  $\delta$ -thio enone was predominantly formed in moderate yield with high enantioselectivity. Configurational control of the extended iminium system

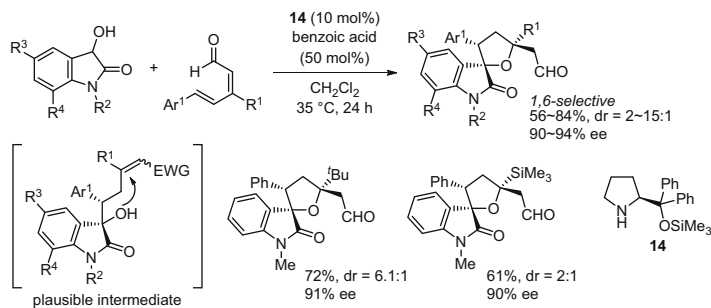
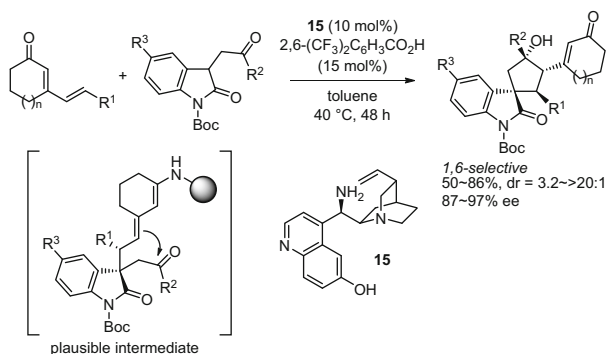
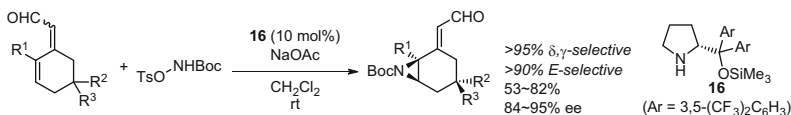


**Scheme 9** 1,6-Selective sulfa-Michael addition via vinylogous iminium activation

and  $\pi$ -facial discrimination at the remote position by the single chiral catalyst are essential for realizing high levels of enantiocontrol. Interestingly, the structure of the acid co-catalyst had a slight effect on the enantioselectivity, and *N*-Boc-protected *L*-valine was identified to be optimal. The remaining enone moiety of the 1,6-adducts was amenable to subsequent functionalization, as demonstrated in the cascade reaction involving both 1,6- and 1,4-addition of benzylic mercaptans. Nearly enantiomerically pure products were isolated with moderate diastereoselectivity under slightly forcing conditions.

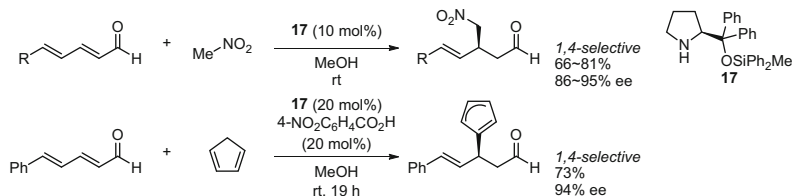
The merger of iminium activation with vinylogy in conjugate additions has been achieved with acyclic electrophiles such as 2,4-dienals. A 1,6-selective conjugate addition/standard oxy-Michael cascade with 3-hydroxyoxindoles and 2,4-dienals was catalyzed by diarylprolinol trimethylsilyl ether **14** to afford tetrahydrofuran spirooxindole derivatives (Scheme 10) [22]. The  $\beta$ -substituent  $R^1$  of the 2,4-dienal was revealed to have a critical impact on the site-selectivity as well as the stereoselectivity. When simple 2,4-hexadienal ( $R^1 = \text{H}$ ,  $\text{Ar}^1 = \text{Me}$ ) was treated with *N*-methyl 3-hydroxyoxindole in the presence of **14** and benzoic acid, 1,4-selective conjugate addition followed by intramolecular acetalization was the predominant pathway. In the reaction with 3,5-diphenyl 2,4-pentadienal ( $R^1 = \text{Ph}$ ,  $\text{Ar}^1 = \text{Ph}$ ) under otherwise similar conditions, complete switching of the reaction pathway to 1,6-selective conjugate addition-initiated spirocyclization was observed, albeit with moderate stereoselectivity ( $\text{dr} = 8:1$ , 46% ee). The enantioselectivity was markedly improved to 88% ee ( $\text{dr} = 5.5:1$ ) by introduction of the bulky *tert*-butyl group ( $R^1 = \text{tBu}$ ,  $\text{Ar}^1 = \text{Ph}$ ), which was accounted for by the configurational stability of the vinylogous iminium intermediate possessing a sterically demanding substituent at the 3-position. Although this requirement could negate the synthetic utility of this protocol, it was secured by the use of the removable trimethylsilyl group which provided a similar effect.

Utilization of a vinylogous enamine generated via 1,6-selective addition to  $\alpha,\beta,\gamma,\delta$ -unsaturated iminium intermediate could potentially provide an intriguing synthetic handle for achieving greater molecular complexity. Experimental demonstration of the feasibility of this approach was provided in the development of a 1,6-selective conjugate addition/vinylogous aldol sequence catalyzed by the

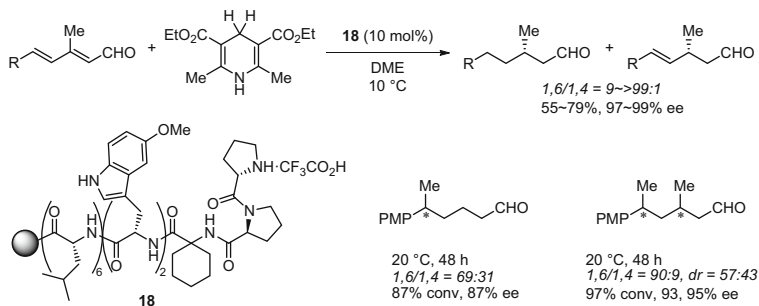
**Scheme 10** 1,6-Conjugate addition-oxy-Michael addition sequence**Scheme 11** 1,6-Conjugate addition-aldol reaction domino sequence**Scheme 12** Remote aziridination of 2,4-dienals

cinchona alkaloid-derived primary amine **15** bearing arylhydroxide and tertiary amine moieties (Scheme 11) [23]. The efficiency of this transformation was greatly affected by the acidity of the co-catalyst. Although the reaction was sluggish in the absence of an additional acid or in the presence of a strong acid such as CF<sub>3</sub>CO<sub>2</sub>H, addition of 2,6-bis(trifluoromethyl)benzoic acid [2,6-(CF<sub>3</sub>)<sub>2</sub>C<sub>6</sub>H<sub>3</sub>CO<sub>2</sub>H] accelerated this cascade-type transformation with high stereoselectivity. This study reveals the power of the catalyst **15** to propagate not only iminium activation but also enamine activation through the conjugated  $\pi$ -system and to transmit the stereochemical information to remote positions.

Similarly, the combined use of LUMO-lowering and HOMO-raising strategies facilitated formation of aziridines at the  $\gamma,\delta$ -olefinic moiety of conformationally restricted cyclic 2,4-dienals (Scheme 12) [24]. The appropriately modified



**Scheme 13** 1,4-Selective conjugate addition to  $\alpha,\beta,\gamma,\delta$ -unsaturated iminium ion



**Scheme 14** Peptide-catalyzed conjugate reduction of  $\alpha,\beta,\gamma,\delta$ -dienals

diarylprolinol trimethylsilyl ether **16** promoted remote aziridination in moderate to good yield with high stereoselectivity.

As illustrated in Scheme 10, conjugate addition to  $\delta$ -monosubstituted 2,4-dienals under iminium catalysis preferentially afforded 1,4-adducts. This phenomenon was further investigated in the addition to unbiased dienal acceptors (Scheme 13), and *ab initio* calculations were carried out to probe the electronic profile of the vinylogous iminium intermediates [25]. The nitronate of nitromethane exclusively attacked the  $\beta$ -position of 2,4-dienals activated by diarylprolinol silyl ether **17** to furnish  $\gamma$ -nitro aldehydes with high enantioselectivity. Interestingly, cyclopentadiene could be employed as a nucleophile in the reaction, where complete 1,4-selectivity was also observed. A rational explanation of this site-selectivity was sought by theoretical analysis of the  $\pi$ -orbital coefficient of the LUMO and the atomic charge (Mulliken and ChelpG) of the vinylogous iminium ion derived from  $\text{Me}_2\text{NH}$  and 5-unsubstituted- or 5-phenyl-2,4-pentadienal. This quantum study suggested that the LUMO of the vinylogous iminium cation and the positive charge on the carbon atoms decrease in the order;  $\text{C}2 > \text{C}4 > \text{C}6$ , which facilitated comprehension of the origin of site-selectivity in this system.

Within the context of chiral secondary amine-catalyzed conjugate reduction, the polyethylene glycol grafted polystyrene resin-supported peptide **18** was developed as an effective catalyst for the 1,6-selective transfer hydrogenation of 3-methyl-2,4-dienals with Hantzsch ester, followed by enantioselective 1,4-reduction (Scheme 14) [26]. The combination of the five terminal residues of the catalyst,

including the turn motif and polyisoleucine unit, was essential to attain high site- and enantioselectivity. The importance of the catalyst structure for achieving site-selectivity was also demonstrated by the attempted use of simple cyclic secondary amines such as pyrrolidine and morpholine as catalysts, where 1,4-reduction of the dienal was predominant. This study was further extended to consecutive 1,6- and 1,4-conjugate additions of thiols by using a similar resin-supported peptide catalyst, namely Pro-D-Pro-Aib-(Trip)<sub>2</sub>-(Leu-Leu-Aib)<sub>2</sub>-(resin) [27].

### 3 Vinylogous Nucleophiles

#### 3.1 Azlactones

Azlactone is commonly utilized as a precursor of  $\alpha$ -quaternary  $\alpha$ -amino acids and various heterocyclic compounds [28–30]. Because the enol form of azlactone has aromatic character, facile deprotonation from the C4-position affords the corresponding enolate under the influence of various bases. Interestingly, the enolate ion shows ambident reactivity and attacks the electrophile at either the C4-position ( $\alpha$ -addition) or the C2-position ( $\gamma$ -addition), thus acting as an  $\alpha$ -amino enolate or an acyl anion equivalent, respectively (Fig. 1). The site-selectivity associated with this enolate seems to be heavily dependent on its stereoelectronic characteristics, and introduction of a bulky substituent into the C2- or C4-position suppresses the nucleophilicity at the particular position.

The effects of substituents on the oxazoline core on the site-selectivity have been empirically determined by investigation of the conjugate addition of azlactones to nitroolefins catalyzed by cinchona alkaloid-derived thioureas **19** (Scheme 15) [31]. Whereas phenylglycine-derived azlactone bearing a phenyl group at the C4-position reacted with nitroolefins selectively at the C4-position ( $\alpha$ -selective), C4-alkyl azlactones exhibited  $\gamma$ -selectivity under similar reaction conditions. In both cases, generally high diastereoselectivity and moderate to good enantioselectivity were attained with appropriately modified catalysts.

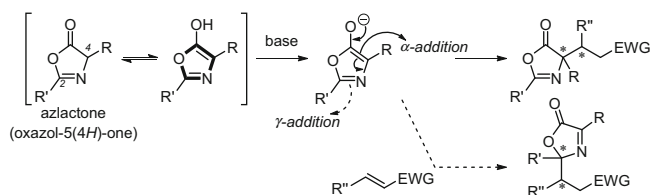
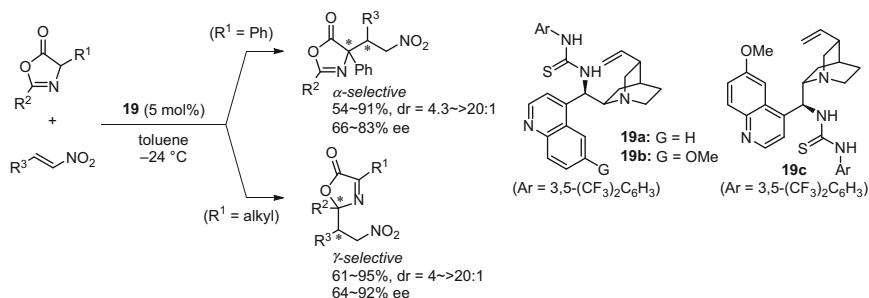
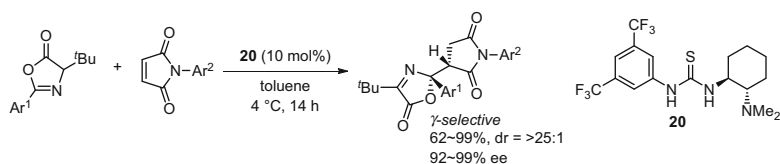


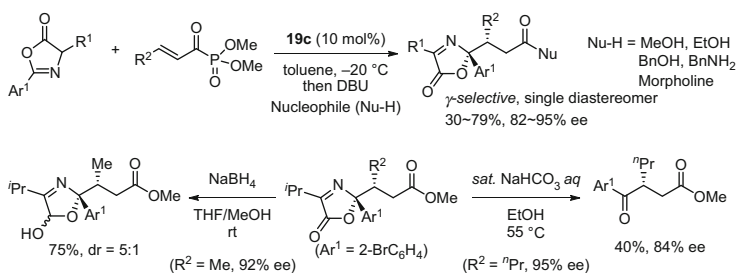
Fig. 1 General addition mode of azlactones



**Scheme 15** Ambident reactivity of azlactones



**Scheme 16**  $\gamma$ -Selective conjugate addition of azlactones to  $N$ -aryl maleimides

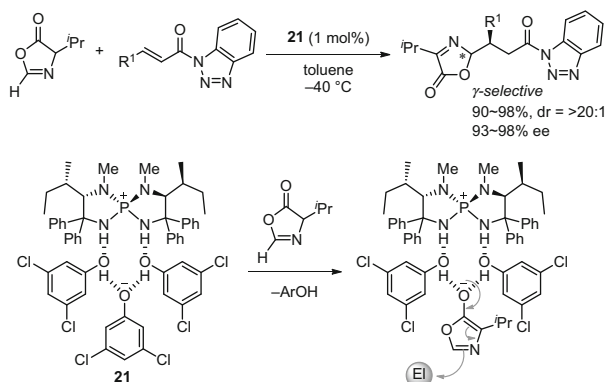


**Scheme 17**  $\gamma$ -Selective conjugate addition to  $\alpha,\beta$ -unsaturated acyl phosphonates

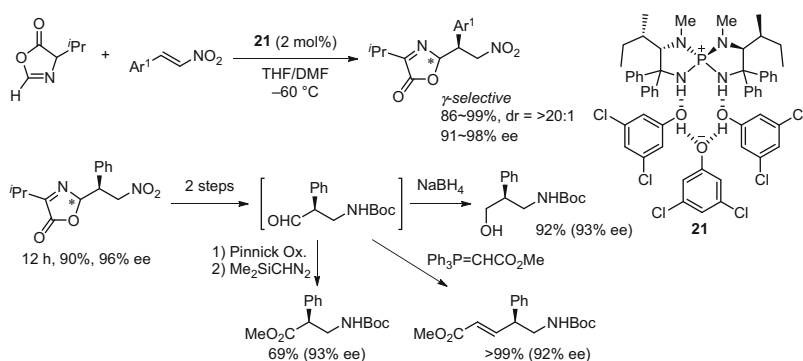
### 3.1.1 $\gamma$ -Addition

Increasing the steric hindrance at the C4-position is a general strategy for realizing complete  $\gamma$ -selectivity in the addition of azlactone enolates. In fact, *tert*-leucine-derived azlactone reacted with  $N$ -aryl maleimides predominantly at the C2-position with excellent diastereo- and enantiocontrol by use of amino thiourea **20** as a bifunctional catalyst (Scheme 16) [32].

In a similar manner, conjugate addition of azlactones possessing isopropyl or isobutyl groups at the C4-position to a series of acyl phosphonates proceeded with  $\gamma$ -selectivity and high stereoselectivity under the catalysis of quinine-derived thiourea **19c**. The phosphonate moiety of the resulting adducts was readily replaced with various heteronucleophiles such as alcohols and amines in situ under the influence of 1,8-diazabicyclo[5.4.0]undec-7-ene (DBU) (Scheme 17) [33]. The synthetic utility of azlactones as an acyl anion equivalent in this  $\gamma$ -selective addition



**Scheme 18**  $\gamma$ -Selective conjugate addition of 2-unsubstituted azlactone



**Scheme 19** Synthesis of  $\beta$ - and  $\delta$ -amino acid derivatives via  $\gamma$ -selective conjugate addition

was also demonstrated by the single-step derivatization of the adduct into the corresponding 1,4-ketoester. Although performing this transformation with weak base under gentle heating for 14 h led to almost complete racemization, the enantiomeric excess of 84% was conserved by quenching the reaction after 2 h.

$\gamma$ -Selective conjugate addition of C2-unsubstituted azlactone was utilized as a platform for the development of the supramolecular ion-pair catalysis of the chiral aminophosphonium aryloxy-arylhydroxide complex **21** (Scheme 18) [34, 35]. Nearly complete diastereo- and enantioselectivity were uniformly observed with a variety of  $\beta$ -aryl- and alkyl-substituted  $\alpha,\beta$ -unsaturated acyl benzotriazole acceptors. Intriguingly, in the proposed catalytic cycle, the enolate of the azlactone was recognized as a phenol equivalent by the aminophosphonium ion in the spontaneous formation of a nucleophilic supramolecular assembly.

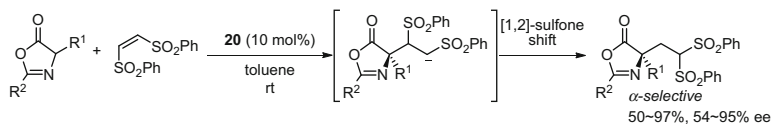
The asymmetric catalysis of the phosphonium aryloxy-arylhydroxide assembly **21** was also applicable to the  $\gamma$ -selective conjugate addition of C2-unsubstituted azlactone to nitroolefins, where use of a polar solvent system was crucial for sufficient reaction efficiency and stereoselectivity (Scheme 19) [36]. Various

aromatic nitroolefins were tolerated, providing the conjugate adducts with excellent stereocontrol, although moderate diastereoselectivity was observed with a single aliphatic example ( $\text{Ar}^1 = \text{cyclohexyl}$ ,  $\text{dr} = 4:1$ ). The oxazolone moiety of the adduct ( $\text{Ar}^1 = \text{Ph}$ ) was converted into a formyl group with minimal loss of enantiopurity, which could serve as a versatile precursor of useful chiral building blocks. Indeed, Wittig olefination of the resulting *N*-Boc amino aldehyde furnished the  $\alpha$ , $\beta$ -unsaturated  $\delta$ -amino acid derivative in quantitative yield, whereas Pinnick oxidation followed by methyl ester formation afforded protected  $\beta^2$ -homophenylglycine, one of the most synthetically challenging classes of  $\beta^2$ -amino acids.

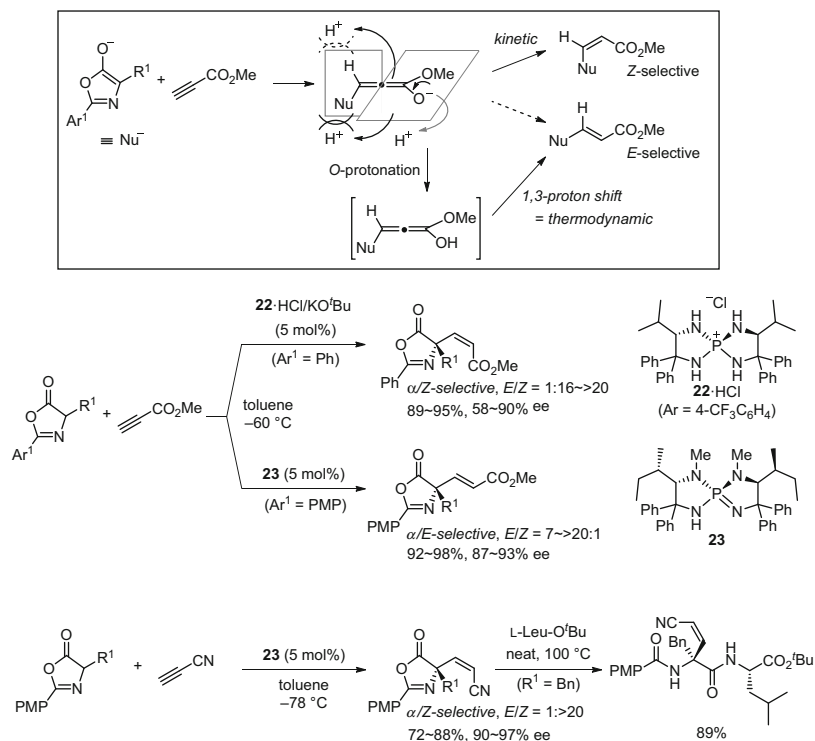
### 3.1.2 $\alpha$ -Addition

Selective  $\alpha$ -addition of C4-substituted azlactones was observed in the Michael addition-[1,2]-sulfone rearrangement sequence, which proceeded with moderate to good enantioselectivity (Scheme 20) [37]. Although 5% of the  $\gamma$ -addition product was detected in the reaction with triethylamine as a base, the use of bifunctional amino-thiourea **20** was pivotal for achieving complete site-selectivity and high enantioselectivity.

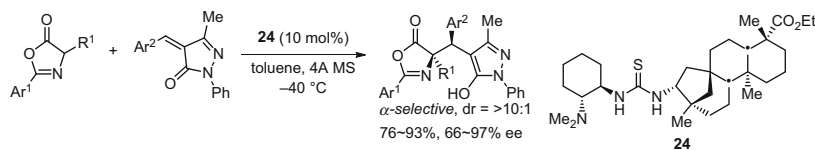
In the conjugate addition of C4-substituted azlactones to electron-deficient terminal alkynes, the azlactones exhibited exclusive  $\alpha$ -preference, and chiral iminophosphorane catalysis enabled geometrically divergent addition of the azlactone to methyl propiolate (Scheme 21, middle) [38]. The geometrical selectivity of the adducts sharply reversed with a change in the spiro-chirality of the catalyst; the *M*- and *P*-isomers of the iminophosphoranes (**22** and **23**) provided *Z*- and *E*-diastereomers, respectively. This unique *E/Z*-selectivity switching was proposed to originate from differences in the protonation pathway. In contrast with the kinetically controlled *Z*-selectivity achieved via *C*-protonation by the phosphonium ion **22**-H, uncommon *O*-protonation of the intermediary allenic enolate followed by 1,3-proton shift was postulated to rationalize the *E*-selectivity observed in the reaction with the sterically demanding iminophosphorane **23**. The validity of this hypothesis was verified through the development of a protocol for highly *Z*- and enantioselective conjugate addition of azlactones to cyanoacetylene using **23** as a catalyst (Scheme 21, bottom). Because the intermediate of this reaction,  $\alpha$ -cyano vinylic anion, has substantial carbanionic character, only *C*-protonation should take place, even with the hindered proton source **23**-H. The substrate scope with respect to azlactones was extensive, and simple heating of the product with an  $\alpha$ -amino acid



**Scheme 20**  $\alpha$ -Selective conjugate addition of azlactone to bis(phenylsulfanyl)ethene



**Scheme 21**  $\alpha$ - and  $E/Z$ -Selective conjugate addition to methyl propiolate and cyanoacetylene

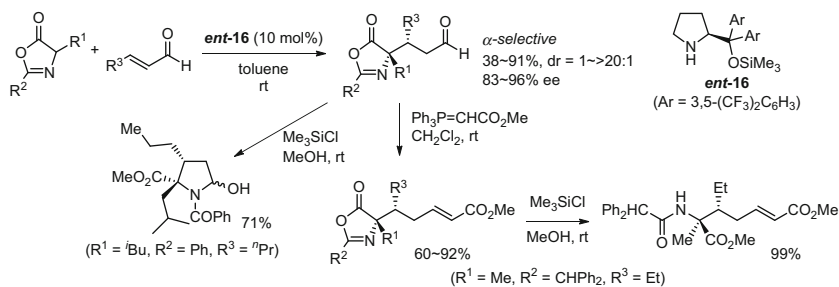


**Scheme 22**  $\alpha$ -Selective conjugate addition/aromatization of  $\alpha,\beta$ -unsaturated pyrazolones

ester ( $L$ -Leu- $O^t$ Bu) gave rise to a non-natural dipeptide without any loss of the enantiopurity.

Complete  $\alpha$ -selectivity was observed in the isosteviol-derived amino-thiourea **24**-catalyzed conjugate addition-aromatization reaction of azlactone with  $\alpha,\beta$ -unsaturated pyrazolones (Scheme 22) [39]. Although generally good to excellent chemical yield and stereoselectivity were obtained with C2-aryl azlactones, the reaction failed with C2-alkyl azlactone ( $Ar^1 = ^t$ Bu,  $R^1 = ^i$ Pr) even at room temperature with 30 mol% catalyst loading.

Because azlactone enolates can be generated under very mild conditions, these species were applied to chiral secondary amine **ent-16**-catalyzed conjugate addition to enals, which proceeded via iminium activation (Scheme 23) [40]. Variable



**Scheme 23**  $\alpha$ -Selective conjugate addition of azlactone via iminium activation

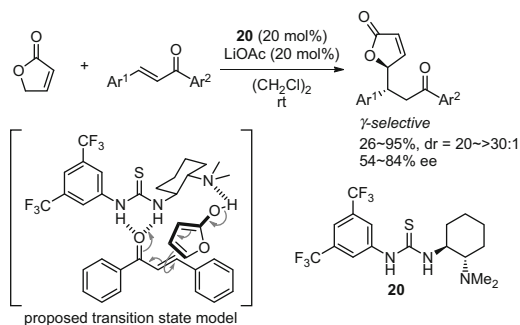
combinations of azlactones and enals were possible in this system and the corresponding adducts were obtained in moderate yield with high enantioselectivity. Notably, the  $\alpha,\beta,\gamma,\delta$ -unsaturated aldehyde ( $\text{R}^3 = (E)$ -prop-1-enyl) reacted at the  $\beta$ -position. The utility of this protocol was highlighted by methanolysis of the oxazolone ring of the products to afford a series of protected  $\alpha$ -quaternary  $\alpha$ -amino acids. Diphenylprolinol *tert*-butyldimethylsilylether was subsequently found to be a superior catalyst for similar conjugate addition of C2-phenyl- and C2-(4-methoxyphenyl)-substituted azlactones to enals [41].

### 3.2 $\gamma$ -Butenolides

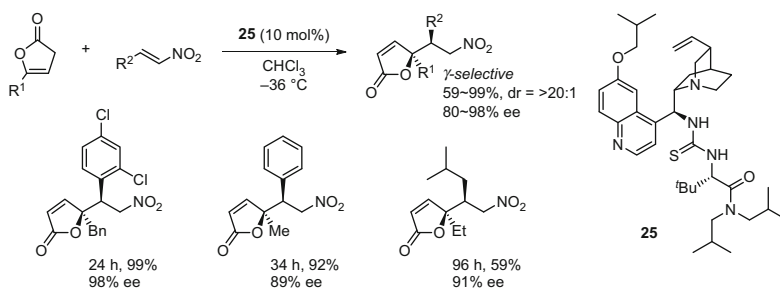
Upon treatment of  $\gamma$ -butenolides with an appropriate base, aromatization-driven enol formation takes place as observed with azlactones. Although the steric environment of the  $\alpha$ - and  $\gamma$ -positions bears a close resemblance, only  $\gamma$ -selective reactions have been reported in the literature. Because the  $\gamma$ -butyrolactone structural motif is frequently found in biologically relevant molecules, development of catalysts for asymmetric introduction of  $\gamma$ -butenolides into organic frameworks in a stereoselective fashion is highly desirable. For conjugate addition of  $\gamma$ -butenolides, bifunctional catalysts seem to be a uniquely effective class of promoters.

In the conjugate addition of bare  $\gamma$ -butenolide to chalcone derivatives, the use of Takemoto's catalyst **20** and lithium acetate was an optimal combination for achieving excellent diastereoselectivity and moderate enantioselectivity (Scheme 24) [42]. The proposed transition-state model suggested the importance of simultaneous recognition of both substrates via hydrogen-bonding interaction between the *tert*-amine moiety of **20** and the enol form of the butenolide, and hydrogen bonding of the thiourea subunit and an enone carbonyl group.

The strong preference of  $\gamma$ -butenolides to react at the  $\gamma$ -position in conjugate addition was demonstrated in the reaction of  $\gamma$ -substituted  $\gamma$ -butenolides with nitroolefins (Scheme 25) [43]. Under the catalysis of aminothiourea **25**, bond formation occurred at the sterically encumbered  $\gamma$ -position with high site- and stereoselectivity. The sense of stereoinduction was dictated by the *tert*-leucine



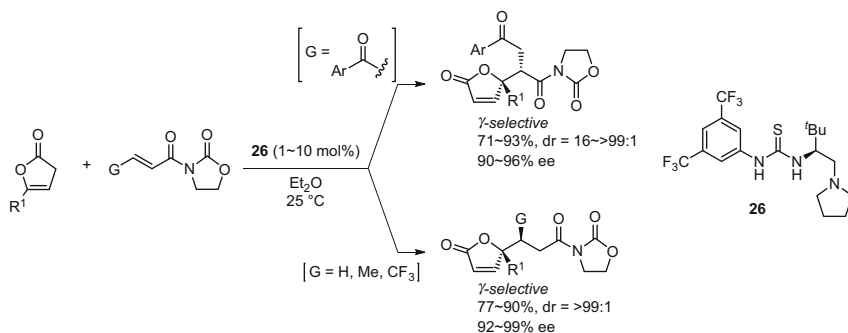
**Scheme 24**  $\gamma$ -Selective addition of butenolides catalyzed by bifunctional organocatalyst



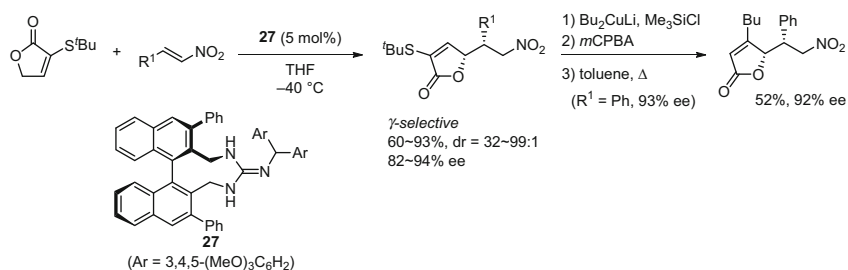
**Scheme 25**  $\gamma$ -Selective addition of butenolides to nitroolefins

segment of **25**, implying the importance of the thiourea moiety in the stereo-determining step. The resulting nitrocarbonyl compound possessing contiguous quaternary-tertiary stereocenters might serve as synthetically versatile chiral building blocks.

Simultaneous control of the site-selectivity with respect to nucleophiles and electrophiles was pursued in the conjugate addition of  $\gamma$ -substituted  $\gamma$ -butenolides to (*E*)-4-oxo-4-arylbutenamides (Scheme 26, top) [44]. Extensive survey of the catalytic potential of a series of bifunctional chiral amines revealed that the amino thiourea **26** bearing a *tert*-butyl group was the best promoter for attaining high stereoselectivity. Although the aryl ketone component in the electrophiles was the primary activating group of the olefinic moiety to dictate the site-selective introduction of the nucleophiles at the  $\alpha$ -position of the imide carbonyl ( $\beta$ -position relative to the ketone), the presence of the oxazolidinone carbonyl was crucial in terms of enantiocontrol. Interestingly, the simple yet  $\gamma$ -selective conjugate addition of  $\gamma$ -butenolides to oxazolidinone enoates was also promoted by **26** with high stereoselectivity, although the carbonyl group responsible for the reacting site of the electrophile differed from that in the doubly site-selective reaction (Scheme 26, bottom). The efficacy of the amino thiourea **26** in a similar reaction with (*Z*)- $\beta$ -trifluoromethyl oxazolidinone enoate demonstrated the potential for development of a diastereodivergent catalyst system.



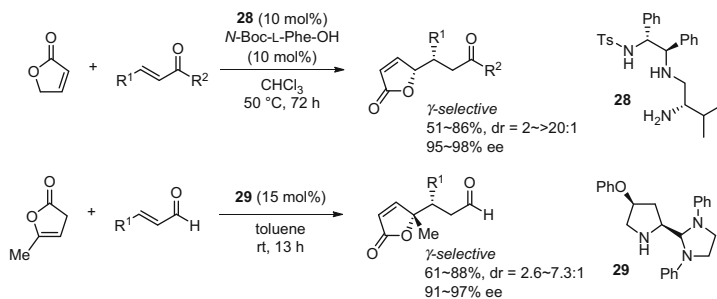
**Scheme 26**  $\gamma$ -Selective addition of  $\gamma$ -substituted butenolides



**Scheme 27**  $\gamma$ -Selective addition of butenolides catalyzed by organic superbase

Axially chiral guanidine **27** was introduced as a highly efficient stereocontroller for the reactions with  $\gamma$ -butenolide enolates, especially 2-thio-substituted derivatives [45]. The characteristic feature of **27** as a chiral organic base catalyst enabled establishment of a highly diastereo- and enantioselective protocol for conjugate addition to nitroolefins, where the structure of the thioether moiety was very important for attaining high enantioselectivity, and *tert*-butylsulfide was an optimal substituent (Scheme 27) [46]. Removability of the sulfide group via an oxidative sequence was demonstrated in the product derivatization process.

Although the  $pK_a$  of the simple  $\gamma$ -butenolide seems to be rather high, multifunctional iminium-activation catalysts bearing an additional amino group can force adoption of the enol form in the keto-enol equilibrium and induce carbon-carbon bond formation with transient iminium species. For example, the in situ-generated salt of the trifunctional primary amine **28** and *N*-Boc-*L*-phenylalanine catalyzed  $\gamma$ -selective conjugate addition of  $\gamma$ -butenolide to  $\alpha,\beta$ -unsaturated ketones in a highly stereoselective manner (Scheme 28, top) [47]. The acidic additive exerted a profound effect on the stereoselectivity, and the steric bulkiness of the acid was proposed to be a critical element. Importantly, the chirality of the amino acid derivative had a negligible impact on the stereoselectivity.



**Scheme 28**  $\gamma$ -Selective addition of  $\gamma$ -butenolides via iminium activation

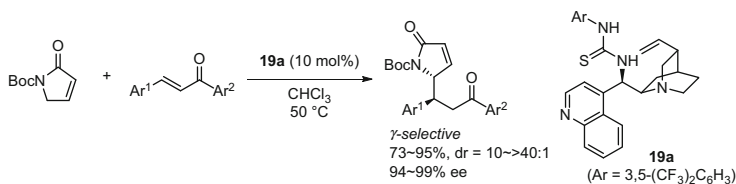
A similar strategy was applied to the conjugate addition of  $\alpha$ -angelicalactone to enals (Scheme 28, bottom) [48]. Because the  $pK_a$  of  $\alpha$ -angelicalactone at the  $\alpha$ -position is relatively low, the chiral secondary amine **29** possessing an aминаl moiety could promote a moderately diastereoselective but highly enantioselective reaction. The skipped enoate structure of  $\alpha$ -angelicalactone was crucial for this transformation and, indeed, treatment of the conjugated isomer ( $\beta$ -angelicalactone) with **29** under otherwise identical conditions produced only a trace amount of the corresponding product (<5% conversion).

### 3.3 $\gamma$ -Butyrolactam

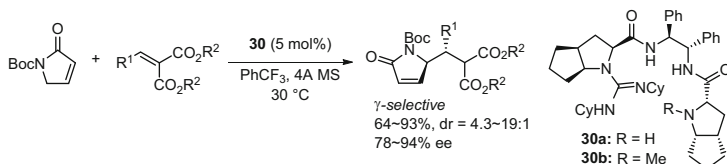
In the conjugate addition of *N*-Boc  $\gamma$ -butyrolactam, the site-selectivity and the efficacy of the catalysts followed almost the same trends with those observed in the reactions with  $\gamma$ -butenolides. Complete  $\gamma$ -selectivity was generally observed under various reaction conditions and highly stereoselective systems were reported, which were mainly based on the use of multifunctional catalysts. However, the effect of nitrogen-protecting groups other than Boc and introduction of substituents at the 3-, 4-, and 5-positions has not been extensively evaluated to date.

Cinchona alkaloid-derived thiourea **19a** was an effective catalyst for the conjugate addition of *N*-Boc  $\gamma$ -butyrolactam to various chalcone derivatives; the corresponding adducts were obtained in good yield with high diastereo- and enantioselectivities, although a relatively long reaction time was required (48–84 h) (Scheme 29) [49]. Chloroform proved to be the best reaction medium; nevertheless, this protocol tolerated other standard organic solvents such as toluene, MeCN, THF, and  $\text{CH}_2\text{Cl}_2$  in terms of stereoselectivity but not catalytic efficiency. The aromatic substituent at the 1-position of the enone ( $\text{Ar}^2$ ) was essential for attaining sufficient reactivity, and only a trace amount of the products was detected in the reactions with aliphatic analogues ( $\text{Ar}^2 = \text{alkyl}$ ).

Alkylidene malonates are good candidates as highly electrophilic acceptors in the  $\gamma$ -selective conjugate addition of  $\gamma$ -butyrolactam under the catalysis of multifunctional chiral guanidine **30a** (Scheme 30) [50]. Nearly complete



**Scheme 29** Bifunctional thiourea catalyzed  $\gamma$ -selective addition of  $\gamma$ -butyrolactam

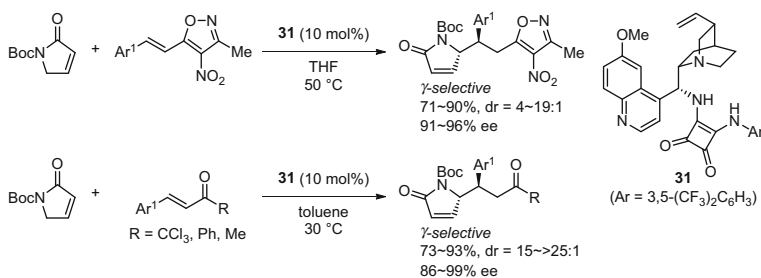
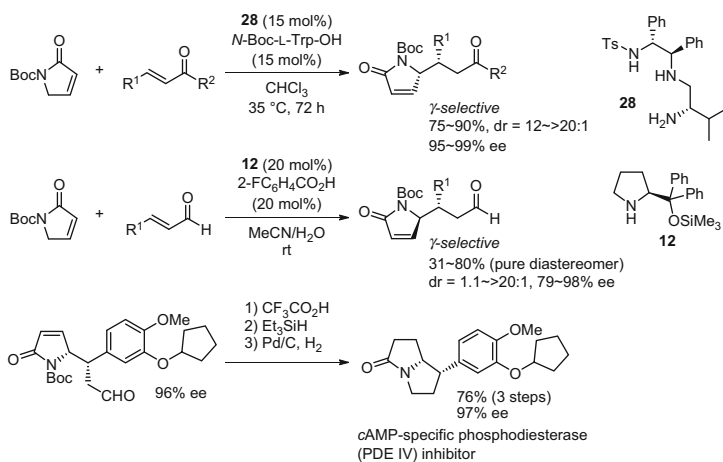


**Scheme 30**  $\gamma$ -Selective addition catalyzed by guanidine possessing a secondary amine subunit

diastereoselectivity and excellent enantioselectivity were observed with aromatic acceptors ( $\text{R}^1 = \text{aryl}$ ), but a slight decrease in stereoselectivity was inevitable in the reaction with acceptors bearing cinnamyl and cyclohexyl substituents at the  $\beta$ -position. The presence of guanidine and secondary amine subunits in the catalyst was indispensable for promotion of the conjugate addition. The *N*-Me analogue **30b** provided the product in only 15% yield with diminished enantioselectivity (71% ee) after 18 h of stirring under the optimized conditions.

In the  $\gamma$ -selective conjugate addition of the  $\gamma$ -butyrolactam to 3-methyl-4-nitro-5-alkenyl isoxazoles, the importance of a hydrogen-bonding site in the bifunctional amine catalysts was argued (Scheme 31, top) [51]. Specifically, the squaramide group of the optimal quinine-derived catalyst **31** had a prominent effect on the reaction efficiency, diastereoselectivity, and enantioselectivity. Various aromatic and heteroaromatic acceptors were amenable to the asymmetric catalysis of **31**. However, introduction of strongly electron-deficient aromatic substituents onto the vinyl terminus ( $\text{Ar}^1 = 4\text{-CF}_3\text{C}_6\text{H}_4$ ,  $4\text{-CNC}_6\text{H}_4$ ,  $4\text{-NO}_2\text{C}_6\text{H}_4$ ,  $3,4\text{-Cl}_2\text{C}_6\text{H}_3$ ) decreased the diastereomeric ratio (dr = 4–7:1). The high performance of the catalyst **31** allowed the accommodation of simple  $\beta$ -aryl  $\alpha,\beta$ -unsaturated ketones, including  $\alpha,\alpha,\alpha$ -trichloromethyl enones, as an acceptor and excellent stereoselectivity was obtained under very mild conditions (Scheme 31, bottom).

The iminium activation strategy with the trifunctional chiral primary amine **28**, which was used in the  $\gamma$ -selective conjugate addition of  $\gamma$ -butenolides (Scheme 28), also proved highly effective for promoting reaction with the  $\gamma$ -butyrolactam (Scheme 32, first line) [52]. Although various chiral diamines, amino thioureas, and amino sulfonamides were evaluated during the optimization study, none of these catalysts gave rise to impressive levels of diastereoselectivity. Eventually, a bulky acid additive, such as the protected tryptophan derivative (*N*-Boc-*L*-Trp-OH),

**Scheme 31**  $\gamma$ -Selective 1,6- and 1,4-addition catalyzed by bifunctional squaramide**Scheme 32** Synthesis of PDE IV inhibitor through  $\gamma$ -selective addition of  $\gamma$ -butyrolactam

was identified as a requisite co-catalyst for enhancing the diastereoselectivity, which mirrors the observation in the  $\gamma$ -butenolide addition. With the optimal catalyst combination, the  $\gamma$ -butyrolactam underwent  $\gamma$ -selective addition to the  $\beta$ -carbon of a wide variety of methyl enones ( $R^2 = \text{Me}$ ) with excellent stereoselectivity.

Conjugate addition of the  $\gamma$ -butyrolactam to enals was promoted by diphenylprolinol trimethylsilyl ether **12** via the iminium activation process (Scheme 32, second line) [53]. A satisfactory level of enantioselectivity was generally observed irrespective of the solvent polarity, although the use of aqueous acetonitrile was superior for optimizing the chemical yield and enantioselectivity. In addition, acidic additives had apparent effects on the reaction profile and the highest diastereoselectivity was attained with 2-fluorobenzoic acid. The synthetic utility of this site- and stereoselective transformation was demonstrated in a series of product derivatizations, including the three-step synthesis of a *c*AMP-specific phosphodiesterase (PDE IV) inhibitor (Scheme 32, third line).

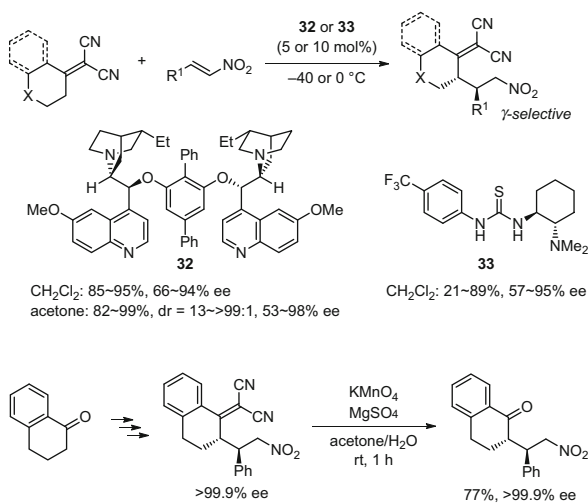
### 3.4 Alkylidene Malononitriles

$\beta,\beta$ -Disubstituted alkylidene malononitriles serve as useful precursors of acyclic vinylogous nucleophiles. Facile deprotonation of the alkylidene malononitriles under very mild conditions allows the generation of vinylogous carbanions because of the extremely strong electron-withdrawing character of the dicyanovinylidene moiety (Hammett constant:  $\sigma_p = 0.84$  [cf:  $\sigma_p = 0.78$  for  $\text{NO}_2$ ]) [54]. In contrast to the  $\alpha$ -selective alkylation under strongly basic conditions [55], this unique class of vinylogous nucleophiles preferentially undergoes  $\gamma$ -addition in conjugate addition reactions.

Site- and stereoselective conjugate addition of the alkylidene malononitriles to nitroolefins was reported by three independent groups, and moderate to high enantioselectivity was obtained by using either the dimeric quinine **32** or amino thiourea **33** as a catalyst (Scheme 33, top) [56–58]. In each case, nearly perfect diastereoselectivity was observed regardless of the structure of the alkylidene malononitriles employed, but the benzoannulated framework appeared to be important for rigorous enantiocontrol. Because the olefinic moiety of the products can be oxidatively cleaved to give the corresponding ketone, the alkylidene malononitrile component can be regarded as an activated carbonyl group. That is, Knoevenagel condensation of a ketone with malononitrile followed by  $\gamma$ -selective transformation would give the  $\gamma$ -functionalized alkylidene malononitrile; the parent carbonyl functionality could subsequently be regenerated upon treatment with  $\text{KMnO}_4$  (Scheme 33, bottom). This three-step sequence enables site- and stereoselective modification at the  $\alpha$ -position of relatively less acidic ketones under mild conditions.

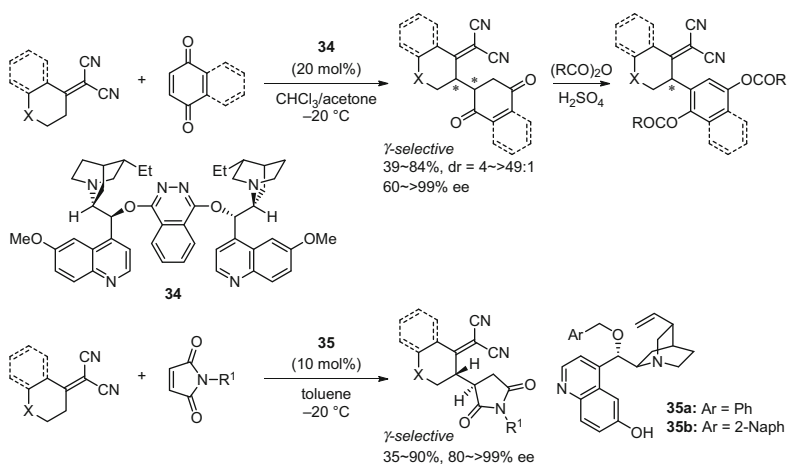
Doubly carbonylated cyclic olefins are reactive candidates as acceptors for  $\gamma$ -selective conjugate addition of alkylidene malononitriles. The highly

**Scheme 33** Conjugate addition of alkylidene malononitriles as vinylogous nucleophiles

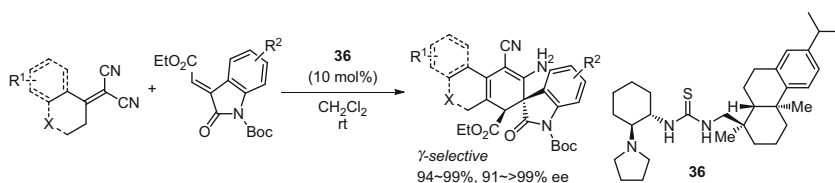


stereoselective coupling between the  $\gamma$ -carbon of the nitriles and the  $\alpha$ -carbon (or  $\beta$ -carbon) of the carbonyl provides adjacent tertiary–tertiary stereogenic carbons having unique synthetic handles. For example, conjugate addition to quinones was catalyzed by dimeric cinchona alkaloid **34** with variable stereoselectivity, and the resulting 1,4-cyclohexanedione motif was converted into the 1,4-diacloxyphenyl group (Scheme 34, top) [59]. Similarly, cinchona alkaloid-derived amine **35** exerted high stereoselectivity in the conjugate addition to maleimides, where an enantiomeric excess of over 80% was achieved, even with non-benzoannulated alkylidene malononitrile (Scheme 34, bottom) [60].

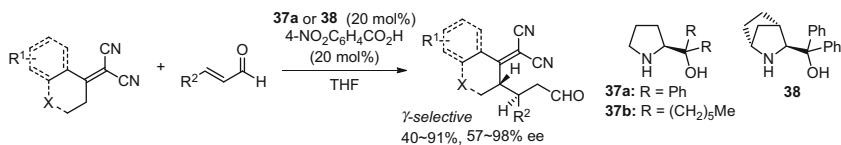
The stereoselective vinylogous Michael addition-cyclization cascade of alkylidene malononitriles and 3-alkylideneoxindoles was effectively catalyzed by rosin-derived thiourea **36** to give spirocyclic oxindoles with excellent stereoselectivity (Scheme 35) [61]. Although simple thiourea **20** (see Scheme 16) provided low stereoselectivity (dr = 3:1, 29% ee), introduction of the rosin unit into the thiourea core significantly improved the diastereoselectivity to >20:1; the pyrrolidine structure was essential for high enantioselectivity. The effect of the chirality of the rosin component on the absolute stereocontrol was negligible and, thus, the major proposed role of this structural unit was to increase the steric hindrance of the catalyst. One of the salient features of this protocol is the



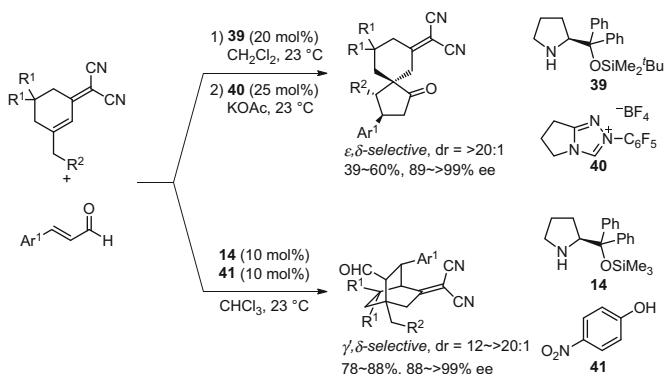
**Scheme 34** Conjugate addition of alkylidene malononitriles to doubly activated electrophiles



**Scheme 35** Vinylogous Michael addition-cyclization cascade reaction to form spiro-oxindoles



**Scheme 36**  $\gamma$ -Selective addition of alkylidene malononitriles via iminium activation



**Scheme 37** Site-selective carbocycloaddition sequence of alkylidene malononitriles

remarkably broad substrate scope. Acyclic, cyclic, and non-benzoannulated alkylidene malononitriles could all be employed and substituents on the 5- and 6-positions of the oxindoles were also tolerated.

The iminium activation strategy is applicable to the  $\gamma$ -selective conjugate addition of alkylidene malononitriles with  $\alpha,\beta$ -unsaturated aldehydes as an acceptor. Readily available diphenylprolinol **37a** and sterically congested bicyclic secondary amine **38** were found to be suitable catalysts in separate screening studies. 4-Nitrobenzoic acid was effective for increasing the turnover frequency (Scheme 36) [62, 63]. It should be noted that the free hydroxy group of the catalyst did not interfere with the catalytic performance, although plausible hemiaminal formation was sometimes problematic in the conjugate addition to enals catalyzed by diarylprolinols. In an analogous manner, prolinol **37b** possessing linear aliphatic chains was found to be an effective catalyst for promoting the same reaction with brine as a solvent [64].

The anion-stabilizing effect of the vinylidene malononitrile unit allows for extended vinylogous reactions. The vinylogous reactivity of cyclohexenylidene malononitriles in the conjugate addition to enals was modulated by using an appropriate set of catalysts for selective production of spiro[4.5]decanones and bicyclo[2.2.2]octane, respectively (Scheme 37) [65]. The former spiro compound was constructed in a stepwise sequence via  $\epsilon,\delta$ -regioselective bis-vinylogous conjugate addition/intramolecular 1,6-Stetter [3 + 2] spiroannulation through sequential treatment with diphenylprolinol silyl ether **39** and *N*-heterocyclic carbene **40**. The initial step was catalyzed by **39** without any additives in relatively less polar

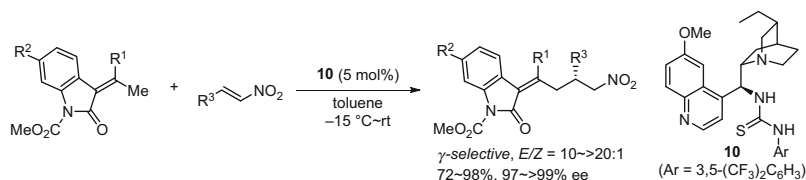
solvents in a highly enantioselective fashion. The second step proceeded via the Breslow intermediate generated from the transient aldehyde and **40** with complete site- and diastereoselectivity. In sharp contrast, catalysis with similar secondary amines in the presence of acidic additives such as carboxylic acids and electron-deficient phenol derivatives selectively generated a bicyclic cage molecule via one-step domino  $\gamma,\delta$ -vinylogous conjugate addition/1,6-Michael [4 + 2] cycloaddition. The optimal catalyst combination, prolinol silyl ether **14** and 4-nitrophenol **41**, provided the desired product in good chemical yield with high stereoselectivity. The same formal [4 + 2] cycloaddition was also effected under prolinol catalysis with basic ( $i$ Pr<sub>2</sub>EtN) or acidic (benzoic acid) additives in a polar aprotic solvent (acetonitrile) [66].

### 3.5 $\alpha$ -Alkylidene Oxindoles and Lactones

$\beta,\beta$ -Disubstituted alkylidene derivatives of oxindole, azlactone, and  $\gamma$ -butyrolactone are used as precursors of vinylogous enolates, which are highly stabilized owing to the heteroaromatic nature of the enolate components. Although these  $\alpha,\beta$ -unsaturated carbonyl systems can act as electrophilic Michael acceptors, the presence of two  $\beta$ -substituents seems to suppress nucleophilic attack on the  $\beta$ -carbon.

The utility of the alkylidene oxindole-derived vinylogous enolates was demonstrated in the  $\gamma$ -selective asymmetric conjugate addition to nitroolefins (Scheme 38) [67, 68]. Dihydroquinine-derived thiourea **10** earned distinction as the most effective catalyst in terms of catalytic efficiency and stereocontrolling ability. The tertiary amine and the thiourea functionalities both appeared to be essential for ensuring catalytic activity. It should be noted that not only perfect  $\gamma$ -selectivity but also very high *E/Z*-selectivity were observed under the optimal conditions. A wide variety of nitroolefins and substituted alkylidene oxindoles were amenable to this protocol.

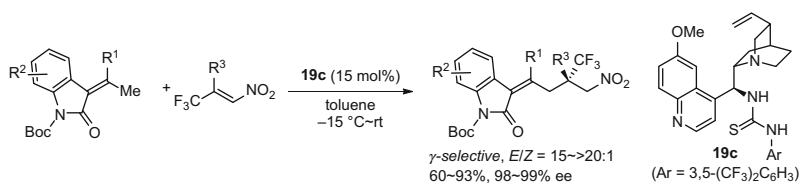
A quaternary stereogenic carbon center was effectively constructed by the  $\gamma$ -selective conjugate addition of this class of nucleophile to highly electrophilic,  $\beta$ -trifluoromethyl nitroolefins using cinchona alkaloid-derived thiourea **19c** as a



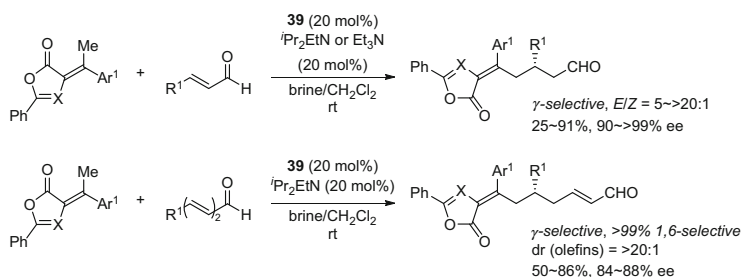
**Scheme 38**  $\gamma$ -Selective addition of  $\beta,\beta$ -disubstituted alkylidene oxindoles

requisite catalyst (Scheme 39) [69]. Nearly complete *E/Z*- and enantioselectivities were attained with a broad range of substrate sets, leading to the generation of almost enantiomerically pure trifluoromethylated quaternary carbon. In the reaction with the ethylidene analogue ( $R^1 = H$ ), the product was formed in less than 10% yield, verifying the importance of two substituents in the  $\beta$ -position of the alkylidene oxindoles.

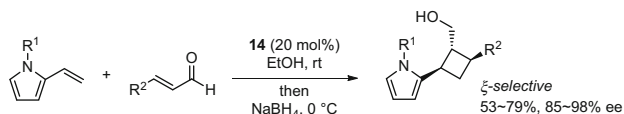
The potential utility of  $\beta,\beta$ -disubstituted alkylidene azlactones and  $\gamma$ -butyrolactones as precursors of vinylogous nucleophiles was substantiated in the development of highly site-, diastereo-, and enantioselective conjugate additions to  $\alpha,\beta$ -unsaturated aldehydes with diphenylprolinol silyl ether **39** as a catalyst (Scheme 40, first line) [70]. In contrast with the reactions with alkylidene malonitriles, the presence of a catalytic amount of organic base was indispensable for facilitating  $\gamma$ -deprotonation of these pronucleophiles to generate the corresponding vinylogous enolate probably because of the lower acidity of the  $\gamma$ -proton of the alkylidene lactones. In addition, the use of water as co-solvent was effective for not only improving the chemical yield but also increasing the *E/Z*- and enantioselectivities. Replacement of the water with brine further ameliorated the reaction profiles. This protocol was successfully extended to a doubly vinylogous conjugate addition to 2,4-dienals, where greater than 99% site-selectivity was uniformly observed with dienals bearing a primary alkyl substituent at the  $\delta$ -position (Scheme 40, second line). However, total loss of site-selectivity was observed in the addition to  $\delta$ -phenyl-substituted 2,4-dienal ( $R^1 = Ph$ ) under otherwise similar reaction conditions.



**Scheme 39**  $\gamma$ -Selective addition of alkylidene oxindoles to  $\beta$ -trifluoromethyl nitroolefins



**Scheme 40** 1,4- and 1,6-Selective  $\gamma$ -addition of alkylidene lactones



**Scheme 41**  $\zeta$ -Selective conjugate addition initiated [2 + 2]-cycloaddition

### 3.6 Miscellaneous

Friedel–Crafts-type vinylogous conjugate addition of 2-vinyl pyrroles to enals was achieved site-selectively with the use of diphenylprolinol trimethylsilyl ether **14** as an iminium-enamine activation catalyst (Scheme 41) [71]. Stepwise, formal [2 + 2] cycloaddition would be a plausible outcome of the reaction for constructing stereochemically enriched cyclobutanes. The polarity of the solvent had a critical impact on the catalytic efficiency. Trace amounts or none of the desired product was formed when less polar toluene or dichloromethane was used. Increasing the polarity of the solvent led to enhancement of the turnover frequency of **14**; the polar protic solvent, ethanol, was optimal.

## 4 Outlook

As outlined in this chapter, significant development of protocols for organocatalytic site- and enantioselective conjugate addition via ionic intermediates has been accomplished over the past decade and this arena continues to be an actively growing field. Various vinylogous electrophiles and nucleophiles have been elaborated for this type of selective bond-forming system, greatly expanding its utility. Notwithstanding, these advances also highlight the dearth of highly stereoselective protocols for controlling the site-selectivity, largely because the intrinsic reactivity of multifunctional substrates governs the reaction site. Therefore, development of novel strategies or catalysts for circumventing the site-selectivity constraints imposed by the inherent attributes of the substrates remains an elusive goal. Synergistic catalysis such as that demonstrated by the system illustrated in Scheme 37 is one potential platform for developing truly catalyst-controlled site-selective transformations.

## References

1. Fuson RC (1934) Chem Rev 16:1–27
2. Csáký AG, de la Herrán G, Murcia MC (2010) Chem Soc Rev 39:4080–4102
3. Biju AT (2011) ChemCatChem 3:1847–1849
4. Silva EMP, Silva AMS (2012) Synthesis 44:3109–3128

5. Bernardi L, López-Cantarero J, Niess B, Jørgensen KA (2007) *J Am Chem Soc* 129:5772–5778
6. Uraguchi D, Yoshioka K, Ueki Y, Ooi T (2012) *J Am Chem Soc* 134:19370–19373
7. Kowalczyk R, Wierzbaj AJ, Boratynski PJ, Bąkowicz J (2014) *Tetrahedron* 70:5834–5842
8. Chu W-D, Zhang L-F, Bao X, Zhao X-H, Zeng C, Du J-Y, Zhang G-B, Wang F-X, Ma X-Y, Fan C-A (2013) *Angew Chem Int Ed* 52:9229–9233
9. Law KR, McErlean CSP (2013) *Chem Eur J* 19:15852–15855
10. Berner OM, Tedeschi L, Enders D (2002) *Eur J Org Chem* 1877–1894
11. Vicario JL, Badía D, Carrillo L (2007) *Synthesis* 2065–2092
12. Yu Z, Liu X, Zhou L, Lin L, Feng X (2009) *Angew Chem Int Ed* 48:5195–5198
13. Chauhan P, Chimni SS (2011) *Adv Synth Catal* 353:3203–3212
14. Chowdhury R, Vamisetti GB, Ghosh SK (2014) *Tetrahedron Asymmetry* 25:516–522
15. Li X-J, Peng F-Z, Li X, Wu W-T, Sun Z-W, Li Y-M, Zhang S-X, Shao Z-H (2011) *Chem Asian J* 6:220–225
16. Uraguchi D, Kinoshita N, Kizu T, Ooi T (2011) *Synlett* 1265–1267
17. Kowalczyk R, Nowak AE, Skarzewski J (2013) *Tetrahedron Asymmetry* 24:505–514
18. Ahrendt KA, Borths CJ, MacMillan DWC (2000) *J Am Chem Soc* 122:4243–4244
19. Melchiorre P, Marigo M, Carlone A, Bartoli G (2008) *Angew Chem Int Ed* 47:6138–6171
20. Jurberg ID, Chatterjee I, Tannert R, Melchiorre P (2013) *Chem Commun* 49:4869–4883
21. Tian X, Liu Y, Melchiorre P (2012) *Angew Chem Int Ed* 51:6439–6442
22. Silvi M, Chatterjee I, Liu Y, Melchiorre P (2013) *Angew Chem Int Ed* 52:10780–10783
23. Tian X, Melchiorre P (2013) *Angew Chem Int Ed* 52:5360–5363
24. Halskov KS, Naicker T, Jensen ME, Jørgensen KA (2013) *Chem Commun* 49:6382–6384
25. Hayashi Y, Okamura D, Umemiya S, Uchimaru T (2012) *ChemCatChem* 4:959–962
26. Akagawa K, Sen J, Kudo K (2013) *Angew Chem Int Ed* 52:11585–11588
27. Akagawa K, Nishi N, Sen J, Kudo K (2014) *Org Biomol Chem* 12:3581–3585
28. Fisk JS, Mosey RA, Tepe JJ (2007) *Chem Soc Rev* 36:1432–1440
29. Alba A-NR, Rios R (2011) *Chem Asian J* 6:720–734
30. Reissig H-U, Zimmer R (2014) *Angew Chem Int Ed* 53:9708–9710
31. Alemán J, Milelli A, Cabrera S, Reyes E, Jørgensen KA (2008) *Chem Eur J* 14:10958–10966
32. Alba A-NR, Valero G, Calbet T, Font-Bardía M, Moyano A, Rios R (2010) *Chem Eur J* 16:9884–9889
33. Jiang H, Paixão MW, Monge D, Jørgensen KA (2010) *J Am Chem Soc* 132:2775–2783
34. Uraguchi D, Ueki Y, Ooi T (2009) *Science* 326:120–123
35. Uraguchi D, Ueki Y, Ooi T (2011) *Angew Chem Int Ed* 50:3681–3683
36. Uraguchi D, Ueki Y, Ooi T (2012) *Chem Sci* 3:842–845
37. Bravo N, Alba A-NR, Valero G, Companyó X, Moyano A, Rios R (2010) *New J Chem* 34:1816–1820
38. Uraguchi D, Ueki Y, Sugiyama A, Ooi T (2013) *Chem Sci* 4:1308–1311
39. Geng Z-C, Chen X, Zhang J-X, Li N, Chen J, Huang X-F, Zhang S-Y, Tao J-C, Wang X-W (2013) *Eur J Org Chem* 4738–4743
40. Cabrera S, Reyes E, Alemán J, Milelli A, Kobbelgaard S, Jørgensen KA (2008) *J Am Chem Soc* 130:12031–12037
41. Hayashi Y, Obi K, Ohta Y, Okamura D, Ishikawa H (2009) *Chem Asian J* 4:246–249
42. Zhang Y, Yu C, Ji Y, Wang W (2010) *Chem Asian J* 5:1303–1306
43. Manna MS, Kumar V, Mukherjee S (2012) *Chem Commun* 48:5193–5195
44. Zhang W, Tan D, Lee R, Tong G, Chen W, Qi B, Huang K-W, Tan C-H, Jiang Z (2012) *Angew Chem Int Ed* 51:10069–10073
45. Ube H, Shimada N, Terada M (2010) *Angew Chem Int Ed* 49:1858–1861
46. Terada M, Ando K (2011) *Org Lett* 13:2026–2029
47. Huang H, Yu F, Jin Z, Li W, Wu W, Liang X, Ye J (2010) *Chem Commun* 46:5957–5959
48. Quintard A, Lefranc A, Alexakis A (2011) *Org Lett* 13:1540–1543
49. Zhang Y, Shao Y-L, Xu H-S, Wang W (2011) *J Org Chem* 76:1472–1474

50. Yang Y, Dong S, Liu X, Lin L, Feng X (2012) *Chem Commun* 48:5040–5042
51. Zhang J, Liu X, Ma X, Wang R (2013) *Chem Commun* 49:9329–9331
52. Huang H, Jin Z, Zhu K, Liang X, Ye J (2011) *Angew Chem Int Ed* 50:3232–3235
53. Feng X, Cui H-L, Xu S, Wu L, Chen Y-C (2010) *Chem Eur J* 16:10309–10312
54. Hansch C, Leo A, Taft RW (1991) *Chem Rev* 91:165–195
55. Grossman RB, Varner MA (1997) *J Org Chem* 62:5235–5237
56. Xue D, Chen Y-C, Wang Q-W, Cun L-F, Zhu J, Deng J-G (2005) *Org Lett* 7:5293–5296
57. Poulsen TB, Bell M, Jørgensen KA (2006) *Org Biomol Chem* 4:63–70
58. Jiang L, Zheng H-T, Liu T-Y, Yue L, Chen Y-C (2007) *Tetrahedron* 63:5123–5128
59. Alemán J, Jacobsen CB, Frisch K, Overgaard J, Jørgensen KA (2008) *Chem Commun* 632–634
60. Lu J, Zhou W-J, Liu F, Loh T-P (2008) *Adv Synth Catal* 350:1796–1800
61. Shi X-M, Dong W-P, Zhu L-P, Jiang X-X, Wang R (2013) *Adv Synth Catal* 355:3119–3123
62. Xie J-W, Yue L, Xue D, Ma X-L, Chen Y-C, Wu Y, Zhu J, Deng J-G (2006) *Chem Commun* 1563–1565
63. Lu J, Liu F, Zhou W-J, Loh T-P (2008) *Tetrahedron Lett* 49:5389–5392
64. Lu J, Liu F, Loh T-P (2008) *Adv Synth Catal* 350:1781–1784
65. Dell'Amico L, Rassu G, Zambrano V, Sartori A, Curti C, Battistini L, Pelosi G, Casiraghi G, Zanardi F (2014) *J Am Chem Soc* 136:11107–11114
66. Li Q-Z, Gu J, Chen Y-C (2014) *RSC Adv* 4:37522–37525
67. Curti C, Rassu G, Zambrano V, Pinna L, Pelosi G, Sartori A, Battistini L, Zanardi F, Casiraghi G (2012) *Angew Chem Int Ed* 51:6200–6204
68. Rassu G, Zambrano V, Pinna L, Curti C, Battistini L, Sartori A, Pelosi G, Zanardi F, Casiraghi G (2013) *Adv Synth Catal* 355:1881–1886
69. Chen Q, Wang G, Jiang X, Xu Z, Lin L, Wang R (2014) *Org Lett* 16:1394–1397
70. Dell'Amico L, Albrecht L, Naicker T, Poulsen PH, Jørgensen KA (2013) *J Am Chem Soc* 135:8063–8070
71. Duan G-J, Ling J-B, Wang W-P, Luo Y-C, Xu P-F (2013) *Chem Commun* 49:4625–4627

# Asymmetric Iridium-Catalyzed C–C Coupling of Chiral Diols via Site-Selective Redox-Triggered Carbonyl Addition

Inji Shin and Michael J. Krische

**Abstract** Cyclometalated  $\pi$ -allyliridium *C,O*-benzoate complexes modified by axially chiral chelating phosphine ligands display a pronounced kinetic preference for primary alcohol dehydrogenation, enabling highly site-selective redox-triggered carbonyl additions of chiral primary-secondary 1,3-diols with exceptional levels of catalyst-directed diastereoselectivity. Unlike conventional methods for carbonyl allylation, the present redox-triggered alcohol C–H functionalizations bypass the use of protecting groups, premetalated reagents, and discrete alcohol-to-aldehyde redox reactions.

**Keywords** Allylation · Dehydrogenation · Diastereoselectivity · Enantioselectivity · Green chemistry · Iridium · Polyketides · Transfer hydrogenation

## Contents

1	Introduction .....	85
2	Redox-Triggered Allylation of Diols .....	88
3	Summary and Outlook .....	96
	References .....	97

## 1 Introduction

As stated by Hendrickson, “The ideal synthesis creates a complex skeleton... in a sequence only of successive construction reactions involving no intermediary refunctionalizations, and leading directly to the structure of the target, not only its

---

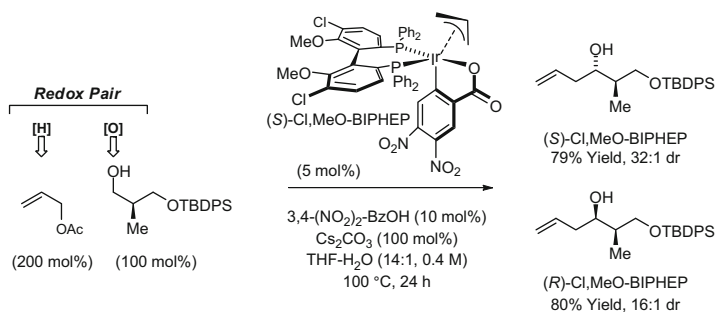
I. Shin and M.J. Krische (✉)

Department of Chemistry, University of Texas at Austin, 1 University Station – A5300, Austin, TX 78712-1167, USA

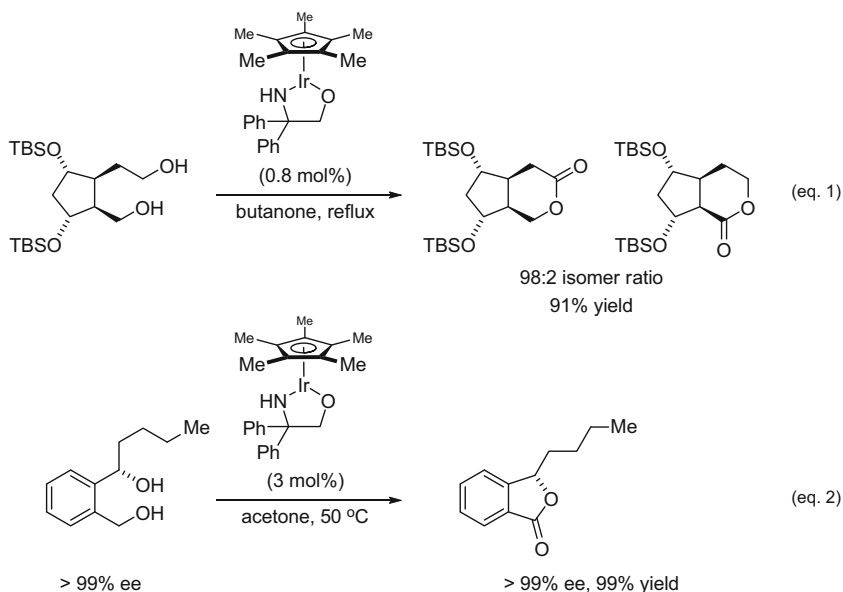
e-mail: [mkrische@mail.utexas.edu](mailto:mkrische@mail.utexas.edu)

skeleton but also its correctly placed functionality” [1]. This perspective elegantly captures many core aspects of synthetic efficiency, including the importance of merged redox-construction events (“redox-economy”) [2], regio-, chemo-, and stereoselectivity [3, 4], as well as protecting group-free chemical synthesis [5–7]. A modernistic revision of this statement would also encompass considerations of atom-efficiency [8, 9] and waste generation [10–12], overall process relevance [13–16], and the minimization of preactivation: the degree of separation between reagent and feedstock [17]. Considerable progress toward these ideals has been made, especially in terms of controlling regio- and stereoselectivity. Indeed, 40 years have elapsed since the first industrial catalytic asymmetric synthesis was reported by Monsanto for the synthesis of L-DOPA, which utilizes a byproduct-free enantioselective hydrogenation [18, 19]. The design of chemoselective catalysts capable of discriminating between like functional groups, so as to transform organic molecules in a “site-selective” manner, poses a more formidable challenge, but offers the benefit of removing steps from a synthetic route otherwise required for the installation and removal of protecting groups. As demonstrated in the work of Kawabata [20–26], Miller [27–35], and Taylor [36–41], the site-selective modification of carbohydrates and other natural polyols directly delivers compounds that would normally require lengthy stepwise preparations, or may be entirely inaccessible by other means.

By exploiting the native reducing ability of alcohols, we have developed a broad, new family of redox-triggered carbonyl additions where hydrogen transfer from alcohols to  $\pi$ -unsaturated reactants results in the formation of electrophile–nucleophile pairs, which combine to give products of formal alcohol C–H functionalization [42–48]. These processes are redox efficient as they merge alcohol oxidation and C–C bond construction events, bypassing discrete alcohol-to-aldehyde redox reactions, and manipulations required for the stoichiometric formation of premetalated reagents. One of the most useful processes based on this pattern of reactivity is the enantioselective iridium-catalyzed coupling of primary alcohols with allyl acetate to form secondary homoallylic alcohols (Scheme 1) [49–53]. Such primary alcohol C-allylations have been applied to the syntheses of



**Scheme 1** Iridium-catalyzed coupling of primary alcohols with allyl acetate to form secondary homoallylic alcohols



**Scheme 2** Examples of site-selective diol oxidation involving discrimination between two primary alcohols (eq. 1) and discrimination between benzylic primary vs secondary alcohols (eq. 2)

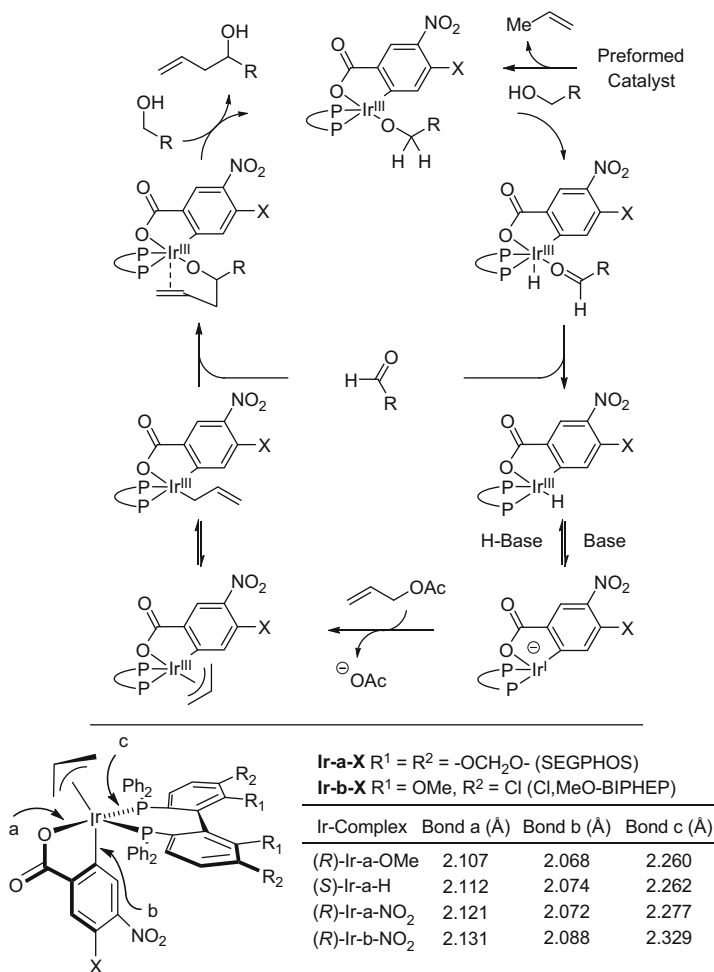
diverse polyketide natural products, resulting in the most concise routes reported to date [54–64].

As documented in the review literature [65], iridium catalysts are remarkably sensitive to the steric environment of reactants and, in the context of diol oxidation, display a pronounced kinetic preference for dehydrogenation of the more accessible alcohol [66–74]. As illustrated in the context of oxidative lactonization, nearly complete levels of discrimination between two primary alcohols are achieved on the basis of remote steric effects: beta- versus gamma-branching (Scheme 2 (eq. 1)) [71]. In the case of benzylic diols, the energetic barrier to dehydrogenation should be lower, potentially diminishing selectivity in the dehydrogenation event. Yet as illustrated in the oxidative lactonization of the enantiomerically-enriched 1,4-diol, oxidation at the primary benzylic alcohol occurs with complete levels of selectivity even though it is more endothermic than oxidation of the secondary benzylic alcohol (Scheme 2 (eq. 2)) [73].

The exceptional levels of chemoselectivity displayed in iridium catalyzed diol oxidation led us to explore the feasibility of redox-triggered diol C-allylations which are both asymmetric and site-selective [75, 76]. Such transformations would represent a significant departure from classical protocols for carbonyl allylation [77–83], as they would forego the requirement of protecting groups, premetallated reagents, chiral auxiliaries, and discrete alcohol-to-aldehyde oxidation, thus representing an additional step toward fulfillment of the “Hendricksonian ideal.” In this review we summarize our progress on chiral diol C–H functionalization via asymmetric redox-triggered carbonyl addition.

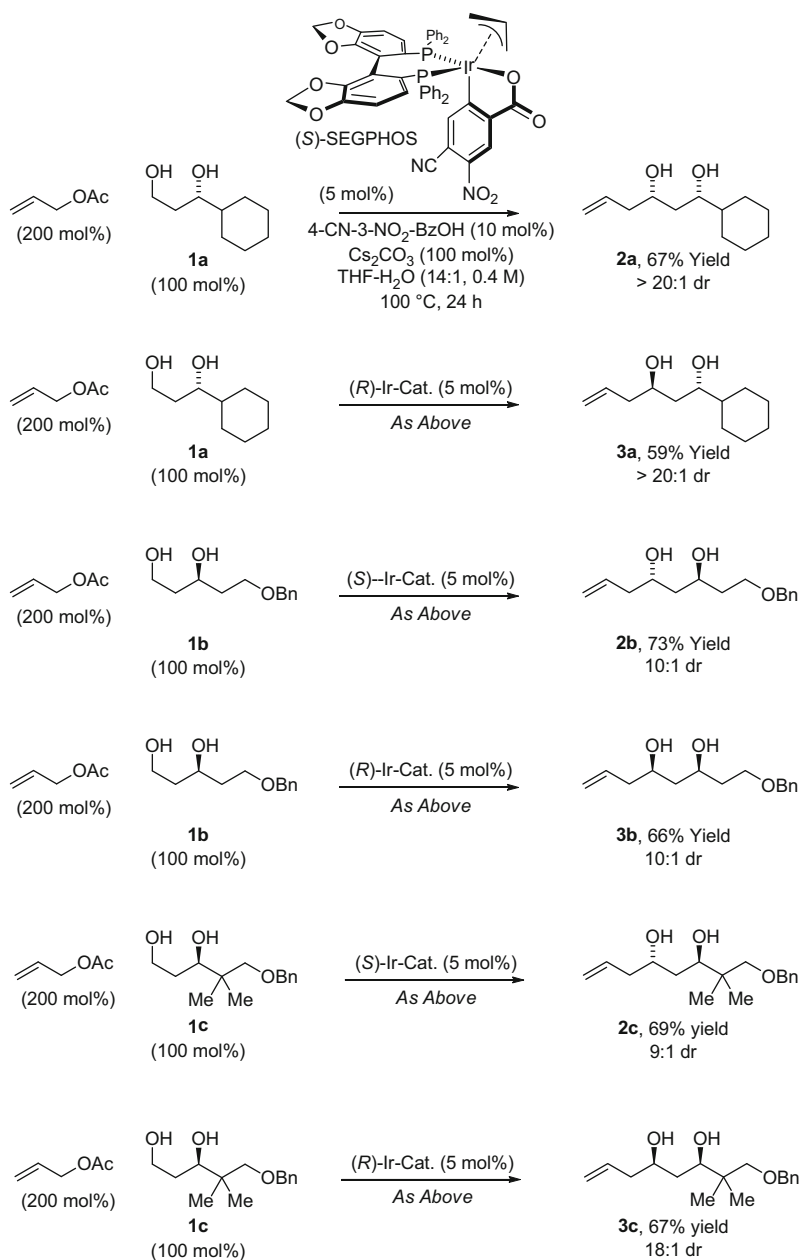
## 2 Redox-Triggered Allylation of Diols

The redox-triggered carbonyl allylations developed in our laboratory are catalyzed by cyclometalated  $\pi$ -allyliridium *C,O*-benzoate complexes bearing chiral phosphine ligands. These reactions proceed in accordance with the indicated general catalytic mechanism (Scheme 3). Entry into the catalytic cycles occurs upon protonolytic cleavage of the  $\pi$ -allyliridium complex by the primary alcohol reactant. The resulting iridium alkoxide suffers  $\beta$ -hydride elimination to furnish an aldehyde and an iridium hydride. Competition experiments demonstrate rapid and reversible  $\beta$ -hydride elimination, that is, alcohol hydrogenation-dehydrogenation,



**Scheme 3** General catalytic mechanism for redox-triggered carbonyl allylation and survey of selected bond lengths from a series of  $\pi$ -allyliridium *C,O*-benzoate complexes

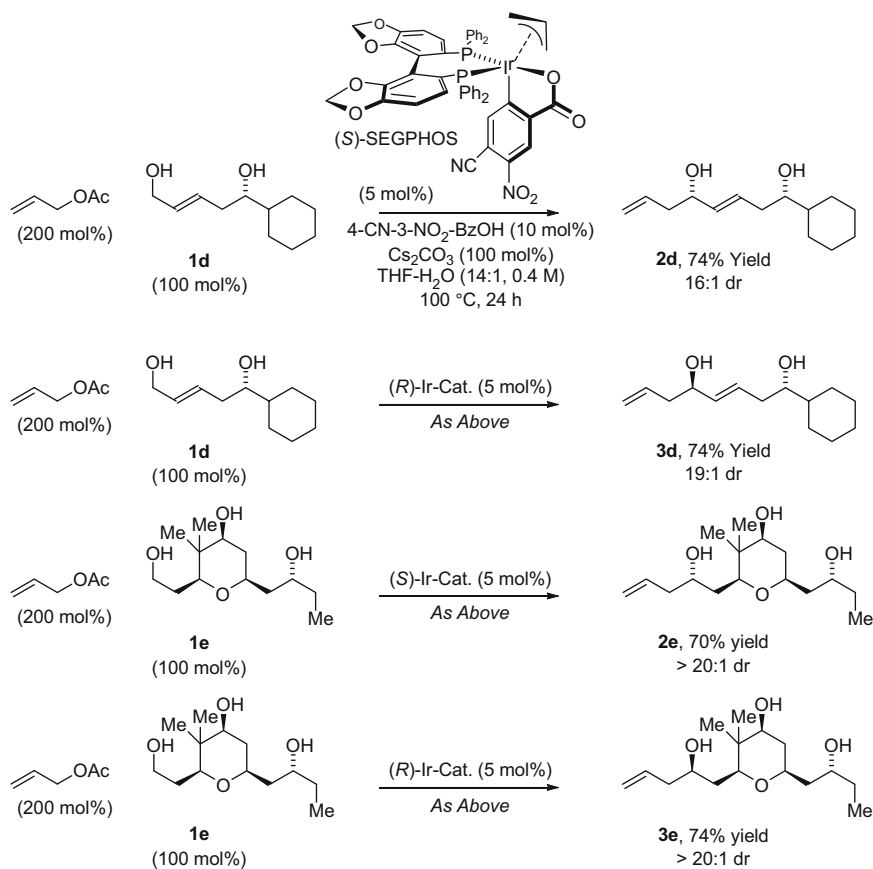
in advance of carbonyl addition [50]. Deprotonation of the iridium hydride provides an anionic iridium(I) intermediate, which undergoes oxidative addition with allyl



**Scheme 4** Catalyst-directed diastereo- and site-selectivity in the asymmetric C-allylation of unprotected 1,3-diols **1a–1c**

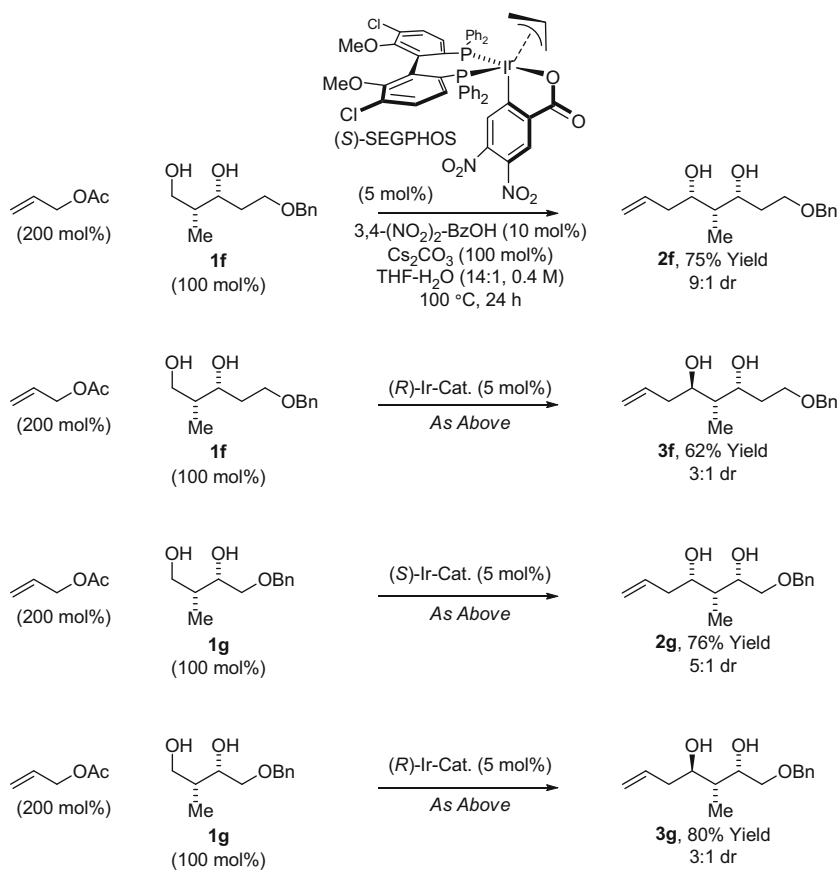
acetate to regenerate the starting  $\pi$ -allyliridium *C,O*-benzoate complex. Now, with aldehyde present, carbonyl addition occurs, resulting in the formation of a homoallylic iridium alkoxide that exchanges with the primary alcohol reactant to close the catalytic cycle. By the use of isotopically labeled allyl acetate with deuterium at the allylic position, intervention of symmetric iridium  $\pi$ -allyl intermediate was corroborated [50]. Interestingly, both catalytic efficiency and stereoselectivity is dramatically influenced by remote substituents at the 4-position of the *C,O*-benzoate moiety. As suggested by single crystal X-ray diffraction data of a series of  $\pi$ -allyliridium *C,O*-benzoate complexes (Scheme 3) [53], more electron-deficient *C,O*-benzoate ligands enhance Lewis acidity at iridium, which may accelerate turnover limiting carbonyl addition with respect to protonolytic cleavage of the  $\pi$ -allyl and other competing processes.

Our initial studies focused on the catalyst-directed diastereo- and site-selective allylation of chiral 1,3-diols **1a–1c**. The feasibility of these processes was rendered



**Scheme 5** Catalyst-directed diastereo- and site-selectivity in the asymmetric *C*-allylation of unprotected 1,5-diol **1d** and 1,5-triol **1e**

uncertain by the well-documented instability of the  $\beta$ -hydroxy aldehyde intermediates, which under equilibrium conditions exist predominantly as dimers [84–86]. Nevertheless, the chromatographically isolated  $\pi$ -allyliridium *C,O*-benzoate complex derived from [Ir(cod)Cl]<sub>2</sub>, (*S*)- or (*R*)-SEGPHOS, 4-cyano-3-nitrobenzoic acid, and allyl acetate proved to be effective in these transformations (Scheme 4) [75]. Specifically, in aqueous THF solvent at 100 °C, 1,3-diols **1a–1c** (100 mol%) were exposed to the (*S*)- or (*R*)-SEGPHOS modified catalyst (5 mol%), allyl acetate (200 mol%), cesium carbonate (100 mol%), and 4-cyano-3-nitrobenzoic acid (10 mol%) to furnish diastereomers **2a–2c** and **3a–3c**, respectively. In each case, the homoallylic alcohols were obtained in good to excellent yields with high levels of catalyst-directed diastereoselectivity. Oxidation of the unprotected secondary alcohol of the reaction products **2a–2c** and **3a–3c** (or reactants **1a–1c**) was not observed. Notably, the synthesis of **3b**, which is accomplished in four steps through iterative redox-triggered allylation, was previously achieved through



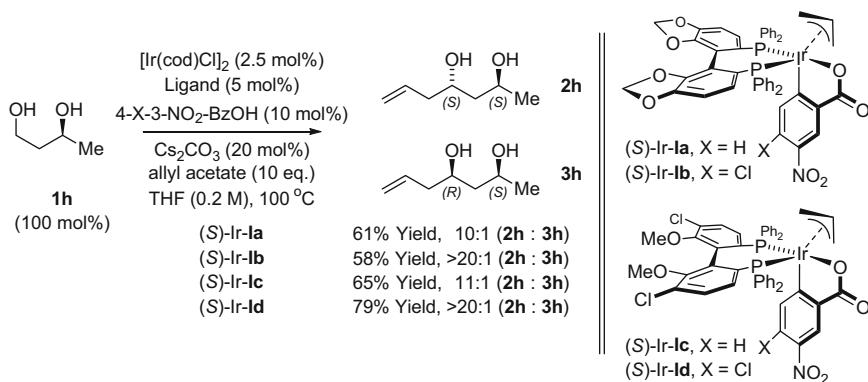
**Scheme 6** Catalyst-directed diastereo- and site-selectivity in the asymmetric C-allylation of unprotected chiral  $\beta,\gamma$ -stereogenic diols **1f** and **1g**

a seven-step sequence from the same starting material [87], illustrating the inherent step-economy of protecting group-free chemical synthesis.

To assess scope further and determine whether a 1,3-relationship between hydroxyl moieties is required to suppress over-oxidation, the 1,5-diol **1d** and 1,5-triol **1e** were exposed to the chromatographically isolated  $\pi$ -allyliridium *C,O*-benzoate modified by (*S*)- or (*R*)-SEGPHOS and 4-cyano-3-nitro-benzoic acid under the aforesaid conditions (Scheme 5) [75]. The corresponding homoallylic alcohols **2d**, **2e** and **3d**, **3e** were obtained in good to excellent yields with high levels of catalyst-directed diastereoselectivity. The site-selective C–C coupling of **1e** to form either **2e** or **3e**, where one of three unprotected alcohols undergoes modification, suggests this technology is applicable to the late stage modification of even more complex polyhydroxylated compounds, such as type I polyketides.

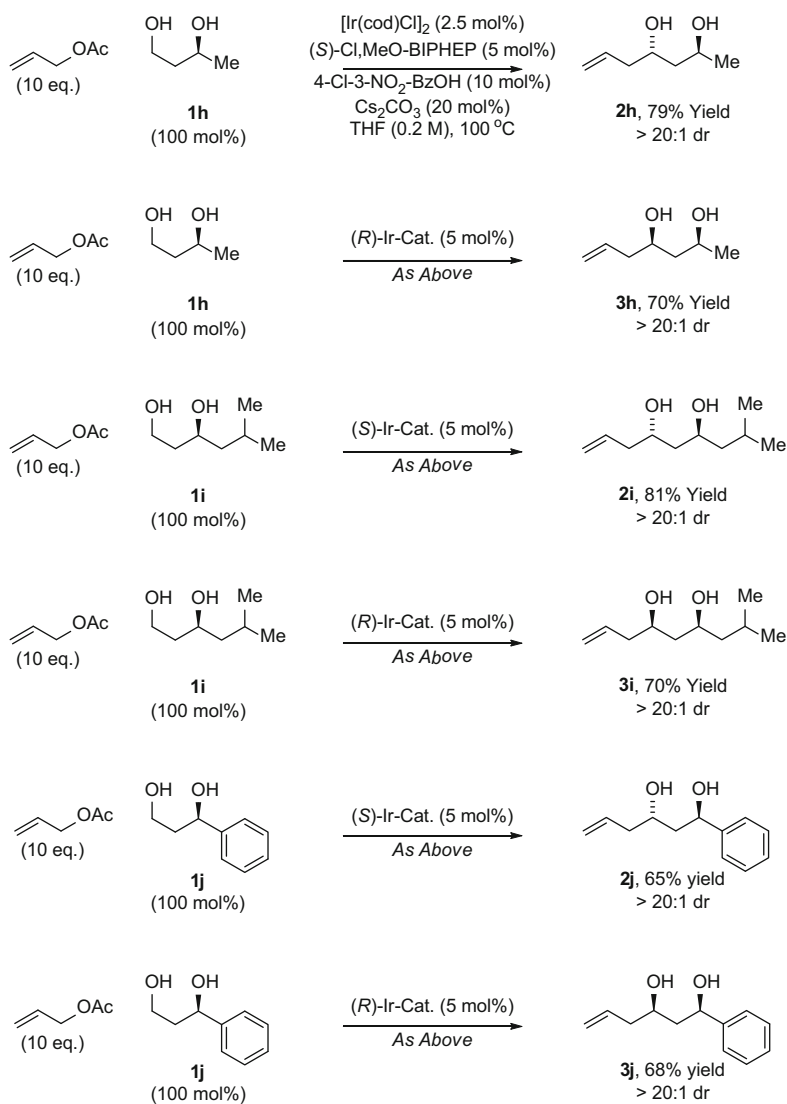
The unprotected chiral  $\beta,\gamma$ -stereogenic alcohols **1f** and **1g** represent an especially challenging class of reactant, as branching adjacent to the transient chiral aldehyde is expected to retard the rate of carbonyl addition with respect to racemization (Scheme 6). For **1f** and **1g**, the chromatographically isolated  $\pi$ -allyliridium *C,O*-benzoate complex derived from [Ir(cod)Cl]<sub>2</sub>, (*S*)- or (*R*)-Cl<sub>2</sub>MeO-BIPHEP, 3,4-dinitro-benzoic acid, and allyl acetate provided the best results [75]. Although site-selectivity proved uniformly high, good levels of diastereocontrol were observed only in cases where the diastereofacial bias of the catalyst matched the intrinsic diastereofacial bias of the transient aldehydes for Felkin-Anh addition [88], as in the formation of **2f** and **2g**. In the mismatched case, represented by the formation of **3f** and **3g**, epimerization of the transient aldehydes erodes diastereoselectivity.

Although use of an isolable, single component catalyst offers certain advantages, generation of the catalyst in situ from commercial precursors is expedient and enables rapid evaluation of structurally diverse complexes. Using the commercially available chiral diol **1h**, a screening of catalysts generated in situ quickly leads to the identification of the  $\pi$ -allyliridium *C,O*-benzoate complex derived from [Ir(cod)

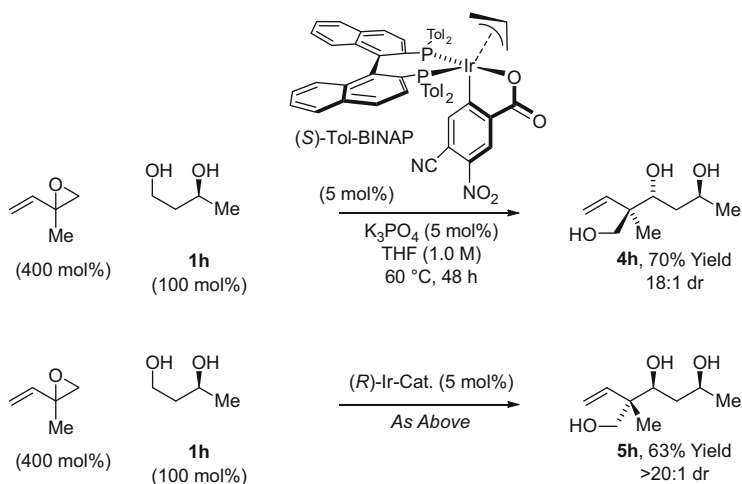


**Scheme 7** Generation of structurally diverse catalysts in situ enables screening and identification of a highly efficient and selective system for *C*-allylation of unprotected diol **1h**

$\text{Cl}]_2$ , (*S*)- or (*R*)-Cl,MeO-BIPHEP, 4-chloro-3-nitro-benzoic acid, and allyl acetate as a highly efficient and selective system for diol *C*-allylation [76]. Under these conditions, diol **1h** is converted to the homoallylic alcohol **2h** in 79% isolated yield as a single diastereomer, as determined by  $^1\text{H}$  NMR analysis of the crude reaction mixture (Scheme 7).



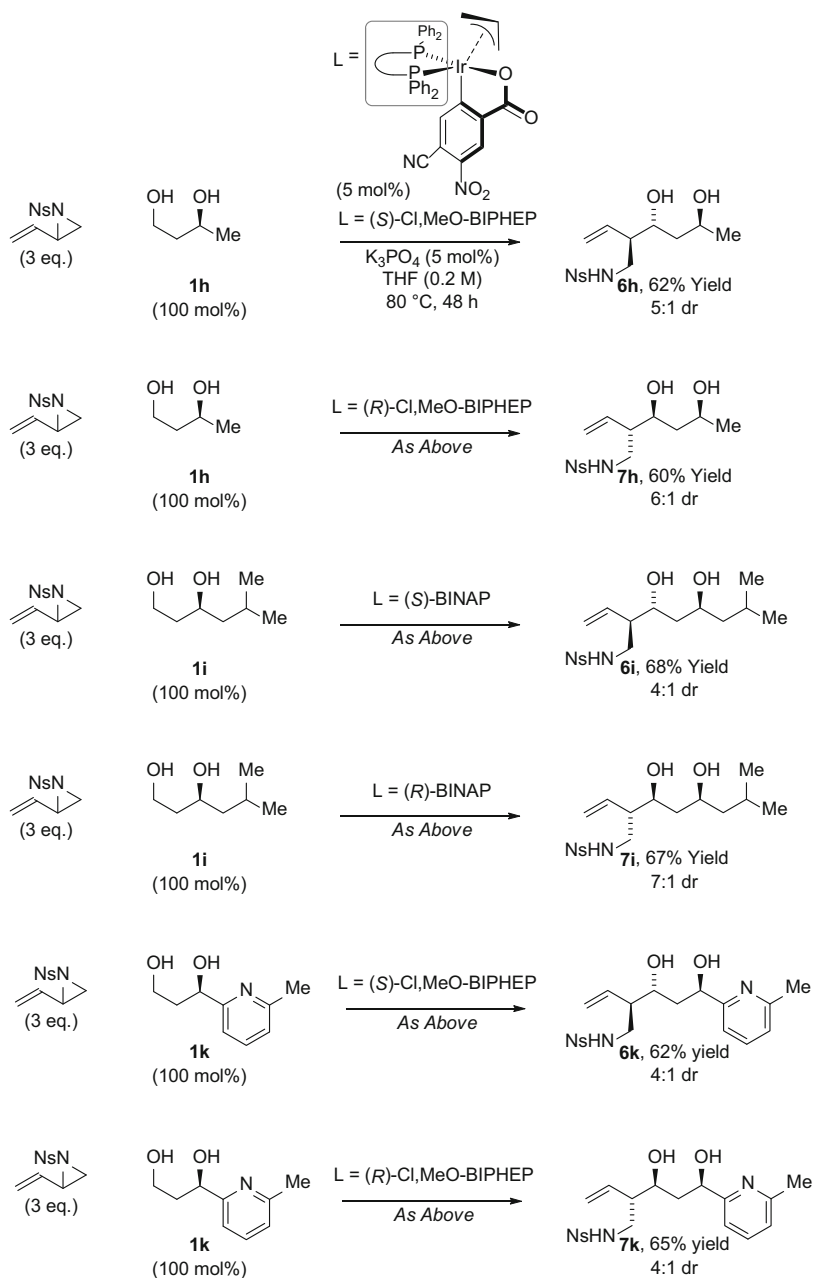
**Scheme 8** Catalyst-directed diastereo- and site-selectivity in the asymmetric *C*-allylation of unprotected 1,3-diols **1h–1j** using in situ generation of catalyst



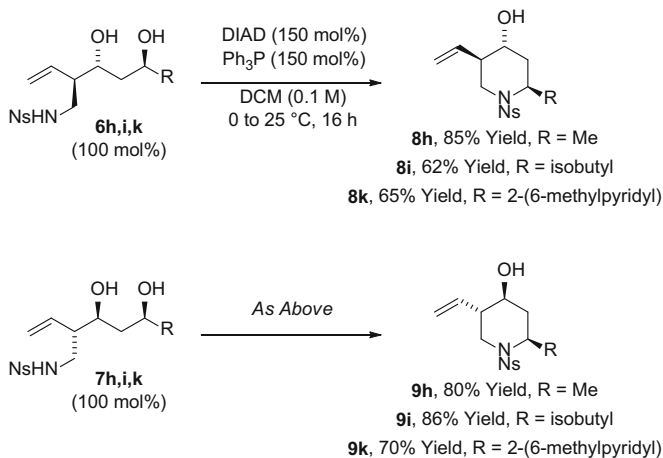
**Scheme 9** Catalyst-directed diastereo- and site-selectivity in the asymmetric *tert*-(hydroxy)-prenylation of unprotected diol **1h**

These conditions for in situ generation of the enantiomeric catalysts (*S*)- or (*R*)-Ir-**Id** were applied to chiral 1,3-diols **1h–1j** (Scheme 8) [76]. The respective diastereomeric products of *C*-allylation **2h–2j** and **3h–3j** were generated in good isolated yields with complete levels of catalyst-directed diastereoselectivity and high levels of site-selectivity. The catalytic C–C coupling of the benzylic diol **1j** is especially noteworthy, as dehydrogenation to form the acetophenone should be far less endothermic than aldehyde formation, yet only trace quantities of the over-oxidized ketone product were observed. Notably, the diastereoselectivities observed in connection with the protocol for in situ catalyst generation were consistently better than those observed previously using the chromatographically purified catalysts [75, 76].

Having established the feasibility of diastereo- and site-selectivity in redox-triggered allylations of unprotected diols, we have begun to explore site-selectivity in related catalytic asymmetric C–C couplings. For example, using the chromatographically purified  $\pi$ -allyliridium *C,O*-benzoate complex derived from [Ir(cod)Cl]<sub>2</sub>, (*S*)- or (*R*)-Tol-BINAP, 4-cyano-3-nitro-benzoic acid, and allyl acetate, primary alcohols react with isoprene oxide to form aldehyde-allyliridium pairs en route to products of *tert*-(hydroxy)-prenylation [89]. To evaluate the feasibility of site-selective coupling, the unprotected chiral diol **1h**, was reacted with isoprene oxide using enantiomeric Tol-BINAP-modified iridium catalysts. The diastereomeric products of *tert*-(hydroxy)-prenylation **4h** and **5h** were formed with excellent levels of diastereo- and site-selectivity. A remarkable feature of this transformation lies in the ability to form an all-carbon quaternary center with control of relative and absolute stereochemistry (Scheme 9).



**Scheme 10** Catalyst-directed diastereo- and site-selectivity in the asymmetric C-( $\alpha$ -aminomethyl)allylation of unprotected 1,3-diols **1h**, **1i**, and **1k** using in situ generation of catalyst



**Scheme 11** Direct conversion of **6h**, **6i**, and **6k** and **7h**, **7i**, and **7k** to trisubstituted piperidines **8h**, **8i**, and **8k** and **9h**, **9i**, and **9k**, respectively

More recently, related redox-triggered C–C couplings of primary alcohols and vinyl aziridines were developed, which furnish products of carbonyl ( $\alpha$ -aminomethyl)allylation [90]. This transformation was applied to the unprotected 1,3-diols **1h**, **1i**, and **1k** using the enantiomeric cyclometalated iridium *C,O*-benzoate catalysts derived from 4-cyano-3-nitro-benzoic acid and either Cl<sub>2</sub>MeO-BIPHEP or BINAP (Scheme 10). The respective diastereomeric products of *C*-allylation **6h**, **6i**, and **6k** and **7h**, **7i**, and **7k** were generated in good isolated yields with good levels of catalyst-directed diastereoselectivity and site selectivity. As illustrated in the conversion of diol **1k** to adducts **6k** and **7k**, the iridium catalyst is tolerant of Lewis basic pyridyl substituents. To illustrate the utility of this methodology, the diol coupling products **6h**, **6i**, and **6k** and **7h**, **7i**, and **7k** were exposed to Mitsunobu reaction conditions, directly providing the diastereomeric trisubstituted piperidines **8h**, **8i**, and **8k** and **9h**, **9i**, and **9k**, respectively (Scheme 11).

### 3 Summary and Outlook

Stereo- and site-selective methods for the assembly of organic molecules that occur with addition, acceptorless removal, or redistribution of hydrogen are natural endpoints in the evolution of methods for process-relevant chemical synthesis. With this objective, we have merged the chemistry of transfer hydrogenation and carbonyl addition by harnessing the native reducing ability of alcohols for the redox-triggered generation of transient organometal–aldehyde pairs. Using chiral cyclometalated  $\pi$ -allyliridium *C,O*-benzoate complexes, primary alcohols dehydrogenate faster than secondary alcohols, enabling site-selective modification of chiral

1,3-diols with exceptional levels of catalyst-directed diastereoselectivity. This and related technologies for the direct, stereo- and site-selective C–C coupling of polyol streamlines de novo chemical synthesis, and offer new possibilities for late-stage modification of natural products, such as type I polyketides.

**Acknowledgment** Acknowledgment is made to the Robert A. Welch Foundation (F-0038) and the NIH-NIGMS (RO1 GM093905) for partial financial support.

## References

1. Hendrickson JB (1975) Systematic synthesis design. IV. Numerical codification of construction reactions. *J Am Chem Soc* 97:5784–5800
2. Burns NZ, Baran PS, Hoffmann RW (2009) Redox economy in organic synthesis. *Angew Chem Int Ed* 48:2854–2867
3. Trost BM (1983) Selectivity: a key to synthetic efficiency. *Science* 219:245–250
4. Newhouse T, Baran PS, Hoffmann RW (2009) The economies of synthesis. *Chem Soc Rev* 38:3010–3021
5. Hoffmann RW (2006) Protecting-group-free synthesis. *Synthesis* 3531–3541
6. Young IS, Baran PS (2009) Protecting-group-free synthesis as an opportunity for invention. *Nat Chem* 1:193–205
7. Roulland E (2011) Protecting-group-free total syntheses: a challenging approach. *Angew Chem Int Ed* 50:1226–1227
8. Trost BM (1991) The atom economy – a search for synthetic efficiency. *Science* 254:1471–1477
9. Trost BM (1995) Atom economy – a challenge for organic synthesis: homogeneous catalysis leads the way. *Angew Chem Int Ed Engl* 34:259–281
10. Sheldon RA (1997) Catalysis and pollution prevention. *Chem Ind* 12–15
11. Sheldon RA (2007) The E factor: fifteen years on. *Green Chem* 9:1273–1283
12. Sheldon RA (2012) Fundamentals of green chemistry: efficiency in reaction design. *Chem Soc Rev* 41:1437–1451
13. Butters M, Catterick D, Craig A, Curzons A, Dale D, Gillmore A, Green SP, Marziano I, Sherlock J-P, White W (2006) Critical assessment of pharmaceutical processes – a rationale for changing the synthetic route. *Chem Rev* 106:3002–3027
14. Carey JS, Laffan D, Thomson C, Williams MT (2006) Analysis of the reactions used for the preparation of drug candidate molecules. *Org Biomol Chem* 4:2337–2347
15. Busacca CA, Fandrick DR, Song JJ, Senanayake CH (2011) The growing impact of catalysis in the pharmaceutical industry. *Adv Synth Catal* 353:1825–1864
16. Dunn PJ (2012) The importance of green chemistry in process research and development. *Chem Soc Rev* 41:1452–1461
17. Han SB, Kim IS, Krische MJ (2009) Enantioselective iridium-catalyzed carbonyl allylation from the alcohol oxidation level via transfer hydrogenation: minimizing pre-activation for synthetic efficiency. *Chem Commun* 7278–7287
18. Knowles WS (1983) Asymmetric hydrogenation. *Acc Chem Res* 16:106–112
19. Knowles WS (2002) Asymmetric hydrogenations (Nobel Lecture). *Angew Chem Int Ed* 41:1998–2007
20. Kawabata T, Muramatsu W, Nishio T, Shibata T, Schedel H (2007) A catalytic one-step process for the chemo- and regioselective acylation of monosaccharides. *J Am Chem Soc* 129:12890–12895

21. Muramatsu W, Kawabata T (2007) Regioselective acylation of 6-O-protected octyl  $\beta$ -d-glucopyranosides by DMAP catalysis. *Tetrahedron Lett* 48:5031–5033
22. Kawabata T, Muramatsu W, Nishio T, Shibata T, Uruno Y, Stragies R (2008) Regioselective acylation of octyl  $\beta$ -d-glucopyranoside by chiral 4-pyrrolidinopyridine analogues. *Synthesis* 747–753
23. Ueda Y, Muramatsu W, Mishiro K, Furuta T, Kawabata T (2009) Functional group tolerance in organocatalytic regioselective acylation of carbohydrates. *J Org Chem* 74:8802–8805
24. Yoshida K, Furuta T, Kawabata T (2010) Perfectly regioselective acylation of a cardiac glycoside, digitoxin, via catalytic amplification of the intrinsic reactivity. *Tetrahedron Lett* 51:4830–4832
25. Muramatsu W, Mishiro K, Ueda Y, Furuta T, Kawabata T (2010) Perfectly regioselective and sequential protection of glucopyranosides. *Eur J Org Chem* 827–831
26. Ueda Y, Mishiro K, Yoshida K, Furuta T, Kawabata T (2012) Regioselective diversification of a cardiac glycoside, lanatoside C, by organocatalysis. *J Org Chem* 77:7850–7857
27. Griswold KS, Miller SJ (2003) A peptide-based catalyst approach to regioselective functionalization of carbohydrates. *Tetrahedron* 59:8869–8875
28. Lewis CA, Sculimbrenne BR, Xu Y, Miller SJ (2005) Desymmetrization of glycerol derivatives with peptide-based acylation catalysts. *Org Lett* 7:3021–3023
29. Lewis CA, Miller SJ (2006) Site-selective derivatization and remodeling of erythromycin A by using simple peptide-based chiral catalysts. *Angew Chem Int Ed* 45:5616–5619
30. Lewis CA, Merkel J, Miller SJ (2008) Catalytic site-selective synthesis and evaluation of a series of erythromycin analogs. *Bioorg Med Chem Lett* 18:6007–6011
31. Lewis CA, Longcore KE, Miller SJ, Wender PA (2009) An approach to the site-selective diversification of apoptolidin A with peptide-based catalysts. *J Nat Prod* 72:1864–1869
32. Fowler BS, Laemmerhold KM, Miller SJ (2012) Catalytic site-selective thiocarbonylations and deoxygenations of vancomycin reveal hydroxyl-dependent conformational effects. *J Am Chem Soc* 134:9755–9761
33. Allen CL, Miller SJ (2013) Chiral copper(II) complex-catalyzed reactions of partially protected carbohydrates. *Org Lett* 15:6178–6181
34. Pathak TP, Miller SJ (2013) Chemical tailoring of teicoplanin with site-selective reactions. *J Am Chem Soc* 135:8415–8422
35. Han S, Miller SJ (2013) Asymmetric catalysis at a distance: catalytic, site-selective phosphorylation of teicoplanin. *J Am Chem Soc* 135:12414–12421
36. Lee D, Taylor MS (2011) Borinic acid-catalyzed regioselective acylation of carbohydrate derivatives. *J Am Chem Soc* 133:3724–3727
37. Chan L, Taylor MS (2011) Regioselective alkylation of carbohydrate derivatives catalyzed by a diarylborinic acid derivative. *Org Lett* 13:3090–3093
38. Gouliaras C, Lee D, Chan L, Taylor MS (2011) Regioselective activation of glycosyl acceptors by a diarylborinic acid-derived catalyst. *J Am Chem Soc* 133:13926–13929
39. Lee D, Williamson CL, Chan L, Taylor MS (2012) Regioselective, borinic acid-catalyzed monoacylation, sulfonylation and alkylation of diols and carbohydrates: expansion of substrate scope and mechanistic studies. *J Am Chem Soc* 134:8260–8267
40. Lee D, Taylor MS (2013) Regioselective silylation of pyranosides using a boronic acid/Lewis base co-catalyst system. *Org Biomol Chem* 11:5409–5412
41. Beale TM, Taylor MS (2013) Synthesis of cardiac glycoside analogs by catalyst-controlled, regioselective glycosylation of digitoxin. *Org Lett* 15:1358–1361
42. Patman RL, Bower JF, Kim IS, Krische MJ (2008) Formation of C–C bonds via catalytic hydrogenation and transfer hydrogenation: vinylation, allylation, and enolate addition. *Aldrichim Acta* 41:95–104
43. Bower JF, Kim IS, Patman RL, Krische MJ (2009) Catalytic carbonyl addition through transfer hydrogenation: a departure from preformed organometallic reagents. *Angew Chem Int Ed* 48:34–46

44. Bower JF, Krische MJ (2011) Formation of C–C bonds via iridium-catalyzed hydrogenation and transfer hydrogenation. *Top Organomet Chem* 34:107–138
45. Hassan A, Krische MJ (2011) Unlocking hydrogenation for C–C bond formation: a brief overview of enantioselective methods. *Org Process Res Dev* 15:1236–1242
46. Moran J, Krische MJ (2012) Formation of C–C bonds via ruthenium-catalyzed transfer hydrogenation. *Pure Appl Chem* 84:1729–1739
47. Dechert-Schmitt A-MR, Schmitt DC, Gao X, Itoh T, Krische MJ (2014) Polyketide construction via hydroxyalkylation and related alcohol C–H functionalizations: reinventing the chemistry of carbonyl addition. *Nat Prod Rep* 31:504–513
48. Ketcham JM, Shin I, Montgomery TP, Krische MJ (2014) Catalytic enantioselective C–H functionalization of alcohols by redox-triggered carbonyl addition: borrowing hydrogen, returning carbon. *Angew Chem Int Ed* 53:9142–9150
49. Kim IS, Ngai M-Y, Krische MJ (2008) Enantioselective iridium-catalyzed carbonyl allylation from the alcohol or aldehyde oxidation level using allyl acetate as an allyl metal surrogate. *J Am Chem Soc* 130:6340–6341
50. Kim IS, Ngai M-Y, Krische MJ (2008) Enantioselective iridium-catalyzed carbonyl allylation from the alcohol or aldehyde oxidation level via transfer hydrogenative coupling of allyl acetate: departure from chirally modified allyl metal reagents in carbonyl addition. *J Am Chem Soc* 130:14891–14899
51. Lu Y, Kim IS, Hassan A, Del Valle DJ, Krische MJ (2009) 1, n-Glycols as dialdehyde equivalents in iridium-catalyzed enantioselective carbonyl allylation and iterative two-directional assembly of 1,3-polyols. *Angew Chem Int Ed* 48:5018–5021
52. Hassan A, Lu Y, Krische MJ (2009) Elongation of 1,3-polyols via iterative catalyst-directed carbonyl allylation from the alcohol oxidation level. *Org Lett* 11:3112–3115
53. Schmitt DC, Dechert-Schmitt A-MR, Krische MJ (2012) Iridium-catalyzed allylation of chiral  $\beta$ -stereogenic alcohols: bypassing discrete formation of epimerizable aldehydes. *Org Lett* 14:6302–6305
54. Han SB, Hassan A, Kim IS, Krische MJ (2010) Total synthesis of (+)-roxaticin via C–C bond forming transfer hydrogenation: a departure from stoichiometric chiral reagents, auxiliaries, and premetalated nucleophiles in polyketide construction. *J Am Chem Soc* 132:15559–15561
55. Lu Y, Woo SK, Krische MJ (2011) Total synthesis of bryostatin 7 via C–C bond-forming hydrogenation. *J Am Chem Soc* 133:13876–13879
56. Gao X, Woo SK, Krische MJ (2013) Total synthesis of 6-deoxyerythronolide B via C–C bond-forming transfer hydrogenation. *J Am Chem Soc* 135:4223–4226
57. Del Valle DJ, Krische MJ (2013) Total synthesis of (+)-trienomycins A and F via C–C bond-forming hydrogenation and transfer hydrogenation. *J Am Chem Soc* 135:10986–10989
58. Waldeck AR, Krische MJ (2013) Total synthesis of cyanolide A in the absence of protecting groups, chiral auxiliaries, or premetalated carbon nucleophiles. *Angew Chem Int Ed* 52:4470–4473
59. Yang Z, Zhang B, Zhao G, Yang J, Xie X, She X (2011) Concise formal synthesis of (+)-neopeltolide. *Org Lett* 13:5916–5919
60. Feng Y, Jiang X, De Brabander JK (2012) Studies toward the unique pederin family member psymberin: full structure elucidation, two alternative total syntheses, and analogs. *J Am Chem Soc* 134:17083–17093
61. Wan S, Wu F, Rech JC, Green ME, Balachandran R, Horne WS, Day BW, Floreancig PE (2011) Total synthesis and biological evaluation of pederin, psymberin, and highly potent analogs. *J Am Chem Soc* 133:16668–16679
62. Kretschmer M, Dieckmann M, Li P, Rudolph S, Herkommer D, Troendlin J, Menche D (2013) Modular total synthesis of rhizopodin: a highly potent G-actin dimerizing macrolide. *Chem Eur J* 19:15993–16018
63. Sejberg JJP, Smith LD, Leatherbarrow RJ, Beavil AJ, Spivey AC (2013) Enantioselective synthesis of (+)-aspericyclide A. *Tetrahedron Lett* 54:4970–4972

64. Willwacher J, Fürstner A (2014) Catalysis-based total synthesis of putative mandelalide A. *Angew Chem Int Ed* 53:4217–4221
65. Suzuki T (2011) Organic synthesis involving iridium-catalyzed oxidation. *Chem Rev* 111:1825–1845
66. Lin Y, Zhu X, Zhou Y (1992) A convenient lactonization of diols to  $\gamma$ - and  $\delta$ -lactones catalyzed by transition metal polyhydrides. *J Organomet Chem* 429:269–274
67. Suzuki T, Morita K, Tsuchida M, Hiroi K (2002) Mild and chemoselective synthesis of lactones from diols using a novel metal–ligand bifunctional catalyst. *Org Lett* 4:2361–2363
68. Suzuki T, Yamada T, Watanabe K, Katoh T (2005) Iridium-catalyzed oxidative lactonization and intramolecular Tishchenko reaction of  $\delta$ -ketoaldehydes for the synthesis of isocoumarins and 3,4-dihydroisocoumarins. *Bioorg Med Chem Lett* 15:2583–2585
69. Suzuki T, Morita K, Ikemiyagi H, Watanabe K, Hiroi K, Katoh T (2006) Synthesis of the hemiacetal pheromone of the spined citrus bug *biprorulus bibax* utilizing an iridium catalyzed oxidative lactonization. *Heterocycles* 69:457–461
70. Königsmann M, Donati N, Stein D, Schönberg H, Harmer J, Sreekanth A, Grützmacher H (2007) Metalloenzyme-inspired catalysis: selective oxidation of primary alcohols with an iridium–aminyl-radical complex. *Angew Chem Int Ed* 46:3567–3570
71. Oger C, Brinkmann Y, Bouazzaoui S, Durand T, Galano J-M (2008) Stereocontrolled access to isoprostanes via a bicycle[3.3.0]octene framework. *Org Lett* 10:5087–5090
72. Arita S, Koike T, Kayaki Y, Ikariya T (2008) Aerobic oxidation of alcohols with bifunctional transition-metal catalysts bearing C–N chelate ligands. *Chem Asian J* 3:1479–1485
73. Kosaka M, Sekiguchi S, Naito J, Uemura M, Kuwahara S, Watanabe M, Harada N, Hiroi K (2005) Synthesis of enantiopure phthalides including 3-butylphthalide, a fragrance component of celery oil, and determination of their absolute configurations. *Chirality* 17:218–232
74. Suzuki T, Morita K, Matsuo Y, Hiroi K (2003) Catalytic asymmetric oxidative lactonizations of meso-diols using a chiral iridium complex. *Tetrahedron Lett* 44:2003–2006
75. Dechert-Schmitt A-MR, Schmitt DC, Krische MJ (2013) Protecting-group-free diastereoselective C–C coupling of 1,3-glycols and allyl acetate through site-selective primary alcohol dehydrogenation. *Angew Chem Int Ed* 52:3195–3198
76. Shin I, Wang G, Krische MJ (2014) Catalyst-directed diastereo- and site-selectivity in successive nucleophilic and electrophilic allylations of chiral 1,3-diols: protecting-group-free synthesis of substituted pyrans. *Chem Eur J* 20:13382–13389
77. Ramachandran PV (2002) Pinane-based versatile “allyl” boranes. *Aldrichim Acta* 35:23–35
78. Denmark SE, Fu J (2003) Catalytic enantioselective addition of allylic organometallic reagents to aldehydes and ketones. *Chem Rev* 103:2763–2793
79. Yu C-M, Youn J, Jung H-K (2006) Regulation of stereoselectivity and reactivity in the inter- and intramolecular allylic transfer reactions. *Bull Korean Chem Soc* 27:463–472
80. Marek I, Sklute G (2007) Creation of quaternary stereocenters in carbonyl allylation reactions. *Chem Commun* 1683–1691
81. Hall DG (2007) Lewis and Brønsted acid catalyzed allylboration of carbonyl compounds: from discovery to mechanism and applications. *Synlett* 1644–1655
82. Lachance H, Hall DG (2008) Allylboration of carbonyl compounds. *Org React* 73:1–573
83. Yus M, González-Gómez JC, Foubelo F (2011) Catalytic enantioselective allylation of carbonyl compounds and imines. *Chem Rev* 111:7774–7854
84. Denmark SE, Ghosh SK (2001) The first catalytic, diastereoselective, and enantioselective crossed-aldol reactions of aldehydes. *Angew Chem Int Ed* 40:4759–4762
85. Rychnovsky SD, Skalitzky DJ (1992) A practical preparation of  $\alpha$ -alkoxylithium reagents: synthesis of syn or anti 1,3-diols. *J Org Chem* 57:4336–4339
86. Marriner GA, Garner SA, Jang H-Y, Krische MJ (2004) Metallo-aldehyde enolates via enal hydrogenation: catalytic cross aldolization with glyoxal partners as applied to the synthesis of 3,5-disubstituted pyridazines. *J Org Chem* 69:1380–1382
87. Fu F, Loh T-P (2009) An asymmetric synthesis of the polyol fragment of the polyene macrolide antibiotic RK-397. *Tetrahedron Lett* 50:3530–3533

88. Mengel A, Reiser O (1999) Around and beyond Cram's rule. *Chem Rev* 99:1191–1223
89. Feng J, Garza VJ, Krische MJ (2014) Redox-triggered C–C Coupling of alcohols and vinyl epoxides: diastereo- and enantioselective formation of all-carbon quaternary centers via tert-(hydroxy)-prenylation. *J Am Chem Soc* 136:8911–8914
90. Wang G, Franke J, Ngo CQ, Krische MJ (2015) Diastereo- and enantioselective iridium catalyzed coupling of vinyl aziridines and alcohols: site-selective modification of unprotected diols and synthesis of substituted piperidines. *J Am Chem Soc* 137:7915–7920

# Site-Selective Peptide/Protein Cleavage

Jizhi Ni and Motomu Kanai

**Abstract** Site-selective peptide/protein degradation through chemical cleavage methods is an important modification of biologically relevant macromolecules which complements enzymatic hydrolysis. In this review, recent progress in chemical, site-selective peptide bond cleavage is overviewed, with an emphasis on postulated mechanisms and their implications on reactivity, selectivity, and substrate scope.

**Keywords** Cleavage • Degradation • Peptide bonds • Proteins • Site-selectivity

## Contents

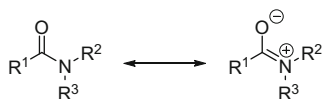
1	Introduction .....	104
2	Metal-Promoted Peptide Hydrolysis/Solvolytic .....	104
2.1	Using Interaction Between Metal Ions and Specific Side Chain Functional Groups of Peptides .....	106
2.2	Using Metal Complexes Bearing Recognition Motifs .....	110
3	Hydrazinolysis .....	113
4	Site-Specific Peptide Cleavage Through Side Chain Modifications .....	113
5	Oxidative Peptide Bond Cleavage .....	115
5.1	Oxidative Cleavage Assisted by Metal Ions/Metal Complexes .....	115
5.2	Peptide Cleavage with Non-Metal Oxidant .....	118
6	Conclusion .....	119
	References .....	119

---

J. Ni and M. Kanai (✉)

Graduate School of Pharmaceutical Sciences, The University of Tokyo, and JST-ERATO, Kanai Life Science Catalysis Project, 7-3-1, Hongo, Bunkyo-ku, Tokyo 113-0033, Japan  
e-mail: [kanai@mol.f.u-tokyo.ac.jp](mailto:kanai@mol.f.u-tokyo.ac.jp)

**Fig. 1** Electron delocalization of the amide functionality



## 1 Introduction

Amide bonds are among the most fundamental and important chemical bonds in nature because of their existence in peptide and protein structures. Amide bonds are stable because of delocalization of the lone pair electrons on the nitrogen atom over the amide functionality (Fig. 1). The half-life of amide bonds in spontaneous hydrolysis is estimated to be 350–600 years in a neutral pH solution at room temperature [1]. Traditional methods for amide hydrolysis generally require harsh reaction conditions, such as strong acids or bases at high temperatures [2].

Protein modifications through chemical methods [3–16] are of great importance in a broad range of research fields, such as chemical biology [17], chemical genetics [18], protein engineering [19, 20], proteomics [21, 22], and drug discovery [23, 24]. Site-specific peptide bond cleavage reactions are valuable chemical tools among such important chemical modifications. Examples include structural determination of peptides and proteins in proteomics, chemical biology, and structural biology studies [25–28].

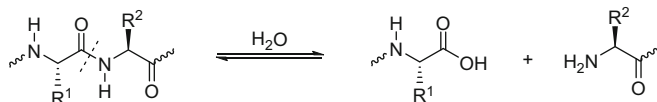
Despite enzymatic (peptidase) hydrolysis of peptide bonds proceeds at specific sites under mild conditions with high fidelity [29, 30], the scope of the scissile substrates is restricted in principle to genetically encoded amino acid sequences. Chemical methods are applicable to substrates containing unnatural or structurally modified amino acids that are not recognized by peptidases. Therefore, the development of artificial peptidases enabling practical and general protein/peptide cleavage is challenging, but of significant utility in a variety of applications ranging from structure determination of chemically modified proteins/peptides to therapeutics.

In this chapter, we survey recent (during the past 10 years) progress in site-selective peptide/protein degradation through chemical cleavage methods that complement enzymatic hydrolysis.

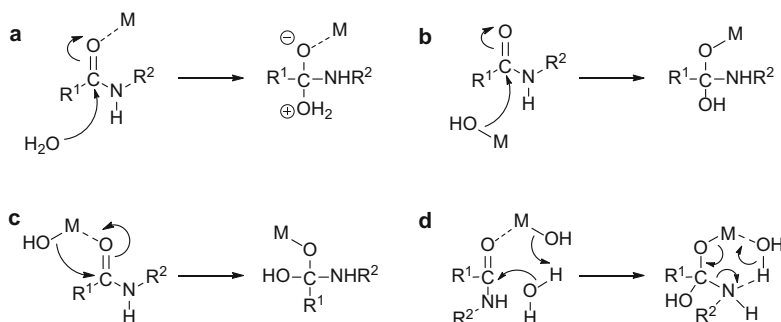
## 2 Metal-Promoted Peptide Hydrolysis/Solvolysis

Hydrolysis (or solvolysis) of peptides and proteins involves addition of a water (or solvent) molecule across an amide bond in peptide backbones without modifying side chain structures (Fig. 2). The hydrolytic approach generates native C-terminal carboxy and N-terminal amino groups. Hence, it is particularly useful and straightforward in protein sequencing, proteomics, and protein engineering applications.

Four representative roles are conceivable for metals in metal-promoted peptide bond hydrolysis (Fig. 3) [31, 32]. First, metals act as a Lewis acid, and activate



**Fig. 2** Peptide bond hydrolysis



**Fig. 3** Four representative pathways for metal-promoted hydrolysis of amide bonds

carbonyl groups toward nucleophilic attack of hydroxide ions or water molecules (Fig. 3a). Second, metals enhance nucleophilicity of water molecules as a Brønsted base through generation of metal hydroxides (Fig. 3b). Third, metals can both activate carbonyl groups as a Lewis acid and deliver hydroxide ions to carbonyl carbons as a counterion (Fig. 3c). These three modes of action facilitate the initial tetrahedral intermediate (TI)-formation step. Elimination of the poor leaving group, RNH, from the generated TI, however, is another difficult step in peptide bond hydrolysis, especially at neutral pH [31, 33]. Because the poor leaving group RNH must be protonated either prior to or in concert with C–N bond cleavage [31], the TI breakdown step at a neutral pH can be accelerated by the fourth mechanism: after forming TI, a metal-bound water molecule works as a proton source for the leaving RNH (Fig. 3d). This M–OH<sub>2</sub> species, serving as a general acid, efficiently facilitates the C–N bond cleavage.

Numerous examples of peptide hydrolysis have been achieved with the assistance of metal ions/metal complexes, including Zn, Co, Zr, Cu, Ni, Mo, Pd, and Pt. Detailed information can be found in a number of excellent and comprehensive review articles written on this subject [32–48]. According to the recognition mode, the site-selective peptide/protein degradation can be achieved in two ways: a direct metal-peptide side chain interaction or a promoter's recognition site-peptide side chain interaction.

## 2.1 Using Interaction Between Metal Ions and Specific Side Chain Functional Groups of Peptides

After metal ions interact with specific peptide side chain functional groups, they act as a Lewis acid to enhance the reactivity of proximal peptide bonds through coordination and polarization of carbonyl groups [49]. Meanwhile, metal ions can also increase the concentration of nucleophilic hydroxide ions by forming metal hydroxides (M–OH). In this way, peptide bond cleavage can be facilitated at specific residues bearing high affinity with metal ions.

Using  $[\text{Pd}(\text{H}_2\text{O})_4]^{2+}$  (**1**), *cis*- $[\text{Pd}(\text{en})(\text{H}_2\text{O})_2]^{2+}$  (**2**; en = ethylenediamine), and other  $\text{Pd}^{\text{II}}$  complexes as catalysts, various polypeptides and proteins containing coordinating residues, such as His, *S*-methyl cysteine (CysMe), and Met, were cleaved (Fig. 4) [44, 50–56]. The cleavage site-selectivity depended on the interaction between the nitrogen or sulfur atom of peptide side chains and the  $\text{Pd}^{\text{II}}$  ions. For dipeptides Ac–His–Xaa, cleavage occurred at the His–Xaa peptide bond with moderate catalytic activity (turnover ~4) by using **2** [55], whereas a turnover of 14 was achieved at 50°C in acetone-*d*<sub>6</sub> containing 2.2% D<sub>2</sub>O for cleavage of Ac–Met–Xaa at the Met–Xaa bond using a dinuclear  $[\text{Pd}_2(\mu\text{-SPh})_2(\text{sol})_4]^{2+}$  complex (sol = H<sub>2</sub>O or acetone, **3**, Fig. 4) [57].

For Met- or His-containing oligopeptides and proteins, however, cleavage using **2** [58] or **1** [59, 60] proceeded at a different site from the above dipeptides, the second peptide bond to the N-terminal side from the anchoring residue (Fig. 5a). In an acidic solution (pH < 2.0), the side chain sulfur atom of Met coordinated to the  $\text{Pd}^{\text{II}}$  complexes to produce **4** (Fig. 5b). Then the  $\text{Pd}^{\text{II}}$  ion preferentially formed a six-membered bidentate chelate complex **5** through covalent bond-formation with the amide nitrogen atom of the Met residue. Generation of a Pd–N bond increased the electron density of this amide bond, thus protecting the amide carbonyl carbon from nucleophilic attack by a water molecule or a hydroxide ion [61]. The bidentate chelate complex **5** was, however, hydrolytically active at the peptide bond adjacent to the N-terminal side because of proximity to the metal. This selective binding mode explained the distinct site-selectivity from the dipeptide substrates Ac–His (Met)–Xaa in [44, 50–57]. At pH 2.3, tridentate chelate complex **6** formed as a major species. When the pH reached 4.5, tetradentate chelate complex **7** was the major species. Both **6** and **7** proved to be hydrolytically inactive.

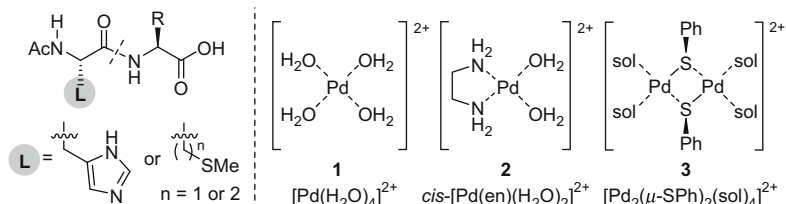
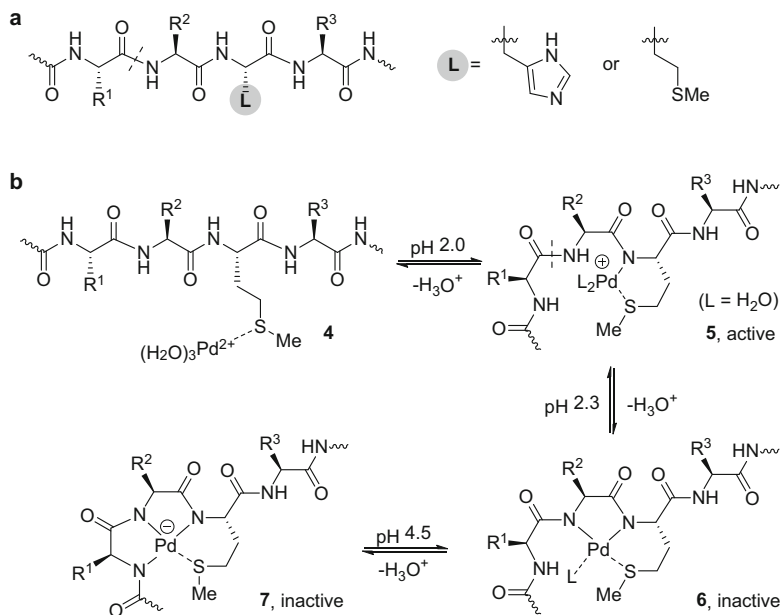


Fig. 4 Hydrolytic cleavage of dipeptides Ac–His(Met or CysMe)–Xaa by  $\text{Pd}^{\text{II}}$  complexes

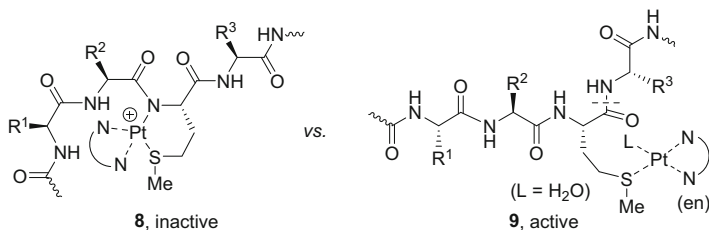


**Fig. 5** Cleavage of oligopeptides and proteins by  $[\text{Pd}(\text{H}_2\text{O})_4]^{2+}$  or *cis*- $[\text{Pd}(\text{en})(\text{H}_2\text{O})_2]^{2+}$

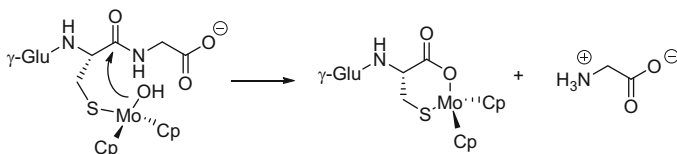
The cleavage site using *cis*- $[\text{Pt}(\text{en})(\text{H}_2\text{O})_2]^{2+}$  differed from that using *cis*- $[\text{Pd}(\text{en})(\text{H}_2\text{O})_2]^{2+}$  (**2**). The  $\text{Pt}^{\text{II}}$  complex cleaved the C-terminal side peptide bond of the anchoring residue; for example, the Met–Zaa bond in Xaa–Yaa–Met–Zaa was cleaved [62]. The stark difference between the Pt and Pd complexes in site-selectivity was because of the stability of metal–en complexes. Complex **2** was not stable in water, and the ethylene diamine ligand (en) was rapidly displaced by water. The *cis*- $[\text{Pt}(\text{en})(\text{H}_2\text{O})_2]^{2+}$  complex was stable, however, and the en ligand remained coordinated to  $\text{Pt}^{\text{II}}$  ion throughout the reaction [63]. Because of the lack of the coordination site, the  $\text{Pt}^{\text{II}}$  ion in a chelate complex **8** did not act as a Lewis acid to activate the proximal peptide bond (Fig. 6), in contrast to the corresponding  $\text{Pd}^{\text{II}}$  complex **5** (Fig. 5). However,  $\text{Pt}^{\text{II}}$  complex **9** was hydrolytically active because of the coordination lability of an aqua ligand (L), leading to cleavage at the indicated site [62].

A  $\text{Cp}_2\text{MoCl}_2$  complex bound with the thiol group of Cys through chloride/thiolate ligand exchange, and mediated regioselective hydrolysis of the Cys–Xaa peptide bond in dipeptides and tripeptides by intramolecular metal hydroxide ( $\text{Mo-OH}$ ) transfer (Fig. 7) [64]. A stoichiometric amount of  $\text{Cp}_2\text{MoCl}_2$  was required because of the very slow ligand exchange of Mo–thiolates.

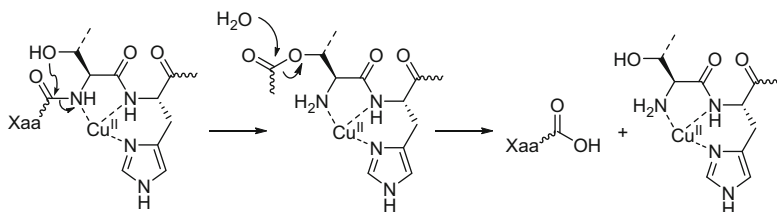
An imidazole group of a histidine residue is a good ligand for  $\text{Cu}^{\text{II}}$  [65–67] and  $\text{Ni}^{\text{II}}$  [40, 66–70] ions. Hydrolysis using  $\text{CuCl}_2$  was specific for the Xaa–Ser(Thr) bond in Xaa–Ser(Thr)–His sequences (at 62°C and pH 8) [65]. Allen proposed that strong binding of the released amino group to  $\text{Cu}^{\text{II}}$  ion prevented the reverse O-to-N



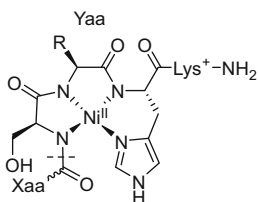
**Fig. 6** Site-selective cleavage of peptides by *cis*-[Pt(en)(H<sub>2</sub>O)<sub>2</sub>]<sup>2+</sup> complex



**Fig. 7** Hydrolysis of  $\gamma$ -L-glutamyl-L-cysteinylglycine (GSH) by Cp<sub>2</sub>MoCl<sub>2</sub>



**Fig. 8** Cu<sup>II</sup>-promoted hydrolysis of Xaa-Ser(Thr)-His sequences



**Fig. 9** Intermediate of Ni<sup>II</sup>-promoted hydrolysis of a Ser-Yaa-His-Lys sequence

acyl migration reaction, which would otherwise be thermodynamically favored in the absence of the metal (Fig. 8) [41]. Using Ni<sup>II</sup>, the Xaa-Ser bond in a Xaa-Ser-Yaa-His-Lys sequence was cleaved at 37°C and pH 7.4 [69] or 10.8 [66]. A stable complex between square planar Ni<sup>II</sup> ion and the Ser-Yaa-His-Lys sequence was formed prior to cleavage (Fig. 9) [67]. In both cases of Cu<sup>II</sup>- and Ni<sup>II</sup>-mediated peptide cleavage, the peptide bond cleavage proceeded through N-to-O acyl migration by participation of the Ser (or Thr) hydroxy group, followed by hydrolysis of the resulting esters.

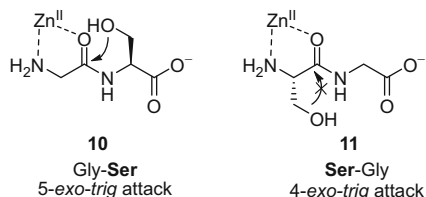
In many metal ion-assisted hydrolytic peptide bond cleavage reactions, the metal ions, such as Pd, Pt, Cu, Mo, and Ni, are trapped by hydrolyzed products. Because free metal ions that are reactive for peptide bond hydrolysis hardly regenerate, examples for metal ion-catalyzed peptide bond cleavage are limited.

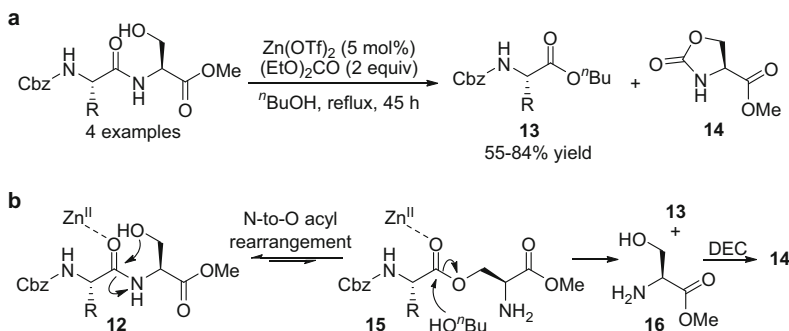
Zn<sup>II</sup> ion possesses several special properties in promoting peptide hydrolysis [71]. First, because Zn<sup>II</sup> ion has a filled d shell, there is no gain in ligand field stabilization energy when it is coordinated by ligands in any geometry. Therefore, Zn<sup>II</sup> may form a variety of ligand geometries without any energy costs. Second, according to hard-soft acid-base theory, Zn<sup>II</sup> is regarded as a borderline acid. It can interact strongly with a variety of ligand types including a sulfur atom of Cys, a nitrogen atom of His, and oxygen atoms of Glu, Asp, and water [72]. Third, ligand exchange on Zn<sup>II</sup> ion is fast, allowing for facile catalyst turnover [39]. Fourth, Zn<sup>II</sup> oxidation state is stable, and thus oxidative side reactions are not conceivable. With these advantages, Zn<sup>II</sup> ions are often found as cofactors in the active sites of proteases (e.g., carboxypeptidase A [73, 74], carboxypeptidase B, and thermolysin [75]).

Early in 1961, Bamann and coworkers reported hydrolysis of Gly-Leu by treatment with stoichiometric Zn<sup>II</sup> for 24 h at pH 8.6 and 70°C [76]. In 2003, Yashiro presented hydrolysis of dipeptides in the presence of stoichiometric ZnCl<sub>2</sub> at pH 7.0 [77]. Hydrolysis of dipeptide sequences containing either a Ser or a Thr residue at the C-terminal position was significantly faster than peptides without these residues. The hydroxy group of the Ser or Thr side chain facilitated peptide bond hydrolysis via promoting N-to-O acyl rearrangement. In Xaa-Ser(Thr) sequences (e.g., Gly-Ser), intramolecular attack of the side chain hydroxy group to the amide carbonyl carbon proceeded through favorable five-membered ring formation (**10**, Fig. 10). In the case of Ser(Thr)-Xaa sequences (e.g., Ser-Gly), however, yield of hydrolysis was low because formation of an unfavorable four-membered ring was required (**11**, Fig. 10).

In 2012, Mashima and co-workers reported that Zn(OTf)<sub>2</sub> acted as a catalyst for Ser-selective scission of peptides (Fig. 11a) [78]. This was the first Zn-catalyzed peptide cleavage. Addition of diethylcarbonate (DEC) as a trapping reagent for the resulting Ser methyl ester (**16**), which was generated after amide bond alcoholysis, was necessary to ensure the cleavage in high yield. On replacing the Ser residue with a Gly residue, only a trace amount of peptide cleavage product was obtained from Cbz-Gly-Gly-OMe, indicating the importance of the Ser hydroxy group participation. With Cbz-Ser-Gly-OMe, no scission occurred, because of the requirement of unfavorable 4-*exo-trig* attack of the Ser hydroxy group. In the

**Fig. 10** Hydrolysis of Gly-Ser and Ser-Gly





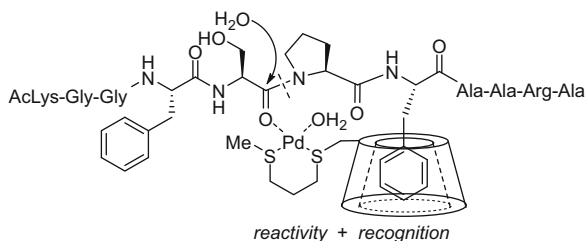
**Fig. 11** Zinc-catalyzed Ser-selective peptide cleavage

proposed mechanism (Fig. 11b), the ester intermediate **15** was first generated after  $\text{Zn}^{\text{II}}$ -catalyzed N-to-O acyl rearrangement [79]. Then, subsequent  $\text{Zn}^{\text{II}}$ -catalyzed *trans*-esterification (**15**) [80–82] released **16**, which was captured by DEC, forming the corresponding carbamate **14**.

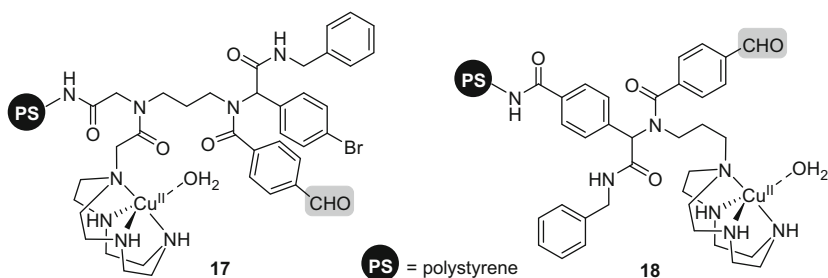
## 2.2 Using Metal Complexes Bearing Recognition Motifs

To facilitate site-selectivity and to avoid strong binding of hydrolysis products to metal ions, a reactive metal ion complex site and a recognition motif for a specific functional group of peptide side chains were separated and conjugated in one molecule. In this way, the metal ion complex moiety positioned itself proximal to a scissile peptide bond, and promoted selective hydrolytic cleavage.

Cyclodextrins (CDs) have affinity for hydrophobic organic moieties. Kostić's group developed a new enzyme-like reagent by conjugating  $\beta$ -CD and a reactive  $\text{Pd}^{\text{II}}$  complex moiety (Fig. 12) [83]. On one hand, the  $\beta$ -CD moiety weakly bound to the aromatic Phe side chain of substrate peptides. On the other hand,  $\text{Pd}^{\text{II}}$  ion selectively activated the peptide bond of the X-Pro group for hydrolysis. Using Ac-Lys-Gly-Gly-Phe-Ser-Pro-Phe-Ala-Ala-Arg-Ala as a substrate, the Ser-Pro bond was selectively cleaved by the Pd- $\beta$ -CD conjugate (10 equiv. of  $\text{Pd}^{\text{II}}$  complex was used to enhance host-guest binding) (Fig. 12). The Gly-Gly bond was not cleaved, however, despite its relative position to another Phe residue being the same as the cleaved Ser-Pro bond to Phe (i.e., the second peptide bond to the N-terminal side from Phe). The difference was because of the coordination ability of the amide carbonyl oxygen atom to Pd; the amide oxygen atom of the Xaa-Pro group possesses the greatest Lewis basicity in proteins [34], thus facilitating coordination and activation of the peptide bond of the Xaa-Pro-Phe sequence. In bradykinin (Arg-Pro-Pro-Gly-Phe-Ser-Pro-Phe-Arg), the Pd- $\beta$ -CD conjugate selectively



**Fig. 12** Hydrolytic cleavage of the Xaa-Pro bond promoted by Phe residue recognition by Pd- $\beta$ -CD conjugate

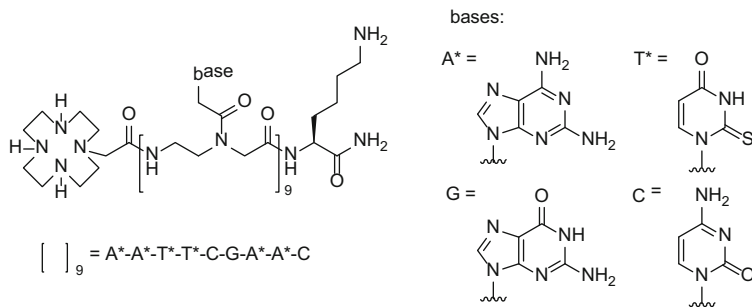


**Fig. 13** Cu complexes bearing a formyl group to recognize Lys side chains on the surface of proteins

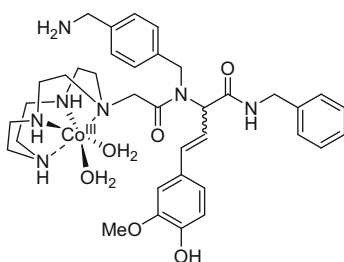
cleaved the Ser-Pro peptide bond, whereas an unconjugated  $[\text{Pd}(\text{H}_2\text{O})_4]^{2+}$  cleaved all three Xaa-Pro bonds.

To achieve high site-selectivity, great reaction rate, and broad substrate generality, peptide cleavage promoter molecules containing a metal complex moiety conjugated with a formyl group were synthesized, in which the formyl group was a recognition motif for Lys residues through imine formation (**17** and **18**, racemic compounds, Fig. 13) [84–87]. With enhanced affinity between the promoter molecules and substrates by reversible imine (covalent bond)-formation, **17** and **18** (100 equiv.) promoted selective cleavage of myoglobin containing 19 Lys residues at the Gln91-Ser92 and Ala94-Thr95 sites. The site-selectivity was attributed to general acid assistance by proximal Tyr146. On replacing the formyl groups of **17** and **18** by hydrogen atoms, protein cleavage was much slower.

Prior to 2000, utility of  $\text{Co}^{\text{III}}$  complexes in peptide bond cleavage was limited only to hydrolysis of the N-terminal peptide bond through coordination of the terminal amino group to the  $\text{Co}^{\text{III}}$  ion [37, 38, 42, 88–90]. This limitation was overcome by Kumar and coworkers, who reported  $[\text{Co}(\text{H}_2\text{O})(\text{NH}_3)_5]^{3+}$ - and  $[\text{Co}(\text{H}_2\text{O})_2(\text{NH}_3)_4]^{3+}$ -promoted hydrolysis of hen egg lysozyme at the internal Ala110-Trp111 bond under extremely mild conditions (at neutral pH and 37°C) [91]. The Trp108 residue anchored the  $\text{Co}^{\text{III}}$  ion in proximity to the scissile Ala110-Trp111 peptide bond. In this sense, this work is categorized in Sect. 2.1. Based on Kumar's



**Fig. 14** Cyclen-PNA conjugates

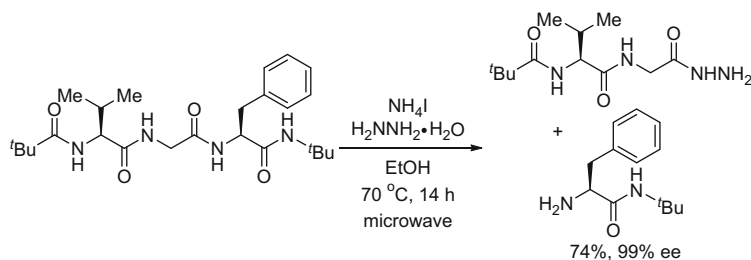


**Fig. 15** An artificial metalloprotease selective for a disease-related enzyme

work, Suh developed a  $\text{Co}^{\text{III}}$  catalyst that selectively hydrolyzed the backbone of a target protein [92, 93]. Designed catalysts comprised a cyclen ligand moiety covalently attached to a peptide nucleic acid (PNA) oligomer that selectively bound to myoglobin (Fig. 14). Using the  $\text{Co}^{\text{III}}$  complex (10 mol%), myoglobin was hydrolyzed at internal Leu72–Gly73 and Leu89–Ala90 bonds under extremely mild conditions (at pH 7.5 and 37°C) with ~50% yield after 30 h. When  $\text{Co}^{\text{III}}$  was replaced by other metals,  $\text{Cu}^{\text{II}}$  was found to be less reactive, whereas  $\text{Fe}^{\text{III}}$ ,  $\text{Hf}^{\text{IV}}$ ,  $\text{Pt}^{\text{IV}}$ ,  $\text{Zr}^{\text{IV}}$ ,  $\text{Pd}^{\text{II}}$ , and  $\text{Ce}^{\text{IV}}$  failed to exhibit any catalyst activity.

In 2005, using a combinatorial library prepared by Ugi condensation, the same group reported an artificial metalloprotease-type catalyst (19 mol%) that selectively hydrolyzed a disease-related enzyme, peptide deformylase (PDF), at the Gln152–Arg153 bond (Fig. 15) [94]. This enzyme is involved in deformylation of proteins in prokaryotic translational systems. The optimal proteolytic activity was produced at pH 7.5. A docking simulation study predicted preferential interaction of PDF with the (S)-enantiomer complex, and hydrogen bonding and van der Waals interactions between the complex with specific amino acid residues near the scissile peptide bond.

Suh's group also developed several  $[\text{Co}^{\text{III}}(\text{cyclen})]$ -based complexes for cleavage of  $\beta$ -amyloid 1–42 ( $\text{A}\beta_{42}$ ) oligomers, a possible etiology of Alzheimer disease, and human islet amyloid polypeptide (h-IAPP, also known as amylin), a cause of type 2 diabetes, typically at pH 7.5 and 37°C [95–99]. The stable  $\text{Co}^{\text{III}}$  complexes



**Fig. 16** Hydrazinolysis in peptide bond cleavage

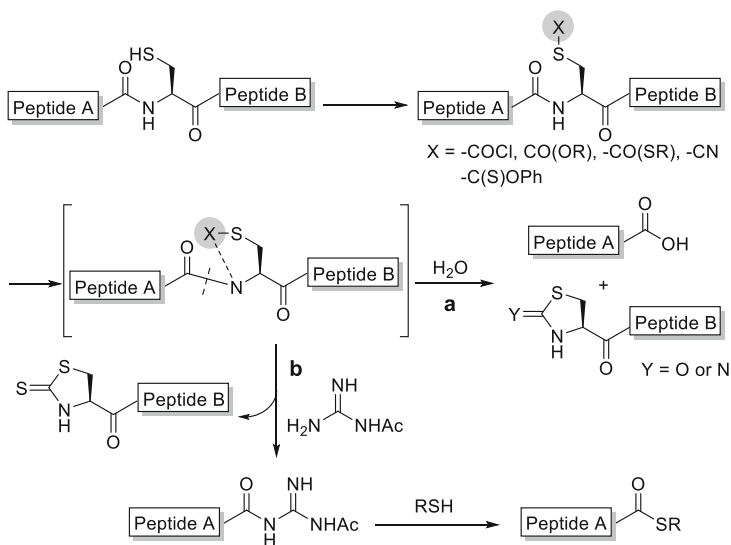
could ensure that the metal ion would not be released, even in clinical applications. Li et al. and Jeong et al. reported that exchange-labile  $[\text{Cu}^{\text{II}}(\text{cyclen})]$ -based complexes also worked as artificial proteases for cleavage of  $\text{A}\beta_{42}$  oligomers and h-IAPP [100–104]. It was expected that the ligand-conjugated apocyclens themselves could be used, instead of  $\text{Cu}^{\text{II}}$  complexes, because the cyclens would capture  $\text{Cu}^{\text{II}}$  ions bound to amyloids and generate catalytically active ligand-conjugated  $\text{Cu}^{\text{II}}$  complexes. These results indicate that ligand-conjugated peptide-cleavage catalysts might be useful drugs for targeting particular amyloid diseases (e.g., Alzheimer's disease, type 2 diabetes, and Parkinson's disease).

### 3 Hydrazinolysis

In 2012, Ohshima and co-workers reported microwave-assisted transamidative deacylation of unactivated amides with a combination of an ammonium salt and ethylene diamine at  $50\text{--}90^\circ\text{C}$  [105]. In 2014, the same group realized hydrazinolysis of unactivated amide bonds [106]. The reaction proceeded at moderate temperature ( $50\text{--}70^\circ\text{C}$ ) to provide *N*-acyl hydrazines and amines in good yield. They applied the reaction conditions to cleave peptides (Fig. 16). Selective cleavage of the Gly–Phe bonds in two peptides was realized. No epimerization at the  $\alpha$ -position of the Phe residue was observed. The site-selectivity was likely caused by both steric and electronic factors.

### 4 Site-Specific Peptide Cleavage Through Side Chain Modifications

Selective activation of peptide side chain functional groups is an important approach in site-selective cleavage of peptide bonds. In 1950, Edman reported a stepwise peptide cleavage from the N-terminal using phenyl isothiocyanate [107]. Thereafter, selective peptide bond cleavage methods at specific residues

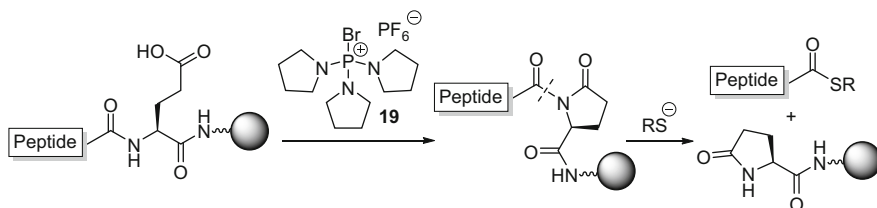


**Fig. 17** Cleavage of a peptide bond initiated by selective *S*-carbonylation of Cys or Met residue

have been reported for protein sequencing. Cys and Met are among the most studied cleavage sites because of the high nucleophilicity of sulfur atoms. Thus, Cys- and Met-selective peptide cleavage reactions were developed initiated by *S*-cyanation of a Met [108, 109] or a Cys [110, 111] residue and *S*-acylation of a Cys [112, 113] residue (Fig. 17a). In these methods, an electrophilic auxiliary group (X) was introduced to the sulfur atom of a Met or a Cys side chain, which induced activation of the peptide bond through N-acylation and subsequent hydrolysis.

In 2012, Kajihara and Okamoto reported a method for cleavage of the N-terminus side peptide bond of a Cys residue and generation of a thioester (Fig. 17b) [114]. This method involved three steps: (1) selective thiocarbonylation of the thiol group of Cys by using *O*-phenyl chlorothionoformate [PhOC(S)Cl], (2) cyclization to generate thiazolidine-2-thione moiety, followed by amidolysis with *N*-acetylguanidine, and (3) thiolysis of the obtained peptidyl-*N*-acetylguanidine to give the peptide thioester. Product thioesters are the key components for chemical ligation, such as native chemical ligation.

A similar concept for site-selective thiolysis of peptide bonds via backbone peptide bond activation can be found in Jensen's work (Fig. 18) [115]. The key step involves activation of the carboxy group of a Glu side chain by PyBrOP (19), resulting in the on-resin formation of the pyroglutamyl imide moiety. The activation renders the imide C–N bond susceptible to thiolysis, after which protected peptide thioesters were released from the solid support.



**Fig. 18** N-Terminal side peptide bond thiolysis at the Glu residue

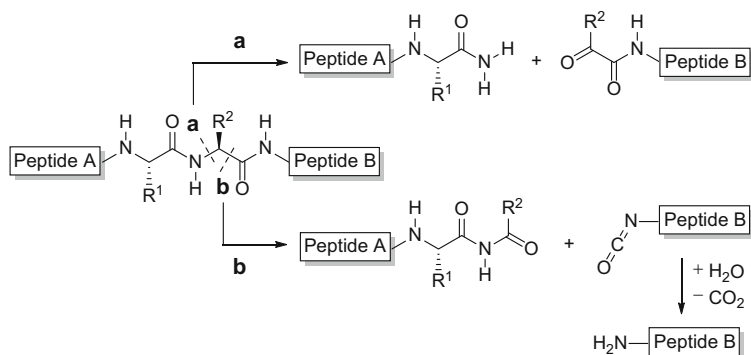
## 5 Oxidative Peptide Bond Cleavage

### 5.1 Oxidative Cleavage Assisted by Metal Ions/Metal Complexes

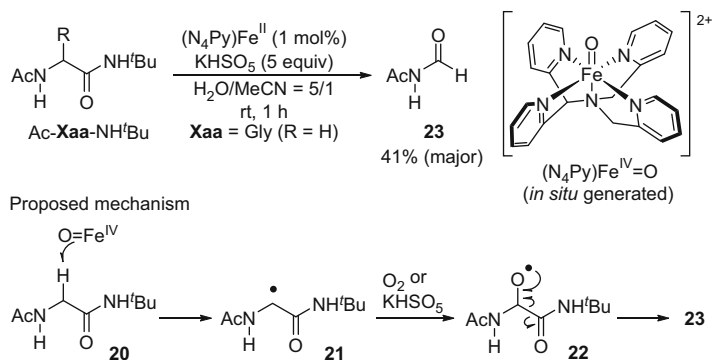
The oxidative peptide cleavage can be classified into two main types (Fig. 19): **a**) hydroxylation at the  $\alpha$ -carbon ( $C\alpha$ ) followed by cleavage of the  $C\alpha$ -N bond, and **b**) oxidative cleavage of the  $C\alpha$ -C(O) bond [116–123].

Redox active metal ions/metal complexes (e.g.,  $Cu^{II}$  [123–127],  $Cr^{III}$  [118],  $Cr^V$  [128],  $Fe^{II}$  [129–138],  $Fe^{III}$  [126, 138–144],  $Ni^{II}$  [145, 146], and  $V^V$  [147–150]) were employed to promote site-selective oxidative degradation of folded proteins under non-denaturing conditions. In the presence of oxidants (e.g.,  $O_2$  or  $H_2O_2$ ), hydroxy radicals or in situ-generated metal-oxo species abstracted an H atom at  $C\alpha$ . This event was followed by oxidation at  $C\alpha$  and cleavage of the  $C\alpha$ -N or  $C\alpha$ -C(O) bond [118, 126, 141, 142]. In those methods, backbone cleavage sites were determined by the affinity to metal complexes [127].

Nature uses heme- [151] and non-heme [152–156] iron-containing enzymes for oxidation of small molecules as an important metabolic transformation. High-valent iron(IV)-oxo species are postulated as the key reactive intermediates. Que reported that a non-heme iron(IV)-oxo complex,  $[(N_4Py)Fe^{IV} = O]^{2+}$  (the structure is shown in Fig. 20), oxidatively cleaved aliphatic C-H bonds (e.g., C-H bonds of cyclohexane) at room temperature [157]. In 2007, Kodanko reported oxidative amide cleavage of protected amino acids using an iron catalyst  $[Fe^{II}(N_4Py)(MeCN)](ClO_4)_2$  (1 mol%) in the presence of 5 equiv.  $KHSO_5$  as an oxidant through pattern **b**) in Fig 19 (Fig. 20) [158, 159]. Oxidation of Ac-Xaa-NH<sup>t</sup>Bu, where Xaa = Gly, produced *N*-acetylformamide as the major product through  $C\alpha$ -C(O) bond cleavage.  $\alpha$ -Alkyl-substituted amino acid derivatives (Xaa = Ala or Val) did not react under the same conditions. With substrates where Xaa = Phe, Tyr, Trp, or Met, oxidation of the amino acids' side chain was observed with greater reaction rates than C-C bond cleavage. According to the proposed mechanism, the first step was formation of glycyl radical intermediate **21** through abstraction of a hydrogen atom at  $C\alpha$  by the iron(IV)-oxo species. Then, **21** was trapped by oxygen species and alkoxy radical intermediate **22** was generated. Finally, radical fragmentation of **22** produced the cleavage product **23**.



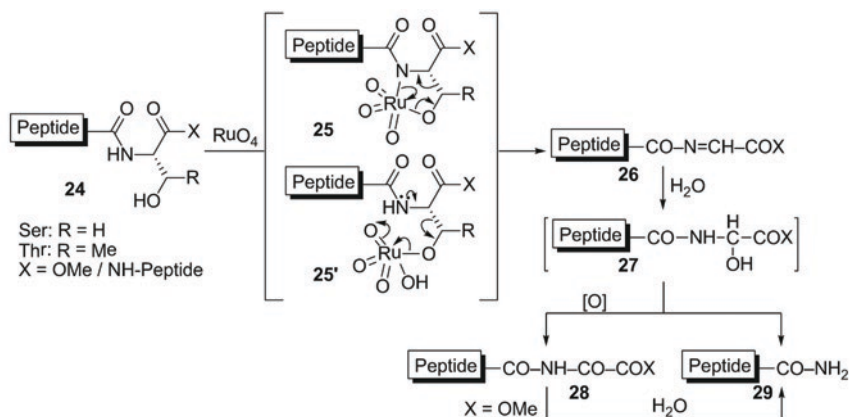
**Fig. 19** Two types of oxidative peptide backbone cleavage



**Fig. 20** Gly-selective oxidative amide cleavage catalyzed by  $(N_4Py)Fe^{II}$

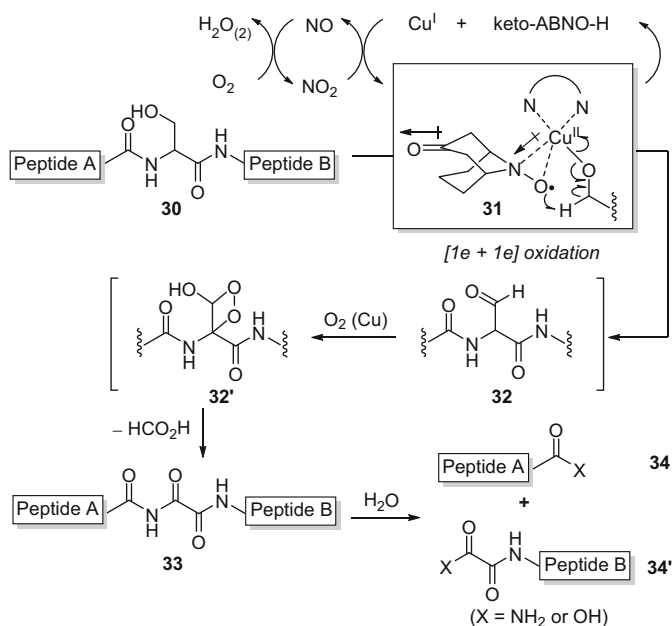
$Ru(VIII)$  oxo species ( $RuO_4$ ), generated *in situ* from  $RuCl_3$  and  $NaIO_4$ , is a powerful oxidizing agent. Ranganathan reported selective catalytic peptide backbone cleavage at serine and threonine residues through  $RuCl_3/NaIO_4$  oxidation (Fig. 21) [160, 161]. This facile C–N bond cleavage was induced by oxidative scission of the C $\beta$ –C $\alpha$  bond at Ser/Thr side-chains, involving either a cyclic (**25**) or an open-chain (**25'**) ruthenium intermediate. Subsequently, addition of water to acylimine **26** gave carbinolamide intermediate **27**. This intermediate underwent further oxidation to oxalimido esters **28** and then hydrolysis to terminal amides **29**. Because of the high reactivity of  $Ru(VIII)$  oxo species, other amino acid (e.g., Tyr, Trp, Cys, and Met) residues were also oxidized or decomposed under these reaction conditions.

Recently, Kanai and Oisaki developed catalytic aerobic oxidation of amines using a combination of a Cu complex and a redox mediator keto-ABNO (**31**, Fig. 22) [162]. Keto-ABNO has greater oxidation potential than other N-oxyl radicals such as TEMPO and ABNO because of the electron-withdrawing ability



**Fig. 21** Ser/Thr-selective peptide bond scission through  $\text{RuO}_4$  oxidation. Typical conditions:  $\text{RuCl}_3$  (2 mol%) and  $\text{NaIO}_4$  (18 equiv.) in  $\text{CH}_3\text{CN}/\text{CCl}_4/\text{pH 3 phosphate buffer}$  (1/1/2) at room temperature

of the keto group. In 2014, the same group achieved Ser-selective aerobic cleavage of peptides and a protein (ubiquitin) using stoichiometric amounts of a water-soluble Cu complex and **31** (**30–34** and **34'**, Fig. 22) [163]. Because of the mild reaction conditions, broad substrate generality compatible with various amino acid residues was realized (19 examples, including peptides comprising unnatural D-amino acids, Thr residues, or disulfide pairings). The postulated mechanism for the Ser-selective peptide cleavage is depicted in Fig. 22. First, an oxidatively active complex of  $\text{Cu}^{\text{II}}$  and keto-ABNO was generated under oxygen atmosphere. Oxidation of the Ser residue proceeded through the formation of  $\text{Cu}^{\text{II}}$ -alkoxide species, single electron oxidation of the alkoxide species by  $\text{Cu}^{\text{II}}$ , and concomitant abstraction of a hydrogen radical from the  $\alpha$ -carbon atom by keto-ABNO ([1e + 1e] oxidation process: **31**), affording aldehyde **32** ( $\alpha$ -formylglycineamide) and reduced  $\text{Cu}^{\text{I}}$  + keto-ABNO-H. Regeneration of the oxidatively active complex ( $\text{Cu}^{\text{II}}$  + keto-ABNO) was promoted by  $\text{NO}_2$ , generated from  $\text{NaNO}_2$  and acetic acid. The resulting NO was re-converted to  $\text{NO}_2$  through aerobic oxidation. Oxidative deformylation of  $\alpha$ -formylglycineamide **32** proceeded through presumed intermediate **32'** to produce oxalimide **33**. Oxalimide **33** was hydrolyzed under mild conditions to produce fragments **34** and **34'**. As for the alcohol oxidation step, a controversial mechanism was recently published based on both experiments and calculations [164, 165].



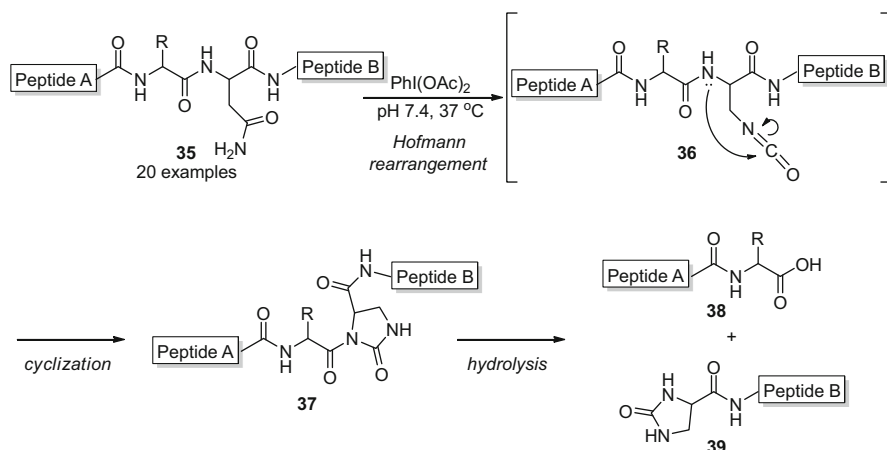
**Fig. 22** Serine-selective aerobic oxidative peptide cleavage and its proposed mechanism. Typical conditions: Cu<sup>I</sup>, bathophenanthroline salt, keto-ABNO (100 mol% each), and NaNO<sub>2</sub> (150 mol% at 0 h + 150 mol% at 5 h) in CH<sub>3</sub>CN/H<sub>2</sub>O/AcOH (9/9/2, 5 mM) at room temperature for 20 h under O<sub>2</sub> (1 atm)

## 5.2 Peptide Cleavage with Non-Metal Oxidant

Early in 1968, Shiba et al. reported Asp-selective peptide cleavage through Hofmann rearrangement promoted by Br<sub>2</sub>. The reaction proceeded in moderate yield under alkaline solution at 60°C [166]. Because of the harsh reaction conditions, however, the method was not applicable to substrates longer than tripeptides.

In 2014, Kanai and Sohma reported a mild method for Asp-selective peptide bond cleavage using diacetoxyiodobenzene (DIB) in an aqueous neutral solution at 37°C (Fig. 23) [167]. The transformation was initiated by oxidation of the primary amide group of an asparagine side chain, providing the corresponding isocyanate **36** through Hofmann rearrangement [168, 169]. Then, intramolecular nucleophilic attack of the amide nitrogen atom of the peptide backbone afforded a kinetically favorable five-membered *N*-acylurea **37** [170–173]. Hydrolysis of **37** at the *N*-acylurea moiety cleaved the peptide chain into the N-terminal fragment **38** and cyclic urea-containing C-terminal fragment **39**.

This asparagine-selective peptide cleavage was of wide substrate generality (20 examples), including an unnatural peptide sequence comprising D-amino acids and chemically modified (oxidized) amino acids that were not cleaved by peptidases.



**Fig. 23** Asp-selective peptide cleavage using DIB in neutral aqueous solution

## 6 Conclusion

In the past 10 years, methods for site-selective chemical cleavage of peptides and proteins have significantly advanced. Metal complexes with high catalyst turnovers, especially those containing  $\text{Zn}^{\text{II}}$ ,  $\text{Co}^{\text{III}}$ , and  $\text{Fe}^{\text{IV}}$ , have been rationally designed and synthesized for hydrolytic or oxidative cleavage of peptide bonds. Meanwhile, site-selective peptide cleavage methods under metal-free conditions using reactivity of side chain functional groups have also proved to be useful for thioester formation toward chemical ligation and for structural determination of unnatural amino acid-containing peptides. Although important progress has been made, the abilities of peptide cleavage methods are still far behind natural peptidases regarding catalyst activity, cleavage site-fidelity, and substrate specificity. Research continues to fill those gaps. Development of truly useful and practical artificial peptidases that can complement enzymes opens up new biology and medicine. To do so requires fundamental chemical breakthroughs

## References

1. Radzicka A, Wolfenden R (1996) *J Am Chem Soc* 118:6105
2. Wuts PGM, Greene TW (2006) *Protective groups in organic synthesis*, 4th edn. Wiley, Hoboken, p 773–789
3. Antos JM, Francis MB (2006) *Curr Opin Chem Biol* 10:253
4. Pellois JP, Muir TW (2006) *Curr Opin Chem Biol* 10:487
5. Hackenberger CPR, Schwarzer D (2008) *Angew Chem Int Ed* 47:10030
6. Heal WP, Tate EW (2010) *Org Biomol Chem* 8:731
7. Wu YW, Goody RS (2010) *J Pept Sci* 16:514
8. Hao Z, Hong S, Chen X, Chen PR (2011) *Acc Chem Res* 44:742

9. Takaoka Y, Ojida A, Hamachi I (2013) *Angew Chem Int Ed* 52:4088
10. Antos JM, Francis MB (2004) *J Am Chem Soc* 126:10256
11. Bang D, Pentelute BL, Kent SBH (2006) *Angew Chem Int Ed* 45:3985
12. Bernardes GJL, Chalker JM, Errey JC, Davis BG (2008) *J Am Chem Soc* 130:5052
13. Tsukiji S, Miyagawa M, Takaoka Y, Tamura T, Hamachi I (2009) *Nat Chem Biol* 5:341
14. Ban H, Gavriluyk J, Barbas CF III (2010) *J Am Chem Soc* 132:1523
15. Popp BV, Ball ZT (2010) *J Am Chem Soc* 132:6660
16. Sato S, Nakamura H (2013) *Angew Chem Int Ed* 52:8681
17. Schreiber SL (2005) *Nat Chem Biol* 1:64
18. O' Conner CJ, Laraia L, Spring DR (2011) *Chem Soc Rev* 40:4332
19. Leisola M, Turunen O (2007) *Appl Microbiol Biotechnol* 75:1225
20. Smith BA, Hecht MH (2011) *Curr Opin Chem Biol* 15:421
21. Aebersold R, Mann M (2003) *Nature* 422:198
22. Morrison RS, Kinoshita Y, Johnson MD, Conrads TP (2003) *Adv Protein Chem* 65:1
23. Gallop MA, Barrett RW, Dower WJ, Fodor SPA, Gordon EM (1994) *J Med Chem* 37:1233
24. Cruz-Migoni A, Fuentes-Fernandez N, Rabbitts TH (2013) *Med Chem Commun* 4:1218
25. Thorner J, Emr S, Abelson J, Simon M (ed) (2000) *Applications of chimeric genes and hybrid proteins, part A: gene expression and protein purification. Methods Enzymol* 326:3–617
26. Thomas JJ, Bakhtiar R, Siuzdak G (2000) *Acc Chem Res* 33:179
27. Durek T, Becker CFW (2005) *Biomol Eng* 22:153
28. Muir TW (2003) *Annu Rev Biochem* 72:249
29. Arnau J, Lauritzen C, Petersen GE (2006) *Protein Expr Purif* 48:1
30. Hancock WS (ed) (1996) *New methods in peptide mapping for the characterization of proteins. CRC, Boca Raton*
31. Sayre LM (1986) *J Am Chem Soc* 108:1632
32. Chin J (1991) *Acc Chem Res* 24:145
33. Polzin GM, Burstyn JN (2001) *Met Ions Biol Syst* 38:103
34. Martin RB (2001) *Met Ions Biol Syst* 38:1
35. Bamann E, Trapmann H (1959) *Adv Enzymol* 21:169
36. Nakahara A, Hamada K, Nakao Y, Higashiyama T (1968) *Coord Chem Rev* 3:207
37. Hay RW, Morris PJ (1976) *Met Ions Biol Syst* 5:173
38. Sutton PA, Buckingham DA (1987) *Acc Chem Res* 20:357
39. Hegg EL, Burstyn JN (1998) *Coord Chem Rev* 173:133
40. Bal W, Kozłowski H, Kasprzak KS (2000) *J Inorg Biochem* 79:213
41. Allen G (2001) *Met Ions Biol Syst* 38:197
42. Buckingham DA, Clark CR (2001) *Met Ions Biol Syst* 38:43
43. Komiyama M (2001) *Met Ions Biol Syst* 38:25
44. Milović NM, Kostić NM (2001) *Met Ions Biol Syst* 38:145
45. Kasprzak KS, Bal W, Karaczyn AA (2003) *J Environ Monit* 5:183
46. Komiyama M, Takarada T (2003) *Met Ions in Biol Syst* 40:355
47. Suh J (2003) *Acc Chem Res* 36:562
48. Suh J (2014) *Asian J Org Chem* 3:18
49. Wolfenden R (2006) *Chem Rev* 106:3379
50. Zhu L, Kostić NM (1992) *Inorg Chem* 31:3994
51. Zhu L, Kostić NM (1993) *J Am Chem Soc* 115:4566
52. Zhu L, Kostić NM (1994) *Inorg Chim Acta* 217:21
53. Korneeva EN, Ovchinnikov MV, Kostić NM (1996) *Inorg Chim Acta* 243:9
54. Parac TN, Kostić NM (1996) *J Am Chem Soc* 118:5946
55. Parac TN, Kostić NM (1996) *J Am Chem Soc* 118:51
56. Chen X, Zhu L, You X, Kostić NM (1998) *J Biol Inorg Chem* 3:1
57. Karet GB, Kostić NM (1998) *Inorg Chem* 37:1021
58. Milović NM, Kostić NM (2002) *Inorg Chem* 41:7053
59. Milović NM, Kostić NM (2002) *J Am Chem Soc* 124:4759

60. Milović NM, Kostić NM (2003) *J Am Chem Soc* 125:781
61. Sigel H, Martin RB (1982) *Chem Rev* 82:385
62. Dutcă L-M, Ko K-S, Pohl NL, Kostić NM (2005) *Inorg Chem* 44:5141
63. Milović NM, Dutcă LM, Kostić NM (2003) *Inorg Chem* 42:4036
64. Erxleben A (2005) *Inorg Chem* 44:1082
65. Allen G, Campbell RO (1996) *Int J Pept Protein Res* 48:265
66. Mylonas M, Krężel A, Plakatouras JC, Hadjiliadis N, Bal W (2005) *J Mol Liq* 118:119
67. Mylonas M, Plakatouras JC, Hadjiliadis N (2004) *Dalton Trans* 4152
68. Bal W, Lukszo J, Bialkowski K, Kasprzak KS (1998) *Chem Res Toxicol* 11:1014
69. Bal W, Liang R, Lukszo J, Lee S-H, Dizdaroglu M, Kasprzak KS (2000) *Chem Res Toxicol* 13:616
70. Krężel A, Kopera E, Protas AM, Poznański J, Wyślouch-Cieszyńska A, Bal W (2010) *J Am Chem Soc* 132:3355
71. Berg JM, Shi Y (1996) *Science* 271:1081
72. Berg JM, Merkle DL (1989) *J Am Chem Soc* 111:3759
73. Christianson DW, Lipscomb WN (1989) *Acc Chem Res* 22:62
74. Xu D, Guo H (2009) *J Am Chem Soc* 131:9780
75. Matthews BW (1988) *Acc Chem Res* 21:333
76. Bamann E, Hass JG, Trapmann H (1961) *Arch Pharm* 294:569
77. Yashiro M, Sonobe Y, Yamamura A, Takarada T, Komiyama M, Fuji Y (2003) *Org Biomol Chem* 1:629
78. Kita Y, Nishii Y, Higuchi T, Mashima K (2012) *Angew Chem Int Ed* 51:5723
79. Sträter N, Lipscomb WN (1995) *Biochemistry* 34:14792
80. Ohshima T, Iwasaki T, Maegawa Y, Yoshiyama A, Mashima K (2008) *J Am Chem Soc* 130:2944
81. Iwasaki T, Maegawa Y, Hayashi Y, Ohshima T, Mashima K (2009) *Synlett* 1659
82. Otera J, Nishikido J (eds) (2003) *Esterification*, 2nd edn. Wiley-VCH, Weinheim
83. Milović NM, Badjić JD, Kostić NM (2004) *J Am Chem Soc* 126:696
84. Yoo SH, Lee BJ, Kim H, Suh J (2005) *J Am Chem Soc* 127:9593
85. Kim MG, Yoo SH, Chei WS, Lee TY, Kim HM, Suh J (2010) *J Biol Inorg Chem* 15:1023
86. de Oliveira MCB, Scarpellini M, Neves A, Terenzi H, Bortoluzzi AJ, Szpoganics B, Greatedi A, Mangrich AS, de Souza EM, Fernandez PM, Soares MR (2005) *Inorg Chem* 44:921
87. Yashiro M, Kawakami Y, Taya J-I, Arai S, Fujii Y (2009) *Chem Commun* 1544
88. Bentley KW, Creaser EH (1973) *Biochem J* 135:507
89. Buckingham DA, Collman JP (1967) *Inorg Chem* 6:1803
90. Buckingham DA, Collman JP, Happer DAR, Marzilli LG (1967) *J Am Chem Soc* 89:1082
91. Kumar CV, Buranapruk A, Cho A, Chaudhari A (2000) *Chem Commun* 597
92. Jeon JW, Son SJ, Yoo CE, Hong IS, Song JB, Suh J (2002) *Org Lett* 4:4155
93. Jeon JW, Son SJ, Yoo CE, Hong IS, Suh J (2003) *Bioorg Med Chem* 11:2901
94. Chae PS, Kim M-S, Jeung C-S, Lee SD, Park H, Lee S, Suh J (2005) *J Am Chem Soc* 127:2396
95. Suh J, Yoo SH, Kim MG, Jeong K, Ahn JY, Kim M-S, Chae PS, Lee TY, Lee J, Lee J, Jang YA, Ko EH (2007) *Angew Chem Int Ed* 46:7064
96. Suh J, Chei WS, Lee TY, Kim MG, Yoo SH, Jeong K, Ahn JY (2008) *J Biol Inorg Chem* 13:693
97. Chei WS, Ju H, Suh J (2011) *J Biol Inorg Chem* 16:511
98. Chei WS, Ju H, Suh J (2012) *Bioorg Med Chem Lett* 22:1533
99. Lee TY, Chei WS, Ju H, Lee M-S, Lee JW, Suh J (2012) *Bioorg Med Chem Lett* 22:5689
100. Wu W-H, Lei P, Liu Q, Hu J, Gunn AP, Chen M-S, Rui Y-F, Su X-Y, Xie Z-P, Zhao Y-F, Bush AI, Li Y-M (2008) *J Biol Chem* 283:31657
101. Hu J, Yu Y-P, Cui W, Fang C-L, Wu W-H, Zhao Y-F, Li Y-M (2010) *Chem Commun* 46:8023

102. Jeong K, Chung WY, Kye Y-S, Kim D (2010) *Bioorg Med Chem* 18:2598
103. Jeong K, Chung WY, Kye YS, Kim D, Song S (2011) *Bull Kor Chem Soc* 32:1751
104. Jeong K, Cho HR, Choi SH, Park Y, Chae PS (2012) *Chem Commun* 48:588
105. Shimizu Y, Morimoto H, Zhang M, Ohshima T (2012) *Angew Chem Int Ed* 51:8564
106. Shimizu Y, Noshita M, Mukai Y, Morimoto H, Ohshima T (2014) *Chem Commun* 50:12623
107. Edman P (1950) *Acta Chem Scand* 4:283
108. Gross E, Witkop B (1962) *J Biol Chem* 237:1856
109. Kaiser R, Metzka L (1999) *Anal Biochem* 266:1
110. Nakagawa S, Tamakashi Y, Hamana T, Kawase M, Taketomi S, Ishibashi Y, Nishimura O, Fukuda T (1994) *J Am Chem Soc* 116:5513
111. Tanaka M, Kajiwara K, Tokiwa R, Watanabe K, Ohno H, Tsutsumi H, Hata Y, Izumi K, Kodama E, Matsuoka M, Oishi S, Fujii N (2009) *Bioorg Med Chem* 17:7487
112. Degani Y, Patchornik A, Maclaren JA (1966) *J Am Chem Soc* 88:3460
113. Degani Y, Patchornik A (1974) *Biochemistry* 13:1
114. Okamoto R, Morooka K, Kajihara Y (2012) *Angew Chem Int Ed* 51:191
115. Kasper APT, Sorensen KK, Conde-Frieboes KW, Hoeg-Jensen T, Jensen KJ (2009) *Angew Chem Int Ed* 48:7411
116. Bateman RC, Youngblood WW, Busby WH, Kizer JS (1985) *J Biol Chem* 260:9088
117. Platis IE, Ermácora MR, Fox RO (1993) *Biochemistry* 32:12761
118. Shrivastava HY, Nair BU (2001) *Biochem Biophys Res Commun* 285:915
119. Halliwell B, Gutteridge JMC (1984) *Methods Enzymol* 105:47
120. Johnson GRA, Nazhat NB (1987) *J Am Chem Soc* 109:1990
121. Masarwa M, Cohen H, Meyerstein D, Hickman DL, Bakac A, Espenson JH (1988) *J Am Chem Soc* 110:4293
122. Shi X, Dalal NS (1993) *Arch Biochem Biophys* 307:336
123. Gallagher J, Zelenko O, Walts AD, Sigman DS (1998) *Biochemistry* 37:2096
124. Wu J, Perrin DM, Sigman DS, Kaback HR (1995) *Proc Natl Acad Sci U S A* 92:9186
125. Shimon MB, Goldshleger R, Karlsh SJD (1998) *J Biol Chem* 273:34190
126. Hoyer D, Cho H, Schultz PG (1990) *J Am Chem Soc* 112:3249
127. Buranaprapuk A, Leach SP, Kumar CV, Bocarsly JR (1998) *Biochim Biophys Acta* 1387:309
128. Shrivastava HY, Nair BU (2000) *Biochem Biophys Res Commun* 279:980
129. Soundar S, Coleman RF (1993) *J Biol Chem* 268:5264
130. Wei C-H, Chou W-Y, Huang S-M, Lin C-C, Chang G-G (1994) *Biochemistry* 33:7931
131. Zaychikov E, Martin E, Denissova L, Kozlov M, Markovtsov V, Kashlev M, Heumann H, Nikiforov V, Goldfarb A, Mustaev A (1996) *Science* 273:107
132. Grodsky NB, Soundar S, Colman RF (2000) *Biochemistry* 39:2193
133. Hlavaty JJ, Benner JS, Hornstra LJ, Schildkraut I (2000) *Biochemistry* 39:3097
134. Schepartz A, Cuenoud B (1990) *J Am Chem Soc* 112:3247
135. Ettner N, Metzger JW, Lederer T, Hulmes JD, Kisker C, Hinrichs W, Ellestad GA, Hillen W (1995) *Biochemistry* 34:22
136. Baichoo N, Heyduk T (1999) *Protein Sci* 8:518
137. Montigny C, Jaxel C, Shainskaya A, Vinh J, Labas V, Møller JV, Karlsh SJD, le Maire M (2004) *J Biol Chem* 279:43971
138. Mocz G, Gibbons IR (1990) *J Biol Chem* 265:2917
139. Rana TM, Meares CF (1990) *J Am Chem Soc* 112:2457
140. Rana TM, Meares CF (1991) *J Am Chem Soc* 113:1859
141. Greiner DP, Hughes KA, Gunasekera AH, Meares CF (1996) *Proc Natl Acad Sci U S A* 93:71
142. Goldshleger R, Karlsh SJD (1997) *Proc Natl Acad Sci U S A* 94:9596
143. Colland F, Fujita N, Ishihama A, Kolb A (2002) *Genes Cells* 7:233
144. Ermácora MR, Delfino JM, Cuenoud B, Schepartz A, Fox RO (1992) *Proc Natl Acad Sci U S A* 89:6383
145. Cuenoud B, Tarasow TM, Schepartz A (1992) *Tetrahedron Lett* 33:895
146. Brown KC, Yang SH, Kodadek T (1995) *Biochemistry* 34:4733

147. Mocz G (1989) *Eur J Biochem* 179:373
148. Cremo CR, Loo JA, Edmonds CG, Hatlelid KM (1992) *Biochemistry* 31:491
149. Grammer JC, Loo JA, Edmonds CG, Cremo CR, Yount RG (1996) *Biochemistry* 35:15582
150. Hua S, Inesi G, Toyoshima C (2000) *J Biol Chem* 275:30546
151. Denisov IG, Makris TM, Sligar SG, Schlichting I (2005) *Chem Rev* 105:2253
152. Bruijninx PCA, van Koten G, Gebbink RJMK (2008) *Chem Soc Rev* 37:2716
153. Solomon EI, Brunold TC, Davis MI, Kemsley JN, Lee S-K, Lehnert N, Neese F, Skulan AJ, Yang Y-S, Zhou J (2000) *Chem Rev* 100:235
154. Merckx M, Kopp DA, Sazinsky MH, Blazyk JL, Müller J, Lippard SJ (2001) *Angew Chem Int Ed* 40:2782
155. Neumann CS, Fujimori DG, Walsh CT (2008) *Chem Biol* 15:99
156. Costas M, Mehn MP, Jensen MP, Que L Jr (2004) *Chem Rev* 104:939
157. Kaizer J, Klinker EJ, Oh NY, Rohde J-U, Song WJ, Stubna A, Kim J, Münck E, Nam W, Que L Jr (2004) *J Am Chem Soc* 126:472
158. Ekkati AR, Kodanko JJ (2007) *J Am Chem Soc* 129:12390
159. Abouelatta AI, Campanali AA, Ekkati AR, Shamoun M, Kalapugama S, Kodanko JJ (2009) *Inorg Chem* 48:7729
160. Ranganathan D, Saini S (1991) *J Am Chem Soc* 113:1042
161. Ranganathan D, Vaish NK, Shah K (1994) *J Am Chem Soc* 116:6545
162. Sonobe T, Oisaki K, Kanai M (2012) *Chem Sci* 3:3249
163. Seki Y, Tanabe K, Sasaki D, Sohma Y, Oisaki K, Kanai M (2014) *Angew Chem Int Ed* 53:6501
164. Hoover JM, Ryland BL, Stahl SS (2013) *J Am Chem Soc* 135:2357
165. Ryland BL, McCann SD, Brunold TC, Stahl SS (2014) *J Am Chem Soc* 136:12166
166. Shiba T, Koda A, Kusumoto S, Kaneko T (1968) *Bull Chem Soc Jpn* 41:2748
167. Tanabe K, Taniguchi A, Matsumoto T, Oisaki K, Sohma Y, Kanai M (2014) *Chem Sci* 5:2747
168. Zhdankin VV, Stang PJ (2008) *Chem Rev* 108:5299
169. Moriarty RM (2005) *J Org Chem* 70:2893
170. Karrer P, Schlosser A (1923) *Helv Chim Acta* 6:411
171. Sola R, Sagner P, David M-L, Pascal R (1993) *J Chem Soc Chem Commun* 23:1786
172. Angelici G, Contaldi S, Green SL, Tomasini C (2008) *Org Biomol Chem* 6:1849
173. Angelici G, Castellucci N, Contaldi S, Falini G, Hofmann H-J, Monari M, Tomasini CA (2010) *Cryst Growth Des* 10:244

# Catalyst-Controlled, Regioselective Reactions of Carbohydrate Derivatives

Mark S. Taylor

**Abstract** Carbohydrates generally possess multiple hydroxyl groups of similar reactivity, and selective monofunctionalization is often difficult. Catalysis provides a versatile and potentially general solution to this problem. This chapter provides an overview of catalyst-controlled methods for the regioselective activation of carbohydrate derivatives. The catalysts discussed include organocatalysts (Lewis bases, Brønsted acids/bases, and others) as well as those based on main group and transition metal elements.

**Keywords** Carbohydrates · Catalysis · Glycosylation · Lewis acids · Lewis bases · Organocatalysis · Protective groups · Regioselectivity

## Contents

1	Introduction .....	127
2	Lewis Base Catalysis .....	128
2.1	Pyridine Derivatives .....	128
2.2	Other Nitrogen Heterocycles .....	131
3	Brønsted Base Catalysis .....	134
4	Brønsted Acid Catalysis .....	135
5	Other Classes of Organocatalysts .....	137
5.1	Phase Transfer Catalysts .....	137
5.2	<i>N</i> -Oxoammonium Salts .....	137
6	Lewis Acid Catalysis .....	138
6.1	Organotin Catalysts .....	138
6.2	Organoboron Catalysts .....	142
6.3	Lanthanide(III) Catalysts .....	146

---

M.S. Taylor (✉)

Department of Chemistry, University of Toronto, 80 St. George Street, Toronto, ON,  
Canada, M5S 3H6

e-mail: [mtaylor@chem.utoronto.ca](mailto:mtaylor@chem.utoronto.ca)

7	Transition Metal Catalysis .....	147
7.1	Transition Metal-Based Lewis Acids .....	147
7.2	Other Transition Metal-Catalyzed Reactions .....	149
8	Summary, Conclusions, and Outlook .....	150
	References .....	151

## Abbreviations

[TPhA] <sup>+</sup>	Trimethylphenylammonium
Ac	Acetyl
acac	Acetylacetonate
AIBN	Azobis(isobutyronitrile)
Ala	Alanine
Alloc	Allyloxycarbonyl
Ar	Aryl
BINOL	2,2'-Dihydroxy-1,1'-binaphthyl
Bn	Benzyl
Boc	<i>tert</i> -Butoxycarbonyl
BOX	Bis(oxazoline)
Bu	Butyl
Bz	Benzoyl
Cbz	Benzyloxycarbonyl
COD	Cyclooctadiene
DCB	2,6-Dichloro-1,4-benzoquinone
DMAc	<i>N,N</i> -Dimethylacetamide
DMAP	4-(Dimethylamino)pyridine
DME	1,2-Dimethoxyethane
DMF	Dimethylformamide
DPG	Directing-protecting group
EPPS	4-(2-Hydroxyethyl)-1-piperazinepropanesulfonic acid
Et	Ethyl
Gal	Galactose
Glc	Glucose
GlcNAc	<i>N</i> -Acetylglucosamine
<i>i</i> -Pr	Isopropyl
M	Mole per liter
Man	Mannose
Me	Methyl
MES	2-( <i>N</i> -Morpholino)ethanesulfonic acid
Ms	Methanesulfonyl
MS	Molecular sieves
NMR	Nuclear magnetic resonance
PEMP	1,2,2,6,6-Pentamethylpiperidine
Ph	Phenyl
Phe	Phenylalanine

PMH	$\pi$ -Methylhistidine
PMP	4-Methoxyphenyl
PPY	4-Pyrrolidinopyridine
Pr	Propyl
<i>T</i>	Temperature
TBDPS	<i>tert</i> -Butyldiphenylsilyl
TBS	<i>tert</i> -Butyldimethylsilyl
<i>t</i> -Bu	<i>tert</i> -Butyl
TES	Triethylsilyl
Tf	Trifluoromethanesulfonyl (triflyl)
THF	Tetrahydrofuran
THP	Tetrahydropyranyl
TMEDA	<i>N,N,N',N'</i> -Tetramethylethylenediamine
Trp	Tryptophan
Trt	Triphenylmethyl
Ts	Tosyl, 4-toluenesulfonyl
U	Uracil
X	Generic leaving group

## 1 Introduction

The use of readily available sugars as chemical feedstocks for the preparation of oligosaccharides, novel therapeutic agents, or biological probes generally requires methods for regioselective manipulation of hydroxyl (OH) groups. The best-established approach takes advantage of intrinsic differences in the reactivity of OH groups under a particular set of reaction conditions [1]. Examples include protection of the least sterically hindered OH group using bulky electrophiles [2, 3], functionalization of the most acidic OH group under strongly basic conditions [4, 5], and formation of ketals or acetals from 1,2- or 1,3-diol pairs [6, 7]. Although this approach is often effective, in many cases it necessitates multi-step sequences involving installation and removal of orthogonal protective groups. In certain instances, the differences in reactivity of the OH groups are too small to enable synthetically useful mono-protection.

Over the past decade, catalytic activation of OH groups has emerged as an attractive, alternative strategy for selective functionalization of carbohydrate derivatives. In addition to providing rate acceleration, catalysts can amplify relatively subtle differences in the reactivity of OH groups, or can override intrinsic differences, thus providing access to products that otherwise would be difficult to obtain. Given that the majority of enzymatic transformations of carbohydrates display catalyst-controlled regioselectivity, there is a biomimetic aspect to this approach. The synthetic catalysts that have been employed for regioselective carbohydrate activation are diverse in their structures and functions, and include several classes of Lewis bases, main group element- and transition metal-centered Lewis acids,

Brønsted acids, and others. The types of reactivity are likewise diverse, encompassing the major classes of protective group installations (acylation, silylation, alkylation, and acetal formation) as well as oxidations and glycosylations.

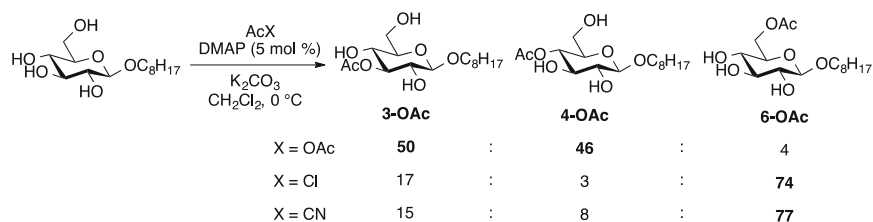
This chapter documents advances in the use of catalysis for regioselective transformations of carbohydrate derivatives. For this discussion, the catalysts are grouped into broad structural or functional classes (Lewis bases, Brønsted acids, Lewis acids, transition metals). Processes that make use of enzyme catalysis (chemoenzymatic methods or metabolic engineering) are not discussed here [8–10]. Emphasis is placed on recent results that were not discussed in previous reviews on this and related topics [11–13].

## 2 Lewis Base Catalysis

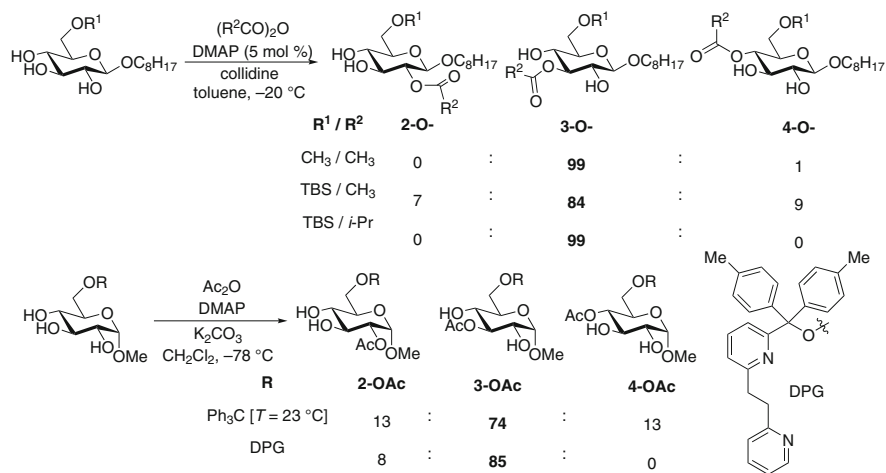
Lewis base acceleration of acylation, silylation, sulfonylation, and phosphorylation is generally understood to involve attack of the electrophilic reagent by the catalyst, generating an adduct that displays enhanced reactivity [14]. Each of the transformations listed above has been effected in a regioselective fashion on carbohydrate-derived substrates using Lewis base catalysis. Functionalizing the catalyst with groups capable of noncovalent or reversible covalent interactions with the sugar derivative has proved to be a versatile and broadly useful design strategy.

### 2.1 *Pyridine Derivatives*

In 1999, Yoshida and co-workers described a systematic study of acylation reactions of unprotected pyranoside substrates catalyzed by 4-dimethylaminopyridine (DMAP) [15]. In the presence of acetic anhydride and potassium carbonate in chloroform solvent, a surprising level of selectivity for acetylation of secondary over primary OH groups was observed for octyl  $\beta$ -glucopyranoside,  $\alpha$ -glucopyranoside, and  $\beta$ -mannopyranoside. The authors proposed that networks of intramolecular hydrogen bonding interactions between OH groups were responsible for this behavior. A subsequent study by Kattnig and Albert revealed that the regiochemical outcome of the acetylation of octyl  $\beta$ -glucopyranoside is dependent on the leaving group  $X^-$  of the acyl donor  $AcX$  (Scheme 1) [16]. Whereas selective acetylation of the 3- and 4-OH groups was observed using  $Ac_2O$ , the 6-*O*-acetylated product predominated using  $AcCl$  and  $AcCN$ . Using pyridine, which would likely act as a Brønsted rather than a Lewis base, the 6-*O*-acetyl derivative was obtained using  $Ac_2O$ , albeit at a low rate. These findings pointed to a role for acetate as a general base catalyst in the DMAP-catalyzed reaction with  $Ac_2O$ . Two-point hydrogen bonding interactions between acetate and diol groups in the



**Scheme 1** Leaving group dependence in the DMAP-catalyzed acetylation of octyl  $\beta$ -D-glucopyranoside

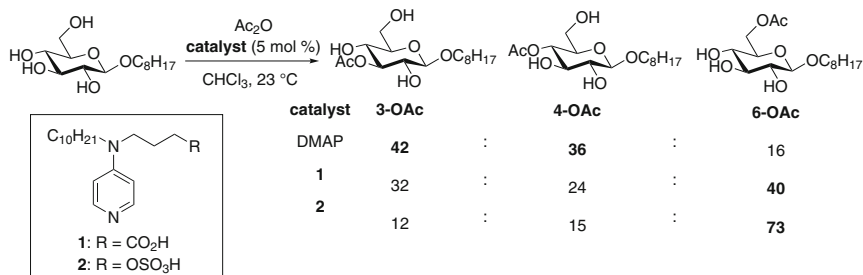


**Scheme 2** DMAP-catalyzed monoacylations of 6-*O*-protected glucopyranosides

glucopyranoside substrate were proposed to give rise to the observed selectivity for the secondary OH groups.

DMAP-catalyzed acylations of D-glucopyranoside derivatives lacking a free 6-OH group have been studied in detail (Scheme 2). Octyl 6-*O*-methyl- $\beta$ -D-glucopyranoside, which bears a sterically unencumbered blocking group, underwent selective 3-*O*-acetylation in toluene at  $-20$  °C [17]. High selectivity for the 3-OH group was also observed using isobutyric and benzoic anhydride. Polar, Lewis basic media such as THF and DMF gave rise to less selective acylations, pointing to a role for hydrogen bonding interactions (either intramolecular in the pyranoside substrate, or between the anhydride-derived carboxylate and the substrate) in the regiochemical outcome of the reaction. For reasons that are not readily apparent, acylation of the corresponding 6-*O*-TBS derivative took place with lower regioselectivity. However, the isobutyryl group could be installed in a selective fashion at O-3, presumably because of the increased steric demand and lower uncatalyzed reaction rate of (*i*-PrCO)<sub>2</sub>O.

Acylations of substrates in the  $\alpha$ -glucopyranoside series have been explored by the group of Moitessier [18]. Modest levels of selectivity for the 3-OH group were

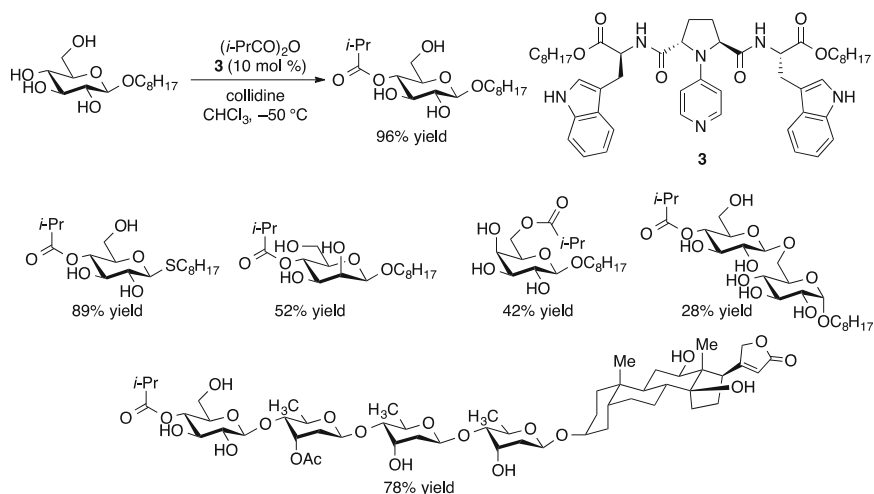


**Scheme 3** Acetylation of octyl  $\beta$ -D-glucopyranoside using functionalized DMAP derivatives

obtained (THF or  $CH_2Cl_2$ , 23 °C) using derivatives having a bulky 6-*O*-protective group such as triphenylmethyl. The yield of the 3-*O*-acetylated product was increased using a bis(pyridyl)-functionalized “directing–protecting group” (DPG), although the magnitude of the effect was not large. Supported by  $^1H$  NMR spectroscopic studies, the authors proposed that hydrogen bonding interactions between pyridyl and glucopyranoside OH groups contributed to this behavior. More dramatic effects of DPGs on regiocontrol were observed for glycosylations using trichloroacetimidate donors [19].

Derivatives of DMAP in which the amino group bears a tethered carboxylic or sulfonic acid group have been explored as catalysts for acetylation of hexopyranoside substrates [20]. These functionalized catalysts were found to give rise to altered regioselectivity relative to DMAP in acetylation reactions (Scheme 3). An analog of catalyst **1** in which the carboxylic acid was replaced by a methyl ester gave regioselectivity similar to that obtained using unfunctionalized DMAP. This observation, along with the fact that both the carboxylate- and sulfonate-functionalized catalysts favored the same regioisomer, suggested that these groups acted as acceptors of hydrogen bonds from OH groups of the carbohydrate substrate.

Kawabata and co-workers have employed chiral 4-pyrrolidinopyridine (PPY) derivatives as catalysts for selective acylations of carbohydrates. Tryptophan ester-substituted,  $C_2$ -symmetric derivative **3** promoted the acylation of the 4-OH group of octyl  $\beta$ -glucopyranoside (Scheme 4) [21]. This was a reversal of the preference for 6-*O*-acylation (albeit modest: 36% regioselectivity, along with significant amounts of diacylated material and recovered substrate) obtained using simple DMAP as catalyst. Replacement of the indolyl groups of **3** with *N*-methylindolyl or 2-naphthyl groups resulted in diminished regioselectivity, pointing towards a role for the N–H groups as hydrogen bond donors. Donation of a hydrogen bond from the 6-OH group of the substrate to an amide group of the catalyst was also proposed as a key interaction, supported by the poor regiocontrol observed for a 6-*O*-methylated glucopyranoside substrate. The 4-*O*-acylated glucopyranoside product obtained using this method served as a useful starting point for the preparation of orthogonally protected derivatives through sequential, substrate-controlled transformations [22]. In addition to alkyl and thioglycosides, disaccharide derivatives



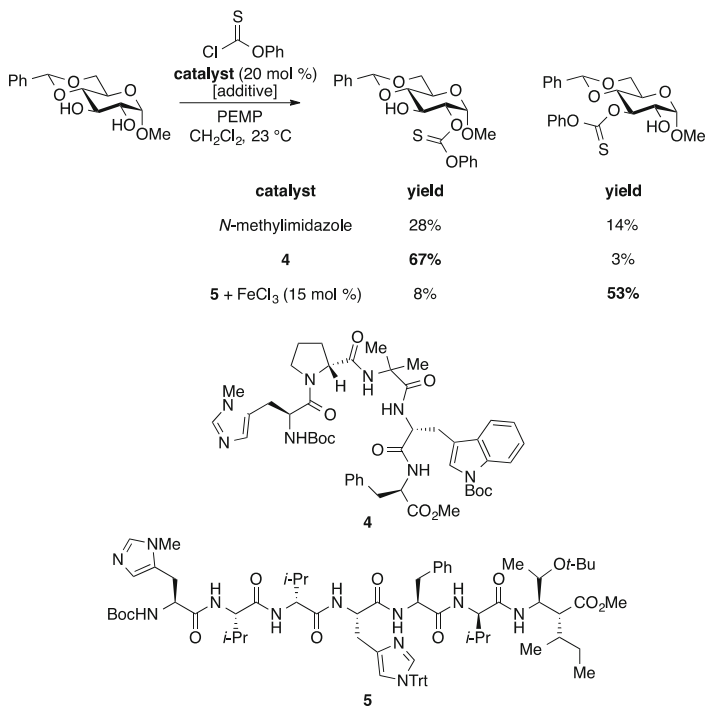
**Scheme 4** *Top*: selective monoacylation of octyl  $\beta$ -D-glucopyranoside catalyzed by C2-symmetric PPY derivative **3**. *Bottom*: monoacylated pyranosides prepared using catalyst **3**

and the complex cardiac glycosides digitoxin and lanatoside were selectively monoacylated using catalyst **3** [23–25]. Catalyst architectures based on *trans*-4-hydroxy-L-proline have also been explored by the Kawabata group [26].

## 2.2 Other Nitrogen Heterocycles

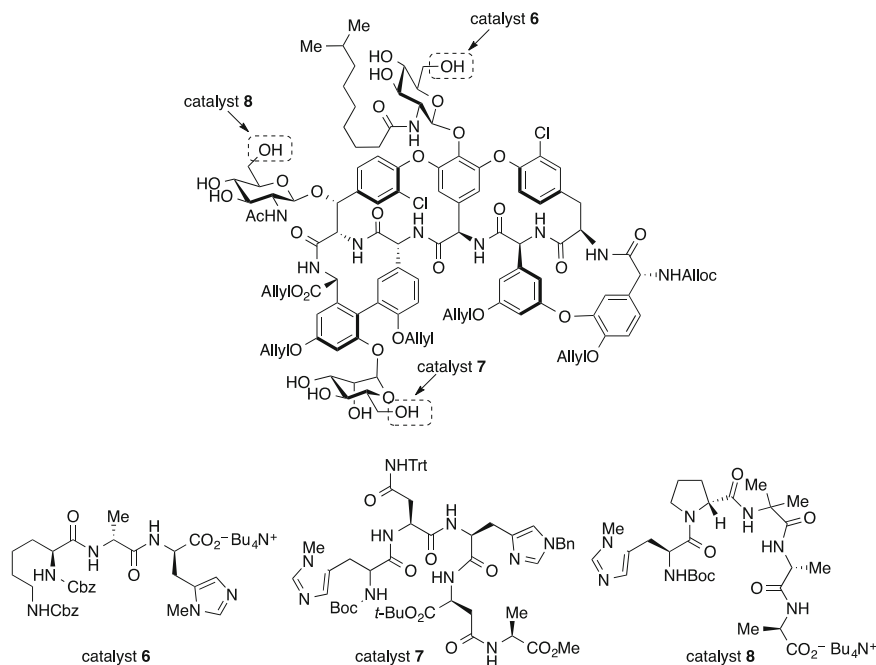
Using peptides functionalized with Lewis basic *N*-alkylimidazole moieties as catalysts, the group of Scott Miller has accomplished the selective acylation, thiocarbonylation, and phosphorylation of pyranosides [27–30]. Peptide-based catalysts **4** and **5** provided complementary regiochemical outcomes in the thiocarbonylation of benzylidene-protected methyl  $\alpha$ -glucopyranoside in the presence of phenyl chlorothionoformate and 1,2,2,6,6-pentamethylpiperidine (PEMP, Scheme 5) [28]. Iron trichloride was found to increase the reaction rate, presumably by Lewis acid activation of the chlorothionoformate, and, in the case of catalyst **5**, provided an improved level of selectivity for the 3-OH group. A control experiment using *N*-methylimidazole as catalyst revealed that functionalization of the 2-OH group was favored, although not to a synthetically useful extent. The thiocarbonylated products were subjected to Barton–McCombie reaction conditions ( $\text{Bu}_3\text{SnH}$ , AIBN initiator, refluxing toluene), providing expedient access to the corresponding deoxysugars. Substrates as complex as the natural product vancomycin were amenable to this approach [29].

By virtue of its structural complexity and potent antibiotic activity, the glycopeptide natural product teicoplanin is a substrate of great interest for site-selective catalysis. Miller and co-workers' approach to discovering catalysts for selective



**Scheme 5** Selective thiocarbonylation of a glucopyranoside-derived diol mediated by *N*-methylimidazole-bearing peptide catalysts. PEMP denotes 1,2,2,6,6-pentamethylpiperidine

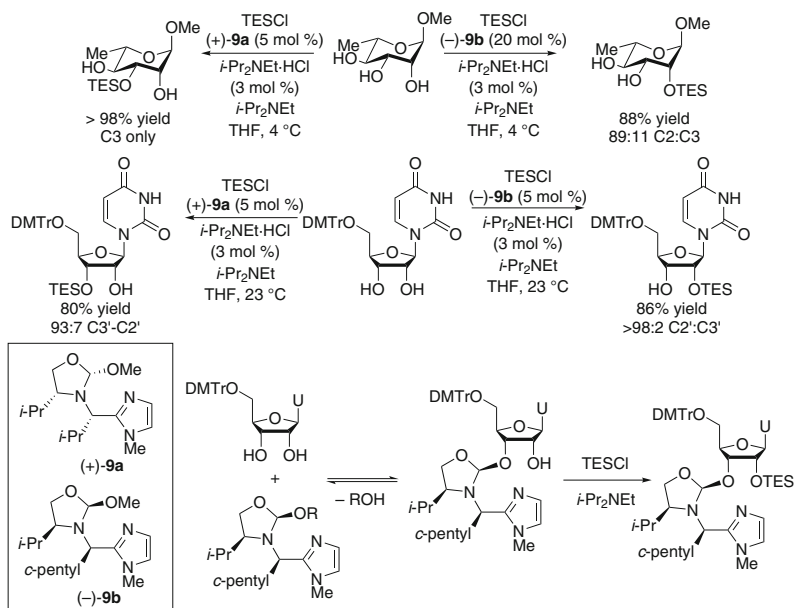
mono-phosphorylation of each of the three primary hydroxyl groups of teicoplanin (associated with the *N*-decanoylglucosamine, *N*-acetylglucosamine, and mannose moieties) was based on a combination of crystallography-assisted design and catalyst structure–activity relationship studies (Scheme 6). Teicoplanin interacts selectively with D-Ala–D-Ala motifs of the growing bacterial peptidoglycan chain, a property that is thought to be key to its antibacterial activity. In catalyst **6**, this D-Ala–D-Ala binding motif is replaced with a D-Ala–D-Pmh sequence (Pmh denotes  $\pi$ -methylhistidine). Based on the structure of a crystallographically characterized teicoplanin–peptide complex, it was anticipated that catalyst **6** would place its Lewis basic imidazole group in the vicinity of the *N*-decanoylglucosamine group. Indeed, phosphorylation of a derivative of teicoplanin (protected at the carboxylic acid, phenol, and amine groups, but still possessing ten free OH groups) in the presence of catalyst **6** occurred predominantly at the 6-OH group of the *N*-decanoylglucosamine sugar. A similar strategy of embedding a D-Pmh catalytic group into the D-Ala–D-Ala motif was envisioned for functionalization of the mannosyl 6-OH group, but was unsuccessful. However, a screen of *N*-alkylhistidine-bearing peptides which had been useful catalysts for other transformations revealed that catalyst **7** was able to promote phosphorylation at this position. This screen also provided a hint on how to address the



**Scheme 6** Catalyst-controlled phosphorylation of a teicoplanin derivative. *Arrows* indicate the position of phosphorylation in the presence of the indicated catalyst (diphenylphosphoryl chloride, PEMP, THF/CH<sub>2</sub>Cl<sub>2</sub>, 23 °C)

*N*-acetylglucosamine moiety, as catalyst **4** (see Scheme 5 above) provided a modest level of selectivity for this position. The authors identified the  $\beta$ -turn-promoting proline–aminoisobutyric acid element and the pair of *D*-amino acids at the C-terminus as key structural attributes of catalyst **4**. Replacing the *D*-Trp(Boc)–*D*-Phe sequence of **4** with the *D*-Ala–*D*-Ala teicoplanin binding motif resulted in a catalyst (**8**) that displayed enhanced activity and selectivity for the GlcNAc 6-OH group. The observation of competitive inhibition by a *D*-Ala–*D*-Ala-containing tripeptide was consistent with the authors’ proposal of catalyst–substrate binding through the *D*-Ala–*D*-Ala motif of **8**, followed by remote functionalization. These results demonstrate the feasibility of using the specific interactions between natural products and their target motifs as a starting point for devising catalyst–substrate complexation modes.

The concept of “scaffolding catalysis” [31] underlies the design of imidazole-substituted orthoamides **9a–9b**, which promote regioselective monoacylations, silylations, and sulfonylations of diol motifs belonging to pyranoside and furanoside substrates, including monosaccharide derivatives, nucleosides, and glycosylated natural products and drugs (Scheme 7) [32, 33]. A useful and impressive feature of this system is the ability to activate selectively either of the two OH groups of a *cis*-1,2-diol pair by selection of the catalyst enantiomer, thus

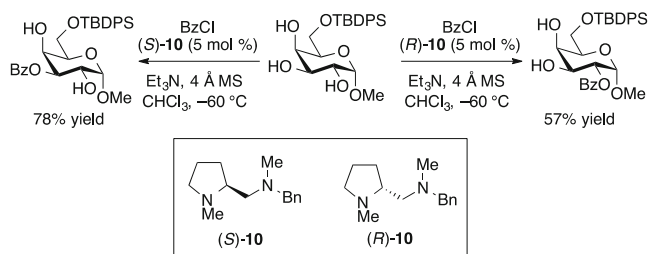


**Scheme 7** Selective silylations of carbohydrate derivatives mediated by chiral scaffolding catalysts

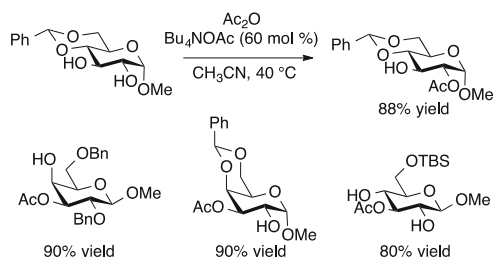
overcoming intrinsic differences in reactivity. The syntheses of the 2-*O*-silylated rhamnopyranoside and 3-*O*-silylated uridine derivative shown in Scheme 7 illustrate this property. The orthoamide group serves as the site of substrate complexation via reversible, covalent interactions with a hydroxyl group, positioning the second OH group in proximity to the catalytically active *N*-alkylimidazole group. Based on studies of desymmetrizations of *meso*-1,2-diols promoted by this class of catalysts, it is likely that substrate coordination occurs *cis* to the isopropyl group of the oxazolidine, with the enantioselectivity being dictated by the relative reactivities of the resulting complexes towards OH functionalization (rather than the relative affinities of catalyst for the substrate OH groups) [34]. Whether the imidazolyl group acts as a Brønsted or Lewis base in each of the transformations promoted by catalysts **9a** and **9b** is not fully clear [35].

### 3 Brønsted Base Catalysis

Hu and Vasella explored the use of chiral, proline-derived diamine catalyst **10** – previously employed by Oriyama for kinetic resolutions and enantioselective desymmetrizations of 1,2-diols – for regioselective benzoylations of hexopyranosides [36]. Scheme 8 depicts one of several instances in which some level of regiochemical complementarity was achieved using the two enantiomers of



**Scheme 8** Complementary regiochemical outcomes for benzoylation of an  $\alpha$ -D-galactopyranoside using enantiomeric diamine catalysts



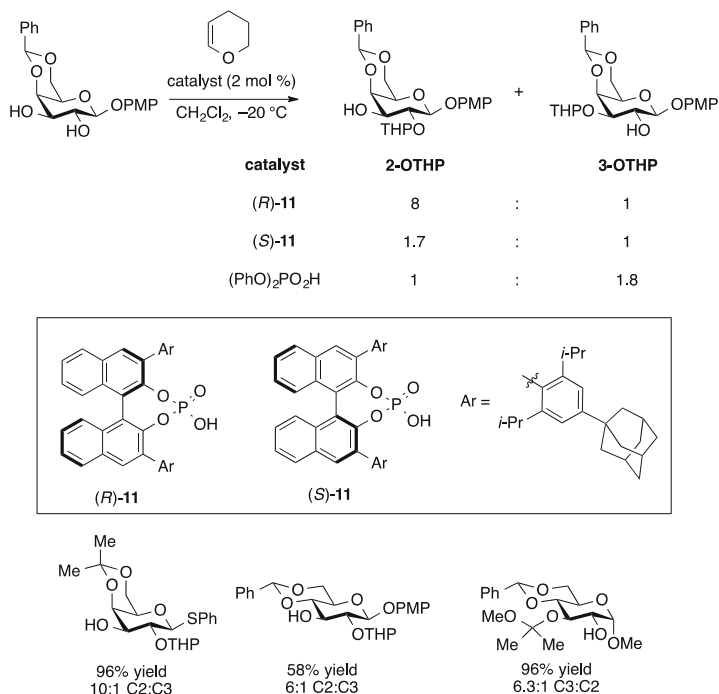
**Scheme 9** Tetrabutylammonium acetate-accelerated monoacetylations of pyranoside-derived di- and triols

catalyst **10**. Based on mechanistic studies of other amine-catalyzed enantioselective acylations, Brønsted base catalysis by **10** is the most likely reaction pathway.

Tetrabutylammonium acetate has been found to provide rate acceleration in monoacetylations of pyranoside-derived diols (Scheme 9) [37]. In general, it was the least sterically hindered OH group belonging to a 1,2- or 1,3-diol moiety that underwent selective acetylation. The authors' proposal of two-point hydrogen bonding interactions between acetate and the 1,2- or 1,3-diol motif echoes the mechanistic hypotheses advanced earlier for selective acetylations of sugars using DMAP-derived catalysts. The scope of this study was later expanded to encompass 6-*O*-protected pyranosides, as well as fully unprotected pyranoside substrates [38]. The former gave rise to 3-*O*-acetylation for gluco-, galacto-, and manno-configured variants, whereas the latter generally led to 3,6-di-*O*-acetylation.

## 4 Brønsted Acid Catalysis

The regiochemical outcomes of Brønsted acid-catalyzed reactions of carbohydrate derivatives have been studied in detail, particularly in the context of the selective formation or hydrolysis of acetals and ketals [6, 7]. The group of Nagorny has added a new dimension to this strategy by employing chiral Brønsted acids for the selective formation of mixed acetals and ketals from pyranoside-derived 1,2-diol



**Scheme 10** Selective acetalization of pyranoside-derived *trans*-vicinal diols using a chiral phosphoric acid catalyst

groups [39]. The BINOL-derived chiral phosphoric acids employed for this purpose have been used extensively in asymmetric catalysis over the past decade, especially for enantioselective additions to imine electrophiles [40, 41]. Most relevant to the reactivity under discussion are enantioselective, catalytic reactions involving putative oxacarbenium–phosphate ion pairs as intermediates (e.g., aldol-type additions to enol ethers, (*trans*)acetalizations, and spiroketalizations). It should also be noted that control of diastereoselectivity in glycosylation reactions using chiral phosphoric acids of this type [42], as well as other organic Brønsted acids (i.e., thioureas) [43–45], has been explored.

Scheme 10 illustrates the types of matching/mismatching effects observed by Nagorny and co-workers upon acetalization of substrates having vicinal equatorial OH groups using the enantiomeric catalysts (*R*)-11 and (*S*)-11. Achiral phosphate catalyst (PhO)<sub>2</sub>PO<sub>2</sub>H displayed modest selectivity for the 3-OH group of the benzylidene-protected β-D-galactopyranoside substrate, perhaps reflecting a preference for the less sterically hindered position. In contrast, catalyst (*R*)-11 enabled selective tetrahydropyranylation of the 2-OH group. The mismatched combination of catalyst (*S*)-11 with this substrate also yielded the 2-O-THP derivative as the major product, but with appreciably lower regioselectivity. As illustrated by the representative products shown in Scheme 10, the configuration of the anomeric substituent has a significant influence on the regiochemical outcome of reactions of

gluco- or galactopyranoside-derived diols: functionalization of the 2-OH group was favored for  $\beta$ -configured substrates, whereas the 3-O-THP product was obtained from an  $\alpha$ -glucopyranoside. Extending this type of catalysis to reactions of carbohydrate-derived oxocarbenium ions (thus enabling regioselective glycosylations) would be an appealing goal for future studies.

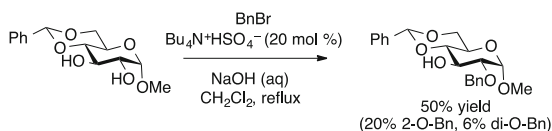
## 5 Other Classes of Organocatalysts

### 5.1 Phase Transfer Catalysts

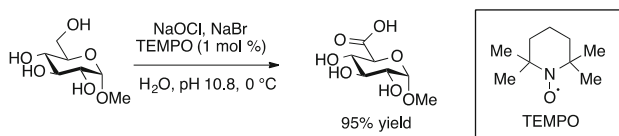
Tetraalkylammonium salts have been used as phase transfer catalysts for alkylation [5], sulfonylation [46], and benzylation reactions [47] of carbohydrate derivatives in mixed organic/aqueous solvent. For example, benzylidene-protected methyl  $\alpha$ -glucopyranoside underwent selective benzylation at the more acidic 2-OH group in the presence of a phase transfer catalyst (Scheme 11).

### 5.2 N-Oxoammonium Salts

Selective oxidation of primary OH groups in carbohydrate derivatives has been achieved using *N*-oxoammonium salts generated from (2,2,6,6-tetramethylpiperidin-1-yl)oxy (TEMPO) and its derivatives as catalysts. The stoichiometric oxidants employed include sodium hypochlorite [48–50], sodium hypobromite [51, 52], and ammonium peroxodisulfate (using silver on alumina as a co-catalyst) [53, 54]. A representative protocol is shown in Scheme 12.



**Scheme 11** Benzylation of a glucopyranoside-derived diol using phase transfer catalysis



**Scheme 12** Selective oxidation of methyl  $\alpha$ -glucopyranoside using TEMPO as a pre-catalyst

## 6 Lewis Acid Catalysis

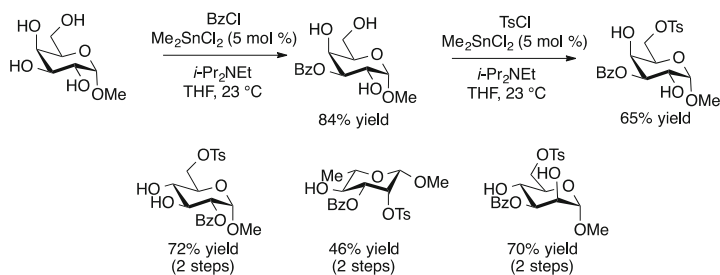
Lewis acids are employed routinely as catalysts for reactions of carbohydrate derivatives, including the formation and cleavage of acetals and ketals, glycosidation, and glycoside hydrolysis. An exciting development in this area has been the design of elegant, multistep Lewis acid-catalyzed processes that take advantage of the selective formation and reductive cleavage of benzylidene-type protective groups to deliver differentially protected pyranoside derivatives in a single reaction flask [55–58]. Applications of Lewis acids in regioselective activation of OH groups in carbohydrates have expanded significantly over the past decade. This mode of catalysis most often takes advantage of the selectivity displayed by Lewis acids in their interactions with carbohydrate derivatives having several free OH groups [59]. Acidification of a bound OH group can accelerate reactions with electrophilic species.

### 6.1 Organotin Catalysts

Applications of organotin(IV) compounds as stoichiometric promoters for regioselective reactions of carbohydrate derivatives date back more than 40 years [60]. Both diorganotin and triorganotin promoters – giving rise to stannylene acetal and stannyl ether intermediates, respectively – have been employed, enabling selective acylation, alkylation, sulfonylation, phosphorylation, and glycosylation reactions [61, 62]. In recent years, reaction conditions have been identified that enable the application of sub-stoichiometric quantities of the organotin compound.

Initial reports of organotin-catalyzed transformations of carbohydrate derivatives were isolated examples described in the context of broader synthetic methodology or target-oriented synthesis efforts. In 1998, Matsumura and co-workers reported the organotin-catalyzed monobenzoylation of 1,2-diols, including a 4,6-*O*-benzylidene-protected  $\alpha$ -glucopyranoside substrate, which reacted preferentially at the 2-OH group [63, 64]. The combination of a diorganotin halide catalyst and inorganic base promoter ( $\text{Me}_2\text{SnCl}_2$  and  $\text{K}_2\text{CO}_3$  in this instance) has been conserved in many of the subsequently developed organotin-catalyzed transformations of carbohydrates (see below). Monosulfonylations were reported in a similar timeframe: Martinelli, Vaidyanathan and co-workers described selective tosylations of 1,2-diol groups in glucofuranoside and xylopyranoside substrates, along with numerous other types of chelation-prone alcohol substrates [65, 66]. The *de novo* synthesis of the sialic acids reported by Burke provided another pioneering example of selective, organotin-catalyzed tosylation: a pyranoside-derived tetraol was bis-sulfonylated at the primary OH group and the equatorial position of a *cis*-1,2-diol group [67].

A systematic study of the regiochemical outcomes of organotin-catalyzed benzoylations of unprotected pyranosides was reported in 2008 [68]. The hierarchy of reactivities that emerged from this study was: (1) equatorial OH groups having a *cis*-vicinal OH group; (2) equatorial OH groups having a *cis*-vicinal alkoxy group;

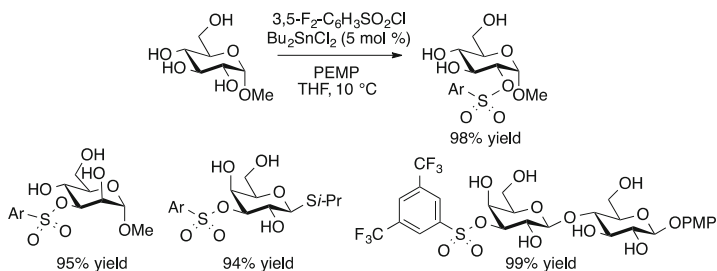


**Scheme 13** Sequential regioselective monobenzylation and sulfonylation of pyranosides using  $\text{Me}_2\text{SnCl}_2$  as catalyst

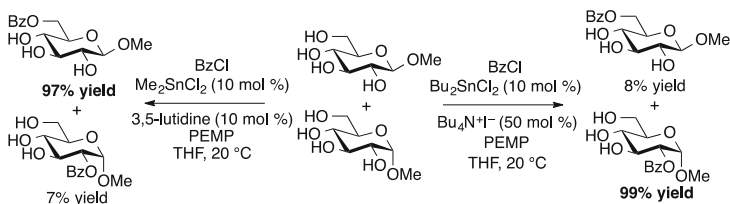
and (3) primary OH groups belonging to 1,3-diol pairs. The ability to activate secondary over primary OH groups reliably is a powerful feature of this catalyst system. The monobenzyolated products obtained were subjected to organotin-catalyzed sulfonylation, giving rise to regiochemical outcomes that were generally consistent with the reactivity hierarchy described above (Scheme 13). A comprehensive investigation of  $\text{Bu}_2\text{SnCl}_2$ -catalyzed sulfonylations of unprotected pyranosides was subsequently reported by Muramatsu (Scheme 14) [69]. The use of an electron-deficient arenesulfonyl chloride was essential to the success of the reaction: 3,5-difluorobenzenesulfonyl chloride was employed in the majority of cases, with other electron-withdrawing substituents (e.g., 4- $\text{NO}_2$ , 3- $\text{NO}_2$ , 3- $\text{CF}_3$ , 3-halo) also being tolerated. Significantly lower yields of monosulfonylation product were obtained using  $\text{MsCl}$ ,  $\text{PhSO}_2\text{Cl}$ ,  $\text{TsCl}$ , and  $\text{Tf}_2\text{O}$ . Again, selective activation of secondary OH groups in a *cis*-1,2-relationship with OH or OR groups, even in the presence of unprotected primary OH groups, was generally observed. The monosulfonylation of a disaccharide bearing five secondary and two primary OH groups provides an impressive illustration of this behavior.

Kinetic resolutions of epimeric carbohydrate derivatives have been achieved using organotin catalysis [70]. The  $\alpha$  and  $\beta$  anomers of methyl *D*-glucopyranoside gave rise to distinct regiochemical outcomes, with the former undergoing benzylation at the 2-OH group and the latter at the 6-OH group (Scheme 15). The anomers reacted at different rates, permitting isolation of the 6-*O*-benzyolated  $\beta$ -isomer using  $\text{Me}_2\text{SnCl}_2$  in the presence of 3,5-lutidine as a co-catalyst. Remarkably, the relative reaction rates of  $\alpha$  and  $\beta$  anomers could be inverted by variation of the catalyst and additive: using  $\text{Bu}_2\text{SnCl}_2$  and  $\text{Bu}_4\text{NI}$ , the  $\alpha$ -anomer underwent preferential activation. Other epimeric pairs (e.g.,  $\alpha$ -*D*-Glc/ $\alpha$ -*D*-Man,  $\alpha$ -*D*-Glc/ $\alpha$ -*D*-Gal,  $\beta$ -*D*-Glc/ $\beta$ -*D*-Gal) were successfully subjected to kinetic resolutions of this type.

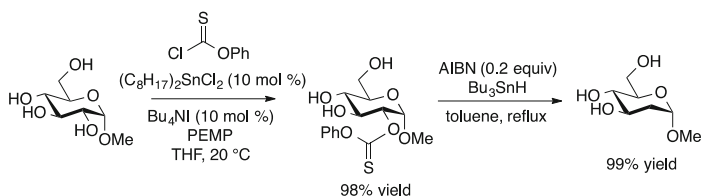
Organotin-catalyzed regioselective thiocarbonylations have been developed as the key step of a protective-group-free synthesis of deoxy sugars [71]. According to the selectivity patterns described above for acylation and sulfonylation, a variety of substrates, including gluco-, manno-, galacto-, xylo-, rhamno-, and fucopyranosides, underwent selective coupling with phenyl chlorothionoformate.



**Scheme 14** Organotin-catalyzed sulfonations of pyranosides. PEMP and Ar denote 1,2,2,6,6-pentamethylpiperidine and 3,5-difluoroaryl, respectively



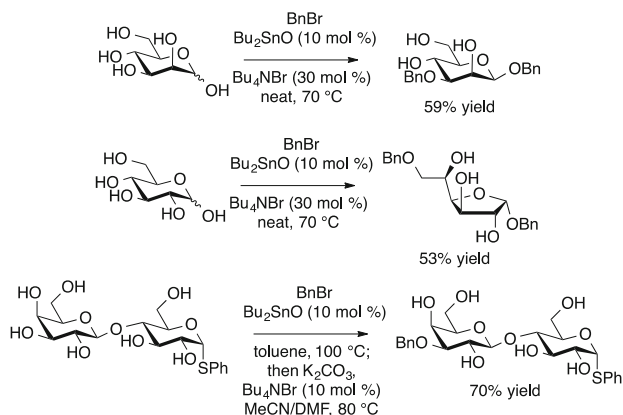
**Scheme 15** Organotin-catalyzed kinetic resolution of an  $\alpha/\beta$  mixture of methyl D-glucopyranosides. PEMP denotes 1,2,2,6,6-pentamethylpiperidine



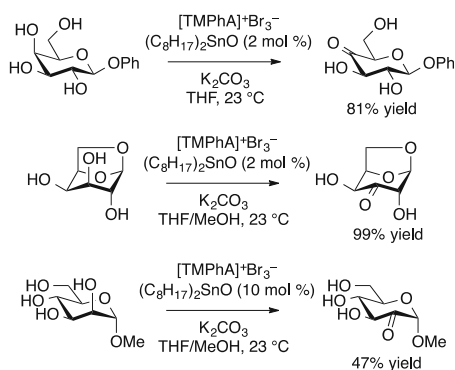
**Scheme 16** Two-step deoxygenation of sugars based on regioselective, organotin-catalyzed thiocarbonylation

The two-step, protective-group-free deoxygenation of methyl  $\alpha$ -D-glucopyranoside is depicted in Scheme 16.

Extensions of organotin-catalyzed pyranoside activation to include reactions with alkyl halides were reported independently by two research groups in 2014. Giordano and Iadonisi developed a solvent-free protocol for benzylation and allylation, using Bu<sub>2</sub>SnO as catalyst in the presence of tetrabutylammonium iodide (Scheme 17) [72]. Reactions of fully unprotected (reducing) sugars under these conditions gave rise to particularly interesting results: for instance, a  $\beta$ -1,3-di-*O*-benzylated mannopyranoside – a stereochemical outcome that would be challenging to access by selective glycosidation – was synthesized directly from mannose. The selective preparation of a glucofuranoside is another noteworthy result. Dong and co-workers described similar conditions (Bu<sub>2</sub>SnO, K<sub>2</sub>CO<sub>3</sub>, Bu<sub>4</sub>NBr, MeCN/DMF, 80 °C) for the selective monobenzylation of secondary OH groups in a variety of sugar-derived di-, tri-, and tetraols [73]. Several instances of benzylation



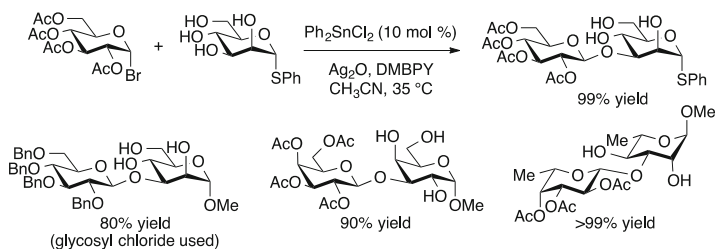
**Scheme 17** Organotin-catalyzed benzylations of carbohydrate derivatives



**Scheme 18** Preparation of keto sugars by regioselective, organotin-catalyzed oxidation. [TMPhA]<sup>+</sup>Br<sub>3</sub><sup>-</sup> denotes trimethylphenylammonium tribromide

of a secondary OH group in the presence of a free 6-OH group were documented, including the monobenylation of the lactose-derived thioglycoside shown in Scheme 17.

Selective oxidations of pyranosides to keto sugars have been accomplished using dioctyltin dichloride ((C<sub>8</sub>H<sub>17</sub>)<sub>2</sub>SnCl<sub>2</sub>) as catalyst and trimethylphenylammonium tribromide ([TMPhA]<sup>+</sup>Br<sub>3</sub><sup>-</sup>) as a mild oxidant (Scheme 18) [74]. Under these conditions, oxidation of the axial OH group of a *cis*-1,2-diol moiety was generally observed, presumably reflecting a preference for abstraction of the less sterically hindered equatorial hydrogen from a catalyst-derived stannylene acetal. The method was found to be best suited for the synthesis of 4-keto sugar derivatives from galactopyranosides, although oxidation of the 3-OH group was observed for 1,6-anhydro-β-D-galactopyranose, which is locked in the <sup>1</sup>C<sub>4</sub> conformation. The yields of 2-keto sugars from manno-configured substrates were significantly lower, perhaps reflecting a deactivating inductive effect of the adjacent anomeric position.



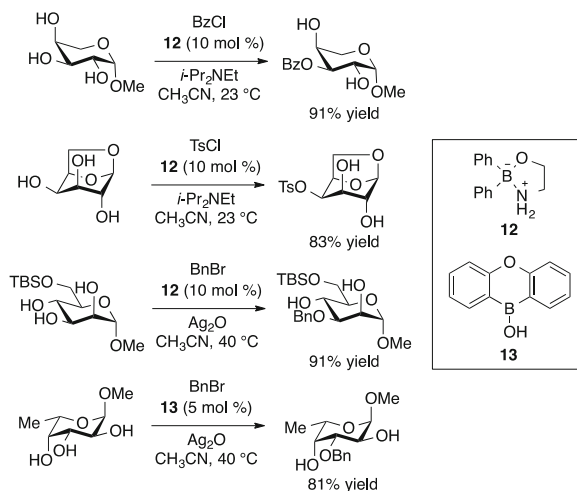
**Scheme 19** Catalytic activation of glycosyl acceptors by  $\text{Ph}_2\text{SnCl}_2$ . DMBPY denotes 5,5'-dimethyl-2,2'-bipyridyl

Although the selective glycosylation of stannylene acetals was reported more than 35 years ago [75], it was not until 2014 that a catalytic variant of this process was developed [76]. The optimized conditions involved the use of the glycosyl bromide (or chloride, in the case of per-benzylated glucose and per-acetylated *N*-acetylglucosamine-derived donors) and  $\text{Ph}_2\text{SnCl}_2$  as catalyst along with  $\text{Ag}_2\text{O}$  and 5,5'-dimethyl-2,2'-bipyridyl (DMBPY) as halide abstracting reagent and base, respectively (Scheme 19). Significantly lower yields were obtained using dialkyltin dichlorides in place of  $\text{Ph}_2\text{SnCl}_2$  as catalyst. Activation occurred at equatorial OH groups of *cis*-1,2-diol motifs in galacto- and manno-configured substrates, resulting in the formation of 1,2-*trans*-configured glycosidic linkages. The fact that the 1,2-*trans*-linkage was obtained using a per-benzylated glycosyl chloride – where neighboring group participation is precluded, opening the possibility of either stereochemical outcome – supports the proposal of an  $\text{S}_{\text{N}}2$ -type glycosylation mechanism.

## 6.2 Organoboron Catalysts

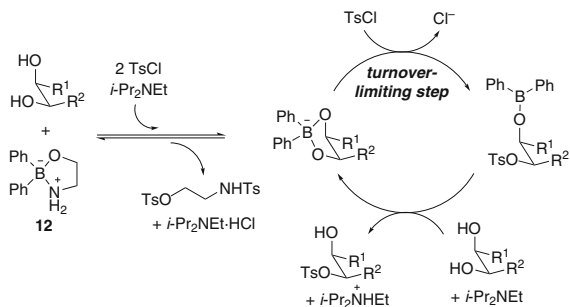
In a manner similar to the development of the tin-based catalysts described above, organoboron-catalyzed methods for activation of sugar derivatives were preceded by protocols that employed stoichiometric amounts of a boron-based promoter. As reported by the group of Aoyama, tetracoordinate adducts generated upon binding of Lewis bases to sugar-derived boronic esters display enhanced reactivity towards electrophiles. Regioselective 3-*O*-alkylations of fuco- and arabinosides were accomplished by activation of the corresponding phenylboronic esters with triethylamine [77]. Building on this concept, intramolecular Lewis base coordination using a hydroxymethyl-substituted boronate was employed to achieve regioselective glycosylations of unprotected pyranoside acceptors [78]. The enhanced nucleophilicity of the tetracoordinate organoboron complexes stands in contrast to the behavior of tricoordinate boronic esters as protective groups for 1,2- and 1,3-diol groups in carbohydrate derivatives.

**Scheme 20** Borinic acid-catalyzed monoacylations, sulfonylations and alkylations of *cis*-1,2-diol groups in pyranoside substrates

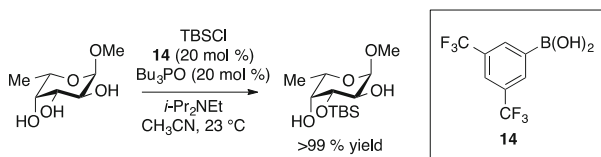


My research group has identified arylborinic acid derivatives ( $\text{Ar}_2\text{BOR}$ ) as useful catalysts for regioselective activation of carbohydrate substrates [79]. Borinic acids are generally more Lewis acidic than the corresponding boronic acids, and their interactions with diols result in tetracoordinate adducts without the need for an auxiliary Lewis base. We found that diphenylborinic acid, and its more conveniently handled ethanolamine ester **12**, were able to accelerate the monobenzylation of 1,2- and 1,3-diol motifs [80]. Phenylborinic acid and other substituted arylborinic acids displayed significantly lower activity than **12** for this transformation. When pyranoside-derived substrates were employed, selective acylation of the equatorial position of *cis*-1,2-diol groups was observed (Scheme 20). This selectivity pattern is consistent with the known affinity of organoboron compounds (in particular, boronic acids) for *cis*-1,2-diol motifs in furanosides and pyranosides. Selective acylation of a secondary OH was not achieved in reactions of hexopyranosides having a free 6-OH group, presumably because of competing 4,6-*O*-borinate formation. The scope of the method thus encompasses 6-*O*-protected manno- and galactopyranosides, as well as fuco-, rhamno-, and arabinopyranosides. Variation of the electrophilic component was also tolerated, with sulfonylations [81] and alkylations (using benzylic halides or chloromethyl ethers, activated by  $\text{Ag}_2\text{O}$ ) [82] giving rise to the same pattern of regioselectivity as was observed for acylations (Scheme 20).

A study of the kinetics of sulfonylation of *cis*-1,2-cyclohexanediol led to the proposed catalytic cycle shown in Scheme 21. Entry of pre-catalyst **12** into the cycle is triggered by rapid and irreversible reaction of the ethanolamine ligand with TsCl. The first-order kinetics in TsCl and catalyst, zero-order kinetics in *i*-Pr<sub>2</sub>NEt, and pseudo-zero-order (saturation) kinetics in substrate were consistent with the turnover-limiting step being the sulfonylation of the substrate-derived borinic ester. Computational modeling suggested that, in addition to the steric factors that might favor this outcome, electronic differences between the two boron-bound



**Scheme 21** Proposed catalytic cycle for sulfonylation of diols in the presence of borinic ester **12**

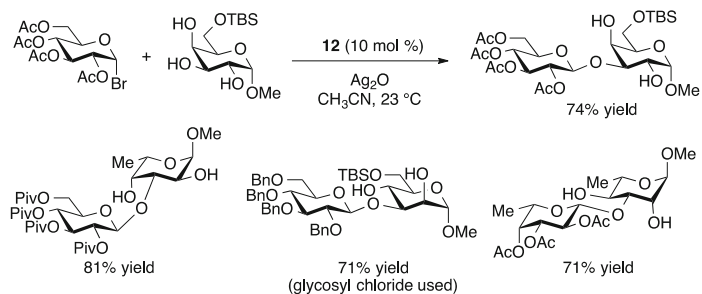
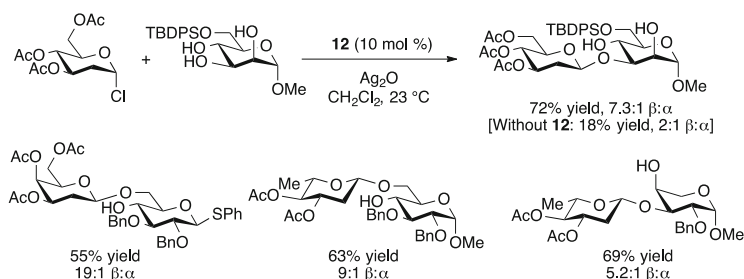


**Scheme 22** Regioselective silylation of a fucopyranoside using boronic acid and Lewis base co-catalysts

oxygen atoms of a pyranoside-derived borinic ester could contribute to the observed selectivity for the equatorial position. The mechanistic hypothesis shown in Scheme 21 helped to guide the identification of heteroboranthracene-derived borinic acids (e.g., **13**, Scheme 20) as second-generation catalysts for diol functionalization [83]. In addition to their improved activity for several representative transformations, these cyclic borinic acids displayed improved stability towards air oxidation, eliminating the need to employ an ethanolamine-derived pre-catalyst.

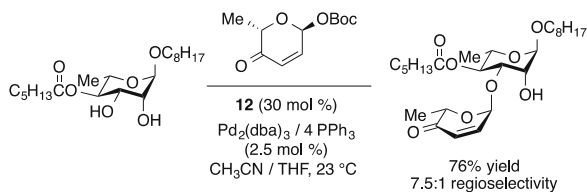
Silylation of equatorial OH groups in fuco-, rhamno-, arabino-, galacto-, and mannopyranoside substrates has been achieved using a two-component catalyst system consisting of a boronic acid and a Lewis base (Scheme 22) [84]. This system constitutes a catalytic variant of the organoboron-promoted methods developed previously by the group of Aoyama (see above), and presumably functions by formation of a tetracoordinate adduct between the Lewis base and a transiently generated, substrate-derived boronic ester.

Regioselective activation of glycosyl acceptors has been achieved using borinic ester **12** under Koenigs–Knorr-type conditions (glycosyl halide donors, activated by  $\text{Ag}_2\text{O}$ ; Scheme 23) [85, 86]. Gluco- and galacto-configured donors gave rise to 1,2-*trans*-glycosidic linkages at the equatorial sites of *cis*-1,2-diol groups, for acceptors ranging in complexity from 6-*O*-protected pyranosides to the steroidal glycoside digitoxin (having five free OH groups). An  $\text{S}_{\text{N}}2$ -type displacement mechanism was proposed, based on the following data: (1) both per-*O*-acylated and per-*O*-benzylated glycosyl halides gave rise to the 1,2-*trans*-stereochemical outcome; (2) whereas  $\alpha$ -configured acetobromoglucose and acetochloroglucose

**Scheme 23** Borinic acid-catalyzed regioselective glycosylation**Scheme 24** Organoboron-catalyzed synthesis of  $\beta$ -2-deoxyglycosides

donors resulted in  $\beta$ -configured disaccharides, the  $\beta$ -configured glycosyl chloride reacted to form the corresponding orthoester; and (3) first-order kinetic dependence on glycosyl donor, glycosyl acceptor, and catalyst was observed.

The idea that an  $S_N2$ -type pathway could be accelerated by borinic acid activation of the glycosyl acceptor motivated us to explore the construction of stereochemically challenging linkages using catalyst **12**. In particular, we envisioned that organoboron catalysis could enable an efficient stereo- and regioselective synthesis of  $\beta$ -2-deoxyglycosides from readily available  $\alpha$ -2-deoxyglycosyl halides by inversion of configuration [87]. Obtaining this outcome is difficult because of the ionization-prone nature of 2-deoxyglycosyl donors, as well as the kinetic anomeric effect that favors formation of the  $\alpha$ -anomer. The ability of catalyst **11** to influence the stereochemical outcome of 2-deoxyglycosylations is shown in Scheme 24: in the absence of catalyst, both the yield of disaccharide and the level of  $\beta$ -selectivity were significantly diminished. This protocol was applied to  $\beta$ -selective couplings of a variety of per-acetylated 2-deoxy and 2,6-dideoxyglycosyl chlorides. Modifications of the donor structure that would be expected to favor ionization (for example, substitution of acyl for benzyl protective groups) resulted in lower  $\beta$ -selectivity, consistent with the hypothesis of a catalyst-promoted  $S_N2$  pathway.

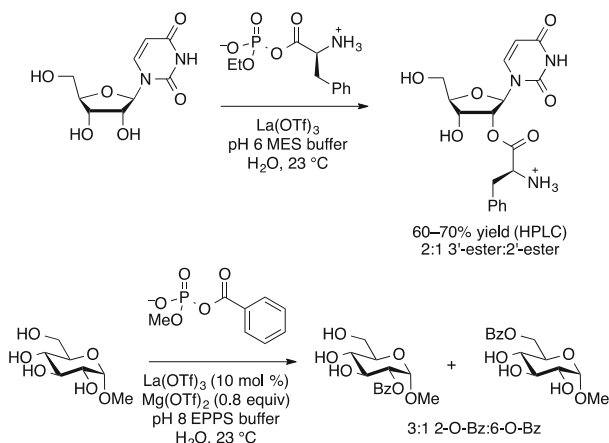


**Scheme 25** Dual B-/Pd-catalyzed regioselective glycosylations using pyranone-derived allylic carbonates

Palladium(0)-catalyzed couplings of pyranone-derived allylic carbonates with alcohols form the basis for an efficient de novo synthesis of oligosaccharides developed by the group of O'Doherty. Control over the regiochemical outcomes of these reactions was achieved through the use of an organoboron/Pd(0) dual catalyst system (Scheme 25) [88]. C–O bond formation was proposed to occur through the reaction of two catalytically generated intermediates: the acceptor-derived nucleophilic borinate and the pyranone-derived electrophilic  $\pi$ -allylpalladium complex. Regioselective glycosylations of this type were used to construct the  $\alpha$ -1,3-linkages present in the mezzettiaside class of oligorhamno-pyranoside natural products.

### 6.3 Lanthanide(III) Catalysts

Kluger and co-workers have developed  $\text{La}(\text{OTf})_3$ -catalyzed, regioselective condensations of carbohydrate derivatives with acyl phosphates in aqueous solution. This chemistry has primarily been explored as a way to access aminoacyl tRNAs by selective coupling of amino acid-derived acyl phosphates with the terminal 2',3'-diol group of the oligoribonucleotide [89–91]. Scheme 26 illustrates the  $\text{La}^{3+}$ -promoted, protective-group-free synthesis of an aminoacyl ribonucleoside: chemoselectivity for the OH groups over the amino group was achieved by carrying out the reaction in pH 6 buffer, with chelation of the Lewis acid to the *cis*-diol accounting for the observed selectivity for secondary over primary OH groups. A mixture of 3'- and 2'-*O*-acyl products was obtained because of relatively rapid equilibration of the regioisomers. This strategy has also been applied to the acylation of pyranoside derivatives [92, 93]. Whereas stoichiometric or superstoichiometric quantities of the Lewis acid catalyst were employed in the aminoacylations of nucleosides and oligonucleotides, a catalytic protocol was developed for benzoylation of pyranosides. Turnover of the  $\text{La}(\text{OTf})_3$  was accomplished by addition of  $\text{Mg}(\text{OTf})_2$  to sequester the released methyl phosphate, thus preventing catalyst inhibition.



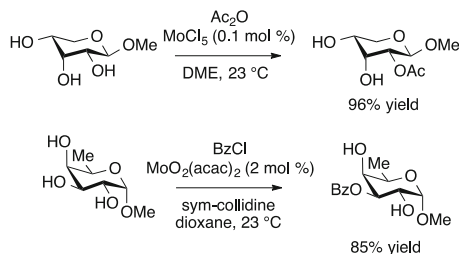
**Scheme 26**  $\text{La(OTf)}_3$ -promoted reactions of acyl phosphates with carbohydrate derivatives

## 7 Transition Metal Catalysis

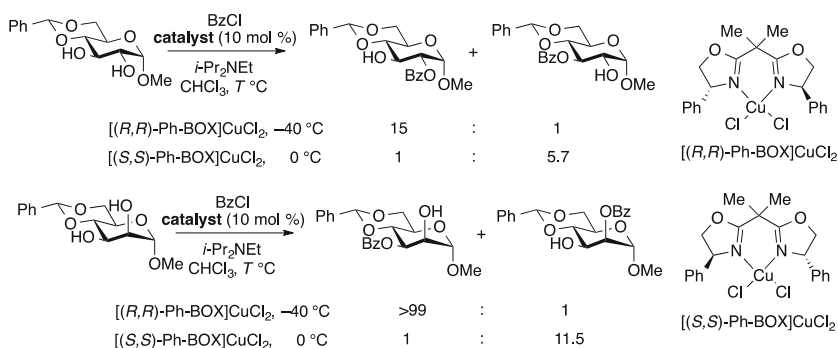
The effects of stoichiometric quantities of transition metal-based additives on the outcomes of acylation, sulfonylation, and alkylation reactions of carbohydrates were explored as early as the 1980s. Copper(II), mercury(II), nickel(II), and silver(I)-promoted transformations have been reported [94–98]. In recent years, increasing attention has been paid to the use of catalytic amounts of transition metal complexes for regioselective transformations of sugar derivatives. In the majority of the applications reported to date, the transition metal acts as a Lewis acid catalyst. The ability to influence catalytic activity and/or regioselectivity by variation of ancillary ligands has been demonstrated in several cases, including examples of chiral ligand-controlled regioselectivity. Transformations that take advantage of more unique reactivity of transition metal complexes (e.g., hydrosilylation, oxidation) have also been reported.

### 7.1 Transition Metal-Based Lewis Acids

Molybdenum-based complexes have been employed as catalysts for the selective acylation of *cis*-1,2-diol groups in pyranoside substrates [99, 100]. Reactions with acetic anhydride were carried out using  $\text{MoCl}_5$  as catalyst, whereas benzoylations proceeded most efficiently using  $\text{MoO}_2(\text{acac})_2$  (Scheme 27). Activation generally took place at the 3-OH groups of galacto- or manno-configured substrates, although 2-*O*-acylation of methyl  $\beta$ -rhamnopyranoside was observed under both sets of reaction conditions.



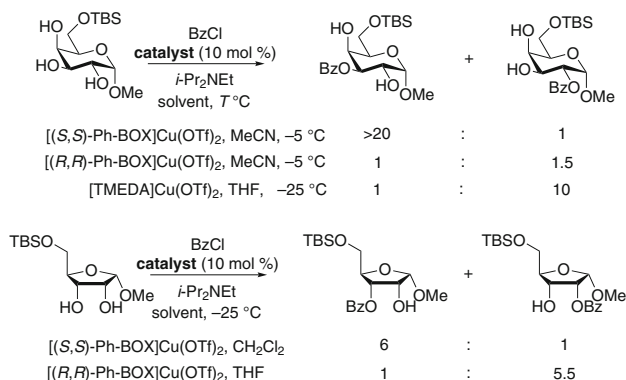
**Scheme 27** Acetylation and benzylation of pyranoside derivatives using molybdenum-based complexes



**Scheme 28** Complementary regiochemical outcomes of benzylation reactions catalyzed by chiral  $\text{CuCl}_2$ -Ph-BOX complexes

Complexes of copper(II) with chiral bis(oxazoline) (BOX) ligands activate diols towards enantioselective acylations and sulfonylations, either via desymmetrization or kinetic resolution [101–103]. Recently, chiral complexes of this type have been used for regioselective transformations of carbohydrate-derived di- and triols. Allen and Miller explored the acylation of 4,6-*O*-benzylidene-hexopyranosides in the presence of the  $\text{CuCl}_2$ -Ph-BOX complex [104]. The ability to obtain complementary regiochemical outcomes with enantiomeric catalysts is illustrated by the reactions of the benzylidene-protected  $\alpha$ -glucopyranoside and  $\alpha$ -mannopyranoside shown in Scheme 28. For other substrates (e.g., the corresponding methyl  $\beta$ -glucopyranoside derivative), matching/mismatching effects were evident, but a catalyst-controlled switch in regioselectivity could not be achieved.

Complexes of the same Ph-BOX ligand with  $\text{Cu}(\text{OTf})_2$  have been employed to promote selective acylations and tosylations of a variety of pyranoside and furanoside derivatives [105]. Matching and mismatching effects were evident upon combining the chiral ligand and the carbohydrate-derived substrate. For example, it was the (*S,S*)-configured ligand that gave the highest level of regiocontrol for benzylation at the 3-position of a 6-*O*-silylated methyl  $\alpha$ -galactopyranoside (Scheme 29). An inversion of regiocontrol – albeit modest in magnitude – in favor of the 2-*O*-acylated product was achieved using the corresponding (*R,R*)-



**Scheme 29** Cu(II) catalyst control of regioselectivity in acylations of pyranosides and furanosides

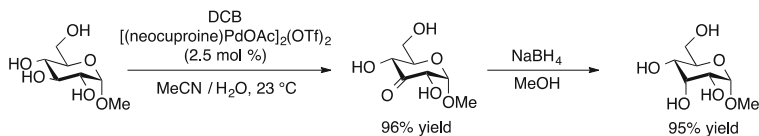


**Scheme 30** Palladium- and iridium-catalyzed silylation of methyl  $\alpha$ -mannopyranoside

Ph-BOX-derived complex. Synthetically useful 2-*O*-acylation was achieved using a complex derived from the achiral ligand *N,N,N',N'*-tetramethylethylenediamine (TMEDA) under slightly different conditions (THF, -25 °C). A clear-cut example of chiral catalyst control of regioselectivity was obtained in the benzylation of a ribofuranoside-derived substrate, with access to either the 2- or the 3-*O*-Bz product being possible through the choice of ligand enantiomer. The ability to alter regiochemical outcomes significantly by varying both the configuration and the steric/electronic properties of the ligands employed is a noteworthy feature of these Cu(II)-catalyzed reactions.

## 7.2 Other Transition Metal-Catalyzed Reactions

Schlaf and co-workers have studied the regiochemical outcomes of palladium- and iridium-catalyzed silylations of pyranosides [106, 107]. Similar distributions of bis- or tris-silylated regioisomers were obtained using heterogeneous (palladium (0) nanoparticles) or homogeneous (iridium(I) phosphine complex) catalysis, as exemplified by the results obtained for methyl  $\alpha$ -mannopyranoside (Scheme 30). In general, these catalyst systems resulted in silylation of the most sterically accessible OH group(s).



**Scheme 31** Palladium-catalyzed, regioselective oxidation of methyl  $\alpha$ -glucopyranoside. DCB denotes 2,6-dichloro-1,4-benzoquinone

Regioselective transformations of glucopyranosides to keto sugars have been achieved under palladium catalysis, using benzoquinone derivatives as stoichiometric oxidants [108]. In the presence of [(neocuproine)Pd(OAc)<sub>2</sub>(OTf)<sub>2</sub>] and 2,6-dichloro-1,4-benzoquinone (DCB), oxidation of the 3-OH group was effected for a variety of  $\alpha$ - and  $\beta$ -configured glucopyranoside derivatives (Scheme 31). This method enabled an efficient, two-step synthesis of methyl  $\alpha$ -D-allopyranoside from the corresponding glucopyranoside. Heterogeneous catalysis has also been employed for selective oxidation of sugar derivatives: in the presence of O<sub>2</sub>, platinum(0) on carbon promotes oxidation of the primary OH group of methyl  $\alpha$ -D-glucopyranoside to the carboxylic acid [109].

## 8 Summary, Conclusions, and Outlook

Despite the significant increase in research activity related to catalyst development for carbohydrate chemistry that has taken place over the past decade, significant challenges and opportunities remain. Many of the catalytic methods described above rely on enhancement of existing differences in the relative reactivity of OH groups. Overcoming these differences is often needed, with chiral catalysts providing a potentially general solution to this problem. To date, selective installation of protective groups has been the primary target for catalyst development. Selective deprotections have been less well-explored, and would also be of value. Finally, glycosylation presents excellent opportunities for further catalyst development. The first examples of synthetic catalysts for regioselective glycosylation have appeared only recently, and expanding the scope of linkages that can be constructed is crucial for future applications in oligosaccharide synthesis and natural product glycodiversification. Glycosidic bond construction presents a challenge not only in regiocontrol, but also in stereocontrol, and it is likely that both types of selectivity can be influenced using well-designed catalyst systems. The drive to unravel the complex roles of carbohydrates in biological systems, and to develop new therapeutic agents from this class of molecules, likely provides continued motivation to explore these and related goals.

## References

1. Wuts PGM, Green TW (2007) Green's protective groups in organic synthesis, 4th edn. Wiley, Hoboken
2. Angyal SJ, Evans ME (1972) Oxidation of carbohydrates with chromium trioxide in acetic acid. III. Synthesis of the 3-hexuloses. *Aust J Chem* 25:1495
3. Robins MJ, Hawrelak SD, Kanai T, Siefert JM, Mengel R (1979) Nucleic acid related compounds. 30. Transformations of adenosine to the first 2',3'-aziridine-fused nucleosides, 9-(2,3-epimino-2,3-dideoxy- $\beta$ -D-ribofuranosyl)adenine and 9-(2,3-epimino-2,3-dideoxy- $\beta$ -D-lyxofuranosyl)adenine. *J Org Chem* 44:1317
4. Schmidt RR, Klotz W (1991) Glycoside bond formation via anomeric *O*-alkylation: how many protective groups are required? *Synlett* 168
5. Garegg PJ, Iversen T, Oscarson S (1976) Monobenzoylation of diols using phase-transfer catalysis. *Carbohydr Res* 50:C12
6. Clode DM (1979) Carbohydrate cyclic acetal formation and migration. *Chem Rev* 79:491
7. Ley SV, Polara A (2007) A fascination with 1,2-diacetals. *J Org Chem* 72:5943
8. Gamblin DP, Scanlan EM, Davis BG (2009) Glycoprotein synthesis: an update. *Chem Rev* 109:131
9. Schmaltz RM, Hanson SR, Wong C-H (2011) Enzymes in the synthesis of glycoconjugates. *Chem Rev* 111:4259
10. Armstrong Z, Withers SG (2013) Synthesis of glycans and glycopolymers through engineered enzymes. *Biopolymers* 99:666
11. Lee D, Taylor MS (2012) Catalyst-controlled regioselective reactions of carbohydrate derivatives. *Synthesis* 44:3421
12. Balmond EL, Galan MC, McGarrigle EM (2013) Recent developments in the application of organocatalysis to glycosylations. *Synlett* 24:2335
13. Böttcher S, Thiem J (2014) Glycosylation employing unprotected carbohydrate acceptor components. *Curr Org Chem* 18:1804
14. Denmark SE, Beutner GL (2008) Lewis base catalysis in organic synthesis. *Angew Chem Int Ed* 47:1560
15. Kurahashi T, Mizutani T, Yoshida J-I (1999) Effect of intramolecular hydrogen-bonding network on the relative reactivities of carbohydrate OH groups. *J Chem Soc Perkin Trans 1*:465
16. Kattnig E, Albert M (2004) Counterion-directed regioselective acetylation of octyl  $\beta$ -D-glucopyranoside. *Org Lett* 6:945
17. Muramatsu W, Kawabata T (2007) Regioselective acylation of 6-O-protected octyl  $\beta$ -D-glucopyranosides by DMAP catalysis. *Tetrahedron Lett* 48:5031
18. Moitessier N, Englebienne P, Chapleur Y (2005) Directing-protecting groups for carbohydrates. Design, conformational study, synthesis and application to regioselective functionalization. *Tetrahedron* 61:6839
19. Lawandi J, Rocheleau S, Moitessier N (2011) Directing/protecting groups mediate highly regioselective glycosylation of monoprotected acceptors. *Tetrahedron* 67:8411
20. Kurahashi T, Mizutani T, Yoshida J-I (2002) Functionalized DMAP catalysts for regioselective acetylation of carbohydrates. *Tetrahedron* 58:8669
21. Kawabata T, Muramatsu W, Nishio T, Shibata T, Schedel H (2007) A catalytic one-step process for the chemo- and regioselective acylation of monosaccharides. *J Am Chem Soc* 129:12890
22. Muramatsu W, Mishiro K, Ueda Y, Furuta T, Kawabata T (2010) Perfectly regioselective and sequential protection of glucopyranosides. *Eur J Org Chem* 827
23. Ueda Y, Muramatsu W, Mishiro K, Furuta T, Kawabata T (2009) Functional group tolerance in organocatalytic regioselective acylation of carbohydrates. *J Org Chem* 74:8802

24. Yoshida K, Furuta T, Kawabata T (2010) Perfectly regioselective acylation of a cardiac glycoside, digitoxin, via catalytic amplification of the intrinsic reactivity. *Tetrahedron Lett* 51:4830
25. Ueda Y, Mishiro K, Yoshida K, Furuta T, Kawabata T (2012) Regioselective diversification of a cardiac glycoside, lanatoside C, by organocatalysis. *J Org Chem* 77:7850
26. Kawabata T, Muramatsu W, Nishio T, Shibata T, Urono Y, Stragies R (2008) Regioselective acylation of octyl  $\beta$ -D-glucopyranoside by chiral 4-pyrrolidinopyridine analogues. *Synthesis* 5:747
27. Griswold KS, Miller SJ (2003) A peptide-based catalyst approach to the regioselective functionalization of carbohydrates. *Tetrahedron* 59:8869
28. Sánchez-Roselló M, Puchlopek ALA, Morgan AJ, Miller SJ (2008) Site-selective catalysis of phenyl thionoformate transfer as a tool for regioselective deoxygenation of polyols. *J Org Chem* 73:1774
29. Fowler BS, Laemmerhold KM, Miller SJ (2012) Catalytic site-selective thiocarbonylations and deoxygenations of vancomycin reveal hydroxyl-dependent conformational effects. *J Am Chem Soc* 134:9755
30. Han S, Miller SJ (2013) Asymmetric catalysis at a distance: catalytic, site-selective phosphorylation of teicoplanin. *J Am Chem Soc* 135:12414
31. Tan KL, Sun X, Worthy AD (2012) Scaffolding catalysis: expanding the repertoire of bifunctional catalysts. *Synlett* 321
32. Sun X, Lee H, Lee S, Tan KL (2013) Catalyst recognition of *cis*-1,2-diols enables site-selective functionalization of complex molecules. *Nat Chem* 5:790
33. Blaisdell TP, Lee S, Kasaplar P, Sun X, Tan KL (2013) Practical silyl protection of ribonucleosides. *Org Lett* 15:4710
34. Sun X, Worthy AD, Tan KL (2011) Scaffolding catalysis: highly enantioselective desymmetrization reactions. *Angew Chem Int Ed* 50:8167
35. Manville N, Alite H, Haeffner F, Hoveyda AH, Snapper ML (2013) Enantioselective silyl protection of alcohols promoted by a combination of chiral and achiral Lewis basic catalysts. *Nat Chem* 5:768
36. Hu G, Vasella A (2003) Regioselective benzylation of 6-*O*-protected and 4,6-*O*-diprotected hexopyranosides as promoted by chiral and achiral ditertiary 1,2-diamines. *Helv Chim Acta* 86:4369
37. Zhou Y, Rahm M, Wu B, Zhang X, Ren B, Dong H (2013) H-Bonding activation in highly regioselective acetylation of diols. *J Org Chem* 78:11618
38. Ren B, Rahm M, Zhang X, Zhou Y, Dong H (2014) Regioselective acetylation of diols and polyols by acetate catalysis: mechanism and application. *J Org Chem* 79:8134
39. Mensah E, Camasso N, Kaplan W, Nagorny P (2013) Chiral phosphoric acid directed regioselective acetalization of carbohydrate-derived 1,2-diols. *Angew Chem Int Ed* 52:12932
40. Terada M (2010) Chiral phosphoric acids as versatile catalysts for enantioselective transformations. *Synthesis* 12:1929
41. Akiyama T, Itoh J, Fuchibe K (2006) Recent progress in chiral Brønsted acid catalysis. *Adv Synth Catal* 9:999
42. Cox DJ, Smith MD, Fairbanks AJ (2010) Glycosylation catalyzed by a chiral Brønsted acid. *Org Lett* 12:1452
43. Reisman SE, Doyle AG, Jacobsen EN (2008) Enantioselective thiourea-catalyzed additions to oxocarbenium ions. *J Am Chem Soc* 130:7198
44. Balmont EI, Coe DM, Galan MC, McGarrigle EM (2012)  $\alpha$ -Selective organocatalytic synthesis of 2-deoxygalactosides. *Angew Chem Int Ed* 51:9152
45. Balmont EI, Benito-Alfonso D, Coe DM, Alder RW, McGarrigle EM, Galan MC (2014) A 3,4-trans-fused cyclic protecting group facilitates  $\alpha$ -selective catalytic synthesis of 2-deoxyglycosides. *Angew Chem Int Ed* 53:8190
46. Garegg PJ, Iversen T, Oscarson S (1977) Monotosylation of diols using phase-transfer catalysis. *Carbohydr Res* 53:C5

47. Garegg PJ, Kvarnström I, Niklasson A, Niklasson G, Svensson SCT (1993) Partial substitution of thioglycosides by phase transfer catalyzed benzylation and benzylation. *J Carbohydr Chem* 12:933
48. Davis NJ, Flitsch SL (1993) Selective oxidation of monosaccharide derivatives to uronic acids. *Tetrahedron Lett* 34:1181
49. Györgydeák Z, Thiem J (1995) Synthesis of methyl (D-glycopyranosyl azide)uricates. *Carbohydr Res* 268:85
50. Bragd PL, Besemer AC, van Bekkum H (2001) TEMPO-derivatives as catalysts in the oxidation of primary alcohol groups in carbohydrates. *J Mol Catal A* 170:35
51. de Nooy AEJ, Besemer AC, van Bekkum H (1994) Highly selective TEMPO mediated oxidation of primary alcohol groups in polysaccharides. *Recl Trav Chim Pays Bas* 113:165
52. Li K, Helm R (1995) A practical synthesis of methyl 4-O-methyl- $\alpha$ -D-glucopyranosiduronic acid. *Carbohydr Res* 273:249
53. Kochkar H, Morawietz M, Hölderich WF (2000) Regioselective oxidation of primary hydroxyl groups of sugar and its derivatives using a new catalytic system mediated by TEMPO. *Stud Surf Sci Catal* 130:545
54. Kochkar H, Lassalle L, Morawietz M, Hölderich WF (2000) Regioselective oxidation of hydroxyl groups of sugar and its derivatives using silver catalysts mediated by TEMPO and peroxodisulfate in water. *J Catal* 194:343
55. Wang CC, Lee J-C, Luo S-Y, Kulkarni SS, Huang Y-W, Lee C-C, Chang K-L, Hung S-C (2007) Regioselective one-pot protection of carbohydrates. *Nature* 446:896
56. Français A, Urban D, Beau J-M (2007) Tandem catalysis for a one-pot regioselective protection of carbohydrates: the example of glucose. *Angew Chem Int Ed* 46:8662
57. Bourdreaux Y, Lemétais A, Urban D, Beau J-M (2011) Iron(III) chloride-tandem catalysis for a one-pot regioselective protection of glycopyranosides. *Chem Commun* 47:2146
58. Tran A-T, Jones RA, Pastor J, Boisson J, Smith N, Galan MC (2011) Copper(II) triflate: a versatile catalyst for the one-pot preparation of orthogonally protected glycosides. *Adv Synth Catal* 353:2593
59. Gyurcsik B, Nagy L (2000) Carbohydrates as ligands: coordination equilibria and structure of the metal complexes. *Coord Chem Rev* 203:81
60. Wagner D, Verheyden JPH, Moffatt JG (1974) Preparation and synthetic utility of some organotin derivatives of nucleosides. *J Org Chem* 38:24
61. David S, Hanessian S (1985) Regioselective manipulation of hydroxyl groups via organotin derivatives. *Tetrahedron* 41:643
62. Grindley TB (1998) Applications of tin-containing intermediates to carbohydrate chemistry. *Adv Carbohydr Chem Biochem* 53:17
63. Maki T, Iwasaki F, Matsumura Y (1998) A new convenient method for selective monobenzylation of diols. *Tetrahedron Lett* 39:5601
64. Iwasaki F, Maki T, Onomura O, Nakashima W, Matsumura Y (2000) Chemo- and stereoselective monobenzylation of 1,2-diols catalyzed by organotin compounds. *J Org Chem* 65:996
65. Martinelli MJ, Vaidyanathan R, Van Khau V (2000) Selective monosulfonylation of internal 1,2-diols catalyzed by di-*n*-butyltin oxide. *Tetrahedron Lett* 41:3773
66. Martinelli MJ, Vaidyanatha R, Pawlak JM, Nayyar NK, Dhokte UP, Doecke CW, Zollars LMH, Moher ED, Van Khau V, Kosmrlj B (2002) Catalytic regioselective sulfonylation of  $\alpha$ -chelatable alcohols: scope and mechanistic insight. *J Am Chem Soc* 124:3578
67. Voight EA, Rein C, Burke SD (2002) Synthesis of sialic acids via desymmetrization by ring-closing metathesis. *J Org Chem* 67:8489
68. Demizu Y, Kubo Y, Miyoshi H, Maki T, Matsumura Y, Moriyama N, Onomura O (2008) Regioselective protection of sugars catalyzed by dimethyltin dichloride. *Org Lett* 10:5075
69. Muramatsu W (2012) Chemo- and regioselective monosulfonylation of nonprotected carbohydrates catalyzed by organotin dichloride under mild conditions. *J Org Chem* 77:8083

70. Muramatsu W, Takemoto Y (2013) Selectivity switch in the catalytic functionalization of nonprotected carbohydrates: selective synthesis in the presence of anomeric and structurally similar carbohydrates under mild conditions. *J Org Chem* 78:2336
71. Muramatsu W, Tanigawa S, Takemoto Y, Yoshimatsu H, Onomura O (2012) Organotin-catalyzed highly regioselective thiocarbonylation of nonprotected carbohydrates and synthesis of deoxy carbohydrates in a minimum number of steps. *Chem Eur J* 18:4850
72. Giordano M, Iadonisi A (2014) Tin-mediated regioselective benzylation and allylation of polyols: applicability of a catalytic approach under solvent-free conditions. *J Org Chem* 79 (1):213–222
73. Xu H, Lu Y, Zhou Y, Ren B, Pei Y, Dong H, Pei Z (2014) Regioselective benzylation of diols and polyols by catalytic amounts of an organotin reagent. *Adv Synth Catal* 356:1735
74. Muramatsu W (2014) Catalytic and regioselective oxidation of carbohydrates to synthesize keto-sugars under mild conditions. *Org Lett* 16:4846
75. Augé C, Veyrières A (1979) Stannylene derivatives in glycoside synthesis. Application to the synthesis of the blood-group B antigenic determinant. *J Chem Soc Perkin Trans* 1:1825
76. Muramatsu W, Yoshimatsu H (2013) Regio- and stereochemical controlled Koenigs–Knorr-type monoglycosylation of secondary hydroxy groups in carbohydrates utilizing the high site recognition ability of organotin catalysts. *Adv Synth Catal* 355:2518
77. Oshima K, Kitazono E-i, Aoyama Y (1997) Complexation-induced activation of sugar OH groups. Regioselective alkylation of methyl fucopyranoside via cyclic phenylboronate in the presence of amine. *Tetrahedron Lett* 38:5001
78. Oshima K, Aoyama Y (1999) Regiospecific glycosidation of unprotected sugars via arylboronic activation. *J Am Chem Soc* 121:2315
79. Taylor MS (2015) Catalysis based on reversible covalent interactions of organoboron compounds. *Acc Chem Res* 48:295–305
80. Lee D, Taylor MS (2011) Borinic acid-catalyzed regioselective acylation of carbohydrate derivatives. *J Am Chem Soc* 133:3724
81. Lee D, Williamson CL, Chan L, Taylor MS (2012) Regioselective, borinic acid-catalyzed monoacylation, sulfonylation and alkylation of diols and carbohydrates: expansion of substrate scope and mechanistic studies. *J Am Chem Soc* 134:8260
82. Chan L, Taylor MS (2011) Regioselective alkylation of carbohydrate derivatives catalyzed by a diarylborinic acid derivative. *Org Lett* 13:3090
83. Dimitrijevic E, Taylor MS (2013) 9-Hetero-10-boraanthracene-derived borinic acid catalysts for regioselective activation of polyols. *Chem Sci* 4:3298
84. Lee D, Taylor MS (2013) Regioselective silylation of pyranosides using a boronic acid / Lewis base co-catalyst system. *Org Biomol Chem* 11:5409
85. Gouliaras C, Lee D, Chan L, Taylor MS (2011) Regioselective activation of glycosyl acceptors by a diarylborinic acid-derived catalyst. *J Am Chem Soc* 133:13926
86. Beale TM, Taylor MS (2013) Synthesis of cardiac glycoside analogs by catalyst-controlled, regioselective glycosylation of digitoxin. *Org Lett* 15:1358
87. Beale TM, Moon PJ, Taylor MS (2014) Organoboron-catalyzed regio- and stereoselective formation of  $\beta$ -2-deoxyglycosidic linkages. *Org Lett* 16:3604
88. Bajaj SO, Sharif EU, Akhmedov NG, O'Doherty GA (2014) *De novo* asymmetric synthesis of the mezzettiaside family of natural products via the iterative use of a dual B-/Pd-catalyzed glycosylation. *Chem Sci* 5:2230
89. Cameron LL, Wang SC, Kluger R (2004) Biomimetic monoacylation of diols in water. Lanthanide-promoted reactions of methyl benzoyl phosphate. *J Am Chem Soc* 126:10721
90. Tzvetkova S, Kluger R (2007) Biomimetic aminoacylation of ribonucleotides and RNA with aminoacyl phosphate esters and lanthanum salts. *J Am Chem Soc* 129(51):15848–15854
91. Her S, Kluger R (2011) Biomimetic protecting-group-free 2',3'-selective aminoacylation of nucleosides and nucleotides. *Org Biomol Chem* 9:676
92. Gray IJ, Kluger R (2007) Chelation-controlled regioselectivity in the lanthanum-promoted monobenzylation of monosaccharides. *Carbohydr Res* 342:1998

93. Dhiman RS, Kluger R (2010) Magnesium ion enhances lanthanum-promoted monobenzoylation of a monosaccharide in water. *Org Biomol Chem* 8:2006
94. Eby R, Webster KT, Schuerch C (1984) Regioselective alkylation and acylation of carbohydrates engaged in metal complexes. *Carbohydr Res* 129:111
95. Osborn HMI, Brome VA, Harwood LM, Suthers WG (2001) Regioselective C-3-O-acylation and O-methylation of 4,6-*O*-benzylidene- $\beta$ -D-gluco- and galactopyranosides displaying a range of anomeric substituents. *Carbohydr Res* 332:157
96. Gangadharmath UB, Demchenko AV (2004) Nickel(II) chloride-mediated regioselective benzoylation and benzylation of diequatorial vicinal diols. *Synlett* 2191
97. Wang H, She J, Zhang L-H, Ye X-S (2004) Silver(I) oxide mediated selective monoprotection of diols in pyranosides. *J Org Chem* 69:5774
98. Evtushenko EV (2012) Regioselective benzoylation of glycopyranosides by benzoic anhydride in the presence of  $\text{Cu}(\text{CF}_3\text{COO})_2$ . *Carbohydr Res* 359:111
99. Evtushenko EV (2006) Regioselective monoacetylation of methyl pyranosides of pentoses and 6-deoxyhexoses by acetic anhydride in the presence of  $\text{MoCl}_5$ . *Synth Commun* 36:1593
100. Evtushenko EV (2010) Regioselective benzoylation of glycopyranosides by benzoyl chloride in the presence of  $\text{MoO}_2(\text{acac})_2$ . *J Carbohydr Chem* 29:368
101. Matsumura Y, Maki T, Murakami S, Onomura O (2003) Copper ion-induced activation and asymmetric benzoylation of 1,2-diols: kinetic chiral molecular recognition. *J Am Chem Soc* 125:2052
102. Matsumura Y, Maki T, Tsurukami K, Onomura O (2004) Kinetic resolution of D,L-myoinositol derivatives catalyzed by chiral Cu(II) complex. *Tetrahedron Lett* 45:9131
103. Demizu Y, Matsumoto K, Onomura O, Matsumura Y (2007) Copper complex catalyzed asymmetric monosulfonylation of *meso-vic*-diols. *Tetrahedron Lett* 48:7605
104. Allen CL, Miller SJ (2013) Chiral copper(II) complex-catalyzed reactions of partially protected carbohydrates. *Org Lett* 15:6178
105. Chen I-H, Kou KGM, Le DN, Rathburn CM, Dong V (2014) Recognition and site-selective transformation of monosaccharides by using copper(II) catalysis. *Chem Eur J* 20:5013
106. Chung M-K, Orlova G, Goddard JD, Schlaf M, Harris R, Beveridge TJ, White G, Hallett FR (2002) Regioselective silylation of sugars through palladium nanoparticle-catalyzed silane alcoholysis. *J Am Chem Soc* 124:10508
107. Chung M-K, Schlaf M (2005) Regioselectively trisilylated hexopyranosides through homogeneously catalyzed silane alcoholysis. *J Am Chem Soc* 127:18085
108. Jäger M, Hartmann M, de Vries HG, Minnaard AJ (2013) Catalytic regioselective oxidation of glycosides. *Angew Chem Int Ed* 52:7809
109. Fabre J, Betheder D, Paul F, Monsan P (1993) Improved synthesis of sodium alkyl-glycopyranuronates. *Synth Commun* 23:1357

# Site-Selective Reactions with Peptide-Based Catalysts

Michael W. Giuliano and Scott J. Miller

**Abstract** The problem of catalyst-controlled site-selectivity can potentially require a catalyst to overcome energetic barriers larger than those associated with enantioselective reactions. This challenge is a signature of substrates that present reactive sites that are not of equivalent reactivity. Herein we present a narrative of our laboratory's efforts to overcome this challenge using peptide-based catalysts. We highlight the interplay between understanding the inherent reactivity preferences of a given target molecule and the development of catalysts that can overcome intrinsic preferences embedded within a substrate.

**Keywords** Asymmetric synthesis · Catalysis · Natural products · Peptides · Site-selective reactions

## Contents

1	Introduction: The Barrier Challenge of Site-Selective Catalysis .....	158
2	Asymmetric Phosphorylation of <i>myo</i> -Inositol as a Proving Ground for Site-Selective Functionalization of Complex Molecules .....	159
3	Parallel Exploration of Site-Selective Acylations .....	166
4	Natural Products as Substrates: Studies of the Relative Reactivity and Remote Functionalization of the Hydroxyl Groups of Erythromycin A and Apoptolidin A .....	167
5	A Connection Between Site-Selective Catalysis in Natural Products and Remote Asymmetric Induction .....	171
6	Development of New Peptide-Catalyzed Reactions to Address Additional Challenges in Chemical Selectivity .....	173
7	Peptide-Catalyzed Diversification of Glycopeptide Antibiotics .....	178

---

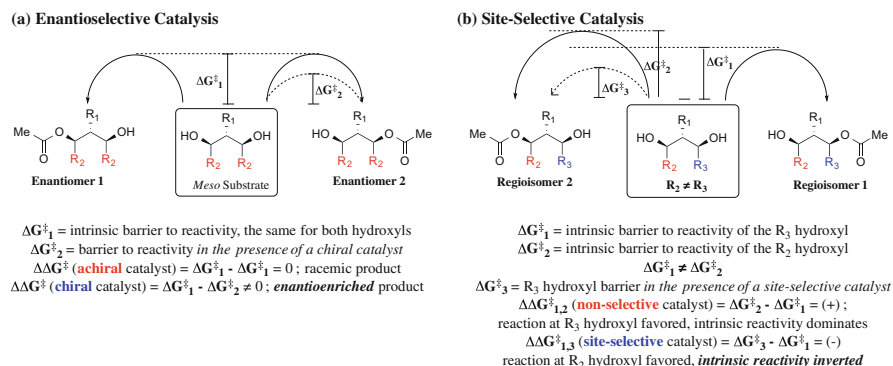
M.W. Giuliano and S.J. Miller (✉)  
Department of Chemistry, Yale University, 225 Prospect Street, New Haven, CT 06520-8107,  
USA  
e-mail: [scott.miller@yale.edu](mailto:scott.miller@yale.edu)

8 Peptide-Based Catalysts for Site-Selective Oxidation .....	188
9 Conclusions .....	191
References .....	192

## 1 Introduction: The Barrier Challenge of Site-Selective Catalysis

Peptide-based catalysts have emerged as a versatile platform for catalytic reactions. Some of the earliest contributions provided opportunities to explore biomimetic ideas, as minimal peptides can be viewed as low molecular weight mimics of the more complicated, naturally occurring enzymes. Fundamental studies have addressed a range of questions, for example, about hydrolysis reactions in analogy to those carried out by proteases [1, 2]. More recently, peptide-based catalysts have become a popular platform for the study of enantioselective catalytic reactions. The Julia–Colonna epoxidation represents the first asymmetric, peptide-catalyzed reaction, reported initially by Julia et al. [3]. Asymmetric peptide catalysis has also been the subject of a number of reviews [4–9]. In our own laboratory, we have examined peptide-based catalysts for a number of enantioselective processes [5–7]. As described below, we made observations that led us to recognize increasingly the potential of these catalysts to mediate selective reactions on “complex” substrates, wherein multiple copies of the same functional group exist within the scaffold of interest. This chapter focuses primarily on our laboratory’s studies of peptide-catalyzed site-selective derivatizations of molecules of this type.

As becomes clear in the discussion below, our analysis of site-selective reactions was shaped by our parallel study of enantioselective reactions. We came to view our goals in the context of an admittedly simplified reaction coordinate diagram model (Chart 1). On the one hand, we viewed enantioselective reactions as a challenge associated with differential transition state stabilization for competing pathways. The intrinsic activation barriers for competing enantiotopic pathways are equivalent by definition. In the site-selective catalysis arena, by contrast, the intrinsic barriers to reaction at similar functional groups may not be equivalent. Thus, a major challenge is the discovery of catalysts that can lead to favored reactions at inherently less reactive positions. For example, if one potential site of derivatization is 100 times less reactive than another, the proverbial 2.7 kcal/mol of transition state stabilization which can lead to >98% ee in an enantioselective reaction only delivers 1:1 in the site-selectivity arena (among many essential contributions, Kagan has discussed the intricacies of the energetics of asymmetric reactions at length in [10–12]). Therefore, from a purely physical organic perspective, achieving highly efficient functionalization at low-reactivity positions is a challenging goal. Of course, there are other scenarios that may lead to selectivity in site-selective reactions. These include a number of possibilities that may differentially destabilize ground states, or which may differentially increase the energies of transition states. Nonetheless, we began our studies with the simplified reaction coordinates of Chart 1 as a guiding principle.



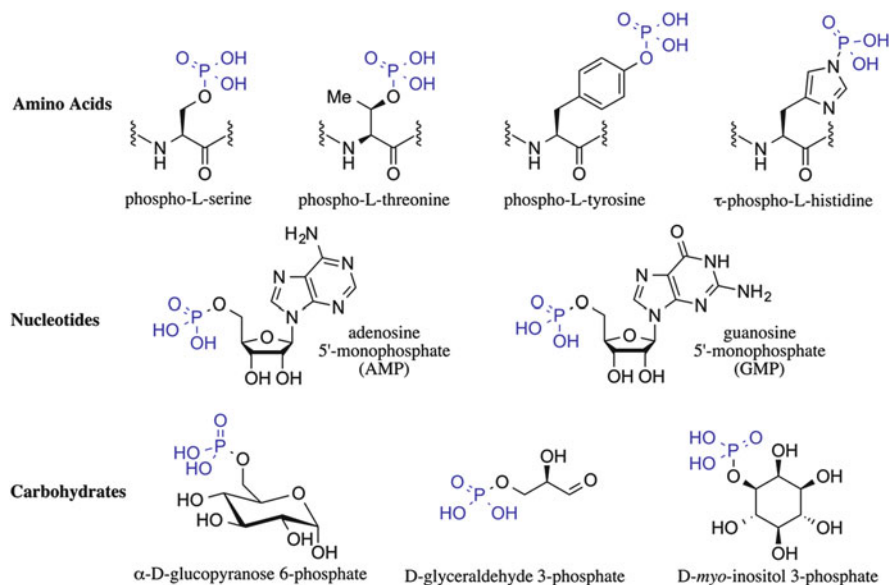
**Chart 1** (a) Simplified reaction coordinate diagram for an enantioselective desymmetrization reaction. (b) Simplified reaction coordinate diagram for a site-selective reaction

## 2 Asymmetric Phosphorylation of *myo*-Inositol as a Proving Ground for Site-Selective Functionalization of Complex Molecules

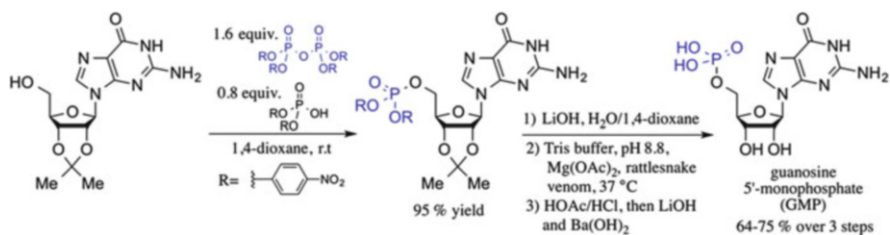
The transfer of phosphate to a specific position in a complex molecule by kinases represents an important and ubiquitous chemical event in biology [13, 14]. Phosphorylation often acts as a switch, imbuing a substrate with biological function different from the non-phosphorylated species. These essential reactions are observed in all classes of important biomolecules, including proteins, nucleic acids and their building blocks, and, particularly relevant to our early studies, carbohydrates (Fig. 1).

Carbohydrates present a significant challenge for efficient synthesis. The site-selective transfer of a reagent to a single functional group within a molecule that contains multiple copies of that functional group is manifest throughout carbohydrate chemistry. Most often, this challenge is met through the implementation of protecting groups [15, 16]. The selective phosphorylation of carbohydrates is a subset of the field, and studies date back at least to the work of Fischer nearly a century ago [17]. In the 1950s, Moffatt and Khorana utilized a stoichiometric pyrophosphate reagent to prepare guanosine 5'-phosphate, commonly known as the ubiquitous metabolite GMP in the presence of a free amine and pyridone-like carbonyl (Scheme 1). This precedent provides a pioneering example of a site-selective phosphorylation used for the chemical synthesis of a biologically important molecule [18, 19].

We were drawn to the catalytic, asymmetric phosphorylation of inositol for several reasons [20–22]. First, *myo*-inositol possesses six hydroxyl groups, any one of which could potentially be phosphorylated by a chiral catalyst. Second, the diverse phosphorylation patterns of inositol phosphates correspond to equally diverse biological functions [23]; excellent strategies for their synthesis existed,



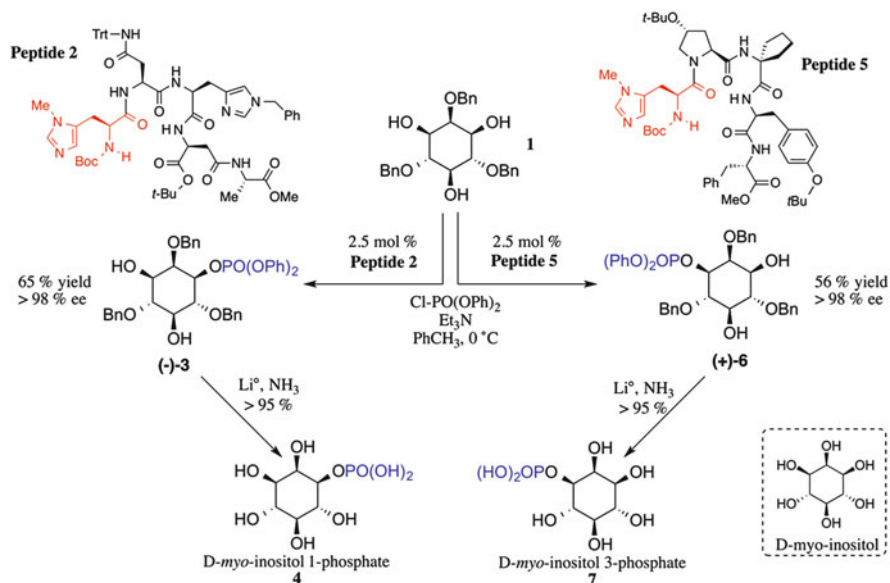
**Fig. 1** Important phosphorylated species. On phosphate protonation state in figures: all phosphate groups, for the sake of simplicity, are shown as fully protonated. We recognize that the protonation state of phosphates and phosphate monoesters is highly dependent upon environment



**Scheme 1** Moffatt and Khorana's GMP synthesis [18, 19]

but were often dependent on protecting groups and classical resolution for asymmetric synthesis [24]. Third, we postulated that peptide-based catalysts might provide a means to reduce the dependence on protective groups for the synthesis of targets. For example, any free hydroxyl groups on an inositol-derived substrate might engage in hydrogen-bonding interactions with a peptide catalyst. In addition, we were inspired by the enzymes of the histidine-dependent kinase family, which utilize an active site histidine (cf. Fig. 1;  $\tau$ -phospho-L-histidine) as a nucleophilic catalyst for phosphoryl group transfer. [25, 26].

Our earliest efforts in peptide catalysis employed a  $\pi$ -methyl histidine residue as the catalytic side chain in acyl transfer reactions [27, 28]. Given this precedent and



**Scheme 2** Enantioselective phosphorylation of **1** by peptide catalysts [20–22]. Catalytic  $\pi$ -methyl histidine residue is highlighted in red

our interest in selective nucleophilic catalysis, we screened a small, randomized library of 39 peptides for the enantioselective phosphorylation of **1**, derived from *D*-myo-inositol (Scheme 2). Derivative **1** was chosen in particular, as the benzyl groups convey solubility in organic solution to the substrate, and the site selectivity challenge is simplified to three unique positions [29]. Peptide **2** was found, under optimized conditions, to give desymmetrized (–)-**3** (65% isolated yield) with excellent enantioselectivity (>98% by HPLC) [20]. Synthetic *D*-myo-inositol 1-phosphate (**4**) was then obtained in excellent yield (96%) following deprotection.

Expansion of this peptide library yielded an additional catalyst scaffold, peptide **5**, which, despite originating from a homochiral peptide library composed of *L*-amino acids, gave the opposite selectivity as peptide **2** (Scheme 2). Intermediate (+)-**6** was obtained in >98% ee (HPLC) and 56% isolated yield under the conditions optimized for the production of **3**. Synthetic *D*-myo-inositol 3-phosphate (**7**) was thus obtained following deprotection once again [21]. It is particularly noteworthy that, in both of these cases, phosphorylation at the 5-position of inositol was observed only as a trace byproduct, with recovered starting material **1** as the only other primary species after reaction. Although peptides **2** and **5** were able to distinguish clearly between the 1- and 3-positions, the 5-position hydroxyl appears to have a higher intrinsic barrier to reaction. We emphasize that we have yet to discover a selective catalyst for derivatization at the 5-position of **1**.

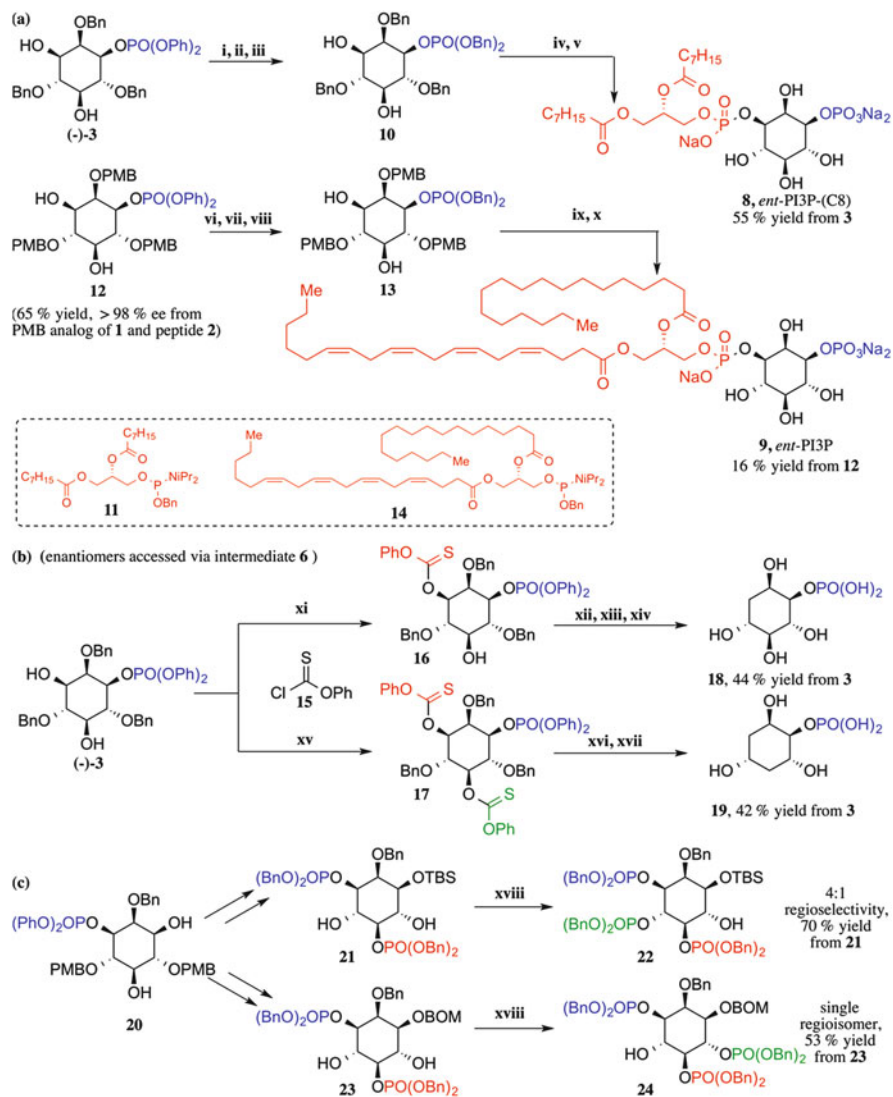
The identification of catalysts **2** and **5** provided some opportunities for synthesis. Inositol phosphates themselves are interesting as targets of site-selective organic reactions, as their diverse structures are observed to result in equally diverse

biological functions. In the same way, the related phosphatidyl inositol phosphates (PIPs) are ubiquitous across biology, serving diverse roles ranging from cell membrane components, to immunopotentiality, to PIP-dependent cellular signaling; this has itself constituted its own field of study in chemical biology [30–32]. With the ability both to install phosphates asymmetrically and to differentiate the functionally important 1- and 3-hydroxyl groups of inositol (see above), we targeted the C8 variant of phosphatidyl inositol-3-phosphate, *ent*-PI3P-(C8), **8**, a common PIP model compound in biological studies, and PI3Ps that contained arachidonate sidechains (**9**) observed in naturally occurring PI3Ps (Scheme 3a) [33]. The lower reactivity of the 5-hydroxyl relative to the 1- and 3-positions was now key to our strategy. Once the 1- and 3-positions were differentiated to yield **3**, the remaining enantiotopic hydroxyl, the 3-position on benzyl derivative **10**, could be functionalized using a phosphoramidite without an asymmetric catalyst. Removal of all protecting groups *via* hydrogenolysis furnished **8**. A degree of 5-hydroxyl reactivity did limit yield.

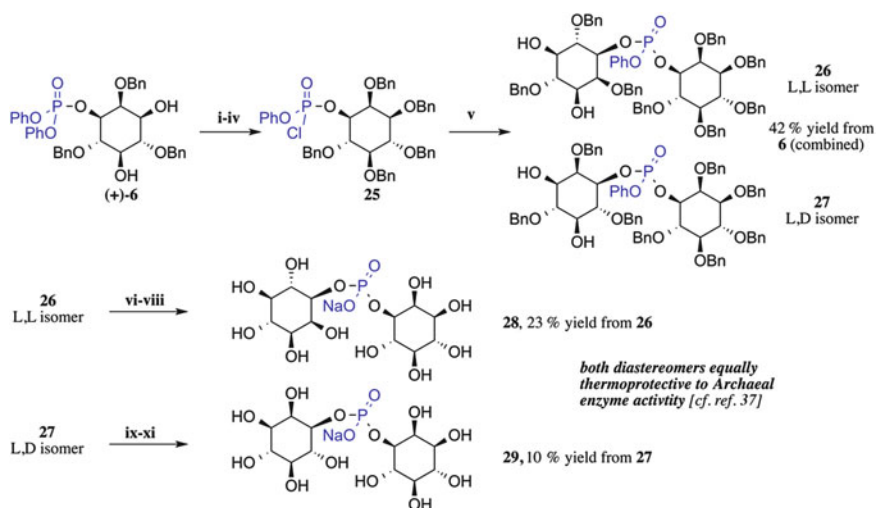
In order to access **9**, which contains an unsaturated arachidonate sidechain, the use of *para*-methoxybenzyl (PMB) protecting groups on the inositol ring was necessary. The deprotection used in the synthesis of **8**, hydrogenolysis, was incompatible with the alkenes of the arachidonate sidechain. Fortunately, intermediate **12** could be prepared from the corresponding tris-PMB-protected *myo*-inositol derivative using peptide **2** in >98% ee. Following, once again, installation of benzyl protecting groups on the phosphate to yield **13**, phosphoramidite coupling using **14**, followed by an optimized global deprotection with TMSBr yielded *ent*-PI3P derivative **9**.

We again exploited the greater reactivity of the 1-hydroxyl of **3** in a selective functionalization sequence this time to target select deoxy-*myo*-inositol phosphates for use as probes of monophosphatase enzyme specificity (Scheme 3b) [34–36]. Either just the 1- or the 3-hydroxyl could be mono-thiocarbonylated (depending on using **3** or **6** as a substrate; **3** is shown in Scheme 3b), or both the remaining enantiotopic position and the 5-hydroxyl could be exhaustively thiocarbonylated, yielding **16** or **17**, depending on reaction time. Compounds **16** and **17** (and their enantiomers) were then subjected to deoxygenation under standard Barton–McCombie conditions and then global deprotection furnished both enantiomers of 3-deoxy-*myo*-inositol, **18**, and 3,5-dideoxy-*myo*-inositol, **19**. These four species along with *L*- and *D*-*myo*-inositol-1-phosphate were used in the kinetic profiling of an archaeal phosphatase [34]. Deoxygenation was also used in a strategy combining the insights from the studies mentioned above to provide an efficient route to various deoxy-PIPs (not shown) [36].

The combination of both asymmetric catalysis and differential innate functional group reactivity also allowed preparation of a number of inositol polyphosphates (Scheme 3c) [35]. Key to this last strategy was the site-selective phosphitylation of the 4-hydroxyl over the 6-hydroxyl of intermediate **21** to yield **22**; the latter hydroxyl was sterically encumbered by a bulky TBS protecting group on the 1-hydroxyl. This hypothesis regarding steric differentiation was supported by the selective phosphitylation of **23** to yield **24**, which, using the smaller BOM



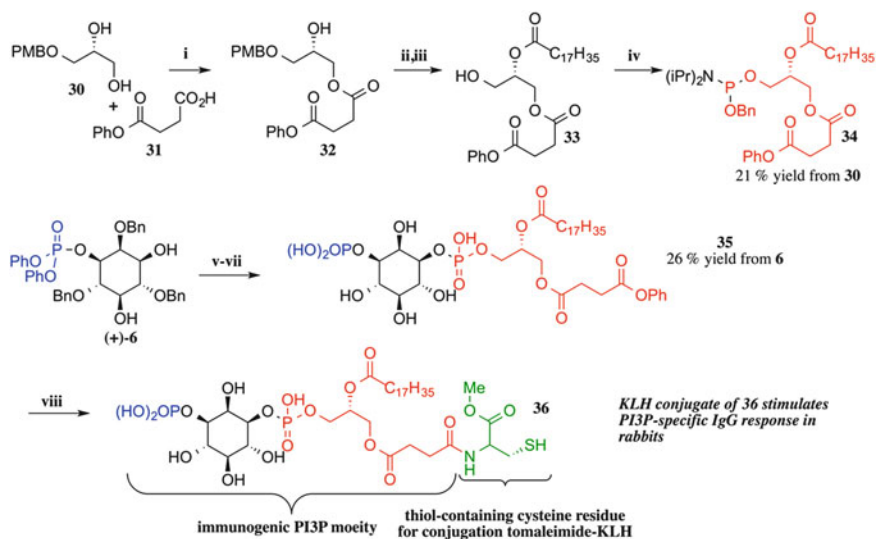
**Scheme 3** (a) Synthesis of PI3P-C8 and arachidonate derivatives **8** and **9**, respectively [33]. (i) TBSCl, imidazole, DMF. 89% (ii) NaH, BnOH, THF. 84% (iii) HF-pyridine, THF. 86% (iv) dicyanoimidazole, toluene/CH<sub>2</sub>Cl<sub>2</sub> (1:1), **11**; then 30% (aq.) H<sub>2</sub>O<sub>2</sub>. (v) H<sub>2</sub>, Pd(OH)<sub>2</sub>/C, *t*-BuOH/H<sub>2</sub>O, NaHCO<sub>3</sub>. 85% (two steps) (vi) TBSCl, imidazole, DMF. 89% (vii) NaH, BnOH, THF. 99% (viii) HF-pyridine, THF. 77% (ix) dicyanoimidazole, toluene/CH<sub>2</sub>Cl<sub>2</sub> (1:1), **14**; then 30% (aq.) H<sub>2</sub>O<sub>2</sub>. 39% (x) TMSBr (20 equiv.), PhCH<sub>3</sub>, 70 °C then NH<sub>4</sub>OH. 61% (b) Synthesis of deoxy-myoinositol phosphates [34]. (xi) **15**, pyridine, DMAP, CH<sub>2</sub>Cl<sub>2</sub>, 2 h. 70% (xii) Ac<sub>2</sub>O, Et<sub>3</sub>N, DMAP, CH<sub>2</sub>Cl<sub>2</sub> (xiii) Bu<sub>3</sub>SnH, AIBN, PhCH<sub>3</sub>, reflux. 64% (two steps) (xiv) Li<sup>0</sup>, NH<sub>3</sub>. 99% (xv) **15**, pyridine, DMAP, CH<sub>2</sub>Cl<sub>2</sub>, t., 48 h. 70% (xvi) Bu<sub>3</sub>SnH, AIBN, PhCH<sub>3</sub>, reflux. 61% (xvii) Li<sup>0</sup>, NH<sub>3</sub>. 99% (c) Synthesis of myo-inositol polyphosphates via modulation of inherent hydroxyl group reactivity [35]. (xviii) (iPr)<sub>2</sub>NP(OBn)<sub>2</sub>, dicyanoimidazole; then 30% (aq.) H<sub>2</sub>O<sub>2</sub>



**Scheme 4** Synthesis of the L,L and L,D isomers of di-*myo*-inositol-1,1'-phosphate [37]. (i) 2-benzyloxy-1-methyl-pyridinium triflate, MgO, C<sub>6</sub>H<sub>5</sub>CF<sub>3</sub>. 73% (ii) LiOH, THF/H<sub>2</sub>O (1:1) (iii) Dowex 50X2-200. quant. (two steps) (iv) (COCl)<sub>2</sub> (2 equiv.), DMF (1 equiv.), CH<sub>2</sub>Cl<sub>2</sub>, 5 min., r.t. (v) Et<sub>3</sub>N (4 equiv.), DMAP (1 equiv.), **1** (2 equiv.), r.t., 12 h, 57% (vi) 2-benzyloxy-1-methyl-pyridinium triflate, MgO, C<sub>6</sub>H<sub>5</sub>CF<sub>3</sub>. 35% (vii) LiOH, THF/H<sub>2</sub>O (1:1); Chelex 100 Na form; 69% (two steps) (viii) H<sub>2</sub>, Pd(OH)<sub>2</sub>/C, EtOAc/MeOH (1:1). 96% (ix) 2-benzyloxy-1-methyl-pyridinium triflate, MgO, C<sub>6</sub>H<sub>5</sub>CF<sub>3</sub>. 27% (x) LiOH, THF/H<sub>2</sub>O (1:1); Chelex 100 Na form; 47% (two steps) (xi) H<sub>2</sub>, Pd(OH)<sub>2</sub>/C, EtOAc/MeOH (1:1). 82%

protecting group at the 1-hydroxyl, resulted exclusively in phosphoramidite transfer to the 6-hydroxyl.

Our synthetic studies enabled study of another aspect of Archaea inositol phosphate biochemistry [37]. Hyperthermophilic organisms have evolved a number of mechanisms by which they survive harsh environments [38, 39], including the use of a variety of charged secondary metabolites to regulate osmotic stress. Another, using dimeric *myo*-inositol phosphates (DIPs), is to convey drastically improved thermostability to the organism's essential enzymes [38, 39]. At the time of our study, it was not established conclusively as to which of the possible di-*myo*-inositol-1,1'-phosphate stereoisomers, e.g., L,L-**28** or L,D-**29** (Scheme 4), was responsible for this function or if one provided any advantage over the other, even though, the L,D isomer is believed to be the more prevalent natural product. Starting from **6**, accessed *via* the phosphorylation of **1** with peptide **5**, we prepared per-benzylated phosphoryl chloride **25**. Reaction of **25** with **1** in the presence of Et<sub>3</sub>N and DMAP furnished a 1:3 mixture of **26** and **27** in 42% combined yield from **6**. Stereochemical assignment was made by analyzing optical rotation following separation and perbenzylation of **26** and **27**, identifying **26** as the L,L isomer and **27** as the L,D DIP isomer. Following deprotection, yielding **28** and **29**, the DIP isomers were evaluated for their ability to preserve enzymatic activity at high temperatures in an effort to trace one or the other as a thermoprotective natural product in certain



**Scheme 5** Synthesis of a thiol-containing PI3P hapten [40]. (i) DCC, DMAP,  $\text{CH}_2\text{Cl}_2$ , r.t., 30 min. 50% (ii) stearic acid, DCC, DMAP,  $\text{CH}_2\text{Cl}_2$ , 7 h. 85% (iii) DDQ,  $\text{CH}_2\text{Cl}_2$ , r.t., 14 h. 89% (iv)  $\text{BnOP}(\text{iPr})_2$ , tetrazole,  $\text{CH}_2\text{Cl}_2$ , r.t., 3 h. 56% (v) tetrazole,  $\text{CH}_2\text{Cl}_2$ , r.t., 1.5 h (vi) 30%  $\text{H}_2\text{O}_2$  (aq.),  $0^\circ\text{C}$ , 1 h, 30% (two steps) (vii)  $\text{Pd}(\text{OH})_2/\text{C}$ , *t*-BuOH,  $\text{H}_2\text{O}$ ,  $\text{H}_2$  (1 atm), r.t., 1 h. 86% (viii) 15 mM L-cysteine methyl ester $\cdot\text{HCl}$ , 5.8 M GdmCl, 40 mM TCEP $\cdot\text{HCl}$ , 2.5 M imidazole,  $\text{CH}_3\text{CN}$  20% by volume, pH 7.1,  $40^\circ\text{C}$ , 135 min

hyperthermophilic Archaea species. Remarkably, both isomers perform this task nearly equally, suggesting, perhaps, that the L,D DIP isomer has its stereochemistry not as a result of evolutionary optimization, but for other biosynthetic happenstance.

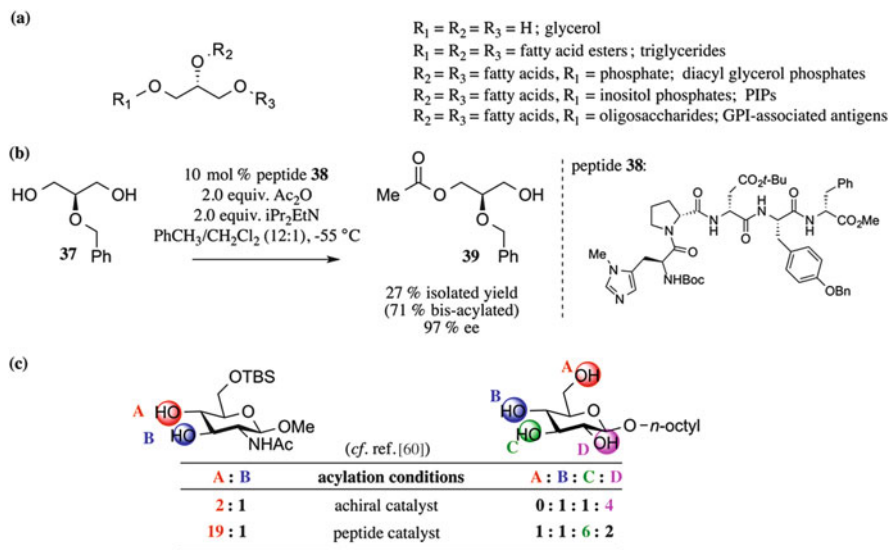
Asymmetric phosphorylation chemistry was also used strategically in the synthesis of a phosphatidyl-*myo*-inositol-3-phosphate-based hapten [40]. Our strategy required the synthesis of a phosphatidyl-*myo*-inositol-3-phosphate-based hapten, **36**, equipped with a thiol group to allow for conjugation to keyhole limpet hemocyanin (KLH), a protein commonly used in immunogenic multicomponent species (Scheme 5) [41–43]. We prepared *D*-*myo*-inositol-3-phosphate precursor **6** using peptide **5** as detailed previously (Scheme 2, [21]). We sought to prepare the PI3P analogue, as we had previously, utilizing phosphorus(III)-based phosphoramidite chemistry. This required the synthesis of phosphoramidite **34**, which was accomplished in four straightforward steps [44]. Conjugation of **34** to **6** was accomplished with tetrazole. Ensuating oxidation to phosphorus(V) and global deprotection proceeded efficiently. A significant hurdle to accessing a PI3P hapten proved to be the installation of a simple thiol group. Standard amide bond-forming conditions used in attempts to couple L-cysteine methyl ester to the free carboxylic acid form of **35** failed to yield product. However, use of native chemical ligation [45–48], employing L-cysteine methyl ester with phenyl ester **35** as the electrophile [48], proceeded in a relatively clean reaction, providing useable hapten in 46% yield

[40]. Subsequent immunological evaluation of the **36**-KLH conjugate revealed the production of highly specific IgG antibodies in rabbit sera. Although the sample size is small, these results suggest that the concise and highly selective synthetic routes derived from peptide-catalyzed reactions can provide a fairly direct route to the production of biochemical tools for the spatiotemporal study of diverse PIPs which are widely distributed within mammalian cells.

### 3 Parallel Exploration of Site-Selective Acylations

The overall arc of study of peptide-catalyzed phosphorylation was encouraging and prompted us to explore related acyl transfer reactions with histidine-based peptides. The existence of a differentially functionalized glycerol in the phosphatidylinositol family also created the motivation to develop catalysts that could break symmetry in glycerols, as part of phosphatidylinositol total syntheses.

Glycerol possesses two enantiotopic primary hydroxyl groups, which most commonly are differentially functionalized with a variety of species, forming the phosphatidyl inositol phosphates, diacyl glycerol phosphates (the major components of all biological membranes), GPI-associated antigens, and fatty acid triglycerides (Fig. 2). A screen based on the libraries of acylation catalysts [27, 28], phosphorylation catalysts [20–22, 33–37], and sulfinylation catalysts [51] developed for group transfer reactions found that benzyl glycerol derivative **37** could be monoacylated by peptide **38** in up 97% ee, with the high levels of enantioinduction



**Fig. 2** (a) Diverse biomolecules that contain glycerol. (b) Enantioselective acylation of glycerol by a peptide catalyst [49]. (c) Reactivity modulation in model carbohydrates [50]

resulting from an initial acylation followed by a secondary kinetic resolution [49, 52].

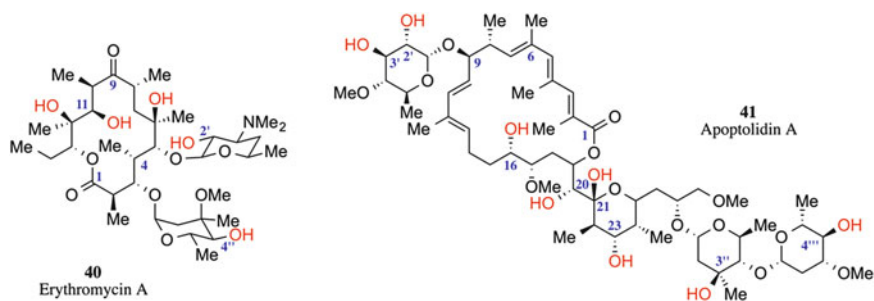
Our results at this stage suggested an opportunity to attempt to contribute to the problem of site-selective catalysts in additional substrates with ever more sites of potential functionalization that are not enantiotopic. Thus, our efforts in site-selective catalysis seemed poised to enter a new phase. We chose to explore selective acylation in simple carbohydrates for this initial challenge (Kawabata and colleagues have used pyrrolidino-pyridine-based catalysts to great effect in the asymmetric and site-selective acylation of alcohols and carbohydrates. Select examples of this work can be found in [53–56]; see also [57–60]). Our initial study addressed two different sugars (Fig. 2c) exhibiting two or four free hydroxyl groups, and led to the discovery of a number of catalysts that, in the case of the simpler sugar, enhanced the intrinsic reactivity preferences to Pmh-catalyzed acylation and in the case of the more complex sugar, led to a significant alteration of the product distribution [50] (Fig. 2c). The results of this study, along with important developments from other labs [53–64], including the N-heterocycle-catalyzed polyol silylation chemistry of Hoveyda, Snapper, Tan, and others [63, 64], helped to solidify site-selective polyol modification as a field with some momentum.

The above studies established (1) that broad peptide sequence space can furnish catalysts that are effective across both a wide array of substrates and for several chemical transformations and (2) that nucleophilic peptide catalysis was effective at modulating barriers to reaction in the context of enantioselective reactions and site-selective reactions such that inherent preferences could be enhanced, e.g., inositols (Fig. 2c), or inverted (Fig. 2c) in a catalyst-controlled manner. At this time it became clear that the stage was set to explore beyond model systems and to begin treating large, complex natural products as substrates themselves.

#### **4 Natural Products as Substrates: Studies of the Relative Reactivity and Remote Functionalization of the Hydroxyl Groups of Erythromycin A and Apoptolidin A**

As we sought to increase the complexity of the substrates upon which the peptide-based catalysts might operate, we were drawn to the polyketide family of natural products [65–70]. Synthetic chemists are attracted to the challenge of constructing these complex architectures, and also providing access to molecules for biological study and evaluation [71–73]. Biochemists have, in the same spirit, learned much about nature's evolved machinery for constructing such molecules [74–78].

For our purposes, we were drawn to erythromycin A (**40**) and the antitumor compound apoptolidin A (**41**) (Fig. 3), as each contains varied arrays of hydroxyl groups [79, 80]. These ubiquitous moieties are often assigned as playing conformational roles in the natural products (for example, see [81, 82]), being targets for enzymes involved in resistance mechanisms [83, 84], or, from the perspective of

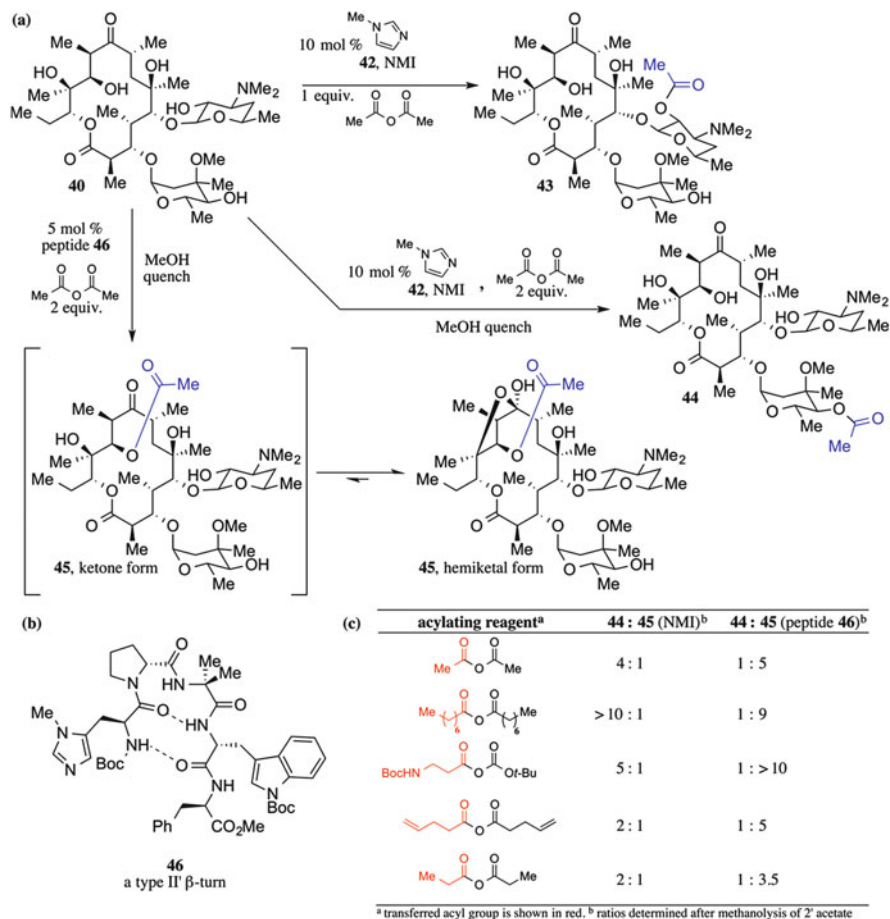


**Fig. 3** Structures of erythromycin A and apoptolidin A. Potentially reactive hydroxyls are shown in red

our research program, serving as handles for modification and interrogation of the important structural and biologically relevant features of a given natural product [85, 86]. As such, we initially targeted erythromycin A as a substrate for site-selective, peptide-catalyzed acyl transfer reactions [87, 88].

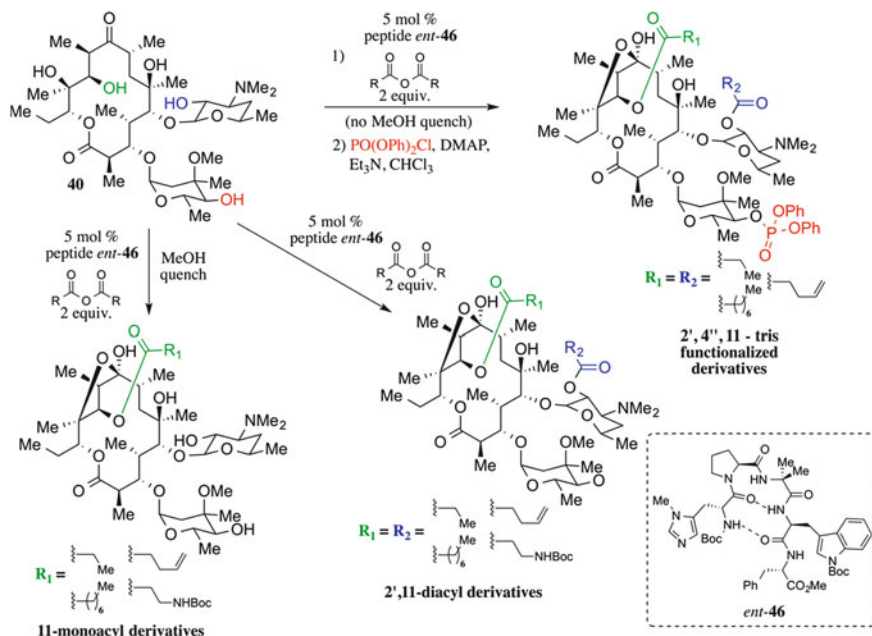
Our investigation began with a study of the innate reactivity preferences of the hydroxyl groups under relevant reaction conditions. Prior studies from Abbott Laboratories had established that, in the presence of DMAP and acetic anhydride, the 2'-hydroxyl of the D-desosamine sugar (5-position of the macrolide) was the most reactive, followed by the 4''-hydroxyl of the L-cladinose sugar (3-position of the macrolide), followed by the 11-position hydroxyl of the macrolide itself [89, 90]. We found these trends to be analogous under reaction conditions in which *N*-methylimidazole (NMI, **42**) served as the catalyst analog of the  $\pi$ -methyl histidine residue (Pmh) in the peptide catalysts (Fig. 4a). The 2'-hydroxyl is sufficiently reactive that it is acylated in the absence of NMI; we thus expected it to persist as an acylated species under most conditions. This acetate group (shown as a monoacetate in **43**), however, is readily removed following reaction by treatment with methanol. Under these conditions, reflective of the innate hydroxyl reactivity of erythromycin A (**40**), it was found that the other two reactive hydroxyls are acylated in approximately a 4:1 ratio of 4'':11 (monoacetates **44** and **45**, respectively). The tertiary alcohols of **40** do not react appreciably under NMI-catalyzed conditions.

With conditions established to determine the ratio of **44**:**45** acylation, 137 Pmh-containing peptides were screened as catalysts from the libraries the group had developed for group transfer reactions. Several catalysts, including those hypothesized to form a  $\beta$ -turn [91–93 and references therein], exhibited the capacity to reverse the intrinsic selectivity exhibited by the substrate in comparison to when NMI was the catalyst. When peptide **46** was employed, the preference of **40** for acylation at the 4'' over the 11-hydroxyl was inverted from approximately 4:1 **44**:**45** (NMI-catalyzed) to 1:5 **44**:**45** (**46**-catalyzed). The 11-hydroxyl of **40** has been implicated in a macrolide-stabilizing hydrogen bond with the C9 carbonyl [94, 95]. The structure of **45** supports this hypothesis as it was observed to exist not as the C9 ketone, but primarily as transannular hemiketal **47**, the structure of which



**Fig. 4** (a) Reactivity profiling of the hydroxyl groups of erythromycin under NMI-catalyzed conditions. (b) Hit peptide **46**. (c) 4'':11-Acylation ratios, following 2'-acetate methanolysis, for different acylating reagents under NMI and peptide-catalyzed conditions [87]. Note: all reactions were run at a concentration of 0.1 M **40** in  $\text{CHCl}_3$  solvent with 5 equiv.  $\text{Et}_3\text{N}$  at 25 °C for 24–72 h [87]

was assigned in analogy to the assignments of Everett et al. for related compounds [94, 95]. Thus, the discovery of site-selective peptide catalyst **46** allowed not just for synthetic access to otherwise cumbersome analogues of **40**, but also resulted in the support of a structural hypothesis regarding macrolide conformation. The site-selectivity of peptide **46** also depended upon the structure of the acylating reagent, with larger groups leading to higher selectivity. Smaller alkyl chains led to selectivities similar to those observed with acetic anhydride (Fig. 4c). In all cases, non-peptide-catalyzed reactions allowed for ready access to 4''-monoacylated derivatives of **40** following methanolysis, whereas peptide-catalyzed reactions led to

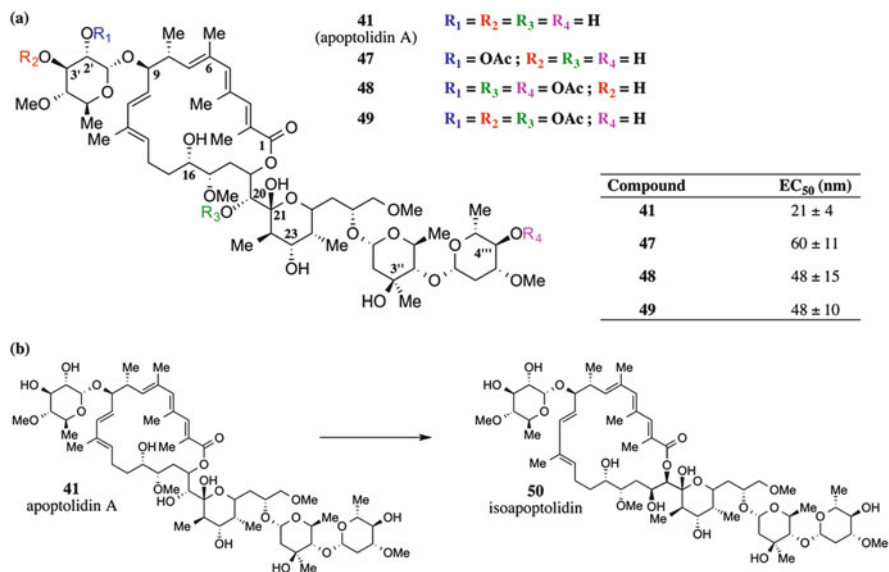


**Scheme 6** Polyfunctionalization of erythromycin A (**40**) [88]

heretofore inaccessible 11-monoacylated derivatives, again following autocatalytic solvolysis of the 2'-acetate (or equivalent group).

We then exploited catalyst **46** for the synthesis of new derivatives of **40** that contained multiple different groups. In the course of these studies, it was discovered that the enantiomer of peptide **46**, *ent-46*, gave even higher catalyst-controlled selectivity for acylation of the 11-hydroxyl over the inherently preferred 4''-hydroxyl [88]. As depicted in Scheme 6, further optimized reactions, according to three different sequences, afforded four 11-monoacyl derivatives of **40**, four 2',11-diacyl derivatives of **40**, and three tris-functionalized derivatives of **40** in which the 4'' hydroxyl was phosphorylated following *ent-46*-catalyzed acylation of the 2'- and 11-hydroxyls. Additionally (not shown), using a methanol quench and additional acylation steps provided access to one unsymmetrical 2',11-diacyl derivative and one tris functionalized compound in which the 2' were different as well (cf. [88]). In total, 14 synthetic analogues, all accessed *via* selective peptide-catalyzed reactions on unprotected erythromycin A, were tested for antibiotic activity against challenging strains of *Staphylococcus* and *Enterococcus*. None provided improved activity (MIC) over **40**. However, the structure activity relationships gleaned from these studies were consistent with some earlier hypotheses [96].

In a related study, which also utilized peptide *ent-46*, we were able to access three hitherto untested acetyl derivatives, **47–49**, of the highly potent and tumor-selective cytotoxic natural product apoptolidin A (**41**) [97]. Triacetates **48** and **49** were particularly significant, as a known problematic structural rearrangement of

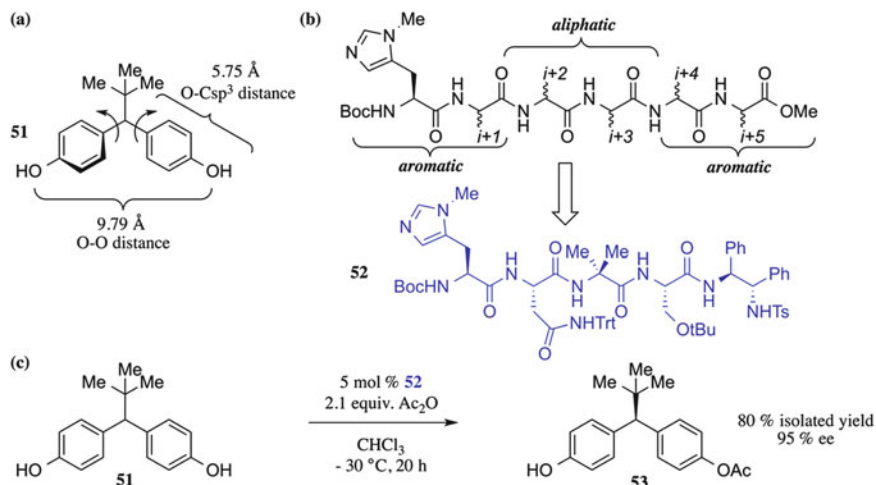


**Fig. 5** (a) Apoptolidin A (**41**) derivatives accessed by site-selective acylation reactions using peptide *ent-46* [97]. (b) Rearrangement of **41** to isoapoptolidin (**50**) [98, 99]

**41** to **50** (isoapoptolidin) that proceeds *via* ring expansion of the macrolide onto the 20-hydroxyl was inaccessible to these derivatives [98, 99]; NMR analysis confirmed that this rearrangement did not occur for **47** as well. The activities of **47–49** were compared to those of **41** in a growth inhibition assay using H292 cells and were found to be comparable (within threefold; inset table in Fig. 5a), suggesting that, as had been proposed earlier, certain modest changes to the array of seven unique hydroxyls on **41** can be made without strong deleterious effects [100].

## 5 A Connection Between Site-Selective Catalysis in Natural Products and Remote Asymmetric Induction

The site-selective catalytic reactions on the inositols and the natural products offered a basis for general musing about the scope and limitations of discovering peptide-based catalysts for targeting substrates possessing several hydroxyl groups that are in unusual stereochemical environments. Among those that seemed appropriate for exploration were those that exhibited the challenges of remote functionality or remote prostereogenic stereochemical elements [101–103]. Bis(phenol) **51** (Fig. 6a), a substrate for enzymatic desymmetrization en route to compounds of interest at Merck Research Laboratories, thus became a testing ground for our hypothesis that peptides could indeed catalyze asymmetric reactions with remotely localized functional groups or prostereogenic centers [104, 105]. Substrates such as



**Fig. 6** Remotely-directed desymmetrization of bis(phenol) **51** by peptide-catalyzed acylation [104, 105] (a) Relevant distances in the structure of bisphenol **51**. (b) General schematic of the library that produced peptide **52**. (c) Desymmetrization of **51** by **52** to yield monoacetate **53**

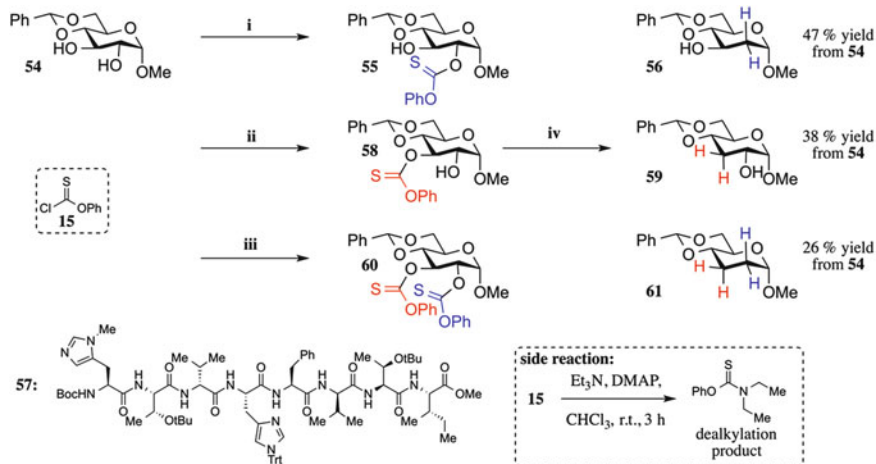
**51** also posed the question of whether or not remote directing functionality could play a role in developing a desymmetrization [106]. In the case of **51**, the enantiotopic hydroxyl groups of **51** are each 5.75 Å away from the molecule's only prochiral center. Additionally, the hydroxyls themselves are separated by almost 1 nm, which seemed to present a significant challenge for the development of a hydroxyl-directed reaction. Although enzymes can be proficient at a variety of reactions where remote sensing of functionality is required (see, for example, steroid biosynthesis and, in particular, the oxidation of steroids by cytochrome P450 enzymes [107–109]), a satisfactory enzymatic solution to the desymmetrization of **51** had not been reported at the time we initiated its study (see below) [104, 105].

We explored libraries of hexapeptides that all contained Pmh at the N-terminus (Fig. 6b); see [105] for detailed discussion of the library design and screening. Notably, peptide **52** catalyzed formation of monoacetate **53** in good yield and excellent enantioselectivity. It should be noted that the high conversion to monoacetate **53** and additional control experiments [104, 105] indicated that minimal secondary resolutions were operative in the ability of peptide **52** to effect a highly enantioselective, remotely-directed chemical reaction [52]; the high ee of **53** was the result of a single remote, catalyst-controlled transformation. Although a high-resolution mechanistic picture of how peptide **52** provides high selectivity remains elusive, we did observe that  $^{13}\text{C}$  resonance degeneracy of the phenolic aromatic carbons of **51** was broken when **51** and **52** were mixed in a 1:1 ratio. Thus, we suspect that peptide **52** is operative for the remote desymmetrization of **51** through formation of a discrete catalyst–substrate complex.

Through our studies of simple and complex substrates, of unnatural and natural origin, we were able to establish the versatility of peptide-based catalysts for a number of site-selective reactions. The next sections illustrate our efforts to generalize these observations to include a number of additional high-value transformations, and ever more complex molecular environments.

## 6 Development of New Peptide-Catalyzed Reactions to Address Additional Challenges in Chemical Selectivity

In the course of our efforts to synthesize PIP and inositol polyphosphate analogs, we utilized stoichiometric quantities of chlorothioformate **15** and then removed hydroxyl groups under standard conditions for the venerable Barton–McCombie deoxygenation reaction [110–112]; cf. Scheme 3 and associated references. We therefore became interested in the possibility that catalytic, site-selective delivery of the thiocarbonyl group might provide a powerful approach to the study of polyol structure–activity relationships. Thus, we wished to establish whether site-selective catalysts could provide access to oxygen atom-deleted analogs in a direct manner [113]. In early studies, we discovered that the catalytic thiocarbonylation was more complex than either phosphorylation or acylation with our approaches. First, the HCl byproduct required the addition of base, but common tertiary alkyl amine bases such as triethylamine underwent dealkylative thiocarbonylation in preference to thiocarbonylation of alcohol substrates (Scheme 7, inset). Thus, we employed 2 equiv. of the hindered base 1,2,2,6,6-pentamethylpiperidine (PEMP) to suppress this undesired reactivity. We also found that, even under these conditions, only a limited set of carbohydrate-derived alcohols were compatible (see [97] for additional details). With these observations in hand, we undertook screening of a sequence and structure-random library of Pmh-containing peptide catalysts for the selective 2- or 3-thiocarbonylation of methyl glucoside **54**. Interestingly, peptide **46**, discovered initially for the site-selective acylation of erythromycin A (**40**, [87]; see above), produced 2-thiocarbonate **55** in a 22:1 ratio relative to the 3-thiocarbonate product in 67% isolated yield. This selectivity was an enhancement of the inherent preferences of **54**, which favors 2-thiocarbonylation in a roughly 2:1 ratio. Standard Barton–McCombie radical deoxygenation yielded deoxyglucoside **56** in 46% yield from **54**. Peptide **57**, previously identified as an effective asymmetric acylation catalyst for small molecules, was found to invert the inherent reactivity preferences of the 2- and 3-hydroxyls of **54**, yielding 3-thiocarbonate **58** in 6.6:1 ratio over **55** in 53% isolated yield. This particular transformation required the addition of 15 mol% FeCl<sub>3</sub> to facilitate turnover [113]. Compound **58** was converted to 3-deoxyglucoside **59** under standard radical conditions in 39% overall isolated yield from **54**. We were also able to access 2,3-dideoxyglucoside **61** from bis(thiocarbonate) **60**, which was the overreaction product of the NMI-catalyzed thiocarbonylation of **54**. Unfortunately, we observed significant drop-off in

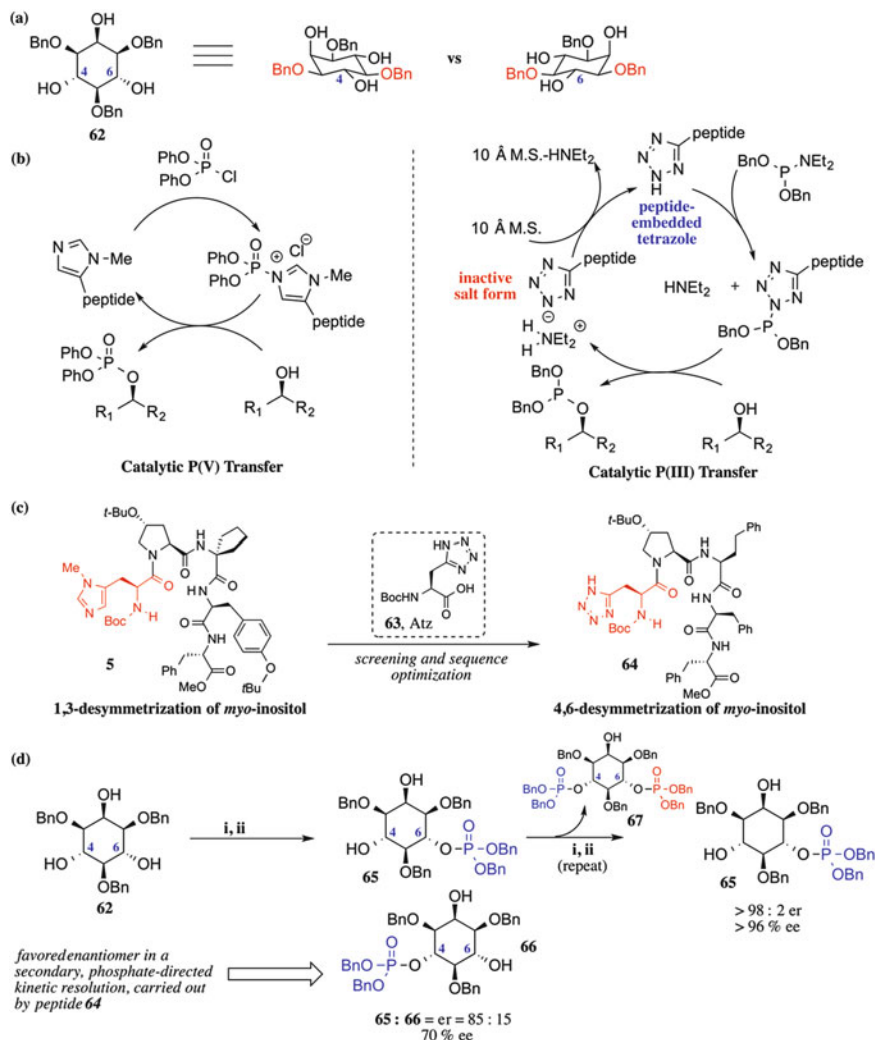


**Scheme 7** Preparation of deoxyglucoside derivatives mediated by peptide-catalyzed thiocarbonylation reactions. (i) 20 mol% peptide **46**, 2 equiv. PEMP, 1.5 equiv. **15**,  $-40\text{ }^{\circ}\text{C}$ , 15 h. 67% (ii) 20 mol% peptide **57**, 15 mol%  $\text{FeCl}_3$ , 2 equiv. PEMP, 1.5 equiv. **15**,  $-25\text{ }^{\circ}\text{C}$ , 5 h. 53% (iii) 20 mol% NMI (**42**), 2 equiv. PEMP, 1.5 equiv. **15**, r.t., 1 h. 40% (iv) 3 equiv.  $\text{Bu}_3\text{SnH}$ , 0.3 equiv. AIBN,  $\text{PhCH}_3$ , reflux, 2 h. Overall yields from **54** over both steps for each deoxysugar are depicted above [113]

selectivity utilizing these catalysts for substrates that were either more complex, such as sucrose, or for substrates which were only changed marginally from **54**, such as its  $\beta$ -anomer. Thus, although useful in some settings, additional approaches to catalytic, site-selective functionalization of polyols that set up deoxygenation are still required.

One additional approach to deoxygenation we have explored involves catalytic phosphoramidite transfer. Our studies along these lines began with the fundamental development of a different catalytic cycle for the site-selective transfer of P(III)-based reagents. We chose to return to the *myo*-inositol scaffold for this basic research, with a focus on the enantiotopic 4- and 6-hydroxyl groups of the substrate (**62**; Fig. 7). The similar steric environment created by the presence of only equatorial flanking groups to these positions renders their differentiation challenging [115].

Carruthers developed methods for the tetrazole-mediated transfer of P(III) compounds, specifically phosphoramidites, enabling the robust synthesis of nucleic acids in work that was truly revolutionary [116]. The key byproduct of the reaction, secondary amines, also deprotonate the key activating tetrazole, thus requiring excess tetrazole to drive the reaction to completion. Therefore, a catalytic cycle based upon a tetrazole-containing amino acid, tetrazolylalanine (Atz, **63**, Fig. 7) [114, 117] must then also include a means for scavenging the amine byproduct of the phosphoramidite transfer reaction. Based on literature precedents, we utilized 10- $\text{\AA}$  molecular sieves for this purpose, which also bore the advantage of rendering the reaction conditions anhydrous [118] (Fig. 7b). Inspired by the sequence of

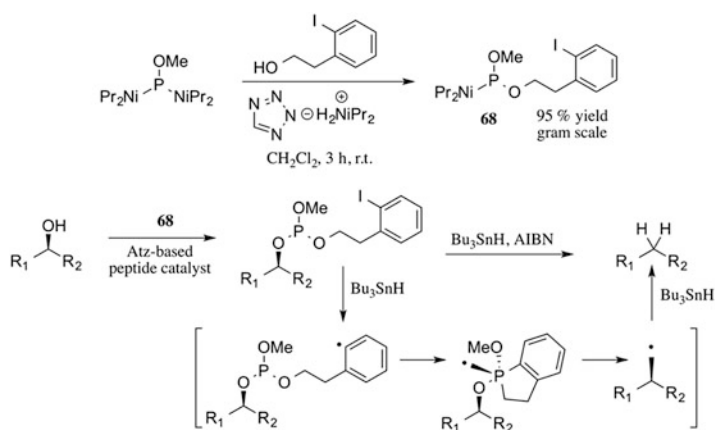


**Fig. 7** (a) Similar equatorially substituted environment about the 4- and 6-hydroxyls of *myo*-inositol derivative **62**. (b) P(III) transfer, catalyzed by a tetrazole sidechain and inspired from previous efforts using Pmh sidechains as nucleophilic catalysts for P(V) transfer among several other transformations. (c) Hit Atz-containing peptide **64**, derived from a library inspired by 1,3-desymmetrization catalyst **5**. (d) Enantioselective preparation of *myo*-inositol-6-phosphate precursor **65** by means of enantioselective phosphitylation followed by a phosphate-directed P(III) transfer that operates as a kinetic resolution ( $k_{rel}$  **65:66**  $\approx$  35). (i)  $\text{Et}_2\text{NP}(\text{OBn})_2$ , 5 mol% peptide **64**, 10 Å M.S.,  $\text{CHCl}_3$ , 4°C. (ii) 30% (aq.)  $\text{H}_2\text{O}_2$ , 0°C, 1 h. 71% yield for 1st pass to yield 85:15 er; 74% yield of **65** in second pass as kinetic resolution with peptide **64** [114]

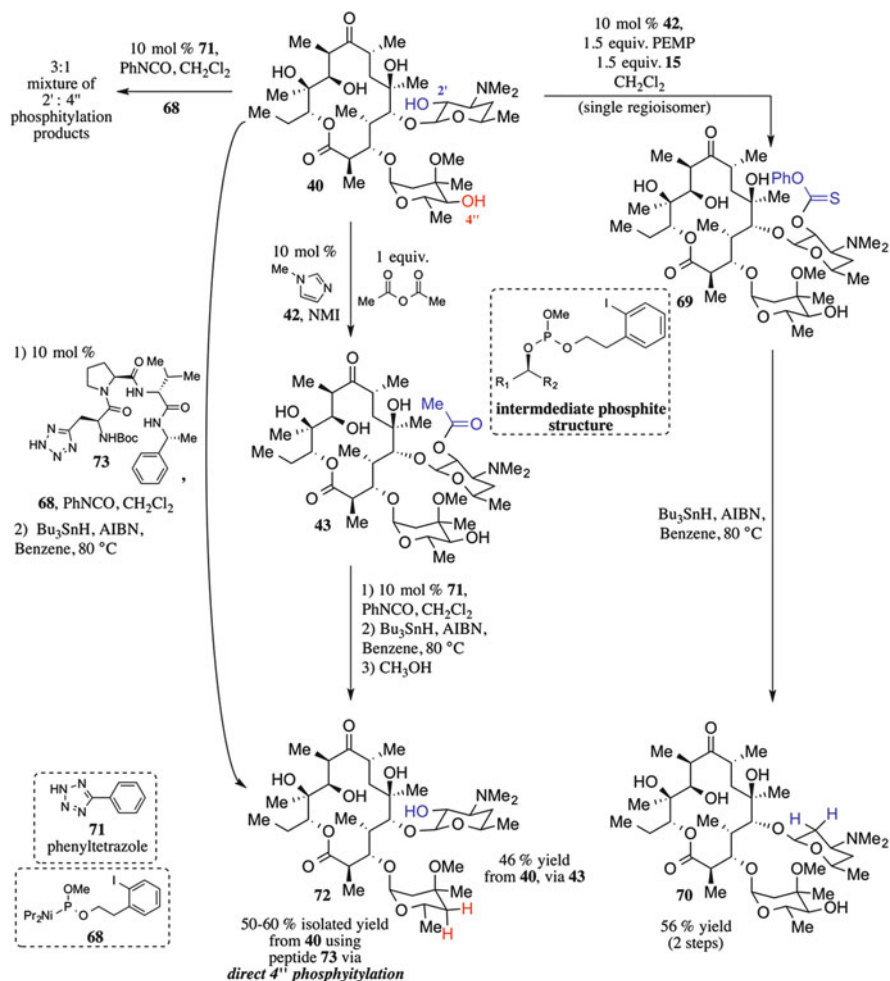
peptide **5**, which was utilized to desymmetrize the 1- and 3-hydroxyl positions of *myo*-inositol derivative **1** (see above) [21], we screened a focused library of peptides that employed Atz, **63**, at the N-terminus as the key catalytic residue for the desymmetrization of **62** via P(III) transfer (Fig. 7c). Hit peptide **64**, which has nearly identical backbone stereochemistry to **5** and differs only in the identity of two sidechains, yielded *myo*-inositol-6-phosphate derivative **65** in good yield (71%) and appreciable enantioselectivity (85:15 er, 70% ee). The minor enantiomer (**66**), which is the protected precursor of *myo*-inositol-4-phosphate, was found to be the faster reacting enantiomer in a kinetic resolution of mixtures of **65** and **66**, such that **65** could be obtained in outstanding enantiopurity by subjecting the oxidized product mixture of the first P(III) transfer to the same reaction sequence a second time (Fig. 7d). The key to the outstanding  $k_{rel}$ , approximately 35 for phosphitylation of **66** over **65** to meso compound **67**, was hypothesized to be interaction between peptide **64** and the Lewis basic phosphate oxygen of **65/66**; this was supported by a lower  $k_{rel}$  of  $\sim 8$  observed in the kinetic resolution of the corresponding phosphorothioate derivatives of **65** and **66** (see [114] for more details).

With these fundamental studies complete, we turned our attention to the adaptation of the method for a site-selective catalysis/deoxygenation sequence [119]. Koreeda and Zhang reported the use of iodoarene-functionalized phosphites as good substrates for deoxygenation [120]. We set out to adapt this work to an Atz-based peptide-based catalytic reaction. Phosphoramidite **68** (Scheme 8) was readily prepared, and found to behave in tetrazole-catalyzed reactions. Its derivatives, upon exposure to appropriate conditions, enabled deoxygenation of a number of alcohols in analogy to literature precedents; see [119] for details.

We were thus equipped with a new tool to explore selective deoxygenation of erythromycin A beyond the 2'-hydroxyl (Scheme 9). It should be noted that this particular effort in site-selective chemistry was preceded by necessary studies in



**Scheme 8** Preparation of a phosphoramidite **68** and mechanism for substrate deoxygenation following a P(III) transfer reaction [119, 120]

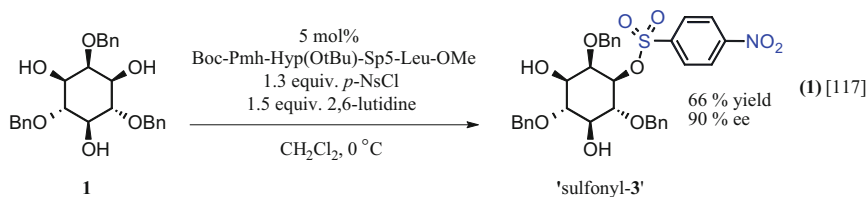


**Scheme 9** Site-selective deoxygenation of Erythromycin A (**40**) to analogs **70** and **72** via exploitation of innate reactivity of 2'-hydroxyl and the peptide catalyzed phosphitylation of the 4''-hydroxyl, respectively [119]

fundamental organic reaction development. Ultimately, both the Pmh-catalyzed thiocarbonylation (Scheme 7) and the Atz-catalyzed phosphitylation (Fig. 7) were employed in our efforts. Specifically, thiocarbonylation was found to enable reaction of the 2'-hydroxyl, to produce thiocarbonate **69**. Utilizing standard Barton–McCombie [110–112] radical conditions, **69** was converted to 2'-deoxyerythromycin, **70**, in 56% yield from the natural product itself (**40**). Notably, this catalytic route to **70** took advantage of the inherently high reactivity of the 2'-hydroxyl of erythromycin A. Thus, initially we sought to use a 2'-acetyl capping strategy applied in an earlier approach to 4''-deoxyerythromycin A (**72**).

Using standard NMI (**42**)-catalyzed acylation, 2'-acetyl erythromycin A was prepared and then subjected to 4''-selective phosphitylation with **68**, catalyzed by phenyltetrazole (**71**). Reduction and deacylation in methanol gave 4''-deoxy erythromycin A in 46% yield over four total transformations. We then explored whether, given the higher inherent reactivity of the 4''-hydroxyl to phosphitylation, a peptide-catalyzed P(III) transfer could direct reaction of **68** preferentially to the 4'' position, circumventing the 2'-hydroxyl altogether in the absence of any protecting groups. Screening of a small library of peptides led to discovery of **73**, which yielded a single  $^{31}\text{P}$ -observed product (as a mixture of P-epimers) identified as the 4''-phosphitylated derivative of **40**. Subsequent deoxygenation yielded **73** in 50–60% isolated yields in only two simple transformations from the parent erythromycin A. Auspiciously, these studies revealed that a peptide-based tetrazole could lead to an alternate product in comparison to that delivered by catalytic phenyltetrazole. Thus, this observation provided another example of selectivity reversal made possible by a peptide-based catalyst.

We have described several experiences in the development of group transfer reactions including acylation [27, 28, 49, 50, 87, 88, 97, 104, 105], phosphorylation [20–22, 33–37], thiocarbonylation [113, 119], sulfonylation [51], and phosphitylation [114, 119]. In the course of our studies we also developed sulfonylation reactions based on the desymmetrization of **1** (**1**) [121]. These reactions proceeded with excellent enantioselectivity to yield the sulfonyl analogues of phosphates **3** and **6** in a catalyst-dependent manner. Sulfonates may bring additional opportunities for site-selective chemistry in the future as they provide entry to cross-coupling, elimination, and substitution chemistry.



## 7 Peptide-Catalyzed Diversification of Glycopeptide Antibiotics

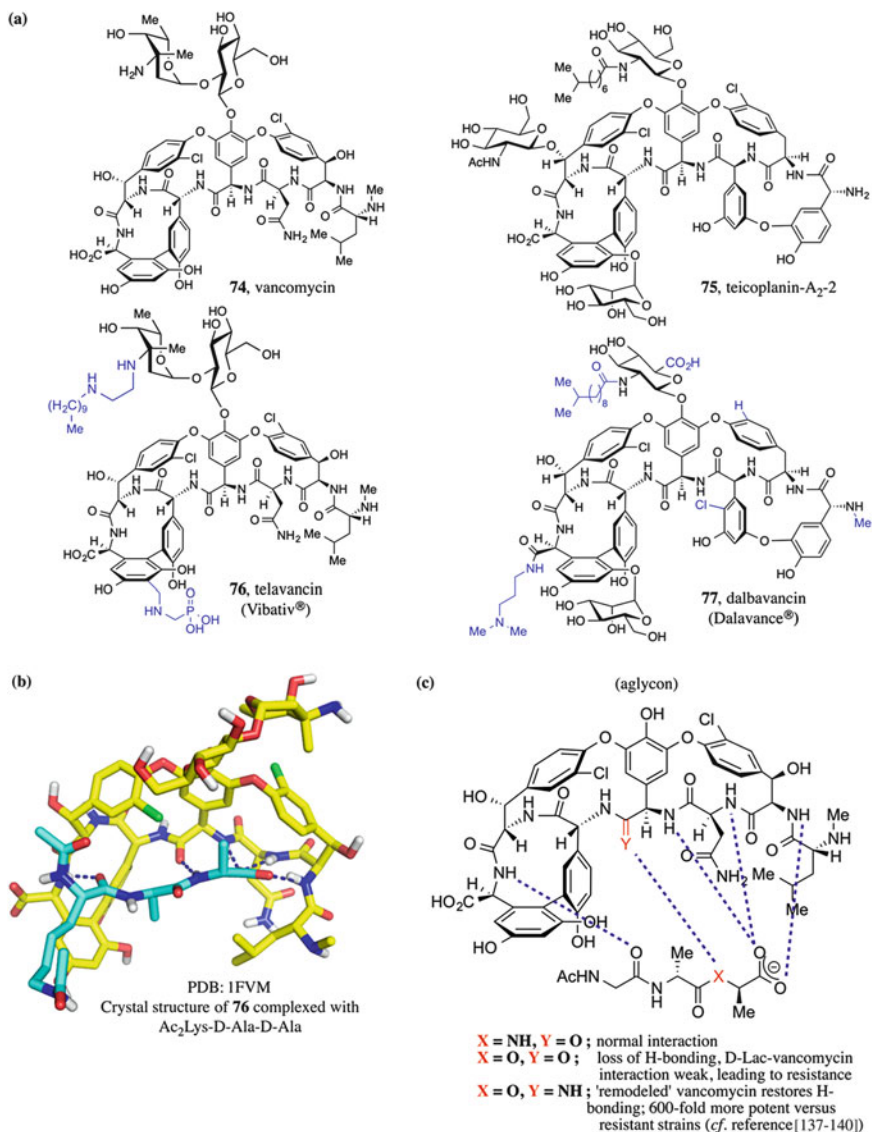
Based on these experiences with a variety of catalyst-dependent, site-selective reactions, we chose to investigate site-selective functionalization of the glycopeptide antibiotics vancomycin (**74**) and the teicoplanins (**75**, the  $A_2$ -2 congener). These decisions were made for primarily chemical reasons – we were inspired by the high level of chemical complexity exhibited by these molecules. However, we also wished to create the opportunity to contribute new, potentially improved analogs of these so-called “antibiotics of last resort” to the field of infectious disease therapy [122–125]. The pursuit of analogs of these storied antibiotics is

an extensive field in and of itself [126–131]. Highlights include the semi-synthetic drug analogs such as telavancin (**76**) and dalbavancin (**77**) [132, 133].

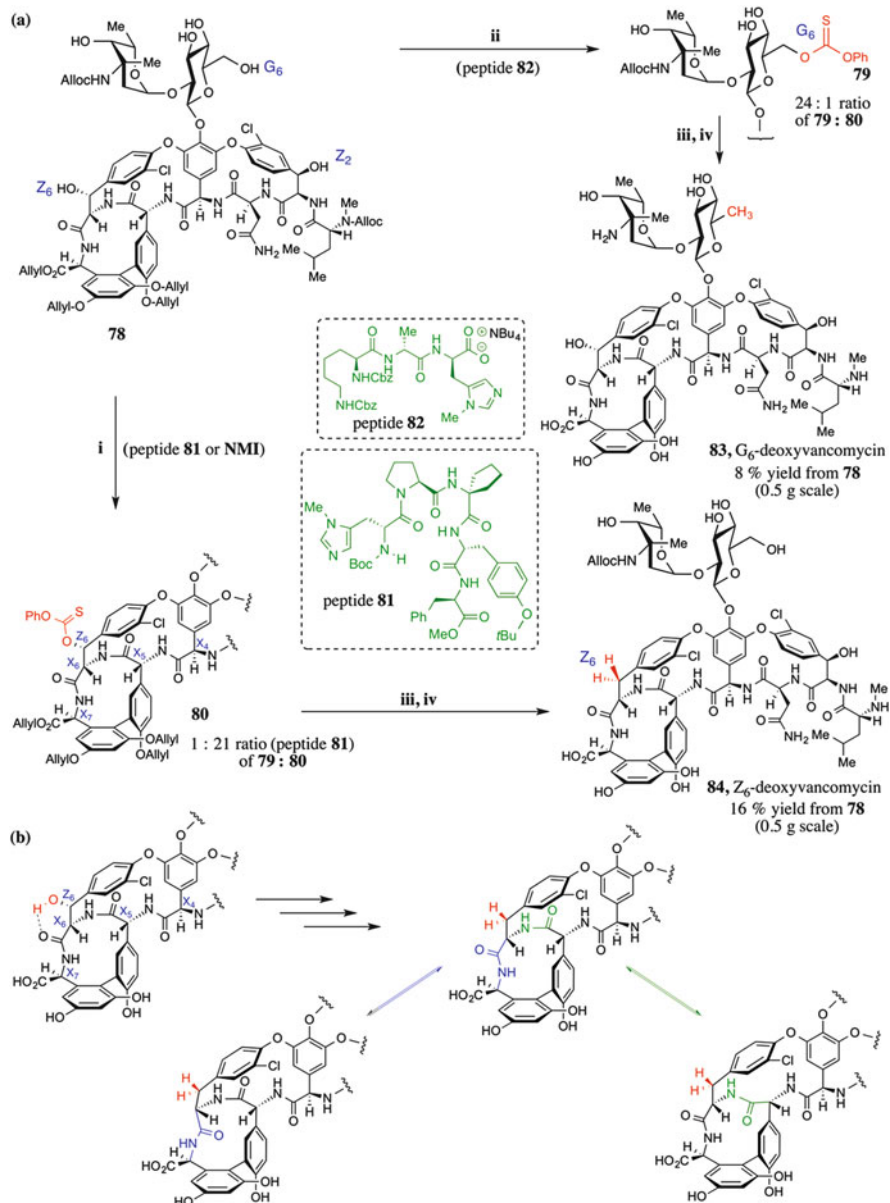
Glycopeptide antibiotics act by disrupting the elaboration of peptidic cross-links that are key to the integrity of the Gram-positive bacterial cell wall [134–136]. This is accomplished *via* binding to a nascent extracellular peptide chain with the sequence (N to C) Lys-D-Ala-D-Ala. The interaction is characterized by the formation of five key hydrogen bonds (Fig. 8b,c). Resistant strains have evolved a mutation such that the D-Ala-D-Ala sequence is mutated to D-Ala-D-Lac (lactic acid), replacing an amide linkage with an ester and eliminating a key hydrogen bond (Fig. 8c, shown for aglycon of **74**). This renders the binding of glycopeptides to the cell wall peptide ineffective [141–143]. Boger and colleagues have provided a remarkable solution to this problem [137–140]. The mutation of the amide oxygen of the central residue of vancomycin instead to an amidine NH restores activity to the aglycon of **74** 600-fold over the parent amide form; the amidine NH restores a key hydrogen bond between the cell wall peptide and the glycopeptide, interacting with the ester oxygen [137–140] (Fig. 8c). Additionally, the amide-amidine mutation reduces an energetically disfavorable electron lone pair repulsion between the D-Ala-D-Lac and the most proximal amide oxygen in the vancomycin binding site. This promising analogue, accessed *via* total synthesis, notably restores much biological activity *via* a single atom change to vancomycin just as the D-Ala to D-Lac mutation was effected by a single atom change to the cell wall peptide. These studies also buttressed our ambition for the study of catalyst-dependent, minimal alterations to the scaffold that might provide similarly dramatic effects. More modestly, if successful, catalysts might expand our understanding of the structure activity relationships within vancomycin.

Single groups or arrays of hydroxyls have been found to be important to drug specificity, potency, and bioavailability; they have also been implicated in the propagation of toxic side effects [144–147] and may be involved in drug resistance mechanisms [83, 84]. Thus, we set out to continue our studies of site-selective deoxygenation with vancomycin. To document the inherent reactivity to thiocarbonylation, we found that NMI-catalyzed reaction of known protected vancomycin derivative **78** [148, 149] yielded a 1:5 mixture of two thiocarbonylated species, **79** and **80**, respectively [150]. Phase-sensitive HSQC led to the assignment of these as belonging to the G<sub>6</sub> and Z<sub>6</sub> thiocarbonylation products, respectively. With this ratio established, we commenced an initial peptide screen, using legacy sequences from our long-standing efforts in selective hydroxyl functionalization. Peptide **81** was found to provide an enhancement of the inherent reactivity of the G<sub>6</sub> and Z<sub>6</sub> hydroxyl groups, especially upon scale-up to a 1:21 ratio of **79**:**80**.

The next step was to search for peptides that would reverse the intrinsic reactivity preferences of the substrate. For this goal, we attempted a strategy of mimicking with a catalyst the intrinsic, well-known affinity of vancomycin for the D-Ala-D-Ala moiety that is a signature of its biological function. Peptide **82** proved effective in this manner, providing a 24:1 ratio of **79** to **80**. Peptide **82** may indeed bind in a manner very similar to the Lys-D-Ala-D-Ala sequence, directing the catalytic amino acid sidechain into the vicinity of the G<sub>6</sub> hydroxyl of **78**, and



**Fig. 8** (a) Chemical structures of vancomycin, teicoplanin, and semisynthetic analogs; differences from parent structures highlighted in blue. (b) Crystal structure of vancomycin (yellow) complexed with substrate analog Ac<sub>2</sub>Lys-D-Ala-D-Ala (cyan; PDB 1FVM). (c) Graphical summary of Boger's key amidine analog of vancomycin aglycon, highlighting the key H-bonding interactions between glycopeptides and, as shown, an analog of the target cell wall peptide [137–140]

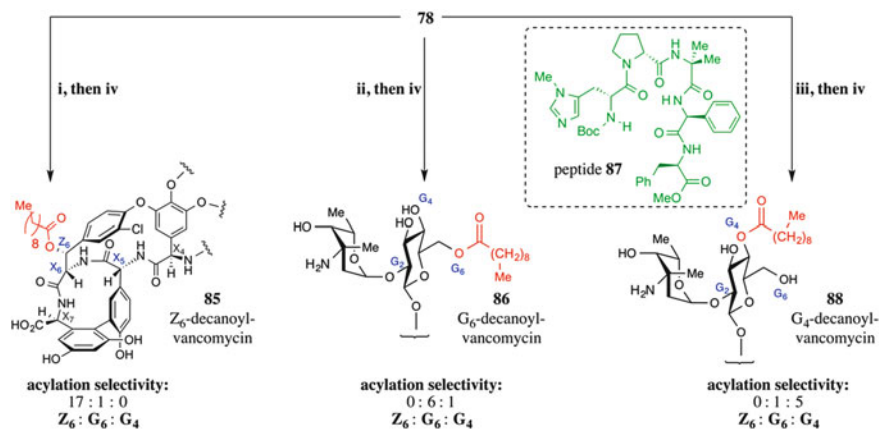


**Scheme 10** (a) Site-selective thiocarbonylation and deoxygenation of vancomycin. (i) 1.5 equiv. **15**, 2.0 equiv. PEMP, 20 mol% peptide **81**, THF/CH<sub>2</sub>Cl<sub>2</sub> (1:3, 10 μM **77**), r.t., 24 h. (ii) 1.5 equiv. **15**, 2.0 equiv. PEMP, 20 mol% peptide **82**, THF/CH<sub>2</sub>Cl<sub>2</sub> (1:3, 10 μM **77**), r.t., 24 h (iii) AIBN, HSnBu<sub>3</sub>, dioxane/PhCH<sub>3</sub>, 70–80 °C, 2 h. (iv) PdCl<sub>2</sub>(PPh<sub>4</sub>)<sub>2</sub>, PhSiH<sub>3</sub>, dioxane/AcOH, r.t., 1 h. (b) Possible conformational movements in Z<sub>6</sub>-deoxyvancomycin [150]

various experiments supported this notion [150]. In contrast, the mode of action of catalyst **81**, which enhances the intrinsic reactivity preferences, remains unknown.

Standard Barton–McCombie deoxygenation of **79** and **80** to **83** and **84** (respectively) led to further interesting observations. Z<sub>6</sub>-deoxyvancomycin **84** exhibited conformational heterogeneity. We speculate that this is produced by loss of a hydrogen bond between the Z<sub>6</sub> hydroxyl with the C<sub>6</sub> amide carbonyl in the native structure. The absence of such an interaction could lead to various forms of medium ring conformational isomerism (Scheme 10b). In terms of biological activity, G<sub>6</sub>-deoxyvancomycin **83** exhibits similar activity with respect to native vancomycin; conformationally mobile **84** is somewhat less effective against certain Gram-positive bacteria. Although this exercise did not yield a more potent analogue of vancomycin vs. resistant strains, our studies of site-selective catalysis unveiled non-obvious features of the antibiotic structure activity relationships.

Lipidation of glycopeptides has been associated with increases in antibiotic activity, as evidenced by the increased activity of the teicoplanins relative to vancomycin [122–125]. We therefore sought to test our catalysts for the site-selective lipidation of vancomycin [151] (Scheme 11). Screening of select legacy sequences from acylation and other group transfer reactions studied by our group led to promising results. Both peptides **81** and **82**, uncovered for functionalization of **78** *via* thiocarbonylation, showed the same site-selectivity trends for acylation that had been observed for thiocarbonylation, producing decanoyl vancomycin derivatives **85** and **86** in 24% and 38% yield, respectively (acylation and global deprotection steps included in yield calculation). Moreover, peptide **87** [152] provided new selectivity capability, targeting the G<sub>4</sub> hydroxyl position over the



**Scheme 11** Site-selective acylation of vancomycin. (i) 20 mol% peptide **81**, PEMP (2 equiv.), decanoic anhydride (2 equiv.), CH<sub>2</sub>Cl<sub>2</sub>/THF (3:1), r.t., 24 h. (ii) 20 mol% peptide **82**, PEMP (2 equiv.), decanoic anhydride (2 equiv.), CH<sub>2</sub>Cl<sub>2</sub>/THF (3:1), r.t., 24 h. (iii) 20 mol% peptide **87**, PEMP (2 equiv.), decanoic anhydride (2 equiv.), CH<sub>2</sub>Cl<sub>2</sub>/THF (3:1), r.t., 24 h. (iv) PdCl<sub>2</sub>(PPh<sub>4</sub>)<sub>2</sub> (1 equiv.), PhSiH<sub>3</sub> (45 equiv.), dioxane/AcOH (4:1), r.t., 3 h [151]

Z<sub>6</sub> and G<sub>6</sub> positions. Deprotection of this intermediate yielded **88** in 24% yield from protected vancomycin (**78**). All three decanoyl derivatives were then tested in growth inhibition assays against resistant strains and **85**, **86**, and **88** all showed excellent activity against MRSA strains and select strains of vancomycin-resistant *Enterococcus*. However, as with vancomycin itself, activity was reduced against the Van A strain. Although these results were interesting, it is clear that these lipidation steps essentially render the vancomycin analogs “teicoplanin-like” in their function, thus making all three highlighted derivatives, despite their increase potency, subject to the same resistance mechanisms that plague related compounds [122–125, 141].

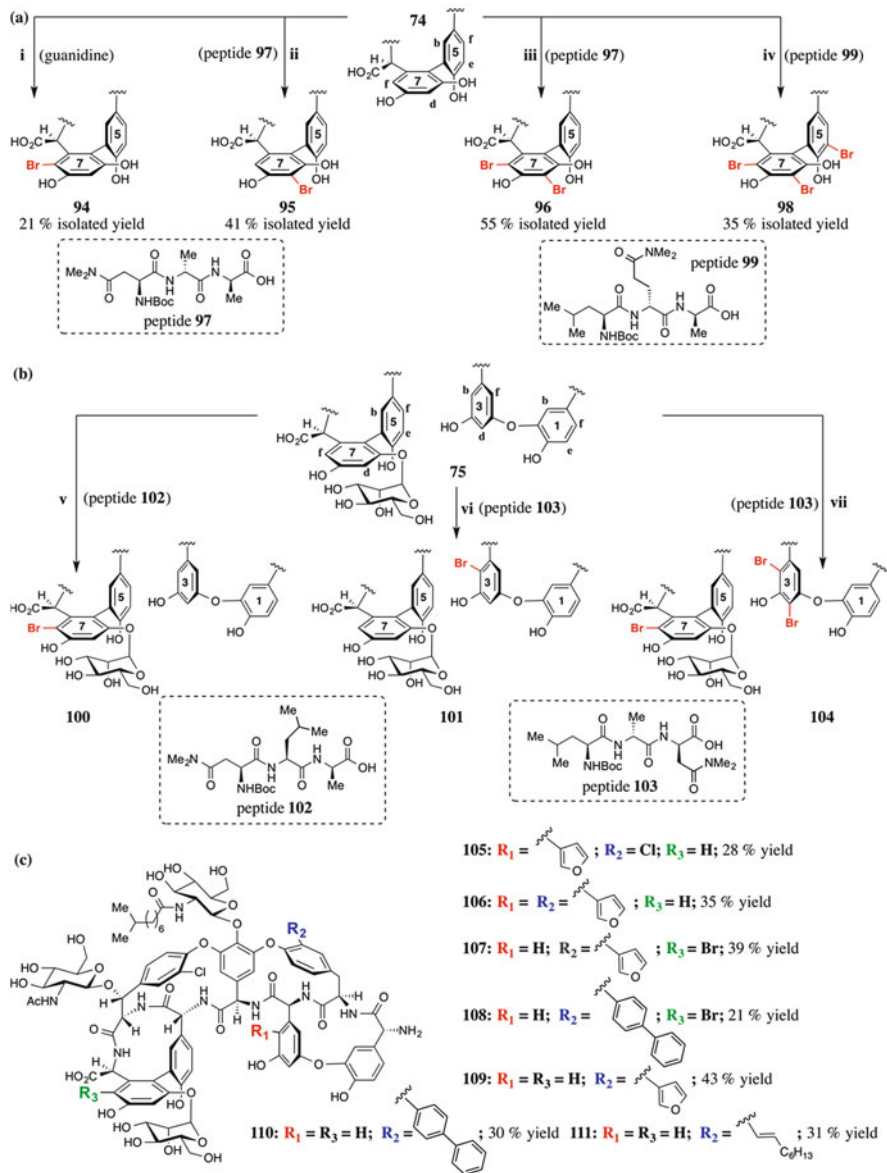
Teicoplanin-A<sub>2</sub>-2 (**75**) is a lipidated relative of vancomycin (**74**). The lipid chain of its topmost glucosamine sugar is believed to enhance its potency by helping the molecule embed itself in the cell membrane, near the location of bacterial cell wall biosynthesis [134–136]. Other mechanisms, independent of D-Ala-D-Ala binding, have also been invoked as potentially operative with the teicoplanins, which are more amphiphilic relative to vancomycin [134–136]. The phosphorylated and lipidated derivative of vancomycin, telavancin (**76**), has shown improved pharmacokinetics over its parent **74** [132, 133]. We wondered whether we could extend the insights gained in our studies of vancomycin to target the site-selective functionalization of individual hydroxyl groups of teicoplanin. We began this work with peptide-catalyzed phosphorylation [153, 154]. In an initial step, to enable solubility in organic solvents, protected teicoplanin-A<sub>2</sub>-2, **89**, was prepared in two steps in 45% overall yield (Fig. 9a). Our initial goal was to see whether catalysis might enable selective functionalization of sites on each of the three sugars on the structure – coded red for the top, green for the left, and blue for the bottom. The primary hydroxyl group of each is separated by 17.7, 11.6, and 16.5 Å, based upon a known crystal structure [155] (Fig. 9b). NMI-catalyzed phosphorylation (not shown) revealed that, indeed, the three targeted hydroxyls were the most reactive under these conditions, with the leftmost (green sugar; *N*-acetylglucosamine) being somewhat less reactive than the primary hydroxyls of the top (red) and bottom (blue) sugars (glucosamine and mannose, respectively), although other products were also detected. We then evaluated peptide-based catalysts (Fig. 9c). First, targeting the top sugar, we found that D-Ala-D-Ala-based peptide **82**, selective for the site-selective thiocarbonylation and acylation of the G<sub>6</sub> primary hydroxyl of vancomycin (see above), catalyzed the analogous site-selective phosphorylation of the primary hydroxyl of the top (red) sugar in **89**. The reaction allowed for isolation of diphenylphosphate **90** in 42% isolated yield. Next, the bottom (blue) mannose unit of **89** was targeted by screening a library of 15 legacy catalysts. Intriguingly, peptide **2**, initially discovered in our efforts toward the phosphorylation of *myo*-inositol [20], provided the best selectivity, and allowed for the isolation of diphenylphosphate **91** in 23% yield. Surprisingly, it was discovered that tripeptide catalysts (not shown) based on D-Ala-D-Ala that attempted to add catalytic sidechains to the internal D-Ala residue (as opposed to peptide **81**, which placed the sidechain at the C-terminal site) did not catalyze selective phosphorylation.



The C-terminal residues of **46** both possess D stereochemistry, and stimulated the design of peptide **93**, which retains a turn-promoting moiety, and replaces the C-terminal residues with the D-Ala-D-Ala motif. This new catalyst allowed for the efficient conversion of **89** to diphenylphosphate **92** in 41% isolated yield. Following deprotection of **90–92**, each phosphorylated analog showed attenuated activity toward most of the tested in antibacterial assays, providing some SAR information for the teicoplanin hydroxyl array [153, 154].

To investigate the mechanism of action for peptide **93** more closely, we sought a crystal structure of the catalyst–substrate complex. Although this effort proved challenging, we were able to obtain insight through achievement of a structure of a complex of native teicoplanin bound to the peptide-catalyst sequence, albeit embedded in a carrier protein context. Inspired by the strategy of Loll [157, 158], we synthesized a peptide **93**-T4-lysozyme conjugate *via* expressed protein ligation [159, 160]. After significant effort to optimize the carrier protein identity, the linking sequence between **93** and the carrier, and the crystallization conditions, the structure was successfully solved to 2.3 Å (PDB: 4PKO). As shown in Fig. 9d, e, the key catalytic Pmh sidechain is situated proximally to the leftmost (green) sugar, upon which it carries out selective phosphorylation.

In looking at vancomycin and teicoplanin, the hydroxyls are but one choice for functionalization reactions. Each natural product also possesses electron-rich arenes, which may be platforms for electrophilic aromatic substitution reactions. In parallel studies of enantioselective and atropisomer-selective bromination reactions [161–164], we were gaining experience with catalyst-controlled brominations, and we wondered whether these might be extended to site-selective reactions. We speculated that an appropriately positioned Lewis base, such as a dimethyl amide unit, could assist in the delivery of electrophilic bromine [165]. Thus, we carried out a reactivity profiling of vancomycin (**74**) toward electrophilic bromination in methanol solvent and found that three products were favored: the 7f and 7d monobromides (**94** and **95**, respectively), and the 7d,f dibromide (**96**), all resulting from halogenation of resorcinol ring 7 (Fig. 10a) [166]. Evaluation of peptides that contained dimethyl amide units as part of their sidechains, as well as a variety of other additives such as guanidine [168], revealed that peptide **97** could promote the formation of 7d-bromide **95** in 41% yield (or 7d, f-dibromide **96** in 55% yield). The location of the dimethyl amide unit of **97** when bound to **74** is hypothesized to be proximal to the resorcinol, perhaps leading to this reactivity. The 7f bromide **94** was not favored by peptide catalysis, but could be observed as the major product in the presence of guanidine, allowing for isolation in 21% yield. The 5e position, although ordinarily quite unreactive relative to the resorcinol, was also found to be brominated along with the 7f and 7d positions during the initial reactivity profiling, yielding tribromide **98**. Transposition of the dimethyl amide unit of a peptide catalyst, as with **99**, to the central portion of the sequence allowed for the selective formation of **98** in 35% isolated yield. The reason for this reactivity is unclear, and many mechanistic questions remain in this work overall. For example, high catalyst loadings of peptides are required for the

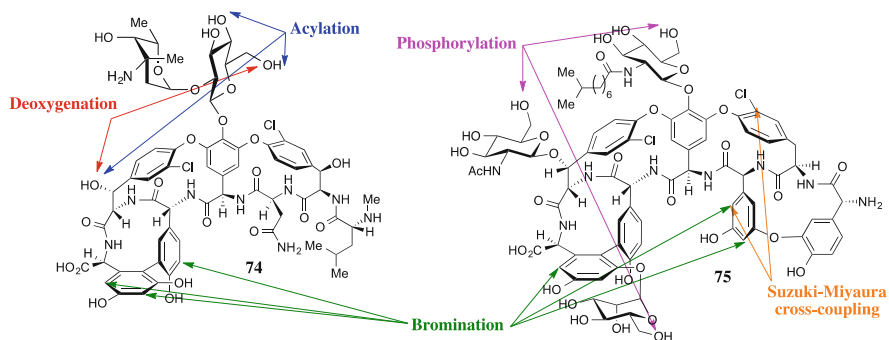


**Fig. 10** (a) Bromination of **74**. (i) 18 equiv. guanidine hydrochloride, 4 equiv. *N*-bromophthalimide (NBP), MeOH, 1 h. (ii) 1 equiv. peptide **97**, 2 equiv. NBP, H<sub>2</sub>O: MeOH (5:1), r.t., 1.5 h. (iii) 1 equiv. peptide **97**, 3 equiv. NBP, H<sub>2</sub>O:MeOH (5:1), r.t., 1.5 h. (iv) 1 equiv. peptide **99**, 4 equiv. NBP, H<sub>2</sub>O:MeOH (5:1), r.t., 2 h. (b) Bromination of **75**. (v) 1 equiv. peptide **102**, 1.1 equiv. NBP, H<sub>2</sub>O:MeOH (1:1), r.t., 1.5 h. (vi) 1 equiv. peptide **103**, 1.1 equiv. NBP, H<sub>2</sub>O:MeOH (1:1), r.t., 1.5 h. (vii) 1 equiv. peptide **103**, 3.3 equiv. NBP, H<sub>2</sub>O: MeOH (1:1), r.t., 0.5 h. (c) Cross-coupled analogs of **75** [166, 167]

best results in these reactions, raising questions about turnover and the balance between peptide binding and catalysis. These issues remain under study in our laboratory.

The analogous experiments were undertaken with teicoplanin A<sub>2</sub>-2 (Fig. 10b) [167]. We were attracted to **75** because of the additional positions available for electrophilic aromatic substitution as a result of the additional aryl rings. Peptide-based promoters yielded the selective formation of several brominated glycopeptides derived from teicoplanin: the 7f and 3b monobromides (**100** and **101**, respectively), favored by peptides **102** and **103**, respectively, and the tribromide **104**, which was formed in a conditions-dependent manner using peptide **103**; the dibromide resulting from both 7f and 3b bromination (not shown) was also isolated as a potential analog. With these halogenated glycopeptides now in hand (in addition to the parent compounds, which possess chloride substituents), we examined further functionalization *via* Suzuki–Miyaura cross-coupling reactions. Conditions were found employing high catalyst loadings and water soluble SPhos phosphine ligand [169] that allowed the preparation of seven novel analogs (**105**–**111**) of teicoplanin A<sub>2</sub>-2, summarized in Fig. 10c (see [167] for further details). Evaluation in biological assays revealed that a number of compounds possessed similar activity to teicoplanin itself, although a select few that were functionalized at the 2-ring *via* cross-coupling showed enhanced activity against various resistant strains of bacteria.

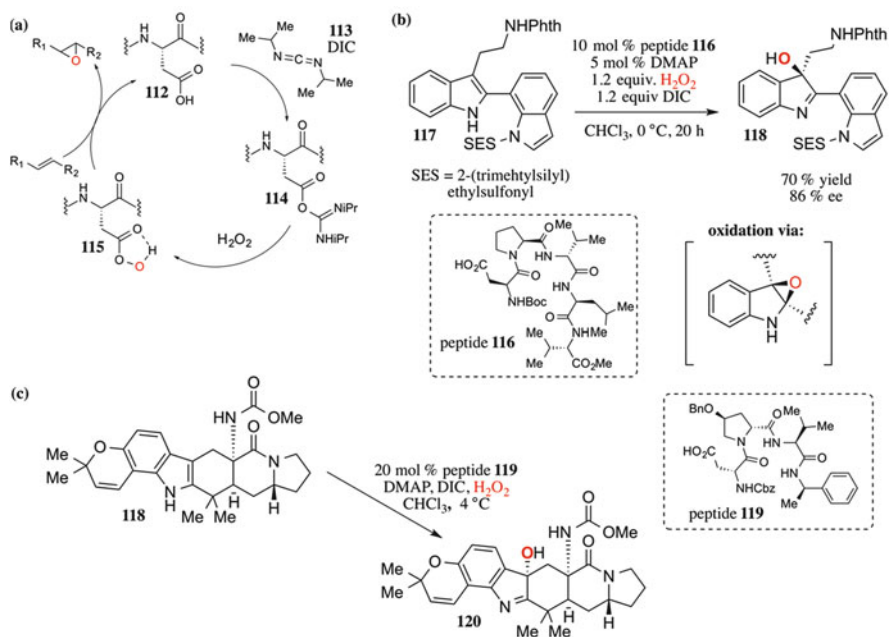
Through our combined efforts in phosphorylation, acylation, deoxygenation, halogenation, and cross-coupling, we reported and evaluated the antimicrobial activity of several dozen glycopeptide analogs, whose availability is enhanced by site-selective peptide-catalyzed reactions (Fig. 11). Our hope is that these results represent an auspicious set of data to justify further studies of this type.



**Fig. 11** Glycopeptides as substrates for site-selective reactions

## 8 Peptide-Based Catalysts for Site-Selective Oxidation

Among the many site-selective reactions carried out by enzymes, we were particularly inspired by the selective epoxidation of squalene to make squalene oxide as a prelude to steroid biosynthesis [170]. Nonenzymatic, peptide-catalyzed oxidations were well known at the outset of our studies, primarily with the Julia–Colonna epoxidation [3], and these have been supplemented with a number of other approaches [171–173]. We thus wished to explore a different approach, which we predicated upon a catalytic cycle based upon the aspartic acid sidechain (Fig. 12a) [174, 175]. Conceptually, the carboxylic acid sidechain (i.e., **112**) is activated by reaction with diisopropylcarbodiimide (DIC, **113**) to form *O*-acyl urea **114**. This activated ester species can then react with hydrogen peroxide to form a reactive peracid oxidant in situ (**115**). This peracid can then react with a substrate, an alkene for the purposes of this discussion, generating oxidized product and regenerating the aspartic acid catalyst sidechain. Although initially developed for substrates that contained carbamates as directing groups [106, 174, 175], we came to explore a number of other applications, including several presenting site-selectivity challenges. Two collaborative studies were particularly inspiring. In the first collaborative effort with the Movassaghi group [176], we observed site-, diastereo-, and enantioselective catalysts for the oxidation of various indoles to afford



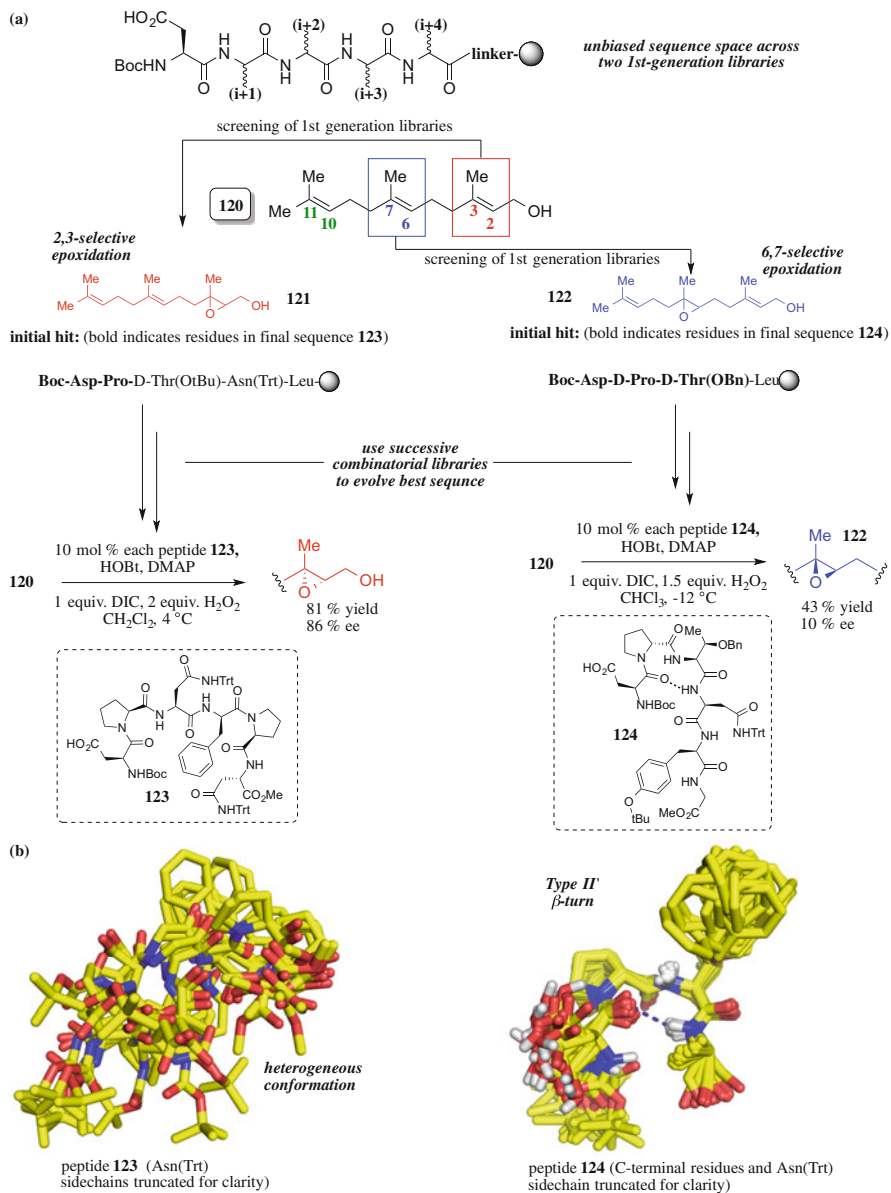
**Fig. 12** (a) Aspartic peracid catalytic cycle for epoxidation and indole oxidation [174, 175]. (b) Enantio- and site-selective oxidation of a complex bis-indole [176]. (c) Site-selective oxidation of an advanced intermediate in natural product total synthesis [177]

3-hydroxyindolenines (Fig. 12b). For example, the work led to peptide **116**, which catalyzed the oxidation of **117** to 3-hydroxyindolenine **118**. Notably, the reaction proceeded with high enantioselectivity and, importantly, only took place at one of two possible indole sites. In the second collaboration, with the Sarpong group [177], we found a catalyst that enabled a challenging late-stage oxidation reaction in the course of their synthesis of congeners of the citrinalin and cyclopiamine natural products (Fig. 12c). In this case, intermediate **118** had proven to be recalcitrant to many known oxidants – all either gave substantial oxidation of the chromene, the wrong hydroxy-indolenine stereoisomer, or both. From a small screen of known peptide sequences, we uncovered peptide **119**, which converted **118** to **120** without chromene oxidation; the site-selective formation of the desired product highlights the function of the mild, catalytically generated oxidant and the likely interaction of the peptide with a carbamate directing group. This particular example of site- and stereoselectivity, with concomitant chemoselectivity, represents an arena that may be a frontier for catalysts of this type which we hope to explore extensively going forward.

These studies proceeded in parallel with a more fundamental investigation of site-selective polyene oxidation [178–181]. We chose hydroxyl-containing terpene natural products as our substrates, projecting that the hydroxyl group might be serviceable as a directing group. As we lacked a hypothesis for the design of a suitable peptide-based catalyst to achieve alternate selectivity in this uncharted arena for our approach, we turned to combinatorial methods and the random peptide sequence space available using the “one-bead-one-compound” approach to library synthesis (Fig. 13a) [185]. We had used this approach earlier for the discovery of enantioselective acylation catalysts [27, 28], harnessing the method’s adaptability to the evolution-like logic employed in studies of the directed evolution of enzymes [186].

We screened our libraries for the site-selective epoxidation of farnesol (**120**) [182]. Either the peracid reagent *m*CPBA, or catalytic *n*-alkyl acids, provided a benchmark for the intrinsic and poorly selective product distribution of monoepoxides (see Fig. 13b inset for schematic of farnesol nomenclature). Hits from the initial libraries, however, showed selectivity toward 2,3-epoxide **121** and 6,7-epoxide **122**, inspiring the development of biased combinatorial libraries to select further for these oxidation sites (Fig. 13b). Further optimization of the sequences after additional library sequences yielded peptide **123**, which provided 2,3-epoxy farnesol **121** with 1:1:>100 site selectivity (10,11:6,7:2,3) in 81% yield and 86% ee. These values are comparable to those provided for this substrate by the venerable Sharpless asymmetric epoxidation [187]. Optimization of the 6,7-biased sequence led to peptide **124**, which provided 6,7-epoxy farnesol **122** in 1.2:8.0:1.0 site selectivity (10,11:6,7:2,3) in 43% yield and 10% ee. Despite the modest ee of **122**, we note that, to our knowledge, no existing catalytic epoxidation method is capable of providing **122** directly in reasonable purity.

Combinatorial discovery of catalysts that exhibit interesting properties invites mechanistic inquiry into the basis of the behavior. As part of these efforts, we obtained NMR solution structures of both catalysts using a standard 2D <sup>1</sup>H–<sup>1</sup>H



**Fig. 13** (a) Schematic summarizing discovery of peptides **123** and **124**. (b) NMR structures of peptides **123** (10 lowest-energy conformers) and **124** (20 lowest-energy conformers) [182–184]

dataset of gCOSY, TOCSY, and ROESY spectra for each and structures were calculated using ROESY-derived distance restraints in simulated annealing protocols [183, 184]. We note the caveat that the structures yielded in these efforts are approximations of the catalyst ground states, not transition state structures. Remarkably, peptide **123** does not adopt a single discrete conformation in solution (Fig. 13b). Rather, the ten lowest energy structures represent a heterogeneous ensemble populated by four conformers. Within this ensemble, we demonstrated that regions of the peptide sequence remain rigid, and the ensemble heterogeneity is generated by only a few non-restrained dihedral angles about the central residues of the peptide. Whatever the nature of the substrate–catalyst complex between peptide **123** and farnesol, the data suggest that it must form dynamically. This may be a departure from modes of action of more rigid catalyst scaffolds which we and others have studied [184].

By contrast, peptide **124** was found to populate a canonical type II'  $\beta$ -turn in its lowest energy ensemble (Fig. 13b). That it was discovered from a random combinatorial library speaks to the possibly privileged nature of this secondary structure element [188]. Furthermore [183], the structure validated a number of hypotheses based on sequence variations and truncation studies that support a remote hydroxyl-directed mechanism of action for the oxidation of the 6,7-position of farnesol by **124**. Importantly, a sidechain ether is implicated as a key acceptor of a hydrogen bond from farnesol.

Our findings with farnesol represent the proverbial preliminary results. A complete set of catalysts that deliver each of the six monoepoxides of farnesol with high site- and enantioselectivity is far from in hand. Nor is a complete mechanistic understanding available for the first two promising catalysts we have found. Yet, it is our hope that a means of moving forward in this area has been grounded, and we hope additional progress is possible.

## 9 Conclusions

Site-selective catalysis is an area of research that is undergoing an exciting expansion of its definition. In many ways, chemists have appreciated its significance and challenges for many years [189–194]. Yet, perhaps it is the case that, as the field of “asymmetric/enantioselective catalysis” has blossomed [195], new opportunities have emerged. Peptide-based catalysts provide just one path forward. It seems obvious that many other approaches can also make important contributions including those based on enzymes and their variants, as well as many other small-molecule catalyst-based metal complexes [196, 197], metalloids [57, 58], and organocatalytic strategies [59]. Catalysts of intermediate dimension are also certain to continue to contribute important advances [198, 199]. Perhaps one inspirational lesson is the expansive variety of catalysts that can be brought to bear on the problem, reflecting its expansive and expanding purview. So too have recent years seen an expansion of the range of reactions that may be studied under the

rubric of site-selective catalysis. Although this chapter has in no way succeeded in capturing all of the important contributions, perhaps it suffices to say that there is probably no known reaction, nor any to be discovered in the future, which could not be conceptualized for a study in a complex molecular environment, with many occurrences of the same functional group. Of course, gaining control of competing, different functional groups also remains a perennial challenge, and this situation too seems likely to remain a challenge for catalysis for many years to come.

## References

1. Matsumoto M, Lee SJ, Gagne MR, Waters ML (2014) Cross-strand histidine-aromatic interactions enhance acyl-transfer rates in beta-hairpin peptide catalysts. *Org Biomol Chem* 12:8711–8718
2. Matsumoto M, Lee SJ, Waters ML, Gagne MR (2014) A catalyst selection protocol that identifies biomimetic motifs from  $\beta$ -hairpin libraries. *J Am Chem Soc* 136:15817–15820
3. Julia S, Masana J, Vega JC (1980) “Synthetic enzymes”. Highly stereoselective epoxidation of a chalcone in a triphasic toluene-water-poly[(S)-alanine] system. *Angew Chem Int Ed* 19:929–931
4. Porter MJ, Roberts SM, Skidmore J (1999) Polyamino acids as catalysts in asymmetric synthesis. *Bioorg Med Chem* 7:2145–2156
5. Jarvo ER, Miller SJ (2002) Amino acids and peptides as asymmetric organocatalysts. *Tetrahedron* 58:2481–2495
6. Miller SJ (2004) In search of peptide-based catalysts for asymmetric organic synthesis. *Acc Chem Res* 37:601–610
7. Colby Davie EA, Mennen SM, Xu Y, Miller SJ (2007) Asymmetric catalysis mediated by synthetic peptides. *Chem Rev* 107:5759–5812
8. Wenemers H (2011) Asymmetric catalysis with peptides. *Chem Commun* 47:12036–12041
9. Lewandowski B, Wennemers H (2014) Asymmetric catalysis with short-chain peptides. *Curr Opin Chem Biol* 22:40–46
10. Kagan HB, Fiaud JC (1979) New approaches in asymmetric synthesis. In: Eliel EL, Allinger NL (eds) *Topics in stereochemistry*, vol 10. Wiley, Hoboken, pp 175–285
11. Kagan HB, Fiaud JC (1988) Kinetic resolution. In: Eliel EL, Wilen SH (eds) *Topics in stereochemistry*, vol 18. Wiley, Hoboken, pp 249–330
12. Fenwick DR, Kagan HB (1999) Asymmetric amplification. In: Denmark SE (ed) *Topics in stereochemistry*, vol 122. Wiley, Hoboken, pp 257–296
13. Manning G, Whyte DB, Martinez R, Hunter T, Sudarsanam S (2002) The protein kinase complement of the human genome. *Science* 298:1912–1934
14. Krebs EG (1983) Historical perspectives on protein phosphorylation and a classification system for protein kinases. *Philos Trans R Soc Lond B Biol Sci* 302:3–11
15. Demchenko AV (ed) (2008) *Handbook of chemical glycosylation: advances in stereoselectivity and therapeutic relevance*. Wiley-VCH, Weinheim
16. Ernst B, Hart GW, Sinay P (2000) Protecting groups: effects on reactivity, glycosylation stereoselectivity, and coupling efficiency. In: Green LG, Ley SV (eds) *Carbohydrates in chemistry and biology*. Wiley-VCH, Weinheim
17. Fischer E (1914) Über Phosphorsäureester des Methyl-glucosids und Theophyllin-glucosids. *Ber Chem* 47:3193–3205
18. Moffatt JG, Khorana HG (1957) Carbodiimides. VII. Tetra-*p*-nitrophenyl pyrophosphate, a new phosphorylating agent. *J Am Chem Soc* 79:3741–3746

19. Chambers RW, Moffatt JG, Khorana HG (1957) Nucleoside polyphosphates. IV. A new synthesis of guanosine-5'-phosphate. *J Am Chem Soc* 79:3747
20. Sculimbrenne BR, Miller SJ (2001) Discovery of a catalytic asymmetric phosphorylation through selection of a minimal kinase mimic: a concise total synthesis of D-*myo*-inositol-1-phosphate. *J Am Chem Soc* 123:10125–10126
21. Sculimbrenne BR, Morgan AJ, Miller SJ (2002) Enantiodivergence in small-molecule catalysis of asymmetric phosphorylation: concise total syntheses of the enantiomeric D-*myo*-inositol-1-phosphate and D-*myo*-inositol-3-phosphate. *J Am Chem Soc* 124:11653–11656
22. Sculimbrenne BR, Morgan AJ, Miller SJ (2003) Nonenzymatic peptide-based catalytic asymmetric phosphorylation of inositol derivatives. *Chem Commun* 1781–1785
23. Agranoff BW, Fisher SK (1991) Inositol phosphates and derivatives: synthesis, biochemistry, and therapeutic potential. In Reitz AB (ed) ACS Symposium series 463, American Chemical Society, Washington, p 20
24. Billington DC (1993) The inositol phosphates: chemical synthesis and biological significance. VCH, New York
25. Pirrung MC (1999) Histidine kinases and two-component signal transduction systems. *Chem Biol* 121:11638–11643
26. Kee JM, Muir TW (2012) Chasing phosphohistidine, an elusive sibling in the phosphoamino acid family. *ACS Chem Biol* 7:44–51
27. Copeland GT, Miller SJ (2001) Selection of enantioselective acyl transfer catalysts from a pooled peptide library through a fluorescence-based activity assay: an approach to kinetic resolution of secondary alcohols of broad structural scope. *J Am Chem Soc* 123:6496–6502
28. Jarvo ER, Copeland GT, Papaioannou N, Bonitatebus PJ, Miller SJ (1999) A biomimetic approach to asymmetric acyl transfer catalysis. *J Am Chem Soc* 121:11638–11643
29. Billington DC, Baker R, Kulagowski JJ, Mawer IM, Vacca JP, deSolms SJ, Huff JR (1989) The total synthesis of *myo*-inositol phosphates via *myo*-inositol orthoformate. *J Chem Soc Perkin Trans 1*:1423–1429
30. Irvine RF, Schell MJ (2001) Back in the water: the return of the inositol phosphates. *Nat Rev Mol Cell Biol* 2:327–338
31. Prestwich GD (2004) Phosphoinositide signaling: from affinity probes to pharmaceutical targets. *Chem Biol* 11:619–637
32. Di Paolo G, de Camilli P (2006) Phosphoinositides in cell regulation and membrane dynamics. *Nature* 443:651–657
33. Sculimbrenne BR, Xu Y, Miller SJ (2004) Asymmetric syntheses of phosphatidylinositol-3-phosphates with saturated and unsaturated side chains through catalytic asymmetric phosphorylation. *J Am Chem Soc* 126:13182–13183
34. Morgan AJ, Wang YK, Roberts MF, Miller SJ (2004) Chemistry and biology of deoxy-*myo*-inositol phosphates: stereospecificity of substrate interactions within an archaeal and a bacterial IMPase. *J Am Chem Soc* 126:15370–15371
35. Morgan AJ, Komiya S, Xu Y, Miller SJ (2006) Unified total syntheses of the inositol polyphosphates: D-I-3,5,6P<sub>3</sub>, D-I-3,4,5P<sub>3</sub>, and D-I-3,4,5,6P<sub>4</sub> via catalytic enantioselective and site-selective phosphorylation. *J Org Chem* 71:6923–6931
36. Xu Y, Sculimbrenne BR, Miller SJ (2006) Streamlined synthesis of phosphatidylinositol (PI), PI3P, PI3,5P<sub>2</sub>, and deoxygenated analogues as potential biological probes. *J Org Chem* 71:4919–4928
37. Longo CM, Wei Y, Roberts MF, Miller SJ (2009) Asymmetric syntheses of L, L- and L, D-di-*myo*-inositol-1,1'-phosphate and their behavior as stabilizers of enzyme activity at extreme temperatures. *Angew Chem Int Ed* 48:4158–4161
38. Cuilla R, Burrgraf S, Stetter KO, Roberts MF (1994) Occurrence and role of di-*myo*-inositol-1,1'-phosphate in *Methanococcus igneus*. *Appl Environ Microbiol* 60:3660–3664
39. Chen L, Spiliotis ET, Roberts MF (1998) Biosynthesis of di-*myo*-inositol-1,1'-phosphate, a novel osmolyte in hyperthermophilic Archaea. *J Bacteriol* 180:3785–3792

40. Chandler BD, Burkhardt AL, Foley K, Cullis C, Driscoll D, D'Amore NR, Miller SJ (2014) A fully synthetic and biochemically validated phosphatidyl inositol-3-phosphate hapten via asymmetric synthesis and native chemical ligation. *J Am Chem Soc* 136:412–418
41. Harris JR, Markl J (1999) Keyhole limpet hemocyanin (KLH): a biomedical review. *Micron* 6:597–623
42. Harlow E, Lane D (1988) *Antibodies: a laboratory manual*. Cold Spring Harbor, New York, Chapter 5
43. Hermanson GT (2008) *Bioconjugate techniques*, 2nd edn. Academic, New York, Chapter 19
44. Martin SF, Josey JA, Wong YL, Dean DW (1994) General method for the synthesis of phospholipid derivatives of 1,2-O-diacyl-*sn*-glycerols. *J Org Chem* 59:4805–4820
45. Dawson PE, Muir TW, Clark-Lewis I, Kent SBH (1994) Synthesis of proteins by native chemical ligation. *Science* 266:776–779
46. Johnson ECB, Kent SBH (2006) Insights into the mechanism and catalysis of the native chemical ligation reaction. *J Am Chem Soc* 128:6640–6646
47. Nilsson BL, Soellner MB, Raines RT (2005) Chemical synthesis of proteins. *Annu Rev Biophys Biomol Struct* 34:91–118
48. Fang GM, Cui HK, Zheng JS, Liu L (2010) Chemoselective ligation of peptide phenyl esters with N-terminal cysteines. *ChemBioChem* 11:1061–1065
49. Lewis CA, Sculimbrene BR, Xu Y, Miller SJ (2005) Desymmetrization of glycerol derivatives with peptide-based acylation catalysts. *Org Lett* 7:3021–3023
50. Griswold KS, Miller SJ (2003) A peptide-based catalyst approach to regioselective functionalization of carbohydrates. *Tetrahedron* 59:8869–8875
51. Evans JW, Fierman MB, Miller SJ, Ellman JA (2004) Catalytic enantioselective synthesis of sulfinate esters through the dynamic resolution of *tert*-butanesulfinyl chloride. *J Am Chem Soc* 126:8134–8135
52. Schreiber SL, Schreiber TS, Smith DB (1987) Reactions that proceed with a combination of enantiotopic group and diastereotopic face selectivity can deliver products with very high enantiomeric excess: experimental support of a mathematical model. *J Am Chem Soc* 109:1525–1529
53. Kawabata T, Nagato M, Takasu K, Fuji K (1997) Nonenzymatic kinetic resolution of racemic alcohols through an “induced fit” process. *J Am Chem Soc* 119:3169–3170
54. Kawabata T, Yamamoto K, Momose Y, Yoshida H, Nagaoka Y, Fuji K (2001) Kinetic resolution of amino alcohol derivatives with a chiral nucleophilic catalyst: access to enantiopure cyclic cis-amino alcohols. *Chem Commun* 2700–2701
55. Kawabata T, Muramatsu W, Nishio T, Shibata T, Schedel H (2007) A catalytic one-step process for the chemo- and regioselective acylation of monosaccharides. *J Am Chem Soc* 129:12890–12895
56. Ueda Y, Muramatsu W, Mishiro K, Furuta T, Kawabata T (2009) Functional group tolerance in organocatalytic regioselective acylation of carbohydrates. *J Org Chem* 74:8802–8805
57. Williamson CL, Chan L, Taylor MS (2012) Regioselective, borinic acid-catalyzed monoacylation, sulfonylation, and alkylation of diols and carbohydrates: expansion of substrate and mechanistic studies. *J Am Chem Soc* 134:8260–8267
58. Taylor MS (2015) Catalysis based on reversible covalent interactions of organoboron compounds. *Acc Chem Res* 48:295–305
59. Sun X, Lee H, Lee S, Tan KL (2013) Catalyst recognition of cis-1,2-diols enables site-selective functionalization of complex molecules. *Nat Chem* 5:790–795
60. Manville N, Alite H, Haeffner F, Hoveyda AH, Snapper ML (2013) Enantioselective silyl protection of alcohols promoted by a combination of chiral and achiral Lewis basic catalysts. *Nat Chem* 5:768–774
61. Blaisdell TP, Lee S, Kasaplar P, Sun X, Tan KL (2013) Practical silyl protection of ribonucleosides. *Org Lett* 15:4710–4713
62. Sun X, Worthy AD, Tan KL (2013) Resolution of terminal 1,2-diols via silyl transfer. *J Org Chem* 78:10494–10499

63. Sun X, Lee H, Lee S, Tan KL (2013) Catalyst recognition of cis-1,2-diols enables site-selective functionalization of complex molecules. *Nature Chem* 5:790–795
64. Zhao Y, Rodrigo J, Hoveyda AH, Snapper ML (2006) Enantioselective silyl protection of alcohols catalysed by amino-acid-based small molecule. *Nature* 443:64–70
65. Rawlings BJ (1999) Biosynthesis of polyketides (other than actinomycete macrolides). *Nat Prod Rep* 16:425–484
66. Shen B (2000) Biosynthesis of aromatic polyketides. *Top Curr Chem* 209:1–51
67. Newman DJ, Cragg GM (2007) Natural products as sources of new drugs over the last 25 years. *J Nat Prod* 70:461–477
68. Walsh CT (2008) The chemical versatility of natural product assembly lines. *Acc Chem Res* 41:4–10
69. Cragg GM, Newman DJ (2013) Natural products: a continuing source of novel drug leads. *Biochim Biophys Acta* 1830:3670–3695
70. Hertweck C (2009) The biosynthetic logic of polyketide diversity. *Angew Chem Int Ed* 48:4688–4716
71. Schetter B, Mahrwald R (2006) Modern aldol methods for the total synthesis of polyketides. *Angew Chem Int Ed* 45:7506–7525
72. Dechert-Schmitt AMR, Schmitt DC, Gao X, Itoh T, Krische MJ (2014) Polyketide construction via hydrohydroxyalkylation and related alcohol C-H functionalizations. Reinventing the chemistry of carbonyl addition. *Nat Prod Rep* 31:504–513
73. Dalby SM, Paterson I (2010) Synthesis of polyketide natural products and analogs as promising anticancer agents. *Curr Opin Drug Discov Devel* 13:777–794
74. Cane DE, Walsh CT, Khosla C (1998) Harnessing the biosynthetic code: combinations, permutations, and mutations. *Science* 282:63–68
75. Khosla C, Herschlag D, Cane DE, Walsh CT (2014) Assembly line polyketide synthases: mechanistic insights and unsolved problems. *Biochemistry* 53:2875–2883
76. Hutchinson CR, Fuji I (1995) Polyketide synthase gene manipulation: a structure-function approach in engineering novel antibiotics. *Annu Rev Microbiol* 49:201–238
77. Jacobsen JR, Hutchinson CR, Cane DE, Khosla C (1997) Precursor-directed biosynthesis of erythromycin analogs by an engineered polyketide synthase. *Science* 277:367–369
78. Hertweck C (2015) Decoding and reprogramming complex polyketide assemblylines: prospects for synthetic biology. *Trends Biochem Sci* 40:189–199
79. Wiley PF, Gerzon K, Flynn EH, Sigal MV, Weaver O, Quarck UC, Chauvette RR, Monahan R (1957) Erythromycin. X. Structure of erythromycin. *J Am Chem Soc* 79:6062–6070
80. Kim JW, Adachi H, Kazuo SY, Hayakwa Y, Seto H (1997) Apoptolidin, a new apoptosis inducer in transformed cells from *Nocardioopsis* sp. *J Antibiot* 50:628–630
81. Taylor RE, Chen Y, Galvin GM, Prabba PK (2004) Conformation-activity relationships in polyketide natural products. Towards to biologically active conformation of epothilone. *Org Biomol Chem* 2:127–132
82. Larsen EM, Wilson MR, Taylor RE (2015) Conformation-activity relationships of polyketide natural products. *Nat Prod Rep* 32:1183–1206
83. Wright GD (2005) Bacterial resistance to antibiotics: enzymatic degradation and modification. *Adv Drug Deliv Rev* 57:1451–1470
84. Walsh CT (2005) Molecular mechanisms that confer antibacterial drug resistance. *Nature* 406:775–781
85. Peddibhotia S, Dang Y, Liu JO, Romo D (2007) Simultaneous arming and structure/activity studies of natural products employing O-H insertions: an expedient and versatile strategy for natural products-based chemical genetics. *J Am Chem Soc* 129:12222–12231
86. Robles O, Romo D (2014) Chemo- and site-selective derivatizations of natural products enabling biological studies. *Nat Prod Rep* 31:318–334
87. Lewis CA, Miller SJ (2006) Site-selective derivatization and remodeling of erythromycin A by using simple peptide-based chiral catalysts. *Angew Chem Int Ed* 45:5616–5619

88. Lewis CA, Merkel J, Miller SJ (2008) Catalytic site-selective synthesis and evaluation of a series of erythromycin analogs. *Bioorg Med Chem Lett* 18:6007–6011
89. Jones PH, Perun TJ, Rowley EK, Baker EJ (1972) Chemical modifications of erythromycin antibiotics. 3. Synthesis of 4'' and 11 esters of erythromycin A and B. *J Med Chem* 15:631–634
90. Martin YC, Jones PH, Perun TJ, Grundy WE, Bell S, Bower RR, Shipkowitz NL (1972) Chemical modification of erythromycin antibiotics. 4. Structure-activity relations of erythromycin esters. *J Med Chem* 15:635–638
91. Haque TS, Little JC, Gellman SH (1994) 'Mirror image' reverse turns promote  $\beta$ -hairpin formation. *J Am Chem Soc* 116:4105–4106
92. Haque TS, Little JC, Gellman SH (1996) Stereochemical requirements for  $\beta$ -hairpin formation: model studies with four-residue peptides and decapeptides. *J Am Chem Soc* 118:6975–6985
93. Gellman SH (1998) Minimal models systems for  $\beta$ -sheet secondary structure in proteins. *Curr Opin Chem Biol* 2:717–725
94. Davies JS, Everett JR, Hutton IK, Hunt E, Tyler JW, Zomaya II, Slawin AMZ, Williams DJ (1991) NMR spectroscopic and X-ray crystallographic studies on the structure, stereochemistry and conformation of a series of 9,11 cyclic aminals of (9S)-9-N-methylerythromyclamine A. *J Chem Soc Perkin Trans 2*:201–214
95. Everett JR, Hunt E, Tyler JW (1991) Ketone-hemiacetal tautomerism in erythromycin A in non-aqueous solutions. An NMR spectroscopic study. *J Chem Soc Perkin Trans 2*:1481–1487
96. Tardrew PL, Mao JCH, Kenney D (1969) Antibacterial activity of 2' esters of erythromycin. *Appl Microbiol* 18:159–165
97. Lewis CA, Longcore KE, Miller SJ, Wender PA (2009) An approach to the site-selective diversification of apoptolidin A with peptide-based catalysts. *J Nat Prod* 72:1864–1869
98. Wender PA, Gullledge AV, Jankowski OD, Seto H (2002) Isoapoptolidin: structure and activity of the ring-expanded isomer of apoptolidin. *Org Lett* 4:3819–3822
99. Pennington JD, Williams HJ, Salomon AR, Sulikowski GA (2002) Toward a stable apoptolidin derivative: identification of isoapoptolidin and selective deglycosylation of apoptolidin. *Org Lett* 4:3823–3825
100. Wender PA, Jankowski OD, Longcore K, Tabet EA, Seto H, Tomikawa T (2006) Correlation of  $F_0F_1$ -ATPase inhibition and antiproliferative activity of apoptolidin analogues. *Org Lett* 8:589–592
101. Linnane P, Magnus N, Magnus P (1997) Induction of molecular asymmetry by a remote chiral group. *Nature* 385:799–801
102. Clayden J, Lund A, Vallverdu L, Helliwell M (2004) Ultra-remote stereocontrol by conformational communication of information along a carbon chain. *Nature* 431:966–971
103. Byrne L, Sola J, Boddaert T, Marcelli T, Adams RW, Morris GA, Clayden J (2014) Foldamer-mediated remote stereocontrol: >1,60 asymmetric induction. *Angew Chem Int Ed* 53:151–155
104. Lewis CA, Chiu A, Kubryk M, Balsells J, Pollard D, Esser CK, Murry J, Reamer RA, Hansen KB, Miller SJ (2006) Remote desymmetrization at near-nanometer group separation catalyzed by a miniaturized enzyme mimic. *J Am Chem Soc* 128:16454–16455
105. Lewis CA, Gustafson JL, Chiu A, Balsells J, Pollard D, Murry J, Reamer RA, Hansen KB, Miller SJ (2008) A case of remote asymmetric induction in the peptide-catalyzed desymmetrization of a bis(phenol). *J Am Chem Soc* 130:16358–16455
106. Hoveyda A, Evans DA, Fu GC (1993) Substrate-directable chemical reactions. *Chem Rev* 93:1307–1370
107. Yoshimoto FK, Guengerich FP (2014) Mechanism of the third oxidative step in the conversion of androgens to estrogens by cytochrome P450 19A1 steroid aromatase. *J Am Chem Soc* 136:15016–15025
108. Pallan PS, Nagy LD, Li L, Gonzalez E, Kramlinger VM, Azumaya CM, Waterman MR, Guengerich FP, Egli M, Wawrzak Z (2015) Structural and kinetic basis of steroid 17 $\alpha$ ,20-

- lyase activity in teleost fish cytochrome P450 17A1 and its absence in cytochrome P450 17A2. *J Biol Chem* 290:3248–3268
109. Payne AH, Hales DB (2004) Overview of steroidogenic enzymes in the pathway from cholesterol to active steroid hormones. *Endocr Rev* 25:947–970
  110. Barton DHR, McCombie SW (1975) A new method for the deoxygenation of secondary alcohols. *J Chem Soc Perkin Trans 1*:1574–1585
  111. Barton DHR, Blundell P, Dorchak J, Jang DO, Jaszberenyi J (1991) The invention of radical reactions. Part XXI. Simple methods for the radical deoxygenation of primary alcohols. *Tetrahedron* 47:8969–8984
  112. Barton DHR, Dorchak J, Jaszberenyi J (1992) The invention of radical reactions. Part XXIV. Relative rates of acylation and radical deoxygenation of secondary alcohols. *Tetrahedron* 48:7435–7446
  113. Sanchez-Rosello M, Puchlopek ALA, Morgan AJ, Miller SJ (2008) Site-selective catalysis of phenyl thionoformate transfer as a tool for regioselective deoxygenation of polyols. *J Org Chem* 73:1774–1782
  114. Jordan PA, Kayser-Bricker KJ, Miller SJ (2010) Asymmetric phosphorylation through catalytic P(III) phosphoramidite transfer: enantioselective synthesis of *D-myo*-inositol-6-phosphate. *Proc Natl Acad Sci U S A* 107:20620–20624
  115. Sculimbrene BR (2004). Catalytic asymmetric phosphorylation. Ph.D. thesis. Boston College, Boston
  116. Carruthers MH (1991) Chemical synthesis of DNA and DNA analogs. *Acc Chem Res* 24:278–284
  117. Vlasuk GP, Webb TR, Abelman MM, Pearson DA, Miller TA (21, 1999) US Patent 5492895
  118. Hayakawa Y, Katoka M (1997) Preparation of short oligonucleotides via the phosphoramidite method using a tetrazole promoter in a catalytic manner. *J Am Chem Soc* 119:11758–11762
  119. Jordan PA, Miller SJ (2012) An approach to the site-selective deoxygenation of hydroxyl groups based on catalytic phosphoramidite transfer. *Angew Chem Int Ed* 51:2907–2911
  120. Zhang L, Koreeda M (2004) Radical deoxygenation of hydroxyl groups via phosphites. *J Am Chem Soc* 126:13190–13191
  121. Fiori KW, Puchlopek ALA, Miller SJ (2009) Enantioselective sulfonylation reactions mediated by a tetrapeptide catalyst. *Nat Chem* 1:630–634
  122. Butler MS, Hansford KA, Blaskovich MAT, Halai R, Cooper MA (2014) Glycopeptide antibiotics: back to the future. *J Antibiot* 67:631–644
  123. Hubbard BK, Walsh CT (2003) Vancomycin assembly: nature's way. *Angew Chem Int Ed* 42:730–765
  124. Nicolaou KC, Boddy CNC, Brase S, Winissinger N (1999) Chemistry, biology, and medicine of the glycopeptide antibiotics. *Angew Chem Int Ed* 38:2097–2152
  125. Williams DH (1996) The glycopeptide story – how to kill the deadly ‘superbugs.’. *Nat Prod Rep* 13:469–477
  126. Min G, Chen Z, Onishi HR, Kohler J, Silver LL, Kerns R, Fukuzawa S, Thompson C, Kahne D (1999) Vancomycin derivatives that inhibit peptidoglycan biosynthesis without binding *D-Ala-D-Ala*. *Science* 284:507–511
  127. Kerns R, Dong SD, Fukuzawa S, Carbeck J, Kohler J, Silver LL, Kahne D (2000) The role of hydrophobic substituents in the biological activity of glycopeptide antibiotics. *J Am Chem Soc* 122:12608–12609
  128. Sun B, Chen Z, Eggert US, Shaw SJ, LaTour JV, Kahne D (2001) Hybrid glycopeptide antibiotics. *J Am Chem Soc* 123:12722–12723
  129. Lin H, Walsh CT (2004) A chemoenzymatic approach to glycopeptide antibiotics. *J Am Chem Soc* 126:13998–14003
  130. Leimkuhler C, Chen L, Barrett D, Panzone G, Sun B, Falcone B, Oberthuer M, Walker S, Kahne D (2005) Differential inhibition of *Staphylococcus aureus* PBP2 by glycopeptide antibiotics. *J Am Chem Soc* 127:3250–3251

131. Ashford PA, Bew SP (2012) Recent advances in the synthesis of new glycopeptide antibiotics. *Chem Soc Rev* 41:957–978
132. Higgins DL, Chang R, Debabov DV, Leung J, Wu T, Krause KM, Sandvik E, Hubbard JM, Kaniga K, Schmidt DE et al (2005) Telavancin, a multifunctional lipoglycopeptide, disrupts both cell wall synthesis and cell membrane integrity in methicillin-resistant *Staphylococcus aureus*. *Antimicrob Agents Chemother* 49:1127–1134
133. Zhanel GC, Calic D, Schweizer F, Zelenitsky S, Adam H, Lagace-Wiens PRS, Rubinstein E, Gin AS, Hoban DJ, Karlowsky JA (2010) New lipoglycopeptides: a comparative review of dalbavancin, oritavancin, and telavancin. *Drugs* 70:859–886
134. Reynolds PE (1989) Structure, biochemistry, and mechanism of action of glycopeptide antibiotics. *Eur J Clin Microbiol Infect Dis* 8:943–950
135. Mackay JP, Gerhard U, Beauregard DA, Williams DH, Westwell MS, Searle MS (1994) Glycopeptide antibiotic activity and the possible role of dimerization: a model for biological signaling. *J Am Chem Soc* 116:4581–4590
136. Dong SD, Oberthuer M, Losey HC, Anderson JW, Eggert US, Peczuh MW, Walsh CT, Kahne D (2002) The structural basis for induction of VanB resistance. *J Am Chem Soc* 124:9064–9065
137. McComas CC, Crowley BM, Boger DL (2003) Partitioning the loss in vancomycin binding affinity of D-Ala-D-Lac into lost H-bond and repulsive lone pair contributions. *J Am Chem Soc* 125:9314–9315
138. Crowley BM, Boger DL (2006) Total synthesis and evaluation of  $[\Psi(\text{CH}_2\text{NH})\text{Tpg}^4]$ vancomycin aglycon: reengineering vancomycin for dual D-Ala-D-Ala and D-Ala-D-Lac binding. *J Am Chem Soc* 128:2885–2892
139. Xie J, Pierce JG, James RC, Okano A, Boger DL (2011) A redesigned vancomycin engineered for dual D-Ala-D-Ala and D-Ala-D-Lac binding exhibits potent antimicrobial activity against vancomycin-resistant bacteria. *J Am Chem Soc* 133:13946–13949
140. Xie J, Okano A, Pierce JG, James RC, Stamm S, Crane CM, Boger DL (2012) Total synthesis of  $[\Psi(\text{C}(=\text{S})\text{NH})\text{Tpg}^4]$ vancomycin aglycon,  $[\Psi(\text{C}(=\text{NH})\text{NH})\text{Tpg}^4]$ vancomycin aglycon, and related key compounds: reengineering vancomycin for dual D-Ala-D-Ala and D-Ala-D-Lac binding. *J Am Chem Soc* 134:1284–1297
141. Bugg TDH, Wright GD, Dutka-Malen S, Arthur M, Courvalin P, Walsh CT (1991) Molecular basis for vancomycin resistance in *Enterococcus faecium* BM4147: biosynthesis of a depsipeptide peptidoglycan precursor by vancomycin resistance proteins VanH and VanA. *Biochemistry* 30:10408–10415
142. Walsh CT, Fisher SL, Park IS, Prahalad M, Wu Z (1996) Bacterial resistance to vancomycin: five genes and one missing hydrogen bond tell the story. *Chem Biol* 3:21–28
143. Walsh CT (1993) Vancomycin resistance: decoding the molecular logic. *Science* 261:308–309
144. Gray KC, Palacios DS, Dailey I, Endo MM, Uno BE, Wilcock BC, Burke MD (2012) Amphotericin primarily kills yeast by simply binding ergosterol. *Proc Natl Acad Sci U S A* 109:2234–2239
145. Hanessian S, Giguere A, Grzyb J, Maianti JP, Saavedra OM, Aggen JB, Linsell MS, Goldblum AA, Hildebrandt DJ, Kane TR, Dozzo P, Gliedt MJ, Matias RD, Feeney LA, Armstrong ES (2011) Toward overcoming *Staphylococcus aureus* aminoglycoside resistance mechanism with a functionally designed neomycin analogue. *ACS Med Chem Lett* 2:924–928
146. Szpilman AM, Cereghetti DM, Manthorpe JM, Wurtz NR, Carreira EM (2009) Synthesis and biophysical studies on 35-deoxy amphotericin B methyl ester. *Chem Eur J* 15:7117–7128
147. Fujisawa KL, Hoshiya T, Kawaguchi H (1974) Aminoglycoside antibiotics. VII. Acute toxicity of aminoglycoside antibiotics. *J Antibiot* 27:677–681
148. Griffith BR, Krepel C, Fu X, Blanchard S, Ahmed A, Edmiston CE, Thorson JS (2007) Model for antibiotic optimization via neoglycosylation: synthesis of liponeoglycopeptides active against VRE. *J Am Chem Soc* 129:8150–8155

149. Thompson C, Ge M, Kahne D (1999) Synthesis of vancomycin from the aglycon. *J Am Chem Soc* 121:1237–1244
150. Fowler BS, Lammerhold KM, Miller SJ (2012) Catalytic site-selective thiocarbonylations and deoxygenations of vancomycin reveal hydroxy-dependent conformational effects. *J Am Chem Soc* 134:9755–9761
151. Yoganathan S, Miller SJ (2015) Structure diversification of vancomycin through peptide-catalyzed, site-selective lipidation: a catalysis-based approach to combat glycopeptide-resistant pathogens. *J Med Chem* 58:2367–2377
152. Fowler BS, Mikochik PJ, Miller SJ (2010) Peptide-catalyzed kinetic resolution of formamides and thioformamides as an entry to nonracemic amines. *J Am Chem Soc* 132:2870–2871
153. Han S, Miller SJ (2013) Asymmetric catalysis at a distance: catalytic, site-selective phosphorylation of teicoplanin. *J Am Chem Soc* 135:12414–12421
154. Han S, Le BV, Hajare HS, Baxter RHG, Miller SJ (2014) X-Ray crystal structure of teicoplanin-A<sub>2</sub>-2 bound to a catalytic peptide sequence via the carrier protein strategy. *J Org Chem* 79:8550–8556
155. Chan HC, Huang YT, Lyu SY, Huang CJ, Li YS, Liu YC, Chou CC, Tsai MD, Li TL (2011) Regioselective deacetylation based on teicoplanin-complexed Orf2\* crystal structures. *Mol Biosyst* 7:1224–1231
156. Nieto M, Perkins HR (1971) The specificity of combination between ristocetins and peptides related to bacterial cell-wall mucopeptide precursors. *Biochem J* 124:845–852
157. Economou NJ, Zentner IJ, Lazo E, Jakonicic J, Stojanoff V, Weeks SD, Gratsky KC, Cocklin S, Loll PJ (2013) Structure of the complex between teicoplanin and a bacterial cell-wall peptide: use of a carrier-protein approach. *Acta Crystallogr D* 69:520–533
158. Economou NJ, Nahoum V, Weeks SD, Gratsky KC, Zentner IJ, Townsend TM, Bhuiya MW, Cocklin S, Loll PJ (2012) A carrier protein strategy yields the structure of dalbavancin. *J Am Chem Soc* 134:4637–4645
159. Muir TW, Sondhi D, Cole PA (1998) Expressed protein ligation: a general method for protein engineering. *Proc Natl Acad Sci U S A* 95:6705–6710
160. Muir TW (2013) Semisynthesis of proteins by expressed protein ligation. *Annu Rev Biochem* 72:249–289
161. Gustafson J, Lim D, Miller SJ (2010) Dynamic kinetic resolution of biaryl atropisomers via peptide-catalyzed asymmetric bromination. *Science* 328:1251–1255
162. Garand E, Kamrath MZ, Jordan PA, Wolk AB, McCoy AB, Miller SJ (2012) Determination of non-covalent docking by IR spectroscopy of cold gas-phase complexes. *Science* 335:694–698
163. Barrett KT, Miller SJ (2013) Enantioselective synthesis of atropisomeric benzamides through peptide-catalyzed bromination. *J Am Chem Soc* 135:2963–2966
164. Barrett KT, Metrano AJ, Rablen PR, Miller SJ (2014) Spontaneous transfer of chirality in an atropisomerically enriched two-axis system. *Nature* 509:71–75
165. Denmark SE, Burk MT (2010) Lewis base catalysis of bromo- and iodolactonization and cycloetherification. *Proc Natl Acad Sci U S A* 107:20655–20660
166. Pathak TP, Miller SJ (2012) Site-selective bromination of vancomycin. *J Am Chem Soc* 134:6120–6123
167. Pathak TP, Miller SJ (2013) Chemical tailoring of teicoplanin with site-selective reactions. *J Am Chem Soc* 135:8415–8422
168. Fu X, Tan CH (2011) Mechanistic considerations of guanidine-catalyzed reactions. *Chem Commun* 47:8210–8222
169. Anderson KW, Buchwald SL (2005) General catalysts for the Suzuki-Miyaura and Songoashira coupling reactions of aryl chlorides and for the coupling of challenging substrate combinations in water. *Angew Chem Int Ed* 44:6173–6177
170. Van Temelen EE, Heys JR (1975) Enzymic epoxidation of squalene variants. *J Am Chem Soc* 97:1252–1253

171. Maayan G, Ward MD, Kirshenbaum K (2009) Folded biomimetic oligomers for enantioselective catalysis. *Proc Natl Acad Sci U S A* 106:13679–13684
172. Berkessel A, Koch B, Toniolo C, Rainaldi M, Broxterman QB, Kaptein B (2006) Asymmetric enone epoxidation by short solid-phase bound peptides: further evidence for catalyst helicity and catalytic activity of individual peptide strands. *Biopolymers* 84:90–96
173. Formagio F, Boncio M, Crisma M, Peggion C, Mezzato S, Polese A, Barazza A, Antonello S, Maran F, Broxterman QB, Kaptein B, Kamphuis J, Vitale RM, Saviano M, Benedetti E, Toniolo C (2002) Nitroxyl peptides as catalysts of enantioselective oxidations. *Chem Eur J* 8:84–93
174. Peris G, Jakobsche CE, Miller SJ (2007) Aspartate-catalyzed asymmetric epoxidation reactions. *J Am Chem Soc* 129:8710–8711
175. Jakobsche CE, Peris G, Miller SJ (2008) Functional analysis of an aspartate-based epoxidation catalyst with amide-to-alkene peptidomimetic catalyst analogues. *Angew Chem Int Ed* 120:6809–6813
176. Kolundzic F, Noshi MN, Tjandra M, Movassaghi M, Miller SJ (2011) Chemoselective and enantioselective oxidation of indoles employing aspartyl peptide catalysts. *J Am Chem Soc* 133:9104–9111
177. Mercado-Marin EV, Garcia-Reynaga P, Romminger S, Pimenta EF, Romney DK, Lodewyk MW, Williams DE, Andersen RJ, Miller SJ, Tantillo DJ, Berlinck RGS, Sarpong R (2014) Total synthesis and isolation of citrinalin and cyclopiamine congeners. *Nature* 509:293–294
178. Gnanadesikan V, Corey EJ (2008) A strategy for position-selective epoxidation of polyprenols. *J Am Chem Soc* 130:8089–8093
179. Chang S, Lee NH, Jacobsen EN (1993) Regio- and enantioselective catalytic epoxidation of conjugated polyenes. Formal synthesis of LTA<sub>4</sub> methyl ester. *J Org Chem* 58:6939–6941
180. Burke CP, Shi Y (2006) Regio- and enantioselective epoxidation of dienes by a chiral dioxirane: synthesis of optically active vinyl cis-epoxides. *Angew Chem Int Ed* 45:4475–4478
181. Barlan AU, Baak A, Yamamoto H (2006) Enantioselective oxidation of olefins catalyzed by a chiral bishydroxamic acid complex of molybdenum. *Angew Chem Int Ed* 45:5849–5852
182. Lichtor PA, Miller SJ (2012) Combinatorial evolution of site- and enantioselective catalysts for polyene epoxidation. *Nat Chem* 4:990–995
183. Lichtor PA, Miller SJ (2014) Experimental lineage and functional analysis of a remotely directed peptide epoxidation catalyst. *J Am Chem Soc* 136:5301–5308
184. Abascal NC, Lichtor PA, Giuliano MW, Miller SJ (2014) Function-oriented investigations of a peptide-based catalyst that mediates enantioselective allylic alcohol epoxidation. *Chem Sci* 5:4504–4511
185. Lichtor PA, Miller SJ (2011) One-bead-one-catalyst approach to aspartic acid-based oxidation catalyst discovery. *ACS Comb Sci* 13:321–326
186. Brustad EM, Arnold FH (2011) Optimizing non-natural protein function with directed evolution. *Curr Opin Chem Biol* 15:201–210
187. Foo K, Usui I, Gotz DCG, Werner EW, Holte D, Baran PS (2012) Scalable, enantioselective synthesis of germacrene and related sesquiterpenes inspired by terpene cyclase phase logic. *Angew Chem Int Ed* 51:11491–11495
188. Yoon TP, Jacobsen EN (2003) Privileged chiral catalysts. *Science* 299:1691–1693
189. Breslow R, Gellman SH (1983) Intramolecular nitrene C-H insertions mediated by transition-metal complexes as nitrogen analogues of cytochrome P-450 reactions. *J Am Chem Soc* 105:6729–6730
190. Breslow R, Gellman SH (1982) Tosylamidation of cyclohexane by a cytochrome P-450 model. *J Chem Soc Chem Commun* 1400–1401
191. Breslow R (1980) Biomimetic control of chemical selectivity. *Acc Chem Res* 13:170–177
192. Xu D, Crispino GA, Sharpless KB (1992) Selective asymmetric dihydroxylation (AD) of dienes. *J Am Chem Soc* 114:7570–7571

193. Becker H, Soler MA, Sharpless KB (1995) Selective asymmetric dihydroxylation of polyenes. *Tetrahedron* 51:1345–1376
194. Kolb HC, VanNieuwenhze MS, Sharpless KB (1994) Catalytic asymmetric dihydroxylation. *Chem Rev* 94:2483–2547
195. Jacobsen EN, Pfaltz A, Yamamoto H (eds) (1999) *Comprehensive asymmetric catalysis*, vol I–III and Supplement 1. Springer, New York
196. Chen MS, White MC (2007) A predictably selective aliphatic C-H oxidation reaction for complex molecule synthesis. *Science* 318:783–787
197. Newhouse T, Baran PS (2011) If C-H bonds could talk: selective C-H bond oxidation. *Angew Chem Int Ed* 50:3362–3374
198. Vohidov F, Coughlin JM, Ball ZT (2015) Rhodium(II) metallopeptide catalyst design enables fine control in selective functionalization of natural SH3 domains. *Angew Chem Int Ed* 54:4587–4591
199. Ball ZT (2012) Designing enzyme-like catalysts: a rhodium(II) metallopeptide case study. *Acc Chem Res* 46:560–570

# Organocatalytic Site-Selective Acylation of Carbohydrates and Polyol Compounds

Yoshihiro Ueda and Takeo Kawabata

**Abstract** Development and scope of conventionally difficult molecular transformation on site-selective acylation of carbohydrates and polyol compounds are described. A salient feature is that the site-selectivity can be controlled independently from the intrinsic reactivity of the substrate, i.e., catalyst-controlled selectivity. Therefore, some substrates undergo acylation with reversal of their intrinsic reactivity. The mechanistic aspects of catalyst-controlled site-selective acylation are discussed with the emphasis on the strategy relying on the accelerative reaction rather than the decelerative one. An unconventional retrosynthetic route based on catalyst-controlled site-selective acylation is proposed toward extremely short-step total synthesis of natural glycosides of an ellagitannin family. Application to the late-stage functionalization of the complex natural products of biological interest is also described.

**Keywords** Accelerative reaction • Acylation • Catalyst-controlled reaction • Molecular recognition • Organocatalyst • Retrosynthesis • Site-selectivity

## Contents

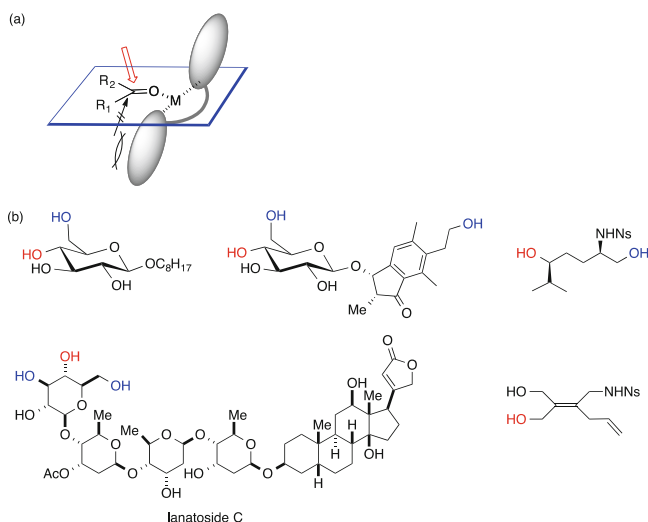
1	Introduction .....	204
2	Backgrounds of Acylation of Carbohydrates .....	205
3	Precedents on Catalyst-Controlled Site-Selective Acylation of Carbohydrates .....	206
4	Our Approach toward Catalyst-Controlled Site-Selective Acylation of Carbohydrates .....	208
5	Mechanistic Investigation for Organocatalytic Site-Selective Acylation .....	210
6	Scope of Site-Selective Acylation of Carbohydrates .....	212
7	Chemoselective Acylation of Linear Diols .....	213
8	Site-Selective Acylation of Amino Diols .....	216

9	Site-Selective Diversification of Polyol Natural Products .....	220
10	Unconventional Retrosynthesis: Application of Site-Selective Acylation to Total Synthesis of Natural Glycosides .....	223
11	Conclusion .....	228
	References .....	229

## 1 Introduction

Organic synthesis has been extensively developed focusing on chemo-, diastereo-, and enantioselectivity. In addition to these selectivities, site-selectivity has been a current focus as a key factor to streamline the synthetic routes to complex molecules. Development of the methods for site-selective functionalization enables late-stage modification of complex molecules, which is expected to provide direct access to structural diversification of biologically active compounds, retaining their original activity [1].

Asymmetric synthesis has been extensively developed during the last few decades. “Steric approach control” is a reliable and generally applicable principle for the development of asymmetric synthesis. Highly enantioselective reaction is expected if one of the two potentially reactive enantiofaces is effectively shielded by steric interaction (Fig. 1a: decelerative selectivity). On the other hand, steric approach control may not be an effective strategy for site-selective functionalization

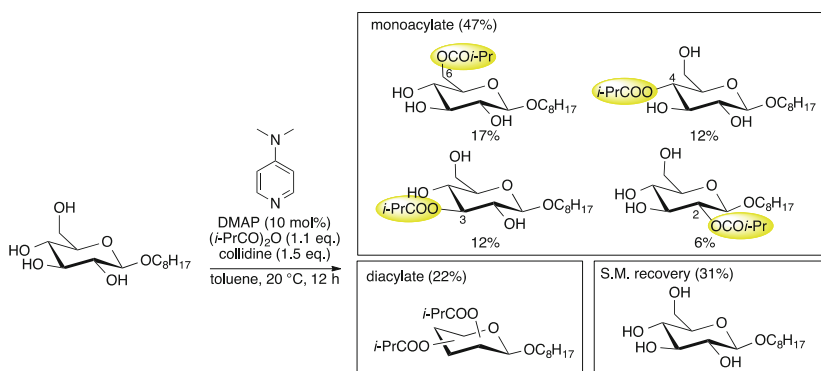


**Fig. 1** (a) Steric approach control for asymmetric synthesis. (b) Examples for site-selective acylation of polyol compounds: OH (shown in red): reactive hydroxy group under catalyst-controlled conditions. OH (shown in blue): reactive hydroxy group under substrate-controlled conditions (hydroxy group with intrinsic high reactivity)

of a particular hydroxy group among multiple hydroxy groups. For example, in order to functionalize one hydroxy group selectively in a huge molecule such as lanatoside C with eight free hydroxy groups (Fig. 1b), seven undesirable potentially reactive hydroxy groups are to be deactivated by steric shielding with the catalyst or the reagent. In contrast to this strategy, one promising approach to achieve site-selective functionalization may be taking advantage of the accelerative reaction at the desired site rather than deceleration of the reactions at many other undesired sites. Several examples of site-selective acylation of carbohydrates and polyol compounds are shown in Fig. 1b. Under catalyst-controlled conditions, a hydroxy group shown in red selectively undergoes acylation in the presence of the intrinsically more reactive hydroxy group(s) shown in blue. The origin of the site-selectivity appears to be the acceleration of the reaction at the desired site resulting from the precise molecular recognition process by the properly designed catalyst.

## 2 Backgrounds of Acylation of Carbohydrates

Carbohydrates play key roles in a wide range of intercellular processes such as infection and differentiation [2, 3]. For the progress in glycobiology and carbohydrate-based therapeutics, organic synthesis of carbohydrates is indispensable. However, efforts regarding carbohydrate synthesis often encounter difficulties associated with selective manipulation of one of the multiple hydroxy groups existing in carbohydrates. Multistep protection/deprotection procedures are usually employed to overcome this problem because direct methods for the chemo- and site-selective molecular transformation of unprotected carbohydrates have rarely been developed [4, 5]. For example, acylation of octyl  $\beta$ -D-glucopyranoside with an acid anhydride in the presence of a typical acylation catalyst, DMAP, proceeds in a random manner to give a mixture of four monoacylates (6-*O*-, 4-*O*-, 3-*O*-, and 2-*O*-acylate in 17%, 12%, 12%, and 6% yields, respectively) with concomitant formation of the diacylates (Scheme 1) [6]. From these backgrounds, selective manipulation of one of the



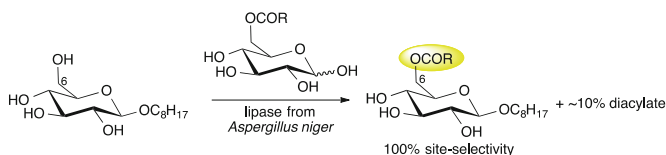
**Scheme 1** Random acylation of octyl  $\beta$ -D-glucopyranoside with DMAP-catalyzed acylation

multiple hydroxy groups of unprotected carbohydrates has been a fundamental challenge in organic synthesis.

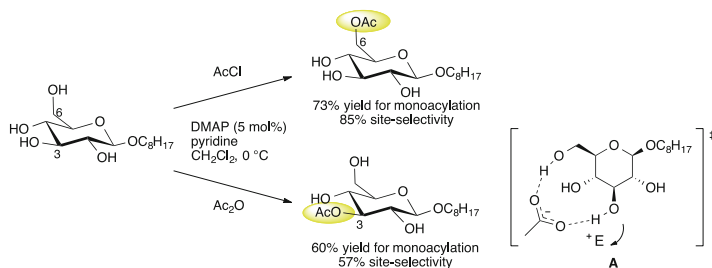
### 3 Precedents on Catalyst-Controlled Site-Selective Acylation of Carbohydrates

Enzymatic methods are powerful tools for introducing an acyl group selectively to one of the multiple hydroxy groups of carbohydrates [7, 8]. Therisod and Klibanov reported selective acylation of a primary hydroxy group in the presence of three secondary hydroxy groups of octyl- $\beta$ -D-glucopyranoside in ca. 100% chemoselectivity by using lipase from *Aspergillus niger* (Scheme 2) [9].

Although selective introduction of an acyl group into the primary hydroxy group of carbohydrates can be effectively achieved by the enzymatic protocol, selective introduction of an acyl group into one of the secondary hydroxy groups in the presence of the intrinsically more reactive primary hydroxy group has been a fundamental challenge in synthetic organic chemistry. Katnig and Albert reported reagent-controlled reversal of chemoselectivity of acylation of octyl  $\beta$ -D-glucopyranoside (Scheme 3) [10]. By treatment with acetyl chloride in the presence of DMAP, acetylation of octyl  $\beta$ -D-glucopyranoside took place at C(6)-OH in 85% site-selectivity and 73% yield for monoacylation. Interestingly, use of acetic anhydride in place of acetyl chloride gave the 3-*O*-acetate predominantly in 57% site-selectivity and 60% yield for monoacylation. It has been proposed that a carboxylate ion, generated as a counter anion of the acylpyridinium cation generated by the



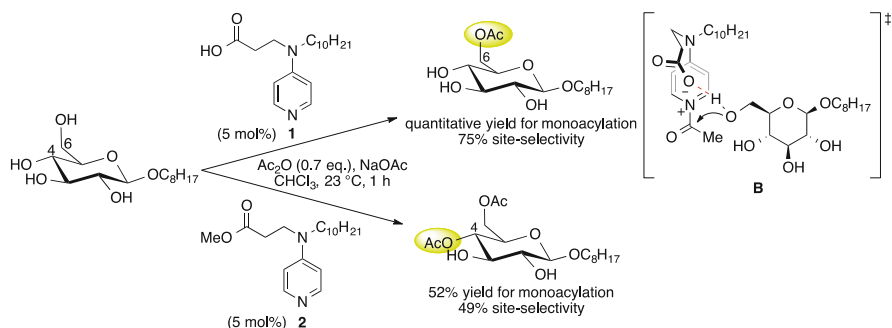
**Scheme 2** Enzymatic site-selective acylation of octyl  $\beta$ -D-glucopyranoside



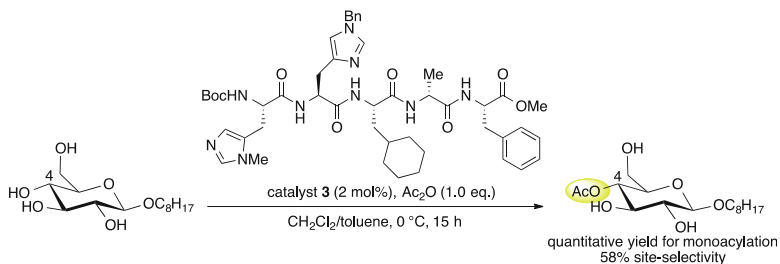
**Scheme 3** Reagent-controlled reversal of chemoselectivity

reaction of an acid anhydride with DMAP, plays an important role in the chemoselectivity as shown at **A** in Scheme 3. These results are in contrast to those in Scheme 1, and suggest that use of even a simple catalyst such as DMAP enables the introduction of an acyl group into the secondary hydroxy group under carefully controlled conditions.

Kurahashi, Mizutani, and Yoshida reported a pioneering example of catalyst-controlled chemoselective acylation of octyl  $\beta$ -D-glucopyranoside (Scheme 4) [11, 12]. In the presence of catalyst **1** with a side chain containing a carboxylic acid moiety, acetylation took place on the primary hydroxy group at C(6) in 75% site-selectivity and quantitative yield for monoacylation, where diacylation was avoided by the use of less (0.7 equiv.) acetic anhydride. On the other hand, the 4-*O*-acylate became the major product in 49% site-selectivity and 52% yield for monoacylation by using catalyst **2** with a side chain containing the corresponding methylester moiety. Hydrogen bonding interaction between catalytically active intermediate and the substrate was proposed to account for the C(6)-*O*-selective acylation (**B** in Scheme 4). Griswold and Miller reported an excellent approach to selective introduction of an acetyl group at the secondary hydroxy group of octyl  $\beta$ -D-glucopyranoside by using peptide-based catalyst **3** (Scheme 5) [13]. Selective C(4)-*O*-acylation has been achieved in a ratio of 22:58:11:9 for 6-*O*, 4-*O*, 3-*O*, and 2-*O*-acylate, respectively, without the formation of diacylates.



**Scheme 4** Catalyst-controlled reversal of chemoselectivity with modified DMAP derivatives



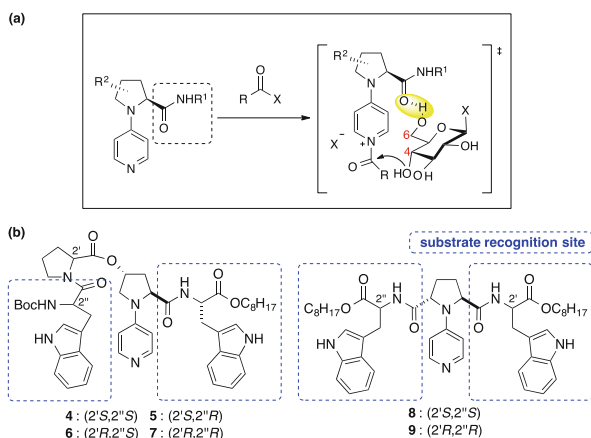
**Scheme 5** Selective acylation of a secondary hydroxy group with a peptide-based catalyst

## 4 Our Approach toward Catalyst-Controlled Site-Selective Acylation of Carbohydrates

In the development of catalysts for chemo- and site-selective acylation of carbohydrates we chose 4-pyrrolidinopyridine (PPY) as a catalytic center because it has been known to be the most powerful catalyst for the acylation of alcohols [14, 15]. Various PPY-type organocatalysts **4–9** with functional side chains for substrate-recognition were prepared (Fig. 2). It has been anticipated that the selective acylation of a secondary hydroxy group of the glucopyranose derivative might be possible even in the presence of a primary hydroxy group according to the hypothetical transition-state model shown in Fig. 2a. Because the primary hydroxy group at C(6) is the most reactive of the four hydroxy groups in the glucopyranose, it would preferentially form a hydrogen bond with a suitably positioned hydrogen-bond acceptor, an amide carbonyl group of the acylpyridinium ion generated from the PPY derivative and an acid anhydride. This interaction between the catalyst and substrate would result in the close proximity of the C(4)-OH to the reactive acyl group in the catalytically active intermediate, and it would preferentially undergo acylation. The R<sup>1</sup> group in the catalyst may participate in the substrate recognition by additional substrate-catalyst interactions. Tryptophan was chosen as a functional side chain of the catalyst because its indole moiety is expected to serve as a hydrogen bond donor and CH- $\pi$  interaction acceptor. After the successful development of catalyst **8** as an excellent catalyst for this purpose, we were surprised to find that two tryptophan moieties are highly preserved in the substrate recognition site of a family of  $\beta$ -glycosidase [16]. PPY-type catalyst **4–7** and **8–9** with dual functional side chains containing two tryptophan substructures were prepared from *trans*-4-hydroxy-L-proline and L-pyroglutamic acid, respectively [17, 18].

Effects of catalyst **4–9** on site-selective acylation of octyl  $\beta$ -D-glucopyranoside in toluene at 20 °C were investigated (Table 1). In reactions catalyzed by DMAP and catalysts **5–7**, acylation took place predominantly at the primary C(6)-OH

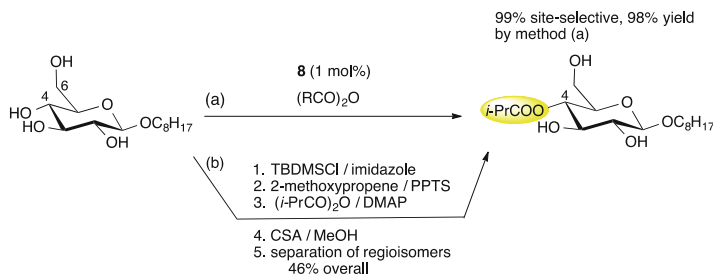
**Fig. 2** (a) Hypothesis for secondary-alcohol-selective acylation. (b) Chiral PPY analogues with dual functional side chains for substrate recognition



**Table 1** Effects of catalysts on site-selectivity in acylation of octyl  $\beta$ -D-glucopyranoside

entry	catalyst	monoacylate (%)	regioselectivity (6-O:4-O:3-O:2-O)	diacylate (%)	recovery (%)
1	DMAP	47	36 : 26 : 26 : 12	22	31
2	<b>4</b>	66	30 : <b>60</b> : 10 : 0	16	16
3	<b>5</b>	67	<b>55</b> : 33 : 10 : 1	19	14
4	<b>6</b>	65	<b>46</b> : 40 : 11 : 3	20	12
5	<b>7</b>	62	<b>49</b> : 39 : 11 : 1	24	10
6	<b>8</b>	84	11 : <b>86</b> : 3 : 0	12	2
7	<b>9</b>	71	20 : <b>73</b> : 7 : 0	17	9
8 <sup>a</sup>	<b>8</b>	98	0 : <b>99</b> : 1 : 0	0	0

<sup>a</sup>) The reaction was run in  $\text{CHCl}_3$  at  $-20\text{ }^\circ\text{C}$  with 1 mol% of catalyst **8**

**Scheme 6** Synthesis of C(4)-O-acylate of octyl  $\beta$ -D-glucopyranoside by (a) catalyst-controlled site-selective acylation, and (b) conventional protection/deprotection procedure

(entries 1, 3–5). On the other hand, catalyst **4** gave the 4-*O*-acylate as the major product, even in the presence of the primary C(6)-OH, which indicated that the relative orientation of two indole groups is critical for the secondary-alcohol-selective acylation. With  $C_2$ -symmetric catalyst **8** and **9**, site-selectivity for the acylation of the C(4)-OH significantly increased to 86% and 73%, respectively (entries 6 and 7). Reaction conditions were further optimized, and finally it was found that treatment of octyl  $\beta$ -D-glucopyranoside with isobutyric anhydride in chloroform at  $-20\text{ }^\circ\text{C}$  in the presence of 1 mol% of catalyst **8** gave the C(4)-*O*-acylate with a perfect chemo- and site-selectivity (entry 8: 99% site-selectivity, 98% yield for monoacylation, and no diacylate formation).

The present method enables the delivery of an acyl group to the secondary hydroxy group at C(4) among four free hydroxy groups, including the primary hydroxy group at C(6), in octyl  $\beta$ -D-glucopyranoside with perfect selectivity (Scheme 6a). This could alternatively be achieved by a conventional protection/deprotection procedure via several steps (Scheme 6b). Thus, catalyst **8** realized a conventionally difficult site-selective molecular transformation.

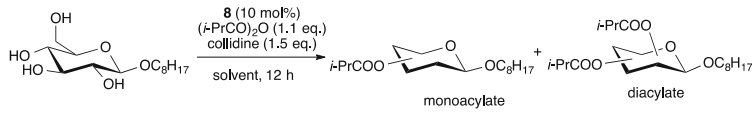
## 5 Mechanistic Investigation for Organocatalytic Site-Selective Acylation

Solvent and temperature effects of site-selective acylation catalyzed by organocatalyst **8** were investigated (Table 2). The highest selectivity for acylation of the C(4)-OH was observed in CHCl<sub>3</sub> (Table 2, entry 1), whereas the 6-*O*-acylate was obtained as the major product from the reaction in a polar solvent, DMF (entry 4). Higher site-selectivity for the C(4)-*O*-acylation was found to be associated with the higher yield for monoacylation and the lower yield for diacylation, which suggests that the selective acylation of C(4)-OH proceeds in an accelerative manner. A decrease in the reaction temperature increased the selectivity (entries 5 and 6 vs 1). All these results indicate that hydrogen bonding interaction between the catalyst and the substrate is a key factor for catalyst-controlled site-selective acylation.

According to the hypothetical structure of the transition-state assembly between the catalyst and the substrate (Fig. 2a), the existence of the primary hydroxy group at C(6) of the substrate seems critical. This idea was supported by the reaction of the 6-*O*-Me derivative **10**, which resulted in random acylation under optimized conditions for site-selective acylation of octyl β-D-glucopyranoside with catalyst **8** (Scheme 7a: 4-*O*:3-*O*:2-*O* = 31:67:2). Competitive acylation between octyl β-D-glucopyranoside and 2-phenylethanol gave the acylated product only from the glucopyranose, retaining the high site-selectivity and high yield (Scheme 7b). These results also suggest that the selective acylation of the C(4)-OH proceeds in an accelerative manner by means of catalyst **8**.

The site-selectivity profile of acylation of octyl β-D-glucopyranoside was further investigated with catalysts **11–14** with various functional side chains (Table 3) [18]. In the presence of **11–13**, acylation took place at C(4)-OH predominantly (58–68% site-selectivity, entries 2–4), which indicates that the amide carbonyl groups, a common substructure among **11–13**, seems essential for the selective acylation at C

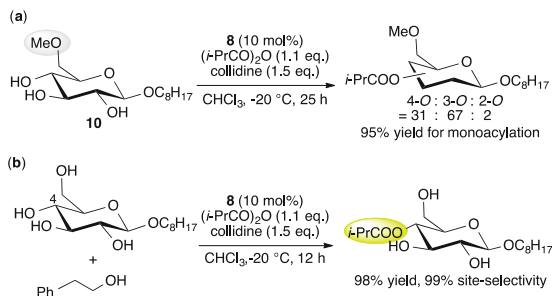
**Table 2** Effects of solvent and temperature on site-selectivity in acylation of octyl β-D-glucopyranoside catalyzed by **8**



entry	solvent	temperature (°C)	monoacylate (%)	regioselectivity (6- <i>O</i> : 4- <i>O</i> : 3- <i>O</i> : 2- <i>O</i> )	diacylate (%)	recovery (%)
1	CHCl <sub>3</sub>	20	90	4 : <b>91</b> : 5 : 0	4	3
2	toluene	20	84	11 : 86 : 3 : 0	12	2
3	THF	20	51	27 : 51 : 22 : 0	28	16
4	DMF	20	46	<b>63</b> : 12 : 24 : 1	<b>26</b>	21
<hr/>						
5	CHCl <sub>3</sub>	0	97	0 : 98 : 2 : 0	2	0
6	CHCl <sub>3</sub>	-20	98	0 : 99 : 1 : 0	0	0

**Scheme 7** Mechanistic implications. (a)

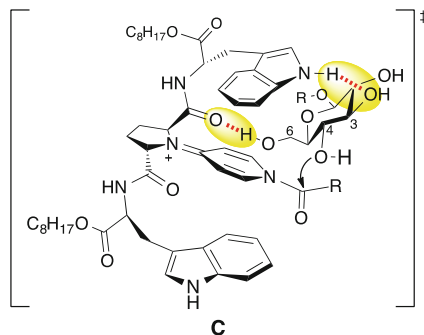
Non-selective acylation of **10** even in the presence of catalyst **8**. (b) Competitive acylation between octyl β-D-glucopyranoside and 2-phenylethanol catalyzed by **8**

**Table 3** Effects of functional side chains of catalysts **11–14** on site-selective acylation

Entry	Catalyst	Monoacylate (%)	Regioselectivity (6- <i>O</i> :4- <i>O</i> :3- <i>O</i> :2- <i>O</i> )	Diacylate (%)	Recovery (%)
1	<b>8</b>	97	0: <b>98</b> :2:0	2	0
2	<b>11</b>	60	23: <b>58</b> :19:0	21	14
3	<b>12</b>	74	7: <b>65</b> :28:0	15	4
4	<b>13</b>	69	14: <b>60</b> :26:0	20	8
5	<b>14</b>	62	13: <b>66</b> :20:1	13	22

(4)-OH and the indole NH of catalyst **8** may participate in further increasing the site-selectivity. Based on these results, transition-state model **C** was proposed (Fig. 3), in which the acylpyridinium ion is expected to recognize the substrate structure precisely via dual hydrogen bonding interaction. The  $C_2$ -symmetric structure of catalyst **8** seems to be important because the substrate approach to the reactive acylpyridinium ion from its  $\beta$ -face should reach the transition state exactly the same as from the  $\alpha$ -face. The decrease in site-selectivity observed in the acylation catalyzed by  $C_1$ -symmetric catalyst **14** is compatible with this rationale

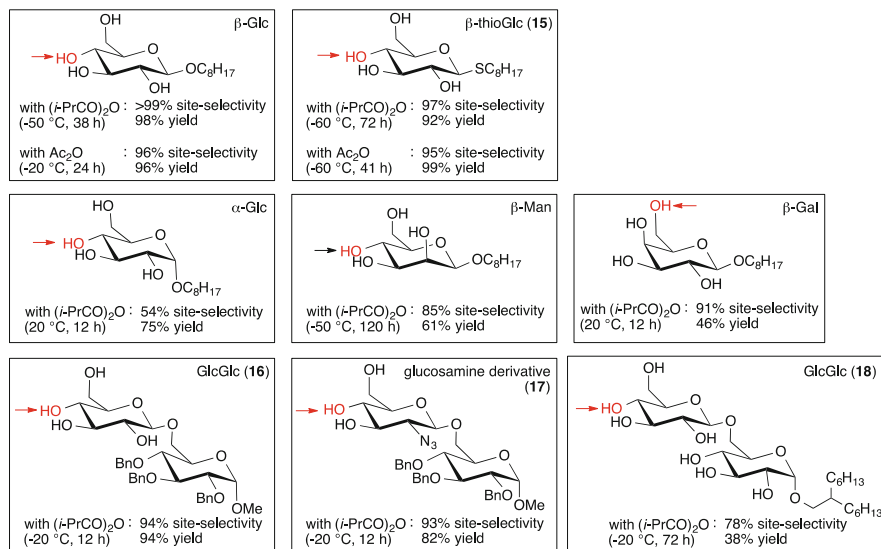
**Fig. 3** A proposed transition state assembly for site-selective acylation of octyl  $\beta$ -D-glucopyranoside promoted by catalyst **8**



(Table 3, entry 5), because substrate approach to the reactive acylpyridinium ion from its  $\alpha$ -face would lead to non-selective acylation, whereas that from its  $\beta$ -face still leads to site-selective acylation.

## 6 Scope of Site-Selective Acylation of Carbohydrates

Scope of the site-selective acylation of various saccharide derivatives is shown in Fig. 4 [19]. Acetylation of octyl  $\beta$ -D-glucopyranoside by using acetic anhydride in place of isobutyric anhydride took place at C(4)-OH selectively (96% site-selectivity and 96% yield for monoacylation). Thioglycoside **15** can be used for the C(4)-OH-selective acylation to provide the 4-*O*-acylate in high selectivity and yield. Acylation of octyl  $\alpha$ -D-glucopyranoside gave the 4-*O*-acylate predominantly, albeit with decreased site-selectivity (54% site-selectivity). Acylation of octyl  $\beta$ -D-mannopyranoside also gave the 4-*O*-acylate selectively (85% site-selectivity and 61% yield for monoacylation), whereas acylation of octyl  $\beta$ -D-galactopyranoside, the C(4)-epimer of octyl  $\beta$ -D-glucopyranoside, took place preferentially at the primary C(6)-OH (91% site-selectivity). The equatorial orientation of the C(4)-OH seems crucial for the selective acylation catalyzed by **8**. Disaccharides **16** with a terminal  $\beta$ -D-glucopyranoside moiety also underwent C(4)-OH-selective acylation (94% site-selectivity and 94% yield for monoacylation). Azide-substituted disaccharide **17** was converted to the corresponding 4-*O*-acylate selectively (93% site-selectivity and 82% yield for monoacylation). Although disaccharide **18** with seven free hydroxy groups also underwent selective acylation at the C(4)-OH of the terminal glucose moiety, the acylation reaction was sluggish because of its low solubility in  $\text{CHCl}_3$  (78% site-selectivity and 38% yield for monoacylation). These results may be explained by the transition state model shown as **C** (Fig. 3).

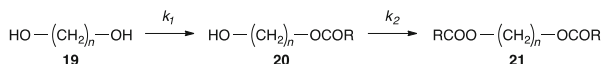


**Fig. 4** Scope of site-selective acylation of various saccharides catalyzed by **8**

## 7 Chemoselective Acylation of Linear Diols

Monoacylation of 1,*n*-linear diols seems to be a simple molecular transformation. However, it is still a challenging subject in current organic synthesis because of the unavoidable over-acylation (Scheme 8) [20, 21]. This transformation seems especially difficult in the case of long-chain linear diols such as **19** ( $n \geq 4$ ) because the reactivity of the free OH in diol **19** is similar to that of the free OH in monoacylated monool **20** ( $k_1 \simeq k_2$ ) because of their similar steric microenvironments. On the other hand, it may be possible if acylation of diol **19** takes place preferentially in the presence of monoacylated monool **20** ( $k_1 \gg k_2$ ) by effective discrimination between **19** and **20** by means of molecular recognition with the catalyst.

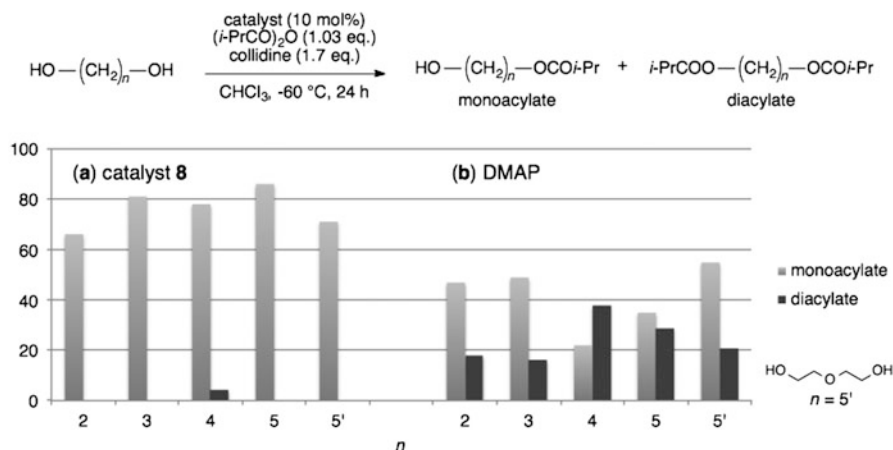
DMAP-catalyzed acylation of 1,5-pentanediol (**19a**) with 1.1 equiv. of isobutyric anhydride gave monoacylate **20a** in 45% yield and diacylate **21a** in 26% yield (Table 4, entry 1, **20a/21a** = 1.7). On the other hand, in the presence of catalyst **8**, chemoselective acylation took place to provide the monoacylate and the diacylate in 92% and 3% yields, respectively (entry 2, **20a/21a** = 31). The reaction of **19a** in DMF resulted in non-chemoselective acylation even in the presence of catalyst **8**, as observed in DMAP-catalyzed acylation (entry 3, **20a/21a** = 1.7). Polarity of the solvent is crucial for the chemoselective acylation of **19a** catalyzed by **8**. The similar tendency was observed in the site-selective acylation of carbohydrates promoted by catalyst **8**. This observation indicates that the hydrogen bonding interaction between the catalyst and the substrate may play a key role for the chemo- and site-selective acylation [22].

**Scheme 8** Mono- and diacylation of 1,*n*-linear diols**Table 4** Chemoselectivity profile in acylation of 1,5-pentandiol (**19a**)

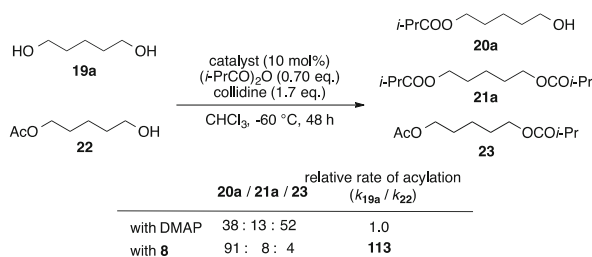
Entry	Catalyst	Solvent	<b>20a</b>	<b>21a</b>	<b>20a/21a</b>
1	DMAP	CHCl <sub>3</sub>	45%	26%	1.7
2	<b>8</b>	CHCl <sub>3</sub>	<b>92%</b>	3%	<b>31</b>
3	<b>8</b>	DMF	48%	29%	1.7

DMAP-catalyzed acylation of various 1,*n*-linear diols ( $n = 2-5$ , and  $5'$ ) with 1.03 equiv. of isobutyric anhydride gave 3:1 ~ 1:1 mixtures of the monoacylates and the diacylates as shown in Fig. 5b. On other hand, almost pure monoacylates were obtained by the acylation of diols in the presence of 10 mol% of catalyst **8** (Fig. 5a). However, a significant amount of the diacylate formed when further longer linear diols ( $n \geq 6$ ) were used as the substrates (data not shown). These results suggest that catalyst **8** is able to distinguish the diol structure from the monoacylated monool in the case where the chain length is shorter or equal to 5.

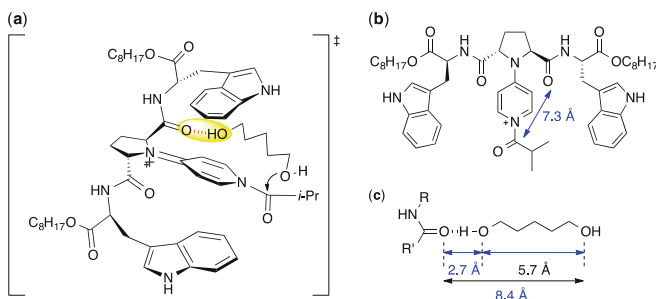
Competitive acylation between **19a** and **22** provides mechanistic insights into the chemoselective acylation (Scheme 9). The relative rate of acylation between **19a** and **22** can be estimated based on the amounts of acylates **20a**, **21a**, and **23** formed, and it was determined to be 1.0 in the DMAP-catalyzed acylation. This indicates no chemoselectivity in the competitive acylation between **19a** and **22**, and this phenomenon is compatible with the formation of the almost equal amounts of the monoacylate and diacylate in DMAP-catalyzed acylation of 1,5-pentandiol (Fig. 5b,  $n = 5$ ). On the other hand, the relative rate was estimated to be 113 in the competitive acylation between **19a** and **22** catalyzed by **8**. This result is also consistent with the chemoselective formation of the monoacylate in the acylation of **19a** catalyzed by **8** (Fig. 5a,  $n = 5$ ). Thus, chemoselective acylation is expected to take place by selective acylation of diol **19a** in an accelerative manner in the presence of the corresponding monoacylate formed in situ. The transition-state model for the monoacylation of **19a** is shown in Fig. 6, in which a hypothetical picture for the distance recognition between two hydroxy groups by hydrogen bonding interaction is shown. This assumption was supported by the experimental results from the competitive acylation between **19a** and its one-carbon-longer homologue (1,6-hexanediol) in the presence of catalyst **8**, which proceeded with the relative rate of 5.2 ( $k_{19a}/k_{1,6\text{-hexanediol}} = 5.2$ ) [22].



**Fig. 5** Ratios of the mono- and diacylates in the acylation of various linear diols catalyzed by (a) catalyst **8** and (b) DMAP



**Scheme 9** Competitive acylation between **19a** and **22**



**Fig. 6** (a) Proposed transition state assembly for acylation of **19a** catalyzed by **8**. (b) Calculated distance between the oxygen atom of the amide carbonyl and the carbon atom of the acyl group of an acylpyridinium ion generated by a molecular modeling. (c) The sum of the length (8.4 Å) of the distance between the two oxygen atoms of the extended conformer of diol **19a** (5.7 Å) and the hydrogen bonding distance (2.7 Å) might roughly account for the preference for selective monoacylation of the 1,5-pentanediol promoted by catalyst **8**

## 8 Site-Selective Acylation of Amino Diols

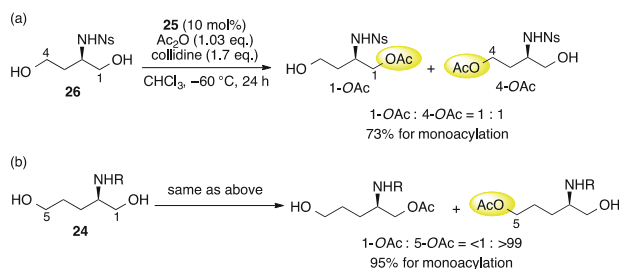
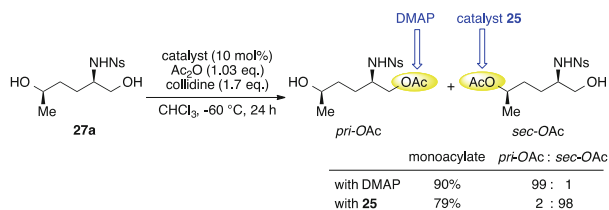
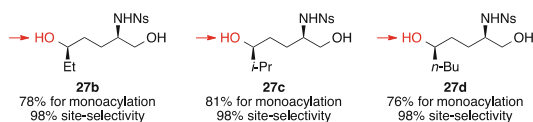
Site-selective manipulation of amino alcohol derivatives is another attractive challenge in organic synthesis, because amino alcohol substructure is widely found in biologically active natural products, pharmaceuticals, and building blocks for molecular catalysts [23–25]. Results of acylation of amino diol **24** containing two primary hydroxy groups are shown in Table 5 [26]. DMAP-catalyzed acylation of **24a** with *Ns* group (*Ns* = 2-nitrobenzenesulfonyl) on the nitrogen atom gave 1-*OAc* and 5-*OAc* in 32% and 6% yields, respectively, with concomitant formation of the diacylate in 30% yield (entry 1). This result indicates that C(1)-OH of **24a** has intrinsic higher reactivity than C(5)-OH. On the other hand, acylation took place at the C(5)-OH in 95% yield and >99% site-selectivity in the presence of catalyst **25** (entry 2). Site-selectivity of the acylation catalyzed by **25** is strongly dependent on the substituents on the nitrogen atom. Among various *N*-substituents examined (entries 2–5), *N-Ns* derivative **24a** showed complete reversal of the intrinsic reactivity of the parent amino diol in the presence of catalyst **25**. This suggests that *NHNs* group may serve as an excellent hydrogen bond donor for the interaction with catalyst **25** at the transition state of the acylation [26].

The distance between functionalities in the substrate seems crucial for the site-selectivity of the acylation catalyzed by **25**. For example, a one-carbon-shorter homologue of **24**, 2-aminobutane-1,4-diol derivative **26**, gave a 1:1 mixture of 1-*OAc* and 4-*OAc* in 73% combined yield under the same conditions for the acylation of **24** (Scheme 10). These results suggest that 1,5-*NHNs*-alcohol substructure is suitable for undergoing preferential acylation in the presence of catalyst **25**. This unique property of catalyst **25** was further demonstrated by chemoselective acylation of amino diols **27a–27d** possessing both primary and secondary hydroxy groups. The primary hydroxy group of substrate **27a** seems to be intrinsically more reactive, and it was selectively acylated almost exclusively in DMAP-catalyzed acylation (Scheme 11). On the other hand, acylation of **27a** catalyzed by **25** took place at the secondary hydroxy group, providing *sec-OAc* in 98% chemoselectivity and 79% yield. Thus, reversal of the chemoselectivity in secondary OH vs primary OH acylation was observed. Surprisingly, this phenomenon on the catalyst-controlled reversal of chemoselectivity was observed even for the substrates **27b–27d** with sterically hindered secondary hydroxy group at C(5) (Fig. 7).

Discrimination of double-bond geometry by the reaction has also been one of the unsolved problems in organic synthesis. Geometry-selective acylation and de-acylation of tri- and tetra-substituted olefins have been well developed by enzymatic methods [27; 28 and references cited therein]. On the other hand, the non-enzymatic counterpart has scarcely been reported before our report in 2012 [29]. We found that double-bond geometry of tri- and tetrasubstituted alkenediols was effectively differentiated on their acylation via hydrogen-bond-mediated molecular recognition of the substrate structure by the catalyst. DMAP-catalyzed acylation of trisubstituted alkenediol **28** with *NHNs* substituent gave almost a 1:1 mixture of *Z-OAc* and *E-OAc* in 55% combined yield, which indicates the similar

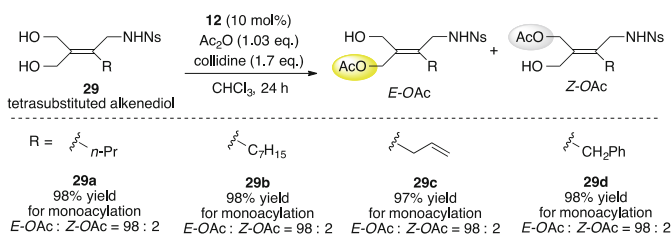
**Table 5** Dependence of the *N*-substituent and the catalyst on the site-selectivity of acylation of 2-amino-1,5-pentandiol derivative **24**

Entry	R ( <b>24</b> )	Catalyst	Monoacylate (%)	1-OAc:5-OAc	Diacylate
1	Ns ( <b>24a</b> )	DMAP	38	<b>84:16</b>	30%
2	Ns ( <b>24a</b> )	<b>25</b>	95	<1:> <b>99</b>	3%
3	Boc ( <b>24b</b> )	<b>25</b>	80	84:16	0%
4	Cbz ( <b>24c</b> )	<b>25</b>	49	69:31	15%
5	Ts ( <b>24d</b> )	<b>25</b>	84	48:52	8%

**Scheme 10** Dependence of the distance between the NHNs and OH groups in the site-selectivity in acylation of (a) **26** and (b) **24****Scheme 11** Catalyst-controlled reversal of chemoselectivity in acylation of **27a****Fig. 7** Secondary-OH-selective acylation of amino diol derivatives in the presence of an intrinsically more reactive primary hydroxy group

**Table 6** Geometry-selective acylation of trisubstituted alkenediol **28**

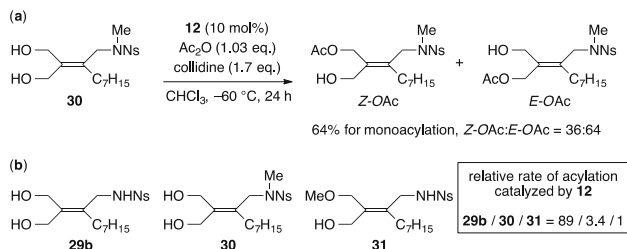
Catalyst	Temperature (°C)	Monoacylate (%)	Z-OAc:E-OAc	Diacylate (%)
DMAP	-40	55	52:48	14
<b>12</b>	-40	90	6:94	2
<b>12</b>	-60	95	5:95	3

**Scheme 12** Geometry-selective acylation of tetrasubstituted alkenediol **29**

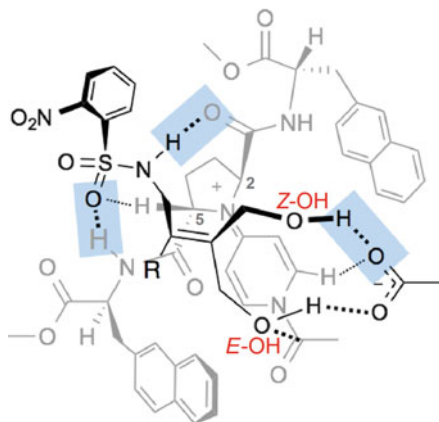
reactivity of two hydroxy groups (Table 6, entry 1). In contrast, highly *E*-OH-selective acylation of **28** took place to provide *E*-OAc in the presence of catalyst **12**, a diastereomeric catalyst of **25** (entry 2). Decrease in the reaction temperature from  $-40$  to  $-60$  °C slightly increases the yield and selectivity for *E*-O-acylation (entry 3, 95% yield, and 95% selectivity).

Geometry-selective acylation of tetrasubstituted alkenediols is generally observed in the presence of catalyst **12**. Acylation of **29** with various alkyl groups (R = *n*-Pr, *n*-C<sub>7</sub>H<sub>15</sub>, allyl, and Bn) took place on the *E*-OH with high geometry-selectivity (*E*-OAc/*Z*-OAc = 98/2) (Scheme 12). The monoool obtained (*Z*-OH) can be readily transformed to diverse tetrasubstituted olefins by the subsequent transformation of the C-OH group into the corresponding C-C, C-N, and C-OR groups [29].

The NHNs group was found to be critical for the geometry-selective acylation by the comparative experiment using the corresponding NMeNs derivative **30**. Acylation of **30** took place predominantly at the *E*-OH, but with much diminished selectivity (*E*-OAc/*Z*-OAc = 64:36) compared to that of **29b** (Fig. 8a). The relative rate of acylation between **29b** and **30** catalyzed by **12** was determined to be  $k_{29b}/k_{30} = 26$  by their competitive acylation reaction. These results indicate that the NHNs group plays an important role for the *E*-selective acylation and accelerative acylation of **29b**. The relative rate of acylation between **29b** and the corresponding *Z*-OMe derivative **31** was found to be  $k_{29b}/k_{31} = 89$ . This result suggests that the unreacting *Z*-OH is essential for the accelerative *E*-OH-acylation. Both NHNs and



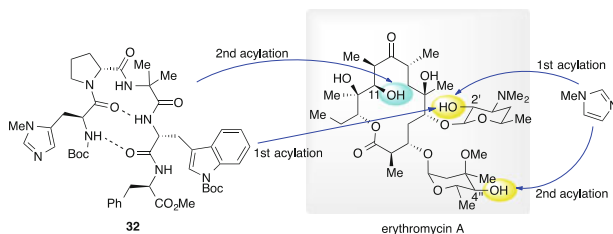
**Fig. 8** (a) Diminished site-selectivity in the acylation of NMeNs derivatives **30**. (b) Relative rates of acylation between **29b**, **30**, and **31** under the optimized conditions for *E*-OH-selective acylation catalyzed by **12**



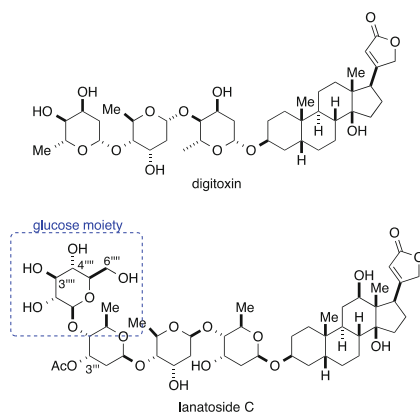
**Fig. 9** A proposed transition-state model for the geometry-selective acylation of tetrasubstituted alkenediols promoted by catalyst **12**

Z-OH in **29b** are assumed to be contributing as hydrogen bond donors for the *E*-selective accelerative acylation. A transition-state model was proposed based on DFT calculation (B3LYP/6-31G\*) (Fig. 9) [30]. The two amide groups at C(2) and C(5) of catalyst **12** participate in the hydrogen-bonding interaction with the NHNs group independently as a hydrogen bond acceptor and donor, respectively. The carboxylate ion, the counter anion of the acylpyridinium cation, binds both *E*-OH and Z-OH to stabilize at the transition state for the *E*-OH selective acylation, in which the *E*-OH located in close proximity to the reactive acyl group is selectively activated as a nucleophile by general base catalysis with the closely located carboxylate anion [30, 31].



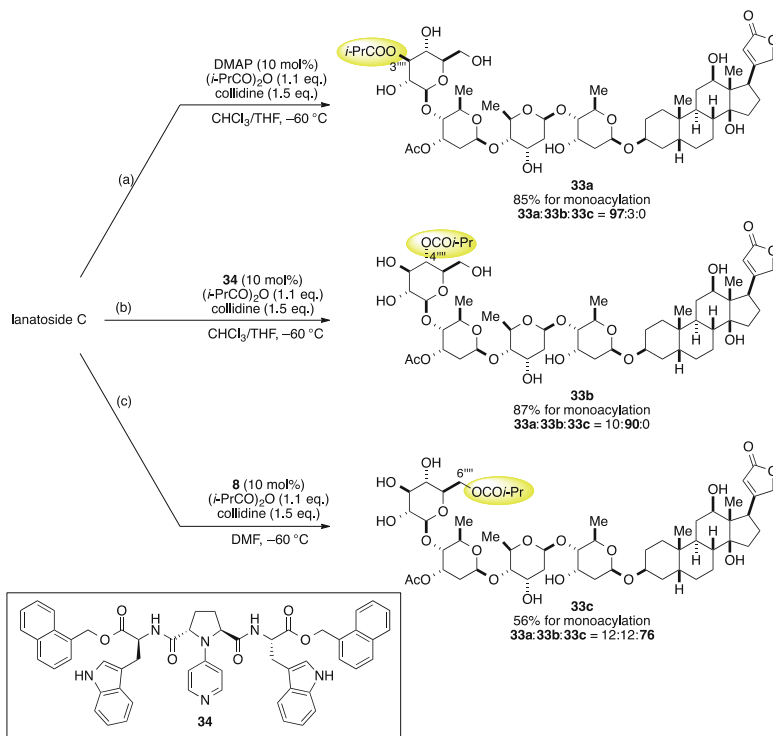


**Fig. 10** Catalyst-controlled site-selective diversification of a polyol macrolide antibiotic, erythromycin A

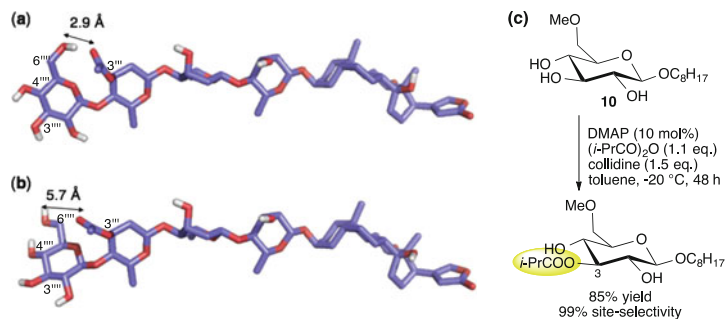


**Fig. 11** Naturally occurring cardiac glycosides, digitoxin and lanatoside C

The site-selectivity profile for the acylation of lanatoside C is shown in Scheme 14. DMAP-catalyzed acylation of lanatoside C in  $\text{CHCl}_3/\text{THF}$  (9/1) at  $-60^\circ\text{C}$  proceeded at the secondary  $\text{C}(3''')$ -OH in 85% yield and 97% site-selectivity (Scheme 14, route (a)). This suggests extremely high intrinsic reactivity of the  $\text{C}(3''')$ -OH among eight hydroxy groups of lanatoside C, i.e., substrate-controlled  $\text{C}(3''')$ -O-acylation. On the other hand, lanatoside C undergoes acylation at  $\text{C}(4''')$ -OH predominantly (90% site-selectivity among 87% yield for monoacylates) in the presence of catalyst **34**, an analogue of **8**, by overcoming the intrinsic high reactivity of  $\text{C}(3''')$ -OH, i.e., catalyst-controlled  $\text{C}(4''')$ -O-acylation (Scheme 14, route (b)). Catalyst **34** seems to be able to recognize the terminal  $\beta$ -glucopyranoside substructure via hydrogen-bonding interaction in a similar manner to catalyst **8** as shown in Fig. 3, even in the presence of many other potential hydrogen bond donors and acceptors in lanatoside C. The site-selectivity of acylation of lanatoside C was found to be highly solvent-dependent. Acylation of lanatoside C in DMF took place at the primary  $\text{C}(6''')$ -OH predominantly catalyzed either by DMAP or **8** (Scheme 14, route (c)), i.e., substrate-controlled  $\text{C}(6''')$ -O-acylation irrespective of the catalyst. Conformational analysis of lanatoside C by molecular modeling suggested the intramolecular hydrogen bond between the C

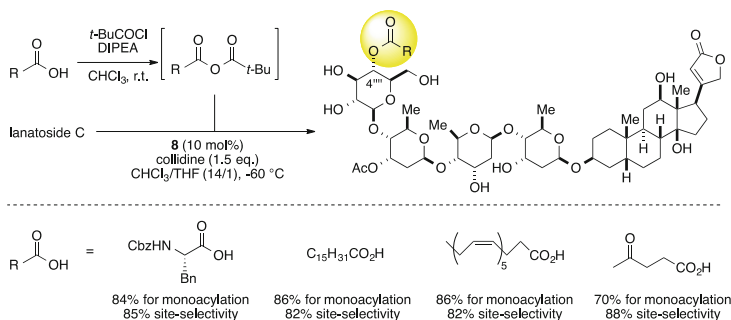


**Scheme 14** Direct site-selective diversification of lanatoside C



**Fig. 12** Calculated structures of lanatoside C in (a) CHCl<sub>3</sub> and (b) water (MacroModel V 9.0 with MM3\* force field). (c) High reactivity of C(3)-OH of 6-*O*-protected β-glucopyranoside **10**

(6''')-OH and the C(3''')-OAc in CHCl<sub>3</sub> (Fig. 12a). Because the primary C(6)-OH is trapped by an intramolecular hydrogen bond in CHCl<sub>3</sub>, the C(3''')-OH is expected to be most reactive, and undergoes highly selective acylation in the presence of DMAP. The observed high reactivity of the C(3)-OH of the β-glucopyranoside substructure in lanatoside C is consistent with our previous result where the C(3)-



**Scheme 15** Catalyst-controlled site-selective introduction of functionalized acyl groups into lanatoside C by a mixed anhydride method

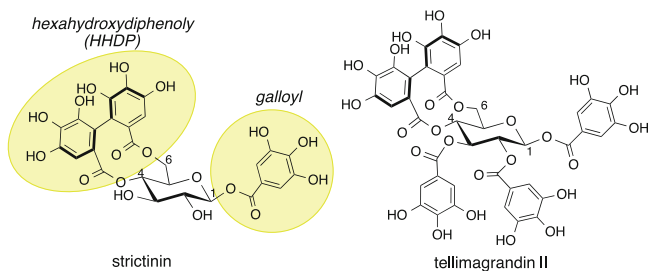
OH of 6-*O*-protected octyl  $\beta$ -D-glucopyranoside **10** showed extremely high reactivity in DMAP-catalyzed acylation (Fig. 12c) [40]. Lack of the hydrogen-bonding interaction of C(6''')-OH in water (Fig. 12b) may be compatible with intrinsic high reactivity of the C(6''')-OH of lanatoside C in DMF solution.

Several functionalized acyl groups can be introduced site-selectively into lanatoside C by using mixed anhydrides generated from the corresponding carboxylic acids and pivaloyl chloride (Scheme 15). Thus, catalyst **8** can deliver various functionalized acyl groups site-selectively onto the C(4''')-OH among eight free hydroxy groups in lanatoside C.

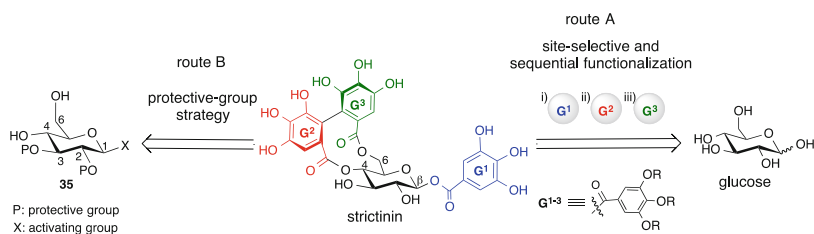
## 10 Unconventional Retrosynthesis: Application of Site-Selective Acylation to Total Synthesis of Natural Glycosides

Retrosynthetic analysis for total syntheses has generally been performed based on chemical transformations with high predictability and reliability [41–43]. In contrast to well established chemical transformations such as chemo-, diastereo-, and enantioselective transformations, site-selective molecular transformation has been scarcely incorporated into retrosynthetic analysis, probably because of the relatively poor reliability of the site-selective transformations. If reliable methods for site-selective molecular transformations are established, they would contribute to the development of innovative retrosynthetic routes, especially for polyfunctionalized complex molecules. Here we introduce several examples of total synthesis of natural glycosides using the unconventional retrosynthetic routes based on organocatalytic site-selective acylation.

Strictinin [44] and tellimagrandin II [45] belong to a family of ellagitannins [46, 47] which consists of a central sugar core, typically D-glucose, to which esterified gallic acid (galloyl) and hexahydroxy diphenolic acid (HHDP) groups are bound (Fig. 13). Strictinin and tellimagrandin II display various biological



**Fig. 13** Structures of strictinin and tellimagrandin II

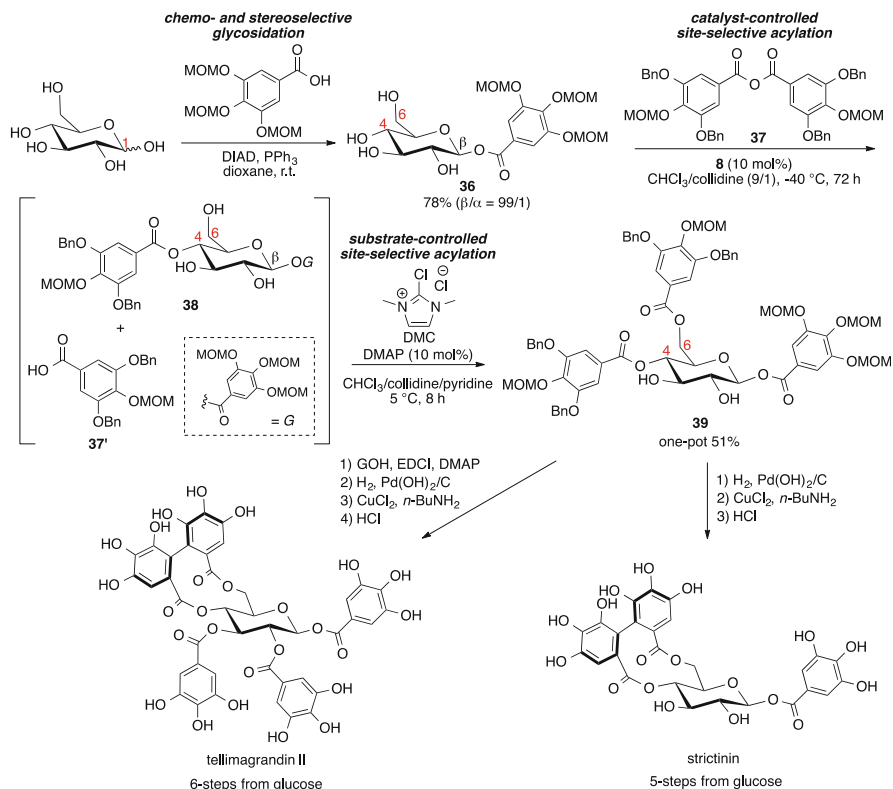


**Scheme 16** Retrosynthetic analyses of strictinin

activities such as anti-HSV, antitumor, anti-influenza virus, and antiallergic activities [48–51].

A rational retrosynthetic analysis of strictinin based on conventional strategy should lead to properly protected precursor **35**, which possesses free C(6)-OH, C(4)-OH, and C(1)-X (X = activating group for glycosidation), C(2)-OPG<sup>1</sup>, and C(3)-OPG<sup>2</sup> aiming at the introduction of an HHDP group at C(4)-O and C(6)-O of the glucopyranose skeleton (Scheme 16, route B). Pioneering works on the total synthesis of strictinin have been reported by Khanbabaee's group and Yamada's group using properly protected precursors such as **35** [52, 53]. Similarly, total synthesis of tellimagrandin II has been reported by Feldman's group [54].

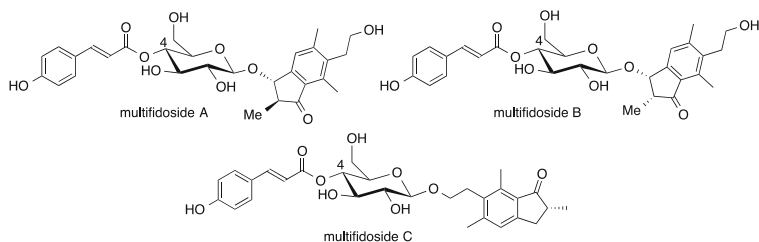
In contrast to these strategies, we propose an unconventional retrosynthetic route to strictinin based on sequential and site-selective introduction of galloyl groups into unprotected glucose (Scheme 16, route A). We envisaged that three galloyl (oxy) groups can be introduced to unprotected glucose in the order C(1) (blue galloyloxy group), C(4)-OH (red galloyl group), and C(6)-OH (green galloyl group). An actual synthetic route for total synthesis of strictinin is shown in Scheme 17 [55]. The first galloyl group was introduced by chemo- and stereo-selective glycosidation employing unprotected glucose as a glycosyl donor under Mitsunobu conditions to provide  $\beta$ -glycoside **36** in 78% yield. The second introduction of a protected galloyl group into intrinsically less reactive C(4)-OH of **36** was achieved by catalyst-controlled acylation with anhydride **37** in the presence of catalyst **8**. The introduction of the third galloyl group at the intrinsically more reactive C(6)-OH is readily achieved employing in situ generated acid **37'** in the



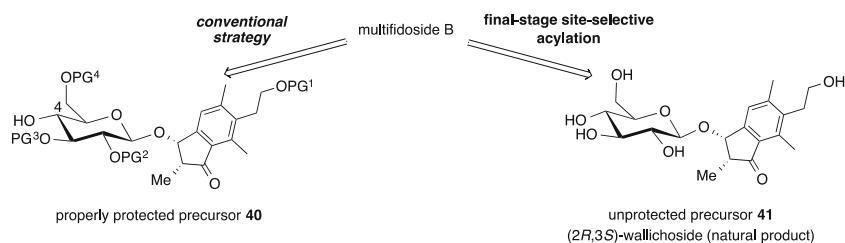
**Scheme 17** Total synthesis of strictinin and tellimagrandin based on sequential site-selective introduction of galloyl groups

presence of condensation agents (DMC and DMAP) to give trigallate **39** in 51% yield by a one-pot operation. Removal of the benzyl groups of **39** by hydrogenation, oxidative phenol coupling of the resulting phenol derivative, followed by removal of MOM groups realized total synthesis of strictinin in five-overall steps and 21% overall yield from naturally abundant glucose without using protecting groups for the glucose moiety. The overall number of the steps for the total synthesis is much less than that previously reported (11–13 steps [52, 53]). In a similar manner, total synthesis of tellimagrandin II was accomplished in six-overall steps and in 18% overall yield from glucose via site-selective sequential introduction of galloyl groups in the order C(1), C(4)-OH, C(6)-OH, and C(2)- and C(3)-OH [55]. The number of steps for the total synthesis is much less than that in previously reported total synthesis of tellimagrandin II (14 steps) [54]. The sequential site-selective functionalization of glucose derivatives was also applied to straightforward preparation of orthogonally protected glucopyranoside derivatives [56].

Multifidosides A, B, and C were isolated from whole plants of *Pteris multifida* used for a traditional Chinese medicine [57]. These glycosides possess a



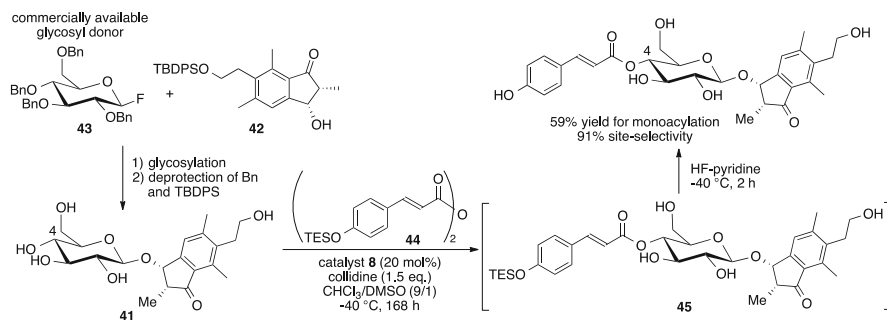
**Fig. 14** Structures of multifidoside A, B, and C



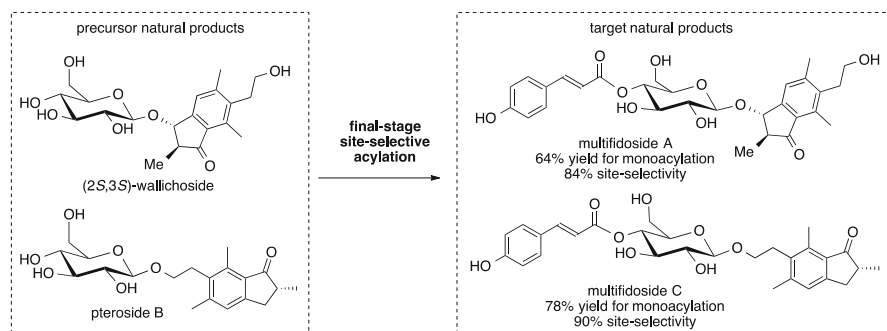
**Scheme 18** Retrosynthetic analyses of multifidoside B

*p*-coumaroyl group at the C(4)-OH of the glucose moiety (Fig. 14). Whereas a rational precursor for the synthesis of multifidoside B is properly protected glycoside **40** with free C(4)-OH based on the conventional retrosynthetic analysis, we propose an unconventional retrosynthetic route based on final-stage site-selective acylation of the protecting-group-free precursor **41** (Scheme 18) [58]. The expected advantages of the latter strategy would involve (1) streamlining the synthetic scheme and (2) avoidance of the risks of the undesired side reactions during the removal of the protecting groups at the later stage. We actually encountered serious undesired side reactions during the attempted total synthesis of multifidoside B during the final deprotection step (Scheme 21). Similarly, undesired side reactions at the late-stage deprotection toward the total synthesis of the related natural glycosides have also been reported [59–62]. The proposed synthetic scheme realizes a one-step conversion from a natural glycoside to another natural glycoside, because precursor **41** is also a natural glycoside, (2*R*,3*S*)-wallichoside [63].

The precursor **41** can be readily prepared by glycosylation of aglycon **42** with commercially available glycosyl donor **43** followed by removal of the TBDPS and Bn groups. By treatment of a protecting-group-free precursor, **41**, with TES-protected acid anhydride **44** in CHCl<sub>3</sub>/DMSO (9/1) in the presence of catalyst **8**, acylation took place selectively on the secondary hydroxy group at C(4) of the glucose moiety in the presence of five free hydroxy groups including two primary hydroxy groups to give directly a natural product, multifidoside B in 91% site-selectivity and 59% yield for monoacylation (54% yield) (Scheme 19). Similarly, the strategy based on final-stage site-selective acylation of the protecting-group-free precursor was further applied to the total synthesis of multifidoside A and C



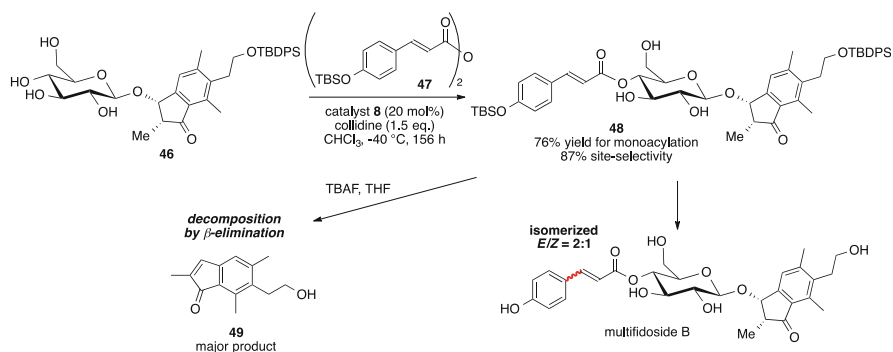
**Scheme 19** Total synthesis of multifidoside B via final-stage site-selective acylation



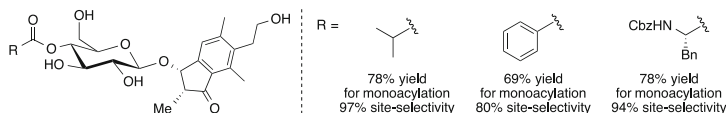
**Scheme 20** Total synthesis of multifidoside A and C via final-stage site-selective acylation

(Scheme 20). In these molecular transformations, CHCl<sub>3</sub>/DMSO (9/1) was found to be a suitable solvent for site-selective acylation. This observation is seemingly inconsistent with the rationale for site-selective catalysis because DMSO, a strong hydrogen-bond acceptor, may disturb the hydrogen bonding interaction between the catalyst and the substrate, which seems critical for the site-selective catalysis shown in Fig. 3. However, tolerated use of DMSO for the catalytic site-selective acylation should provide great advantages to the present strategy, because such a solvent system can dissolve various polar natural and unnatural compounds of biological interest.

Serious undesired side reactions we encountered during the attempted total synthesis of multifidoside B are described here (Scheme 21). Efforts toward the total synthesis was hampered by the final-step deprotection of the partially protected natural product precursor **48**, resulting in giving decomposed product **49** by  $\beta$ -elimination of the glycoside moiety. Use of milder conditions for the deprotection resulted in double-bond isomerization to give an *E/Z* (2/1) mixture of multifidoside B. It has also been reported in the literature that the undesired side reactions such as acyl migration from the desired 4-*O*-acylate to the undesired 6-*O*-acylate and over-reduction, and isomerization of the *p*-coumaroyl moiety have been observed during



**Scheme 21** Problems encountered at the later-stage deprotection toward total synthesis of multifidoside B



**Fig. 15** Various acylates obtained by late-stage diversification of a natural glycoside, (2*R*,3*S*)-wallichoside

the final-step deprotection toward the total synthesis of 4-*O*-acylated glycoside natural products [59–62]. These serious problems could be avoided if the present strategy can be successfully applied. This synthetic strategy is expected to provide a new retrosynthetic route to 4-*O*-acylglycosides such as phenylethanoid glycosides [64] and ellagitannins [46, 47], because the present catalytic site-selective acylation of glycosides takes place with high predictability and reliability.

Another advantage of this strategy involves the direct and facile diversification of natural glycosides. Various kinds of acyl groups can be introduced to the expected C(4)-OH of a natural glycoside, (2*R*,3*S*)-wallichoside (Fig. 15). Late-stage site-selective functionalization of biologically active molecules has recently been receiving great attention because it enables diversification of biologically active compounds retaining their original activity [1]. A proposal for site-selective introduction of various acyl groups at the final stage of the synthesis may be applicable to the search for the analogues with the related biological activity.

## 11 Conclusion

Examples for catalyst-controlled site-selective acylation of carbohydrates and polyol compounds were described. The salient feature of these molecular transformations is that the site-selectivity can be controlled independently from the intrinsic reactivity of the substrate. Some substrates undergo acylation with reversal

of their intrinsic reactivity under catalyst-controlled conditions. The key to achieving the desired site-selective molecular transformation appears to be the strategy relying on the accelerative reaction rather than the decelerative one. An unconventional retrosynthetic route was proposed for total synthesis of natural glycosides based on a site-selective-acylation strategy of carbohydrates. Extremely short-step total syntheses of natural glycosides of an ellagitannin family have been performed by streamlining the synthetic routes based on the proposed unconventional retrosynthetic analysis. Late-stage site-selective acylation of complex natural products of biological interests was also described.

## References

1. Romo D, Robles O (2014) Chemo- and site-selective derivatizations of natural products enabling biological studies. *Nat Prod Rep* 31:318
2. Varki A, Cummings DC, Esko JD, Freeze HH, Stanley P, Bertozzi CR, Hart GW, Etzler ME (2009) *Essentials of glycobiology*. Cold Spring Harbor Press, New York
3. Doores KJ, Gamblin DP, Davis BG (2006) Exploring and exploiting the therapeutic potential of glycoconjugates. *Chem Eur J* 12:656
4. Lee D, Taylor MS (2012) Catalyst-controlled regioselective reactions of carbohydrate derivatives. *Synthesis* 44:3421
5. Bartolozzi A, Seeberger PH (2001) New approaches to the chemical synthesis of bioactive oligosaccharides. *Curr Opin Struct Biol* 11:587
6. Kawabata T, Furuta T (2009) Nonenzymatic regioselective acylation of carbohydrates. *Chem Lett* 38:640
7. Riva S (2008) *Organic synthesis with enzymes in non-aqueous media*. Wiley-VCH, Weinheim
8. Björkling F, Godtfredsen SE, Kirk O (1989) A highly selective enzyme-catalysed esterification of simple glucosides. *J Chem Soc Chem Commun* 934
9. Therisod M, Klibanov AM (1987) Regioselective acylation of secondary hydroxy groups in sugars catalyzed by lipases in organic solvents. *J Am Chem Soc* 109:3977
10. Kattinig E, Albert M (2004) Counterion-directed regioselective acetylation of octyl  $\beta$ -D-glucopyranoside. *Org Lett* 6:945
11. Kurahashi T, Mizutani T, Yoshida J (1999) Effect of intramolecular hydrogen-bonding network on the relative reactivities of carbohydrate OH groups. *J Chem Soc Perkin Trans 1* 465
12. Kurahashi T, Mizutani T, Yoshida J (2002) Functionalized DMAP catalysts for regioselective acetylation of carbohydrates. *Tetrahedron* 58:8669
13. Griswold KS, Miller SJ (2003) A peptide-based catalyst approach to regioselective functionalization of carbohydrates. *Tetrahedron* 59:8869
14. Höfle G, Steglich W, Vorbrüggen H (1978) 4-Dialkylaminopyridines as highly active acylation catalysts. *Angew Chem Int Ed Engl* 17:569
15. Scriven EFV (1983) 4-Dialkylaminopyridines: super acylation and alkylation catalysts. *Chem Soc Rev* 12:129
16. Verdoucq L, Morinière J, Bevan DR, Esen A, Vasella A, Henrissat B, Czjzek M (2004) Structural determinants of substrate specificity in family 1  $\beta$ -glucosidases. *J Biol Chem* 279:31796
17. Kawabata T, Muramatsu W, Nishio T, Shibata T, Uruno Y, Stragies R (2008) Regioselective acylation of octyl  $\beta$ -D-glucopyranoside by chiral 4-pyrrolidinopyridine analogues. *Synthesis* 747

18. Kawabata T, Muramatsu W, Nishio T, Shibata T, Schedel H (2007) A catalytic one-step process for the chemo- and regioselective acylation of carbohydrates. *J Am Chem Soc* 129: 12890
19. Ueda Y, Muramatsu W, Mishiro K, Furuta T, Kawabata T (2009) Functional group tolerance in organocatalytic regioselective acylation of carbohydrates. *J Org Chem* 74:8802
20. Hajjar AB, Nicks PF, Knowles CJ (1990) Preparation of monomeric acrylic ester intermediates using lipase catalyzed transesterifications in organic solvents. *Biotechnol Lett* 12:825
21. Framis V, Camps F, Clapés P (2004) Lipase-catalysed selective monoacylation of 1,n-diols with vinyl acetate. *Tetrahedron Lett* 45:5031
22. Yoshida K, Furuta T, Kawabata T (2011) Organocatalytic chemoselective monoacylation of 1, n-linear diols. *Angew Chem Int Ed* 50:4888
23. Hanessian S, Parthasarathy S, Mauduit M (2003) The power of visual imagery in drug design. Isopavines as a new class of morphinomimetics and their human opioid receptor binding activity. *J Med Chem* 46:34
24. Klingler FD (2007) Asymmetric hydrogenation of prochiral amino ketones to amino alcohols for pharmaceutical use. *Acc Chem Res* 40:1367
25. Ager DJ, Prakash I, Schaad DR (1996) 1,2-Amino alcohols and their heterocyclic derivatives as chiral auxiliaries in asymmetric synthesis. *Chem Rev* 96:835
26. Yoshida K, Shigeta T, Furuta T, Kawabata T (2012) Catalyst-controlled reversal of chemo-selectivity in acylation of 2-aminopentane-1,5-diol derivatives. *Chem Commun* 48:6981
27. Shirmeister T, Otto HH (1993) Enzyme-catalyzed hydrolyses of *E/Z*-diastereotopic and *E/Z*-diastereomeric esters. Affect on selectivity by reaction media. *J Org Chem* 58:4819
28. Miura T, Umetsu S, Kanamori D, Tsuyama N, Jyo Y, Kawashima Y, Koyata N, Murakami Y, Imai N (2008) Convenient synthesis of *Z*-monoacetates of 2-alkylidene-1,3-propanediols. *Tetrahedron* 64:9305
29. Yoshida K, Mishiro K, Ueda Y, Shigeta T, Furuta T, Kawabata T (2012) Nonenzymatic geometry-selective acylation of tri- and tetrasubstituted  $\alpha,\alpha'$ -alkenediols. *Adv Synth Catal* 354:3291
30. Yamanaka M, Yoshida U, Sato M, Shigeta T, Yoshida K, Furuta T, Kawabata T (2015) Origin of high *E*-selectivity in 4-pyrrolidinopyridine-catalyzed tetrasubstituted  $\alpha,\alpha'$ -alkenediol: a computational and experimental study. *J Org Chem* 80:3075
31. Xu S, Held I, Kempf B, Mayr H, Steglich W, Zipse H (2005) The DMAP-catalyzed acetylation of alcohols - a mechanistic study (DMAP = 4-(dimethylamino)pyridine). *Chem Eur J* 11:4751
32. Robles O, Romo D (2014) Chemo- and site-selective derivatizations of natural products enabling biological studies. *Nat Prod Rep* 31:318
33. Clardy J, Walsh C (2004) Lessons from natural molecules. *Nature* 432:829
34. González-Sabín J, Morán-Ramallal R, Rebolledo F (2011) Regioselective enzymatic acylation of complex natural products: expanding molecular diversity. *Chem Soc Rev* 40:5321
35. Gu J, Ruppen ME, Cai P (2005) Lipase-catalyzed regioselective esterification of rapamycin: synthesis of temsirolimus (CCI-779). *Org Lett* 7:3945
36. Lewis CA, Miller SJ (2006) Site-selective derivatization and remodeling of erythromycin a by using simple peptide-based chiral catalysts. *Angew Chem Int Ed* 45:5616
37. Lewis CA, Longcore KE, Miller SJ, Wender PA (2009) An approach to the site-selective diversification of apoptolidin A with peptide-based catalysts. *J Nat Prod* 72:1864
38. Yoshida K, Furuta T, Kawabata T (2010) Perfectly regioselective acylation of a cardiac glycoside, digitoxin, via catalytic amplification of the intrinsic reactivity. *Tetrahedron Lett* 51:4830
39. Ueda Y, Mishiro K, Yoshida K, Furuta T, Kawabata T (2012) Regioselective diversification of a cardiac glycoside, lanatoside C, by organocatalysis. *J Org Chem* 77:7850
40. Muramatsu W, Kawabata T (2007) Regioselective acylation of 6-*O*-protected octyl  $\beta$ -D-glucopyranosides by DMAP catalysis. *Tetrahedron Lett* 48:5031
41. Chen MS, White MS (2007) A predictably selective aliphatic C-H oxidation reaction for complex molecule synthesis. *Science* 318:783

42. Lapointe D, Markiewicz T, Whipp CJ, Toderian A, Fagnou K (2011) Predictable and site-selective functionalization of poly(hetero)arene compounds by palladium catalysis. *J Org Chem* 76:749
43. Gormisky PE, White MC (2013) Catalyst-controlled aliphatic C-H oxidations with a predictive model for site-selectivity. *J Am Chem Soc* 135:14052
44. Okuda T, Yoshida T, Ashida M, Yazaki K (1983) Tannins of *Casuarina* and *Stachyurus* species. Part 1. Structures of penduculagin, casuarictin, strictinin, casuarinin, casuariin, and stachyurin. *J Chem Soc Perkin Trans 1* 1765
45. Wilkins CK, Bohm BA (1976) Ellagitannins from *Tellima grandiflora*. *Phytochemistry* 15:211
46. Quideau S, Deffieux D, Douat-Casassus C, Pouységu L (2011) Plant polyphenols: chemical properties, biological activities, and synthesis. *Angew Chem Int Ed* 50:586
47. Quideau S, Feldman KS (1996) Ellagitannin chemistry. *Chem Rev* 96:475
48. Kurokawa M, Hozumi T, Tsurita M, Kadota S, Namba T, Shiraki K (2001) Biological characterization of eugenin as an anti-herpes simplex virus type 1 compound in vitro and in vivo. *J Pharmacol Exp Ther* 297:372
49. Kashiwada Y, Nonaka G, Nishioka I, Lee KJ-H, Bori I, Fukushima Y, Bastow KF, Lee K-H (1993) Tannins as potent inhibitors of DNA topoisomerase II in vitro. *J Pharm Sci* 82:487
50. Saha RK, Takahashi T, Kurebayashi Y, Fukushima K, Minami A, Kinbara N, Ishitani M, Sagesaka YM, Suzuki T (2010) Antiviral effect of strictinin on influenza virus replication. *Antiviral Res* 88:10
51. Tachibana H, Kubo T, Miyase T, Tanino S, Yoshimoto M, Sano M, Yamamoto-Maeda M, Yamada K (2001) Identification of an inhibitor for interleukin 4-induced epsilon germline transcription and antigen-specific IgE production in vivo. *Biochem Biophys Res Commun* 280:53
52. Khanbabaee K, Schulz C, Lötzerich K (1997) Synthesis of enantiomerically pure strictinin using a stereoselective esterification reaction. *Tetrahedron Lett* 38:1367
53. Michihata N, Kaneko Y, Kasai Y, Tanigawa K, Hirokane T, Higasa S, Yamada H (2013) High-yield total synthesis of (–)-strictinin through intramolecular coupling of gallates. *J Org Chem* 78:4319
54. Feldman KS, Sahasrabudhe K (1999) Ellagitannin chemistry. Syntheses of tellimagrandin II and a dehydrodigalloyl ether-containing dimeric gallotannin analogue of coriariin A. *J Org Chem* 64:209
55. Takeuchi H, Mishiro K, Ueda Y, Fujimori Y, Furuta T, Kawabata T (2015) Total synthesis of ellagitannins via regioselective sequential functionalization of unprotected glucose. *Angew Chem Int Ed* 54:6177
56. Muramatsu W, Mishiro K, Ueda Y, Furuta T, Kawabata T (2010) Perfectly regioselective and sequential protection of glucopyranosides. *Eur J Org Chem* 827
57. Ge X, Ye G, Li P, Tang W-J, Gao J-L, Zhao W-M (2008) Cytotoxic diterpenoids and sesquiterpenoids from *Pteris multifida*. *J Nat Prod* 71:227
58. Ueda Y, Furuta T, Kawabata T (2015) Final-stage site-selective acylation for the total syntheses of multifidosides A-C by organocatalysis. *Angew Chem Int Ed* 54:11966
59. Kawada T, Asano R, Makino K, Sakuno T (2002) Synthesis of isoacteoside, a dihydroxy phenylethyl glycoside. *J Wood Sci* 48:512
60. Kawada T, Asano R, Makino K, Sakuno T (2000) Synthesis of conandroside: a dihydroxy-phenylethyl glycoside from *Conandron ramaidioides*. *Eur J Org Chem* 2723
61. Duynstee HI, de Koning MC, Ovaa H, van der Marel GA, van Boom JH (1999) Synthesis of verbascoside: a dihydroxyphenylethyl glycoside with diverse bioactivity. *Eur J Org Chem* 2623
62. Zhang S-Q, Li Z-J, Wang A-B, Cai M-S, Feng R (1997) Total synthesis of phenylpropanoid glycoside, grayanoside A. *Carbohydr Res* 299:281
63. Sengupta P, Sen M, Niyogi SK (1976) Isolation and structure of wallichoside, a novel pteroside from *Pteris wasslichiana*. *Phytochemistry* 15:995
64. Haslam E, Cai Y (1994) Plant polyphenols (vegetable tannins): gallic acid metabolism. *Nat Prod Rep* 11:591

# Index

## A

Accelerative reaction, 203  
Acyl, 65, 160  
  hydrazines, 113  
  phosphonates, 66  
  transfer reactions, 160  
Acylation, 114, 128, 131, 166, 182, 203  
  site-selective, 166, 203  
Acylimines, 116  
Acylurea, 118, 188  
Alcohols, 39, 46, 51, 66, 85, 96, 138, 146  
  acylation, 167, 209  
  deoxygenation, 176  
  hydrogenation-dehydrogenation, 88  
  oxidation, 117  
  thiocarbonylation, 173  
  unprotected, chiral  $\beta,\gamma$ -stereogenic, 92  
Aldehydes,  $\alpha,\beta$ -unsaturated, 61  
Alkanes, 28, 32, 39, 43, 51  
  oxidation, 32, 35, 40  
Alkylidene lactones, 79  
Alkylidene malonates, 73  
Alkylidene malononitriles, 76  
Alkylidene oxindoles, 79  
Alkyls, C–H oxidation, 27  
2-Alkynylaniline, 20  
2-Alkynylchlorophenol, 17  
Alzheimer disease, 112  
Ambroxide, 38  
Amides, 104, 113, 116, 133  
Amino acids, 57  
Aminopyridine ligands, 27  
Amino sulfonamides, 74  
Amino thiourea, 60, 70, 74  
 $\beta$ -Amyloid, 112

Apoptolidin, 167, 220  
Arabinopyranosides, 143  
Artemisinin, 36, 49  
Arylboronic acids, 5  
Asymmetric synthesis, 84, 160, 204  
Aziridines, 63  
Azlactones, 58, 65

## B

Barton–McCombie reaction, 131  
Benzo[*b*]furans, disubstituted, 20  
Benzoylation, 134, 137, 148  
Benzylation, 137, 140, 164  
Biodegradation, 30  
Bispidine, 34  
2-[Bis-(pyridine)-2-ylmethyl]amino-N-quinolin-8-yl-acetamidate, 34  
Borinic acids, 143  
Boronic esters, sugar-derived, 142  
4-Bromo-2-chlorophenol, 15  
Brønsted acid, 135  
Brønsted base, 105, 134  
 $\gamma$ -Butenolides, 70  
 $\gamma$ -Butyrolactam, 73

## C

Carbohydrates, 86, 125, 159, 166, 173, 203  
Carbonyl( $\alpha$ -aminomethyl)allylation, 96  
Carbonyl compounds,  $\alpha,\beta,\gamma,\delta$ -unsaturated, 56  
Catalysis, 125  
  asymmetric, 55  
  bioinspired, 27  
  site-selectivity, 157

- Catalysts, peptide-based, 157  
 ChelpG, 58  
 Chloroarenes, 18  
 Chlorobenzo**b**/furans, 17  
 4-Chloroindoles, 20  
 C–H, oxidation, 51  
 Cinchona alkaloids, 58  
 Cinchonidinium salt, 57  
*cis*-4-Methylcyclohexyl-1-pivalate, 34  
 Cleavage, 103  
 Conjugate addition, site-selectivity, 55  
 Copper(II), 148  
 Cross-coupling, 1  
     catalyst-controlled, 3  
     chemoselective, 2  
 4-Cyano-3-nitro-benzoic acid, 92  
 Cyclen-PNA conjugates, 112  
 Cycloaddition, 79, 81  
 Cyclobutanes, 81  
 Cyclodextrins (CDs), 110  
 Cyclohexane, 34, 38, 40, 42, 46, 115  
 Cyclohexanediol, 143  
 Cyclohexanedione, 77  
 Cyclohexanones, 40, 61  
 Cyclohexenylidene malononitriles, 78  
 Cyclohexyldiamine, 33  
 Cyclopentadiene, 64  
 Cyclopentanone, 37  
 Cyt P450, 29
- D**
- Decalone, 47  
 Degradation, 103  
 Deoxyglycosides, 145  
 Deoxy sugars, 139  
 Desaturation, 51  
 Diacetyliodobenzene (DIB), 118  
 Diacyl glycerol phosphates, 166  
 Dibromoanilines, 17, 21  
 2,4-Dibromobenzoic acid, 5  
 Dibromoindole, 16  
 1,6-Dibromo-2-naphthol, 15  
 2,5-Dibromothiazoles, 10  
 2,6-Dichloronicotinic acid, 4  
 Dichlorophenols, 17  
 3,5-Dichloropyridazines, 6  
 Dienals,  $\alpha,\beta,\gamma,\delta$ , 64  
     aziridination, 63  
 Difluorobenzene-sulfonyl chloride, 139  
 Digitoxin, 144, 220  
 Dihalides, organic, 3  
 Dihaloarenes, 12  
 2,5-Dihalo-1-methylimidazoles, 10
- Dihalophenols, 16  
 Dihydrocinchoninium salt, 57  
 Dihydropicrotoxinin, 36  
 2,4-Diiodooxazole, 8  
 4-Dimethylaminopyridine (DMAP), 128  
 Dimethyl-2,2-bipyridyl (DMBPY), 142  
 Dimethylcyclohexane, 31  
 Dimethyl-*N,N'*-bis(2-pyridylmethyl)-ethane-1,2-diamine, 32  
 Dioctyltin dichloride, 141  
 Diols, allylation, redox-triggered, 88  
 Dipeptides, 107  
 Diphenylborinic acid, 143  
 Diphenylprolinol silyl ether, 80  
 Diphenylprolinol trimethylsilyl ether, 75  
 6-(1-Dodecynyl)-2-decylbenzo**b**/furan, 19
- E**
- Electrophiles, vinyllogous, 56  
 Ellagitannins, 203  
 Erythromycin, 167, 173, 220  
 Ethanolamine ester, 143
- F**
- Fucopyranosides, 139
- G**
- Galactopyranosides, 141  
 Glucofuranosides, 138, 140  
 Glucopyranosides, 128–132, 137–140, 148, 205–212, 221–225  
 Glycerol, 166  
 Glycosides, 203  
 Glycosylation, 125, 128, 130, 136, 140, 226  
 Guanidine, 73  
 Guanosine 5'-phosphate (GMP), 159
- H**
- Halides, organic, 2  
 Hapten, phosphatidyl-myo-inositol-3-phosphate-based, 165  
 Hexahydroxy diphenolic acid (HHDP), 223  
 Hexopyranosides, 143  
 Hydrazinolysis, 113  
 Hydrogenation, enantioselective, 86  
 Hydrogen peroxide, 27  
 Hydroxylase/desaturase, 52  
 Hydroxylation, 52  
 Hydroxyterphenylphosphines, 14  
 Hyperthermophilic organisms, 164

**I**

Iminium activation, 61  
Indoles, 21, 188  
Inositol, asymmetric  
  phosphorylation, 159  
Inositol phosphates, 161  
Ion-pairing, 55  
Iridium, 149  
Iron coordination complexes, 27, 31  
Iron porphyrins, 29

**J**

Julia–Colonna epoxidation, 158

**K**

Ketones,  $\alpha,\beta$ -unsaturated, 57, 61, 74  
Keyhole limpet hemocyanin  
  (KLH), 165  
Kumada–Tamao–Corriu  
  coupling, 1, 12

**L**

La(OTf)<sub>3</sub>, 146  
Lanatoside, 220  
Lanthanides, 146  
L-DOPA, 86  
Lewis acids, 125, 138  
  transition metal-based, 147  
Lewis bases, 125

**M**

Maleimides, 77  
Malonates,  $\alpha$ -diarylmethylation, 58  
Mannopyranosides, 140  
Menthyl acetate, 36, 38  
Metal hydroxides, 105  
Methyl  $\alpha$ -glucopyranoside, 131  
3-Methyl-4-nitro-5-alkenyl  
  isoxazoles, 74  
4-Methylpentanoic acid, 52  
Mg(OTf)<sub>2</sub>, 146  
Michael addition,  
  sulfa-,1,4-selective, 58  
Molecular recognition, 203  
Molybdenum, 147  
Mono-cross-coupling, 1  
Monophosphatase, 162  
Monosulfonylations, 138  
Multifidocide, 225

**N**

Naphthalene-1,2-dioxygenase (NDO), 30  
Natural products, 157  
Neomenthyl esters, 45  
Nitro compounds,  $\alpha,\beta,\gamma,\delta$ -unsaturated, 59  
Nitroenynes, 60  
Nitroolefins, 59  
*N*-Methyl 3-hydroxyoxindole, 62  
Nonheme oxygenases, 27  
*N*-Oxoammonium salts, 137  
Nucleophiles, vinylogous, 65

**O**

Octyl  $\beta$ -glucopyranoside, 128  
Oligopeptides, 105  
Oligosaccharides, 127  
Organoboron catalysts, 142  
Organocatalysis, 55, 125, 203  
Organotin, 138  
Oxalimide, 117  
Oxazolidinone enoates, 71  
Oxazol-5(4*H*)-one (azlactone), 58  
Oxidation, alkyl C–H, 27  
  selectivity, 27  
Oxindoles, 77, 79  
Oxygenases, nonheme, 27  
Oxygenation, 51

**P**

Palladium, 1, 149  
Pentamethylpiperidine, 131, 140  
Peptide deformylase (PDF), 112  
Peptide nucleic acid (PNA), 112  
Peptides, 103, 157  
  hydrolysis/solvolysis, 104  
Phase transfer catalysts, 137  
Phenylboronic acid, 7  
Phenyl chlorothionoformate, 139  
Phosphatidyl inositol phosphates (PIPs), 162  
Phosphodiesterase (PDE IV) inhibitor, 75  
Phosphoramidite, 162  
Picrotoxinin, 52  
Piperidines, 96  
Polyenyl *N*-acyl pyrroles, 57  
Polyols, 203  
Proteases, 158  
Protective groups, 125  
Proteins, cleavage, 103  
Pseudoaldehydes, 2  
Pyridines, 128  
Pyrrolidinopyridine (PPY), 130, 208

**Q**

Quinone methides, 59

**R**

Rapamycin, 220  
Regioselectivity, 4, 56, 127, 143, 147, 211  
Resorcinarene, 46  
Retrosynthesis, 203  
Rhamnopyranosides, 143  
Rieske oxygenases, 29

**S**

Scaffolding catalysis, 133  
Sclareolide, 38, 49  
SEGPPOS, 92  
Silylation, 144  
Site-selectivity, 55, 103, 157, 203  
Sonogashira coupling, 1, 17  
Stetter reaction, 59  
Strictinin, 223  
Sulfinylation, 166  
Sulfonylation, 137  
Suzuki–Miyaura coupling, 1, 4

**T**

Teicoplanin, 131–133  
Tellimagrandin, 223  
Temsirolimus, 220  
Terphenylphosphine, 12  
*tert*-Butyl-4-iodobenzoate, 15  
Tetraalkylammonium salts, 137

Tetraarylammonium barfate, 60  
Tetrahydrogibberellic acid, 42  
Tetramethylethylenediamine (TMEDA), 149  
Tetramethylpiperidinyloxy (TEMPO), 137  
Thermoprotection, natural products, 164  
Thiocarbonylations, 139  
Thioglycosides, 130  
Thiols, 58  
Thioureas, 60, 65–79, 136  
Toluene monooxygenase, 30  
Transition metal catalyst, 1, 147  
Triaminoiminophosphorane, 58  
Triazamacrocyclic, 32  
Triaza-7-phosphaadamantane, 8  
Triflates, 2  
Trimethylphenylammonium tribromide, 141  
Tripeptides, 107

**V**

Vinylogy, 55  
Vinyl pyrroles, 81

**W**

Wallichoside, 226

**X**

Xanthone, 40  
Xantphos, 8  
Xylopyranosides, 138